CLASS NOTES FOR EXPERIMENTAL METHODS IN FLUID MECHANICS

V.A. SANDBORN

CIVIL ENGINEERING DEPARTMENT
COLORADO STATE UNIVERSITY
Fort Collins, Colorado

CLASS NOTES FOR EXPERIMENTAL METHODS IN FLUID MECHANICS

V. A. SANDBORN

COLORADO STATE UNIVERSITY
FORT COLLINS, COLORADO

1972

REVISION OF NOTES ENTITLED "METROLOGY OF FLUID MECHANICS" 1966

PREFACE

This is a set of notes employed in the teaching of a first year graduate course entitled "Experimental Methods in Fluid Mechanics" at Colorado State University. The notes assume this is the students first introduction to a specific course in experimental methods; although he will be familiar with undergraduate courses and laboratories where basic phenomenon are demonstrated. The course is taught both as a series of lectures and a laboratory. The laboratory, which parallels the notes is designed to teach the experimental techniques. The student is allowed to discover the difficulties and pit falls that can be encountered in making experimental measurements in fluid mechanics.

The notes have been taken from many sources, and as such should not be viewed as totally original. An attempt is made to treat the more basic instruments used in fluid mechanics in some detail. The notes are not intended as a catalogue of all the many different types of instruments that are employed in fluid mechanics. It is hoped that the notes will serve as a starting point for the graduate students venture into experimental research. The student should, however, be forewarned that the present notes are only the first steps into the total field of measurements. Such areas of transient response and servo-mechanism are still in the future for those who would be instrumentation engineers.

I am indebted to Mrs. Arlene Ahlbrandt for the typing and many revisions that the notes have gone through over the last seven years.

Virgil A. Sandborn

Colorado State University
February 1972

CONTENTS

VI. MEASUREMENT OF TEMPERATURE

CHAPTER I
THE THEORY OF MEASUREMENTS

A. Basic Approach. - There is no concise theory of measurements, however, there are a few governing steps that form the start of a theory. Many areas require measurements of one type or another. This means that no one approach will be adequate for all types of measurements. One might contrast the scientific measurement of the speed of light with an engineering test of the strength of a beam. The fundamental difference in the two measurements is the time involved in the measurement. The scientific measurement of the speed of light is one individual number, but it would well require 10 years or more of work to produce the number. On the other hand, the engineering test of the strength of a beam may require a day of work or less. This contrast is of course a simple matter of how accurate a measurement is required. There is a wide division in the approach to a testing type measurement and to that of a scientific type experimental measurement.

The present course is aimed at the wide center ground between the routine test measurement and the elaborate scientific measurement. The routine test will employ about the same type or perhaps a less accurate instrument than those covered in the present approach. The scientific measurement on the other hand will spend a great deal more time in establishing the basic accuracy of each individual step. In each type of measurement it is important that the operator understand the basic function of each part. While it helps to be an electronic engineer, as well as have a Ph. D. in fluid mechanics, to make a measurement in fluid mechanics neither is absolutely necessary.

The basic requirement to successfully carry out a measurement is a driving desire to obtain an understanding of the physical property being measured. It appears that all simple measurements have already been made, so that there is no such thing as a simple measurement. Any measurement that is made is always somewhat questionable. Thus, the experimenter that sets out to make a measurement must start as an optimist and upon obtaining some data he must become a pessimist. It is helpful if the experimenter

can start out as an absolute optimist and back off from this view as the experiment is undertaken. The first view of the results of a new experiment should be absolutely pessimistic and again back off from this view as the results are placed in proper focus.

The above discussion is meant to imply that in experimental research nothing is right the first time. The author after 15 years of setting up experimental programs has developed the superstition that a data sheet is never taken to the site on the first try at making a measurement. There are very few times that a completely new instrument worked the first time that it was tried (the ion beam hot wire calorimeter) led to more confusion than if it had failed. The point is that it is a rare occurrence that an experiment works right the first time it is run. The frequency of working no doubt improves as the experience of the experimenter increases, but each new study produces its share of new problems.

The theory of measurement might well be viewed as what to do when the results are not as expected. First, it can be assumed that the rest of the world is as likely to be right as you are. Thus, if your data disagrees with the rest of the world, do not get too excited about the results. Almost every measurement can at least be checked at some approximate end point, so there is always a rough idea as to what will be obtained from a measurement. After the first attempt and the results differ from that expected, the next step is clear. In many cases it becomes all too clear that it is not possible to obtain all the information considered in the original experiment. In a scientific measurement it is probable that the approach may be altered. For engineering measurements it may be too costly in time and money to make more than minor changes in the research program.

The general approach to making a second step after the first has failed is to examine the results. A decision is made as to why the results differ from what was expected. The second cut at the measurements alters the original approach to correct for the assumed error in the first attempt. After many years of making

this second step, the author has come to feel that it is of only minor importance whether the assumed error was the correct one or not. The important step is to do something. Usually, when one part of the measurement is altered, something new turns up and an insight to the actual problem becomes clear. This should not be taken to imply that everything is cleared up after the second try. Actually, it may require a dozen second steps to get to an acceptable result. With each second try the experimenter must readjust his thinking from the pessimism of the last result to the optimism of the next try. A special attitude is apparently necessary to jump back and forth so quickly. Some very excellent people fail as experimental researchers because of the inability to shake the pessimism of the first failure. Too close a look at any engineering type measurement will turn up a large number of uncertainties. The important thing is to get what ever can be obtained from the experiment and clear up the uncertainties as they arise.

In planning a measurement it is not possible to account for all the problems that might arise. One should take an approach which might best be described as "quick and dirty, but not too dirty". In other words a quick experiment set up at a minimum of expense will show exactly where the major problems will occur. One can usually foresee most of the problems that might arise, but to know just which one will require special consideration is almost impossible. Thus, one can adopt an approach of "leave it alone and it will go away by itself", and then handle only the problems that did not go away. It is always some simple little problem that was thought about, but considered not important, that comes up to give the most trouble.

B. The Measurement.- Each measurement may be broken out into a series of individual steps. Figure 1.1 shows a block diagram of one possible division of the components.

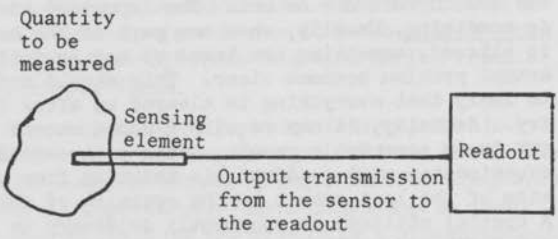

Figure 1.1- Block Diagram of a Measurement

The sensing element may be a probe, as shown in figure 1.1 or it might be a beam of light. We shall term the sensing element as a transducer if it converts the quantity sensed into some other form of output. For example: A thermometer composed of a liquid in a glass tube converts temperature to a height. The main object of this course will be to study the possible transducers that can be used to sense the quantities encountered in fluid mechanics. The problems of evaluating accurately each aspect of how the transducer responds to a given quantity; what other factors affect the transducer; how the transducer effects the quantity measured; and many related problems will be covered.

In order to fully develop the measurement concepts it is necessary to first look at the overall block diagram. A sensing element is of value only if its output can be gotten out of the test facility, and then read on some device that can be calibrated. The linkage between sensor and readout can be very important to a measurement. The linkage will depend on the specific sensing element, so it will be considered with the discussion of specific transducers.

The readout is the major factor in every measurement. Although the sensing element will determine whether a quantity can be sensed, the readout must be able to detect the sensor output or no measurement can be made. For example if a pressure transducer puts out

25 millivolts at 0.01 psi, what is the lowest pressure that can be read? The answer is of course a matter of how low a voltage can be measured. Although, the present course is mainly concerned with fluid mechanics measurements, the first subject must be the readout system.

C. Observation, Readout and Record.- In any scientific undertaking the first step is to observe. Before undertaking a measurement it is equally necessary to observe. In fluid mechanics visual observation is usually the first step. In both liquids and in gases it is a good idea to first try to visualize the flow patterns before making a measurement. Visualization can be made in many ways, such as the introduction of smoke or dye into a fluid. A recent technique for water is to use hydrogen bubbles as tracers. One of the simplest techniques is to employ tufts of flags of string to indicate the direction of flow. Equally important are the many possible techniques that have been developed to indicate flow effects along a surface. Lamp black is a common material employed to indicate regions of large and small shear. Surface wetting and evaporation indicators are good methods of visually observing the mass transfer at a surface. Colora changes are employed for indicating diffusion over surfaces, such as that used in indicating acid and base solutions by a change of paper color from blue to pink.

The present course is mainly concerned with the physical measurement, so that no detailed consideration of flow visualization as such will be made. Specific areas, such as Schleren optics, will deal somewhat with flow visualization. The present area must consider mainly the basic elements outlined in figure 1.1.

For the Readout System, which it appears must be selected at the same time as the sensing element, we must consider all possible types. The different types of readout systems will be covered in detail in the second chapter, even before the transducer concepts are considered. The readout may be considered a black box into which a signal proportional to the quantity to be measured is put. The output of the black box is in some form that can be read visually. In all common

readout systems the output is a physical movement which is calibrated to be sensed by the eye. Some special cases might be a change in color to measure temperature or the newer voltmeters which actually print out numbers. However, the basic system that will be found in the laboratory is still a physical movement, such as a meter. All electrical meters depend on a mechanical linkage to give a reading on a physical scale. Only the cathode-ray tube obtains its deflection by pure electrical means. Even the digital voltmeters depend on some form of mechanical switch to produce the direct reading numbers. In general then, all readout systems are in the final step reduced to roughly three types of physical quantities.

1. A Linear Displacement.
2. An Angular Displacement
3. A Numerical Count

Philosophically, man has only one quantitative sense, that of sight, and this sense requires special training. Thus, the final readings are produced by some kind of mechanical link to render the result readable to the eye.

A study of the design instruments, as such, must devote a good deal of time to the problems of mechanical readouts. The best systems are those with no friction. Unfortunately, mechanical movement does not occur without friction, so the next best approach is an instrument with minimum friction. One means of minimizing friction is to restrict the movement of the mecahnical readout. This minimum movement requirement leads directly to the concept of a null system. For example: the beam balance can be made very sensitive by employing knife edge bearings to minimize friction and also returning the final reading to its original null position. By employing a null systems, such as the beam balance, large magnitude quantities can be measured by indicators that can only detect a small fraction of the actual magnitude. (i.e. The beam balance may easily measure hundreds of grams, while scale deflections marked on its scale are in millionth of a gram.)

The Advantages of a Null System are:

No non-linear effect are introduced due to a change in the equilibrium position of the indicator.

Forces are in balance the same as before the measurement began, so there is less likelyhood of disturbing the quantity being measured.

The final null detector can be made much more sensitive than the magnitude of the quantity measured.

The disadvantages of null systems are:

Requires a mechanical adjust, which is less convenient than a direct reading.

The cost of a null system will in general be greater than the simplier direct reading instrument.

The most accurate measurements will almost always be made with some form of a null system.

Modern readout systems will almost all employ some form of Electronics. The basic requirement for the research engineer employing electronics will not go beyond ohms law, E=IR, and some of the simple resistor current-voltage rules. The advantages of electrical and electronic techniques are impressive:

1. Speed of Response
2. Versatility
3. Economics
4. Sensitivity
5. Recording
6. Transmitting

The main disadvantages have to do with the abilities of the research personal to understand and properly operate the instrument.

D. The Starting Point- Standards and Calibration,- Before a measurement can be made, some agreede unit must be assigned to the quantity to be measured. In this day and age there is usually no question to the units, other than an inmaterial selection of whether metric or English measuring units are to be used. The next step is to setup the measuring system so that its output can be related to the required units. If two or

more readout instruments are required it is extremely important that they agree in the final result. For example; if two electrical readouts are used to evaluate voltage and current, they must be so related that ohms law (where it applies) can be checked. Thus, the major step in setting up an experiment is to establish standards and aline the measuring system to meet the standards.

The National Bureau of Standards has the task of maintaining standards for the United States. All standards are defined in terms of three basic standards; length (meter), time (second) and mass(kilogram). All other physical quantities, such as electrical values, can be derived from these three standards. The time standard has been greatly increased in accuracy in recent years, inorder to meet the requirements of space exploration applications. Figure 1.2 shows, for example the improvements in the accuracy of the U.S. frequency standard over the last forty years.[1]

Research Laboratories maintain a set of secondary standards, which are traceable to the Bureau of Standards. The degree of quality employed in the secondary standards will, of course, be determined by the accuracy of measurements required. Once the readout instruments are calibrated with respect to a laboratory standard, the sensing element must be calibrated with respect to the quantity it measures. If the sensing element is to measure temperature, it must be placed in a know temperature and the readout recorded as a function of temperature. This requires that a standard for temperature be present in the laboratory. Likewise calibration standards must be established for each quantity. That is measured, such as pressure, velocity, length, density, etc. Density, for example might be obtained indirectly from other standards. The establishment of a means of calibrating an instrument for use in an unknown flow can, and usually does, require many more hours of effort than that required for the final measurement.

---

[1]Powell, R.C.; Accuracy in electrical and radio measurements and calibrations, D65. NBS tech. note No. 262-A, 1965

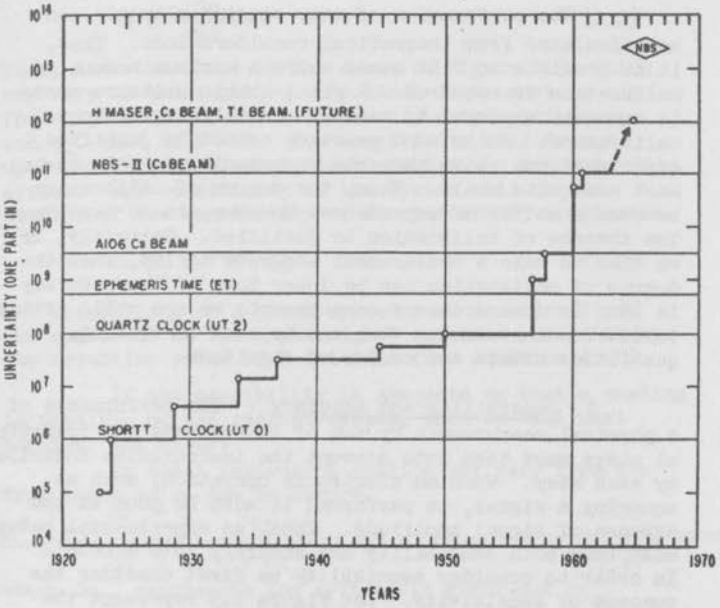

Figure 1.2 - IMPROVEMENTS IN THE ACCURACY OF THE U.S. FREQUENCY STANDARD (USFS)

The performance of many sensing elements can be calculated from theoretical considerations. Thus, it is possible to find cases where a minimum amount of calibration is required. A pitot-static pressure probe is commonly employed to measure air velocity without calibration. While such practice cannot be justified, experience has shown that the uncertainty in this instrument are quite small. Thus, the degree of calibration becomes a matter of experience. However, in no case can the absence of calibration be justified. Certainly, if we wish to make a measurement accurate to 10%, then the degree of calibration can be lower than if the accuracy is 1%. In some areas of measurements we are still trying to develop instruments that can be used to evaluate quantities within one oreder of magnitude.

E. Sensibility and Accuracy.- The performance of a physical measurement by use of instruments and operational steps must take into account the inaccuracies contributed by each step. When an electronic operation, such as squaring a signal, is performed it must be done at the expense of signal amplitude. Thus, an experimental setup must take both sensibility and accuracy into account. In order to consider sensibility we first consider the concept of sensitivity. Let Figure 1.3 represent the relation, between instrument input and output.

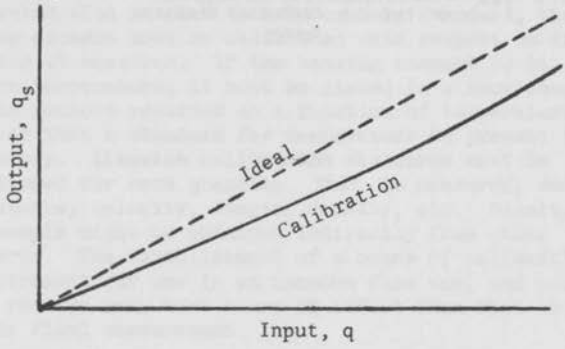

Figure 1.3 Relation Between Input and Output of An Instrument.

The overall sensitivity S is defined as

$$S \equiv \frac{dq_s}{dq} \qquad (1.1)$$

Thus, S is the slope of the curve of figure 1.3, which may vary as the input, q. An ideal instrument is one for which a one to one relationship exists between q and q_s, that is S = 1. The sensitivity will depend upon the sensing element, transmission and readout system. The sensitivity of the system will be the product of the sensitivity of the individual components.

$$S = S_1 S_2 \cdots S_n \qquad (1.2)$$

The sensibility of a given system must consider first the magnitude of the input signal and then reduce it by the resulting value of S obtained from equation (1.2).

If the sensibility is adequate so that a reading is possible on the readout system, then we will next consider the errors.

An ideal instrument reading may vary from the true input value due to errors.

$$\Delta q_s = q_s - q_{true} \qquad (1.3)$$

Instrument errors are divided into random and systematic errors.

$$\Delta q_s = \Delta q_{ss} + \Delta q_{sr} \qquad (1.4)$$

where Δq_{ss} represents the systematic error and Δq_{sr} represents the random error. Random errors are by definition equal likely of being positive or negative. Thus, the average of a large number of measurements should reduce the random errors to zero. Random errors are caused by: scale interpolation on the part of the observer for both calibration and measurements; single events which cause physical effects in the instruments (such as friction, temperature fluctuations, voltage fluctuations, etc.).

Systematic errors are defined as definite effects that are repeatable under a given set of conditions. Typical systematic errors arise from such things as: Scale errors which arise from calibration or shifts of scale due to damage or over extension of the readout mechanism; Environmental errors which arise from such varables as temperature (could cause an expansion within the instrument) or humidity; interaction of the

sensing element with the quantity being measured and response of the sensing element to quantities other than the one being measured: Dynamic errors which arise because the instrument cannot follow the speed of the change in the quantity being measured. In all cases it is possible to correct for systematic errors through calibration, control and adequate calculation of environmental variables. Proper understanding of the dynamics response of the system can make it possible to either avoid measurement where the instrument does no respond of correct for the response. Interaction between the sensing element and the quantity being measured can be predicted and corrected, for if the physics of the sensing element is completely understood. The correction for systematic errors can be presented as a quantity k that is subtracted algebracally from the final readings, q_s

$$X = q_s - k \qquad (1.5)$$

The value of k will in general be a function of q_s although for some systematic errors it may be a simple constant.

The accuracy of a measurement may now be defined as

$$1 - \frac{|\Delta q_{ss}|}{q_s} \qquad (1.6)$$

The absolute value of Δq_{ss} is used in order to keep the accuracy less than or equal to unity. Note that instrument errors may vary with q_s, so that various conventions may be used to specify the accuracy of a given instrument. Two modern conventions are to state accuracy in terms of the local reading, q_s. or in terms of the full scale value of, q_s. For the local reading case, shown in Figure 1.4 the accuracy remains the same at all values of q_s. For the full scale case the accuracy decreases as q_s decreases. For most meters the b) case is found to be true, so that it is desirable to measure at the full scale value of the meter at all times. Note that the accuracy is dependent on the systematic errors only.

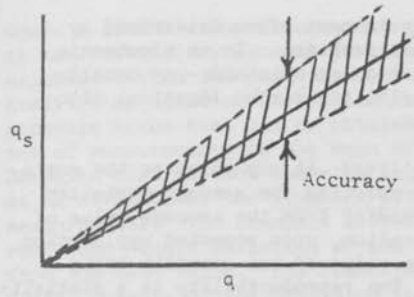

a) Local Reading

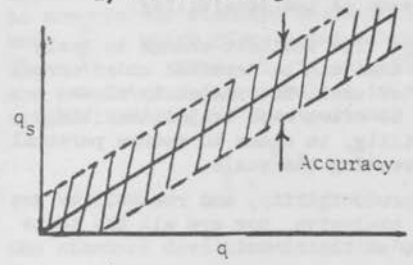

b) Full Scale

Figure 1.4.- Accuracy of an Instrument.

The random errors enter into the precision of a measurement, but not into the accuracy of the instrument. The terms which are employed to discribe instrument performance are:

Range: A statement of the maximum and minimun values of the scale indication, in units of the variable being measured.

Span: The absolute value of the algebraic difference between the maximum and minimum values of the scale indication, in units of the variable being measured.

Sensibility: The smallest change in the variable that can be detected reliably by the instrument. In mechanical readouts,

sensibility is most often determined by backlash and friction. In an electronic instrument such as a cathode-ray oscilloscope, sensibility may be identical with readability.

Reproducibility: At any point on the scale, a term representing the average deviation of scale reading from the average value of scale indication, upon repeated application of the same value of the quantity being measured. The reproducibility is a statistical quantity, and its numerical value is often the same as the sensibility.

Readability: The smallest change in scale indication that can be detected under normal conditions of use. The readabity of an instrument is often made better than its reproducibility, in order to reduce personal errors in reading the scale.

The sensibility, reproducibility, and readability are not always mutually exclusive, nor are all the terms always applicable to an instrument.

F. Statistics of Measurements.- In every measurement we must always seek to define the true value of a quantity. If a set of n readings X_1, X_2, X_3, ...X_i, are made, (free of systematic errors) then these readings must have a mean value which approaches the true value

$$\lim_{n \to \infty} \sum_{i=1}^{n} \frac{X_i}{n} = q \qquad (1.7)$$

The main problem will be to form an estimate of q from a limited number of measurements. In practice it has been found that random errors vary around the true value by a curve defined by the Gaussian Distribution Function

$$y(x) = ke^{-h^2x^2} \qquad (1.8)$$

where x is the error in a measurement X, $y(x)$ is the probability density function, and h is associated with the percision of the measurement. Analysis of equation (1.8) will show that the most probable value that can be obtained from a finite set of measurements is the mean of the set. The Gaussian distribution can also be employed to arrive at an estimate of the standard deviation of the measurements. The standard deviation is defined as root-mean-square deviation of the average measurement from the mean value. The standard deviation is a useful measure of the precision index of a set of measurements. The following procedure can be applied to compute the standard deviation. Choose an estimated mean $\overline{X}$, which gives a set of estimated deviations $(X_i - \overline{X})$ Since $\overline{X}$ is selected, the deviations are tabulated and are smaller in magnitude than the original readings. The true mean is

$$\overline{X} = \frac{\sum_{i=1}^{n}(X_i - \overline{X})}{n} + \overline{X} \qquad (1.9)$$

the standard deviation is given by

$$\sigma^2 = \frac{\sum_{i=1}^{n}(X_i - \overline{X})^2}{n} - (X - \overline{X})^2 \qquad (1.10)$$

More detailed definitions of, such quantities, as the most probable value and its standard deviation, are to be found in the literature.

Least Squares Curve Fitting.- In the previous discussion we were concerned with the best values for a single quantity. For many measurements, particularly in calibrations, two physical quantities x and y must be related. The present discussion is for the case where a linear relation $y = ax + b$, is known to exist

between the two quantities. By some means we must determine the best value of a and b for a given set of experimental values, x_i and y_i. To simplify the problem the assumption is made that errors occur only in the measurement of y.

The error or y deviation for the point $(x_i\ y_i)$ is

$$\Delta y_i = y_i - a\,x_i - b \tag{1.11}$$

The best estimate of the true value is that value that minimizes the standard deviation. Thus, we seek the value of a and b that minimize the sum of the squares of the y-deviation.

$$\sum_{i=1}^{n} (y_i - ax_i - b)^2 = \text{minimum} \tag{1.12}$$

Setting the partial derivatives of equation (1.12) with respect to a and b equal to zero and solving for a and b will give the required minimum. With respect to a

$$\sum_{i=1}^{n} x_i y_i - a \sum_{i=1}^{n} x_i^2 - b \sum_{i=1}^{n} x_i = 0 \tag{1.13}$$

with respect to b

$$\sum_{i=1}^{n} y_i - a \sum_{i=1}^{n} x_i - nb = 0 \tag{1.14}$$

Thus

$$a = \frac{n\Sigma x_i y_i - \Sigma x_i \Sigma y_i}{n\Sigma x_i^2 - \Sigma x_i \Sigma x_i} \qquad b = \frac{\Sigma x_i^2 \Sigma y_i - \Sigma x_i \Sigma x_i y_i}{n\Sigma x_i^2 - \Sigma x_i \Sigma x_i} \tag{1.15}$$

If b is known to be zero, then

$$a = \frac{\Sigma x_i y_i}{\Sigma x_i^2} \tag{1.16}$$

The standard deviation of the y measurement is

$$\sigma_y = \sqrt{\frac{\sum_{i=1}^{n} (y_i - a\,x_i - b)^2}{n}} \tag{1.17}$$

The standard deviation of the parameter a is

$$\sigma_a = \sqrt{\frac{n}{n\Sigma x_i^2 - \Sigma x_i \Sigma x_i}}\ \sigma_y \qquad (1.18)$$

The standard deviation of the parameter b is

$$\sigma_b = \sqrt{\frac{\Sigma x_i^2}{n\Sigma x_i^2 - \Sigma x_i \Sigma x_i}}\ \sigma_y \qquad (1.19)$$

and for b = 0

$$\sigma_a = \frac{\sigma_y}{\sqrt{\Sigma x_i^2}} \qquad (1.20)$$

Specification of errors.- Many engineering measurements are of the single-sample type, where a distribution of errors is not determined. Kline and McClintock[1] propose that uncertainty interval based on specific odds.

$$m \pm w \text{ (b to 1)}$$

where m is the reading (arithmetic mean of the observed reading), w is the uncertainty interval, and b is the odds. As an example

pressure = 50.2 ± 0.5 psia(20 to 1)

This states that the best value for the pressure is believed to be 50.2 psia and the odds are 20 to 1 that the true value lies within ±0.5 psia of this best estimate. This is a statement of the experimenters experience.

The error in a given experiment may depend on several measurements. Kline and McClintock compute the most likely error in the resultant quantity, R, as a linear function of the n independent variables by the following relation

$$w_R = \left[\left(\frac{\partial R}{\partial V_1} w_1\right)^2 + \left(\frac{\partial R}{\partial V_2} w_2\right)^2 + \cdots + \left(\frac{\partial R}{\partial V_n} w_n\right)^2\right]^{\frac{1}{2}} \qquad (1.21)$$

Equation (1.21) is also of specific value in evaluation of the accuracy required in each individual measurement, v_n, inorder to obtain a given overall accuracy for the value R.

---

[1] Kline, S.J., and McClintock, F.A.; Describing uncertainties in single-sample experiments. ASME Mech. Engr. p.3, 1953.

CHAPTER II
READOUT CONCEPTS

The discussion of Chapter I pointed out that the final stage of readout of almost every instrument is a mechanical link. However, for the present chapter we will consider readout systems from a standpoint of what is being measured. This means that meters used in electrical measurements are considered as part of the section on electrical readouts. At the outset the concepts of certain classes of measuring instruments and principles are considered, without specific reference to a particular make of instrument. There are of course many special readout instruments designed for a specific readout application. No attempt is made to survey the specific application, nor to proceed beyond the fundamental concepts. In modern fluid mechanics research a great number of electrical measuring instruments are employed. Mechanical and optical instruments also find many applications in fluid mechanics measurements.

A. Electrical Readout.- The use of electrical readout systems in experimental measurements is increasing each year. Simple measurements of such quantities as pressure and temperature were exclusively mechanical readouts a few years ago. Now both pressure and temperature, through transducers, are quite commonly measured with electrical readout equipment. Thus, electrical systems are a major part of fluid measurements. The section on electrical readout is divided into three parts; first the direct current quantities of voltage, current and resistance are covered; second the alternating quantities of voltage and current are covered; and last the concepts of automatic recording with electronic systems are reviewed.

Direct Current Measurements.- There are six electrical quantities which enter into electrical measurements. (1) charge or quantity of electricity; (2)current; (3) potential difference, or electromotive force; (4) resistance; (5) capacitance; and (6) induction. The first four quantities appear in direct current type measurements. Of the four, current, potential difference and resistance are of major use in fluid mechanic measurements. The basic instrument for measuring direct current is the galvanometer. The principle of operation of a

galvanometer requires the interaction of two magnetic fields, one of which corresponds to the current to be measured. The current produces a magnetic field which interacts with a fixed magnetic field to produce a displacing torque. The displacing torque is usually restored by the action of an elastic mechanical linkage. The modern d-c galvanometer is usually of the d'Arsonval type.

The moving-coil d'Arsonval galvanometer employs a coil (usually rectangular in shape) to carry the current. The coil, which may contain any number of turns is free to rotate about its vertical axis.

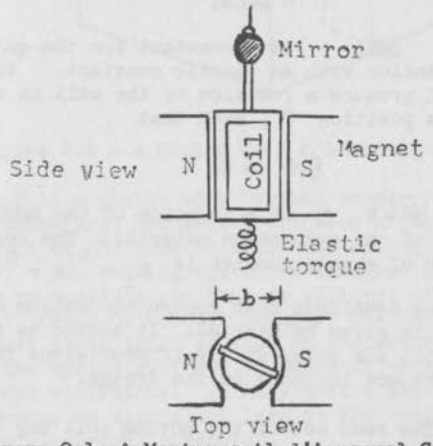

Figure 2.1- A Moving coil d'Arsonval Galvanometer

Figure 2.1 is a sketch of a typical galvanometer arrangement. The coil is allowed to move in a radial path within the horizontal magnetic field of a permanent magnet. Current through the coil causes the coil to rotate. The rotation is opposed by the elastic torque of the supporting suspension. For very sensitive galvanometers the restoring torque is usually supplied by torsion of a taunt wire used to support the coil. For commercial meters the torque is supplied by a hair spring.

The force acting on a vertical element ($d\ell$) of wire carrying a current (i) in a uniform radial horizontal field B is

$$dF = iBdl \tag{2.1}$$

For a length L of the vertical side of the coil and N turns of wire in the coil, the force acting on the coil side is

$$F = BiLN \tag{2.2}$$

and for a coil of width b the total turning moment (torque) is

$$\tau = BNLbi \tag{2.3}$$

where now $BNLb$ is a constant for the galvanometer. For a suspension with an elastic constant the current torque will produce a rotation of the coil to an equilibrium position θ, such that

$$\xi\theta = Gi \tag{2.4}$$

where $G = BNLb$. ξ is a function of the modulus of elasticity of the suspension material. The current sensitivity of a galvanometer is $S_i = \theta/i = G/\xi$.

The detailed equations that govern the motion of galvanometers is given by Harris[1]. It should be obvious that the coil can swing wildly if provisions for clamping are not included in the design.

The read out of the moving coil may be a light beam reflected from a mirror mounted on the suspension, or in the case of a meter a pointer is mounted on the coil to indicate directly the rotation of the coil.

---

[1] Harris, F. K.: Electrical Measurements. Wiley and Son, N. Y. (1962)

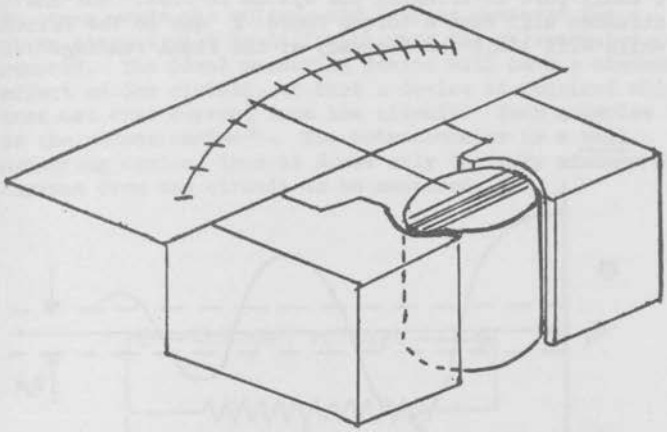

Figure 2.2 - A Moving Coil d'Arsonval type meter

Figure 2.2 is a sketch of a typical commercial d'Arsonval galvanometer. Mechanical friction arises in meters as a result of the need to mount the moving coil in bearings, The bearing system is designed as near frictionless as possible, so that it will not affect the action of torque or counter torque. The instrument spring must be designed so that no inelastic yield can occur. The spring must not be magnetic or change with temperature variations. In many meters the spring may also serve as an electrical lead to the coil, so it must be a good electrical conductor.

In the absence of damping the swinging coil oscillates with a simple harmonic motion about the equilibrium position. Details on the damping of galvanometers are given by Harris[1] and can not be covered in the present discussion. However, some comments on one form of dissipative damping, that of solid friction, are

---

[1] Ibid

necessary. Solid friction is always unavoidably present in the instruments bearings, thus it must play at least a small part in bringing the system to rest. The instrument will have a torque force F due to the friction which will limit the accuracy of the final reading.

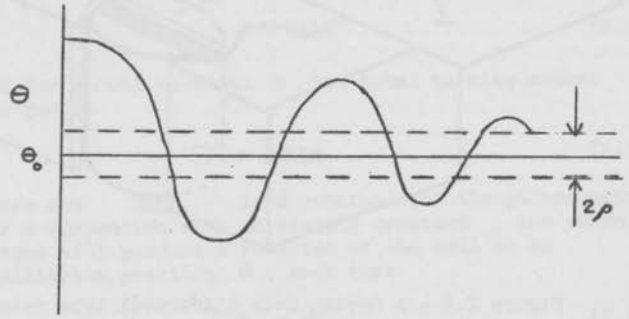

Figure 2.3 - Effect of friction on the reading of a meter

Consider the sketch in figure 2.3 where a galvanometer is oscillating around the equilibrium reading. We assume the oscillation is damped by external forces so that it approached its final reading θ_o . However, once the momentum of the oscillation is smaller than the friction force the movement stops. The angle ρ that corresponds to the friction "dead zone" will be $\pm\rho = \pm\frac{F}{\varepsilon}$. Thus, an individual reading of the meter can only be as good as the error due to the friction ρ . The error due to friction can be either positive or negative, so it represents a random error. This frictional error can be overcome by taking many readings after the system is set into oscillation and allowed to return to equilibrium. It is not uncommon to see an experimenter tapping on a meter to insure that a proper statistical reading is obtained.

The galvanometer requires a flow of current to produce a deflection. Thus, when a galvanometer is employed in a circuit it has a direct effect on the circuit. In other words the voltage and current measured for a given circuit will be different when the galvanometer is removed. The ideal measuring device will have a minimum effect on the circuit, so that a device is required which does not draw current from the circuit. Such a device is the potentiometer[1]. The potentiometer is a null measuring device, thus it draws only the very minimum of current from the circuit to be measured.

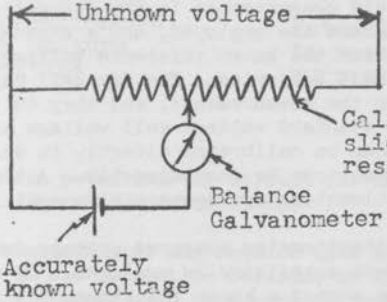

Figure 2.4 - Simple potentiometer

Figure 2.4 shows the simple porentiometer circuit. In order to understand the circuit one need only know the principle of voltage division by a resistor. Consider the current flowing through a resistor, such as the slide wire resistor of Figure 2.4. The current is constant in

[1] The potentiometer principle was first described by Poggendoff, Am. Phys. u. Chemie, Vol. 54 (1841), and is refered to as Poggendoff's compensation method.

the resistor so that the voltage drop to any point in the resistor is a function of the resistance according to Ohm's law, E = IR. Thus, as the slide wire is moved along the resistor the voltage drop increases. A known voltage source and a balance galvanometer is placed in the slider arm circuit. When the unknown voltage drop across the resistor matches the voltage from the known voltage source the galvanometer is in balance. In this way no current flows from the measuring circuit to the galvanometer. A sensitivity galvanometer is employed to indicate the balance or null point. From an accurate knowledge of the potentiometer components the unknown voltage can be determined. Very accurate commercial potentiometers are employed as secondary laboratory voltage standards. A special standard cell is employed as the known voltage source. For field measurements in the laboratory, portable potentiometers are employed, and a standard voltage cell is used to set the known reference voltage of simple commercial dry cell batteries. The dry cell batteries are employed for the measurements, and they in turn are adjusted to the standard voltage cell voltage as required. The slide wire can be calibrated directly in volts, so that the instrument can be read directly. Automatic self-balancing potentiometers are commercially available.

The potentiometer measures voltage drop, thus to measure current a resistor is employed. By measuring the voltage drop across a known resistance the current can be calculated from Ohm's law $I = \frac{E}{R}$. Figure 2.5 shows a typical potentiometer circuit that might be employed to measure an unknown resistance. A standard type resistor is employed with a potentiometer to measure the current flowing in the circuit. The voltage drop across the unknown resistor is measured with the potentiometer, and the resistance is computed from Ohm's law $R = \frac{E}{I}$.

To correctly measure resistance it must be determined that the current in the circuit does not affect the resistance. In general, current flowing through a conductor will heat the conductor and produce a change in resistance. As a result it is desirable to measure the resistance with a minimum amount of current.

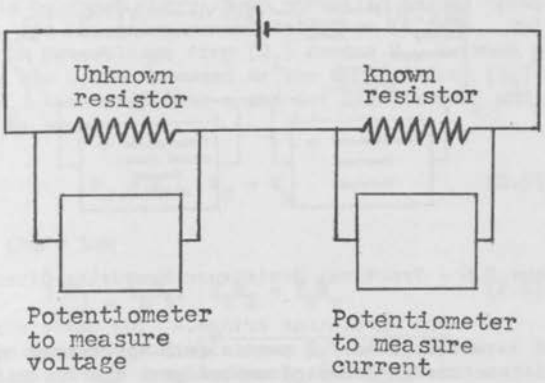

Figure 2.5 - A potentiometer circuit for measuring current and resistance

An accurate measurement may require that a curve of resistance versus current be obtained so that the results can be extrapolated to a zero current.

A practical potentiometer circuit for use with several resistance varying transducers is shown in Figure 2.6. This circuit is employed for steady state measurement such as ion beam studies with the hot wire calorimeter. In general, a potentiometer circuit would not be used in high frequency measurements. More will be said about high frequency effects in the section on alternating current measurements.

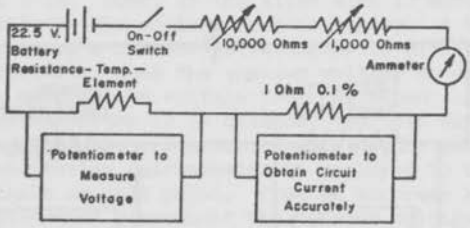

Figure 2.6 - Practical Resistance Measuring Circuit.

The Wheatstone bridge.- The basic circuit that is widely used for precision measurements of resistance is the Wheatstone bridge. The circuit diagram of a Wheatstone bridge is shown in figure 2.7. R_1, R_2 and R_3 are known precision resistors, and R_x is

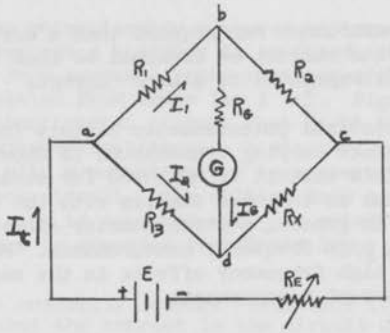

Figure 2.7.- Schematic Wheatstone bridge circuit.

the resistance-temperature element. The galvanometer G, with its resistance R_G, is inserted across terminals b and d to indicate the condition of balance. When the bridge is balanced there is no potential across terminals bd, and the galvanometer defection is zero. This means that the voltage drop (E_1) across R_1, between p points a and b, is the same as the voltage drop (E_3) across R_3, between points a and d. Likewise, E_2 and E_x must be equal.

$$E_1 = E_3, \quad E_2 = E_x \tag{2.5}$$

or from Ohm's law

$$I_1R_1 = I_2R_3, \quad I_1R_2 = I_2R_x \tag{2.6}$$

Dividing the voltage drop across R_1 and R_3 by the respective voltage drop across R_2 and R_x gives

$$\frac{I_1R_1}{I_1R_2} = \frac{I_2R_3}{I_2R_x} \text{ or } \frac{R_1}{R_2} = \frac{R_3}{R_x} \tag{2.7}$$

Thus,

$$R_x = \frac{R_2R_3}{R_1} \tag{2.8}$$

When the bridge is balanced. The current through Rx is

$$I_2 = I_t \frac{\left(R_1 \right)}{R_3 + R_1} \tag{2.9}$$

Equations (2.8) and (2.9) are used extensively in resistance-temperature applications.

For the measurement of an unknown resistance, one of the precision resistors, say R_2, is exchanged with other known resistors until the bridge is

balanced. Commercial Wheatstone bridge units are available to make the measurement of unknown resistance quite easy. In heat transfer applications of the Wheatstone bridge the "cold" resistance of the element is usually determined by the potentiometer method, and then inserted into the bridge. The current I_t of the bridge is increased until Joulean heating increases the resistance (temperature) of the element sufficiently to balance the bridge. The resistors R_1, R_2, and R_3 are able to pass a greater amount of current than the sensing element without becoming heated, so that only the resistance of the element changes with the current. By maintaining the bridge at balance the temperature of the element is kept at a constant elevated temperature. Pre-selection of the resistors R_1, R_2, and R_3 determine exactly the temperature at which the element is operated.

The current flowing through the balance detector galvanometer at time of unbalance will be

$$I_G = \frac{I_t\,(R_2R_3 - R_1R_x)}{R_G(R_1 + R_2 + R_3 + R_x) + (R_2 + R_x)(R_1 + R_3)} \tag{2.10}$$

and the total current into the bridge is approximately

$$I_t = \frac{E}{R_B + \dfrac{(R_1+R_2)(R_3+R_x)}{(R_1+R_2+R_3+R_x)}} \tag{2.11}$$

The bridge sensitivity expressed in terms of the unbalance voltage per volt applied to the bridge is

$$S_e = \frac{e}{E} = \frac{(\gamma)\left(\dfrac{\Delta R_x}{R_x}\right)}{(\gamma+1)^2} \tag{2.12}$$

and in terms of unbalance current per volt applied to the bridge

$$S_I = \frac{I_G}{E} = \frac{\dfrac{\Delta R_x}{R_x}}{\dfrac{R_G}{\gamma(\gamma+1)^2} + R_1 + R_2 + R_3 + R_x} \tag{2.13}$$

where $\tau = (R_2/R_1)$.

For accurate measurements of small changes in resistance, which might be encountered in resistance-temperature calibrations, the high resolution Wheatstone bridge shown in figure 2.8 may be employed.[1] Each of the resistors except R_3 was made from a parallel combination of several 1% deposited carbon resistors. R_3 is a 0.1% linearity multi-turn variable resistor. The particular bridge reported on had resistor values that permitted spanning a 2% range around 129 ohms with a resolution of 0.002%. The variation in balance condition with R_3 is

$$\frac{X(R_3)}{X(0)} = 1 - \left(\frac{R_1}{R_2}\right) \sum_{i=1}^{\infty} \left[-\frac{R_3}{(R_1+R_2)} \right]^i \qquad (2.14)$$

If R_2 is sufficiently larger than R_3 this series can be terminated after one or two terms, and an approximately linear variation of balance with R_3 is obtained.

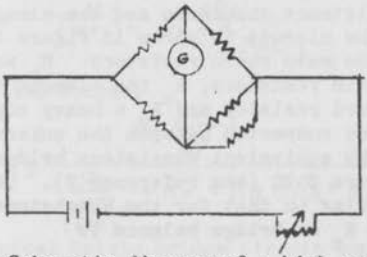

Figure 2.8 - Schematic diagram of a high resolution Wheatstone bridge.

The Kelvin bridge is a specialized version of the Wheatstone bridge. It is so constructed to reduce the effects of lead and contact resistance. This is done by effectively placing relatively high resistance ratio

---

1 McGraw-Hill Encyclopedia of Science and Technology, McGraw-Hill Book Co. N.Y., (1960)

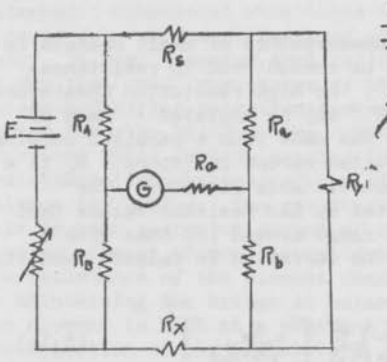

Figure 2.9 - Schematic diagram of Kelvin double bridge.

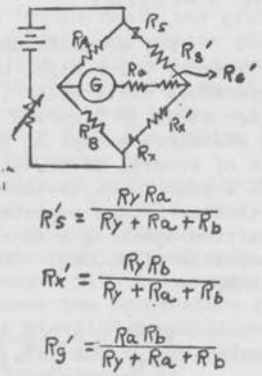

Figure 2.10 - Equivalent Wheatstone bridge circuit.

arms in series with the potential leads and contacts of both the resistance standards and the element to be measured. The circuit is shown in figure 2.9 where R_A and R_B are the main ratio resistors. R_a and R_b the auxiliary ratio resistors, R_x the element to be measured, R_s the standard resistor and R_y a heavy copper yoke of low resistance connected between the unknown and standard resistor. The equivalent Wheatstone bridge circuit is shown in figure 2.10 (see reference 2). Using an analysis similar to that for the Wheatstone bridge, the relation for R_x at bridge balance is

$$R_x = \frac{R_B R_s}{R_A} + R_y\left(\frac{R_b}{R_a + R_b + R_y}\right)\left(\frac{R_B}{R_A} + \frac{R_b}{R_a}\right) \qquad (2.15)$$

---

2 Eklund, K: Rev. Sci. Instr., Vol. 31, (19)

If $\frac{R_B}{R_A} = \frac{R_b}{R_a}$ then the second term of equation (2.15) is zero, and

$$R_X = \frac{R_B}{R_a} R_S \tag{2.16}$$

The Kelvin bridge requires larger total currents than the Wheatstone bridge during the measurements. Care must be taken, however, to insure that the current through the element to be measured does not cause measurable Joulean heating.

The Kelvin bridge sensitivity expressed, as also used for the Wheatstone bridge, in terms of the unbalance voltage per volt applied to the bridge is

$$S_e = \frac{\gamma}{(\gamma+1)^2} \frac{\frac{\Delta R_X}{R_X}}{\frac{R_X}{R_Y}\frac{\gamma}{(\gamma+1)}} \tag{2.17}$$

and for detection current

$$S_I = \frac{E\left(\frac{\Delta R_X}{R_X}\right)}{\frac{R_G}{\frac{\gamma}{(\gamma+1)^2}} + R_A + R_B + R_a + R_b} \tag{2.18}$$

A typical Kelvin bridge circuit employed in hot wire heat loss measurements is described in reference 3. Improvements over both the Wheatstone and Kelvin bridge can be made by the addition of more resistors at the bridge "corners." These circuits become very complex and would only be employed where great precision is required. Bridges used at the National Bureau of Standards [4] for resistance thermometer measurements are

---

3 Lowell, H.H.: NACA TN 2117, (1950)

4 Muller, E.F.: Precision Resistance Thermometry. Temp. Its Meas. and control in Sci. and Ind., Reinholt, N.Y. (1955)

improvements on the Kelvin bridge. An exacting analysis of multiple-bridge circuits for measuring small changes in resistance is reported in reference 5, and should be consulted if the Wheatstone and Kelvin bridges are not accurate enough for a particular application.

---

5 Warshawsky, I: NASA TN 1031 and Rev. Sci. Instr., Vol. 26, (1955)

Alternating Current Measurements - Alternating current measurements can be made in several possible ways. To define a random alternating signal requires more than any single measurement. Thus, several different measuring instruments are often employed. If a sine wave type alternating signal is to be measured only two quantities, frequency and amplitude, are required to completely specify the signal. For the random signal a single frequency has no meaning.

An alternating current may be defined as shown in figure 2.11.

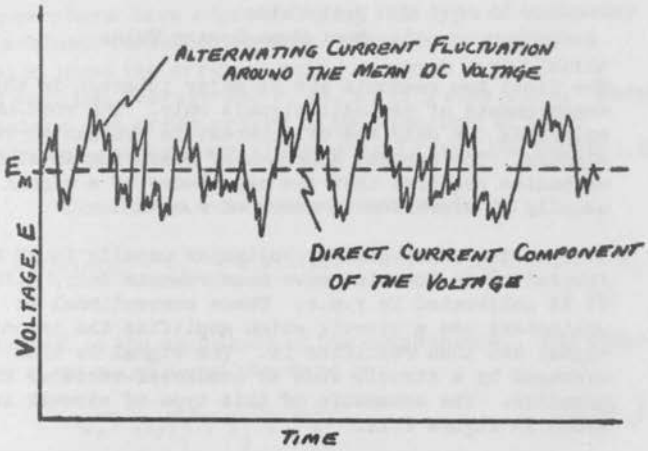

Figure 2.11 - Definition of An Alternating Current

The alternating current is the fluctuation around the direct current component. Thus, a signal may have both a mean and fluctuating part. The direct current measuring instruments are damped so that they can respond only to the dc component, and not to the voltage fluctuations. The dc component is defined by the expression.

$$E_M = \frac{1}{T}\int_0^T E\,dt \qquad (2.18)$$

Thus, the mean of the ac component will correspond to the mean dc voltage. For convenience the ac and dc components are treated separately, so that by definition we look at an ac component and refer to its mean value as zero. In other words we will consider an ac voltage as if it had no dc component in the following discussion.

There are several ways that an alternating current signal may be measured. Typical readouts to be found in the laboratory include:

1. Rectified Mean Value
2. Peak Value
3. Root-Mean-Square Value

The first two readouts are of major interest in the measurements of periodic signals only. The root-mean-square is the only one of interest in evaluating random signals. The present approach of measuring in fluid mechanics requires that the magnitudes of a signal usually be expressed in terms of r.m.s.

The commercial ac voltmeter usually found in the laboratory is for sine wave measurements only, although it is calibrated in r.m.s. These conventional ac voltmeters use a circuit which amplifies the incoming signal and then rectifies it. The signal is then averaged by a circuit such as condenser-resistor in parallel. The schematic of this type of circuit is shown in figure 2.12.

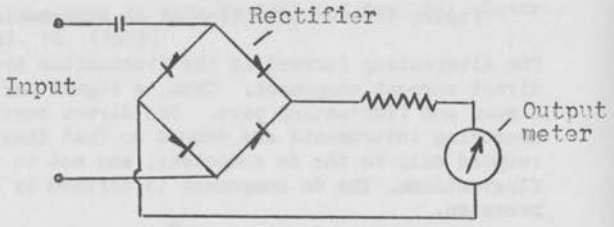

Figure 2.12- Conventional AC voltmeter.

For a sine wave it will be shown that the average is related directly to the r. m.s. by a constant. Thus the meter output of the circuit may be calibrated either as an average or as the r. m. s. of a sine wave. This type of circuit is typical of a great number of commercial ac voltmeters.

Rather than cover the details of the circuit design, the discussion is limited to the ability of the circuit to evaluate a random signal. Several researchers have reported using this type of voltmeter to evaluate turbulent signals. They have suggested that at most the error is only 1.11 which is the factor between the average and r. m. s. of a sine wave. Unfortunately, the error proves to be a function of wave shape and can be many times greater than the factor 1.11.

Consider a complex wave of the form;

$$e = E_1\sin(\omega t + \phi_1) + E_2\sin(2\omega t + \phi_2) + ..E_n\sin(n\omega t + \phi_n) \qquad (2.19)$$

Where E is the amplitude of the components. The effective r. m.s. value of the wave is

$$\sqrt{\overline{e^2}} = \sqrt{E_1^2 + E_2^2 + ..E_n^2} \qquad (2.20)$$

Thus for a pure sine wave

$$\sqrt{\overline{e^2}} = \frac{E}{\sqrt{2}} = 0.707E$$

The ratio between the r. m. s. and the average is .707/.636 = 1.11. Evaluation of E_{AV} for other than a pure sine wave is necessary for the case of a random or turbulent signal. Figure 2.13, shows the effect of considering the second and third harmonics on the relation between average and r. m. s. values. The second harmonic does not lead to large deviations. The harmonic which causes the greatest deviation is the third harmonic. The third harmonic causes a deviation

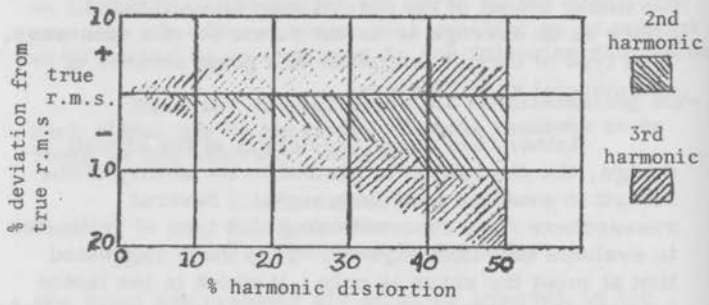

Figure 2.13 - Range of errors due to second and third harmonics in a signal.

of about 33 1/3 per cent of its component percentage. The fifth harmonic can cause a deviation of 20 per cent and the seventh 14.3 per cent of its component percentages.

The analysis demonstrates that the correlation between the average and the r.m.s. can be a strong function of wave shape. For unknown wave shapes a "rule-of-thumb" is that the reading in r.m.s. is no better than one third the total harmonic percentage. Even a filter spectrum instrument which looks at a narrow band of frequencies cannot always be read on an average meter and related directly to the r.m.s. A fluctuation in the amplitude of the frequency out of the filter is equivalent to higher harmonics which can then produce large deviations between average and r.m.s. It was discovered that a particle turbulence signal was greatest affected at the low frequencies and only to a much lesser degree at higher frequencies. However, this may not be generally true, since the "typical" turbulence signal is difficult to define.

There are several possible ways in which a true r.m.s. voltage can be measured. The dynometer, electrostatic voltmeters, and iron vane instruments can

all be made to respond to the r.m.s. value of the wave form. All of these instruments are severely limited in one way or another so that they are of little value for the measurement of the r.m.s. of a turbulent signal. The instruments employed to evaluate r.m.s. of a turbulent signal fall in three classes.

1. a) The electronic r.m.s. meter is based on a parabolic tube or transistor characteristic. This instrument produces a voltage, $e_{out} = Ke_{in}^2$. The average output voltage can be read on a D.C. meter and it will be proportional to the square of the r.m.s. value. The more refined instruments obtained the parabolic transfer characteristic by an approximation with segments from many tubes or transistors. A large number of segments may be employed to keep the errors small.

b) The thermocouple instrument is based on the conversion of electrical energy into thermal energy. The thermal energy is measured through the use of a thermocouple. These instruments can be made to respond to wide ranges of frequency from DC to tens of megecycles. They are, however, susceptible to damage due to overloading, and secondly the low impedance is difficult to match directly to most hot wire circuits.

c) RMS voltmeters are also constructed using various analog computer techniques for multiplying two variables. In this case $e_{out} = e_1 e_2$. The voltage to be measured is fed in as both variables and the average of the output is the square of the r.m.s. value. These multipliers will be considered in the next part of this section.

The electronic r.m.s. meter usually consists of a circuit similar to the average meter circuit shown in figure 2.12 plus an additional rectifier circuit to square the original rectified signal.

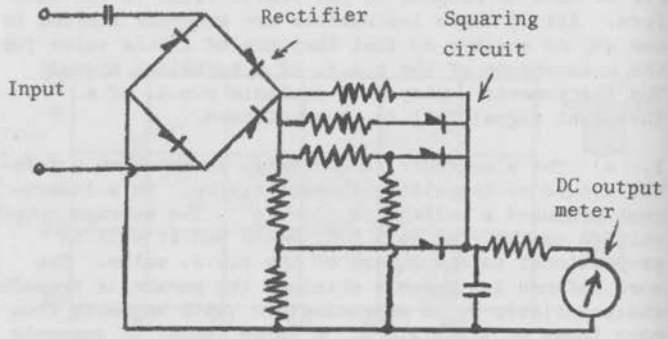

Figure 2.14 - True r.m.s. voltmeter circuit.

Figure 2.14 is a schematic diagram of one type of r.m.s. rectifier circuit. In this circuit the square-law curve is approximated by means of a number o straight line portions. The accuracy of this type of instrument will depend on how well the square curve is approximated. A second factor of importance in some turbulence measurement is the peak or crest factor of the instrument.

The peak factor of a signal is defined as the ratio of the peak value of the signal to its r.m.s. value. The peak factor of a meter is defined as the highest peak factor of signal that the meter can accept without overloading. Peak factors may range from 1 to 10 for commercial r.m.s. meters. To demonstrate the effect of peak factor the idealized rectangular signal shown in figure 2.15 is usually employed, if A is the peak value of the signal, then the r.m.s. value is $A(t/T)^{1/2}$. The peak factor is equal to $(T/t)^{1/2}$.

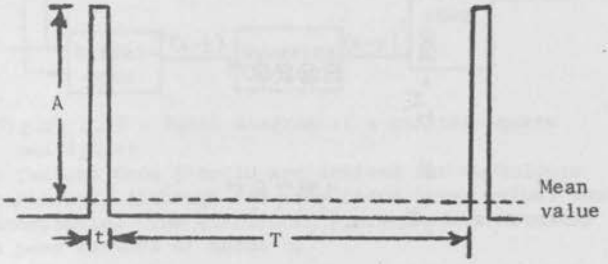

Figure 2.15 - Peak factor representation.

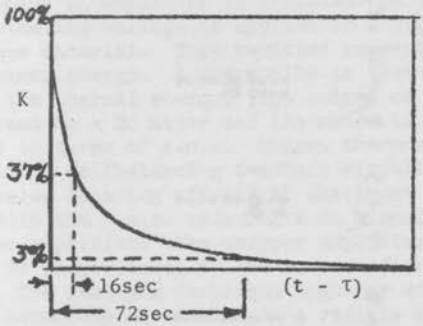

Figure 2.16 - Kernel function for a thermocouple voltmeter.

This means that the criterion as to how far the peaks can be separated and the meter read correctly at full scale depends on the square of the peak factor rather than the peak factor itself. Table 2.I is a comparison of meter readings for a one volt r.m.s. input of different values of

Table 2.I
Readings in Volts

Meter Peak Factor	$T/t = 1$	$T/t = 2$	$T/t = 5$	$T/t = 10$	$T/t = 25$	$T/t = 50$	$T/t = 100$
1	1	.71	.45	.31	.20	.14	.10
2	1	1	.90	.62	.40	.28	.20
3	1	1	1	.93	.60	.42	.30
5	1	1	1	1	1	.70	.50
10	1	1	1	1	1	1	1

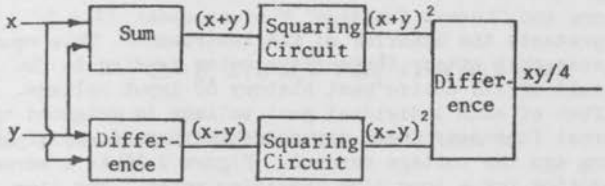

Figure 2.17 - Block diagram of a quarter-square multiplier.

Peak factors from 5 to 10 are desired for turbulence measurements, although for many cases lower values would be acceptable. The electronic r.m.s. meters normally have peak factors of about 5.

For peak factors greater than 5 a thermocouple instrument is used. A typical thermocouple r.m.s. voltmeter would employ an amplifier to increase the input signal. The fluctuating voltage is applied to a highly stable resistance material. This resistor converts the voltage into thermal energy. A thermopile is then used to measure the thermal energy. The output of the thermopile can be read on a DC meter and the meter is calibrated directly in terms of r.m.s. Modern thermocouple meters may employ a selfbalancing feedback circuit in which the r.m.s. value (heating effect) of the input signal is nulled with the r.m.s. value of a dc signal developed by a chopper amplifier. The chopper amplifier output voltage is proportional to the r.m.s. of the AC input signal. The feedback technique together with quick-acting thermocouples results in a rapidly responding meter and a linear voltage scale for r.m.s. rather than the square root scale variation.

For turbulent measurements it may be desirable to have a long time averaging voltmeter. Thus, a quick acting thermocouple system may not be a desirable feature. The relationship between signal voltage e(t) and meter reading m(t), which are expressed as functions of time is

$$m(t) = \int_{-\infty}^{t} K(t-\tau)\, e^2(\tau)\, d\tau \qquad (2.21)$$

where the "Kernal function" K of argument $(t - \tau)$ represents the behavior of the instrument. This equation states that at any instant the meter reading is the result of its entire past history of input voltage. The effect of each individual past voltage is weighted by the kernal function, which expresses the dependency of how long ago the voltage occured. Figure 2.16 is a kernel function for a long time averaging meter. The time interval over which K is substantially different from zero is the averaging time of the instrument. The time constant would be defined much as a hot wire time constant was defined. The point where K has fallen to 37% (or dropped off 63%) of its maximum value corresponds to the instrument time constant.

Equation (2.21) can be further investigated to determine the accuracy of the r.m.s. meter. Let e be a pure sine wave

$$e = E\sin\omega t$$

Then for a true r.m.s. meter

$$\overline{e^2(t)} = \int_{-\infty}^{t} K(\tau-\tau) E^2 \sin^2\omega\tau \, d\tau \qquad (2.22)$$

which may be written as

$$\overline{e^2} = \int_{-\infty}^{\tau} \left[\frac{1}{2}E^2K(t-\tau) - \frac{1}{2}E^2K(t-\tau)\cos 2\omega\tau\right] d\tau \qquad (2.23)$$

The integral of the first term is proportional to the area under the K-curve. The integral of the second term is an error term which vanishes if ω is great enough so that a large number of cycles occur during the time interval over which K is substantially different from zero. For all frequencies satisfying this condition the meter will read correctly, since the area under the K-curve is a fixed quantity. Thus, for low frequency measurements it is important that the "time constant" of the instrument be long. If instead of the pure sine wave, two frequencies were present

$$e = E_1 \sin \omega_1 t + E_2^2 \sin(\omega_2 t + \phi)$$

then it would be found that the error term is

$$\int_{-\infty}^{t} K(t+\tau) E_1 E_2 \left[\cos\{(\omega_1 + \omega_2)(\tau - \phi)\} - \cos\{(\omega_1 + \omega_2)(\tau + \phi)\}\right] d\tau \qquad (2.24)$$

The resultant frequency $(\omega_1 - \omega_2)$ can place a much more restricted requirement on the meter than in the pure sine wave analysis. In particular, for narrow band spectrum analysis where two frequencies are close together the averaging time must be as long as possible.

Special Alternating Current Measurements - Multipliers -

The electronic multiplier is a standard circuit required in analog computers. Slow-speed multipliers usually employ a servomotor-potentiometer technique. Such serve multipliers can be made highly accurate, but their response is limited to 1 or 2 cycles per second. High speed multipliers have been greatly perfected in the last few years, however, they still do not approach the accuracy of the serve system. Although several techniques have been employed in electronic multipliers, it appears that the quarter-square multiplier is the system that has been most fully developed. Figure 2.17 is a block diagram of a typical quarter-square multiplier. Operational amplifiers are employed to obtain the instantaneous values of the sum and the difference of the two signals to be multiplied. The signals are then squared by a circuit, such as shown in figure 2.14. The two squared signals are then summed to give an output

$$e_1 e_2 = \frac{(e_1 + e_2)^2}{4} - \frac{(e_1 - e_2)^2}{4} \qquad (2.25)$$

The term quarter square is derived from the form of equation (2.25).

The frequency response of the quarter-square multipliers have steadily been increased in the past years. Units capable of 4000{000 cycles per second are now commercially available. Most units have good frequency response as far as signal amplitude is concerned. On the other hand the phase shift of the multipliers are more critical. Phase shift is usually troublesome at frequencies above 10,000 cycles. However, for most applications of the multiplier in turbulence research the phase shift at the high frequencies is of minor importance. If the multiplier is used in a spectrum type analysis then phase shift is not of importance.

A multiplier can be used to square an individual signal simply by putting the signal into both inputs. Likewise higher moments of a signal may be obtained by using more multipliers. Once a signal is squared it has a well defined d.c. signal as well as an a.c. signal. Thus when higher moments are obtained with multiplier units the d.c. level must be included and multiplied in the operation. A typical example might be the evaluation of the fourth power of the signal. Since most multipliers multiply both the a.c. and d.c. components, then the first operation is to block any d.c. signal from reaching the first multiplier stage. Out of the first multiplier a d.c. and a.c. signal is obtained which is proportional to the instantaneous square of the signal. This instantaneous square signal is then fed into the two inputs of a second multiplier which multiplier both the d.c. and a.c. components to obtain a signal proportional to the instantaneous fourth power. Note for instance that the instantaneous square signal could not be fed into a true r.m.s. (or mean square) meter to obtain a mean fourth measure, since the true r.m.s. meter blocks the d.c. component and then would rectify an already positive a.c. signal. Although multipliers work with a fixed gain (attentuation) between input and output, it was found from experience that it is best to calibrate the complete bank of multipliers with a sine wave during each set of measurements. The relation between the measured r.m.s. of a sine wave and its mean fourth power is*

$$\overline{e^4} = \frac{3}{2}\left(\sqrt{\overline{e^2}}\right)^4 \qquad (2.26)$$

---

et $e = E\cos\omega t$

then

$$\overline{e^4} = \frac{1}{T}\int_0^T E^4\cos^4\omega t\,dt$$

$$= \frac{E^4\omega}{2\pi}\int_0^{\frac{2\pi}{\omega}} \cos^4\omega t\,dt$$

$$= \frac{E^4}{4} + \frac{E^4}{8}$$

Then using $\sqrt{\overline{e^2}} = E/\sqrt{2}$, equation (2.26) is obtained.

The mean fourth power can be read from the multiplier by a common DC vacuum tube voltmeter. A typical calibration curve obtained by the author for a set of two Philbrick multipliers is shown in figure 2.18.

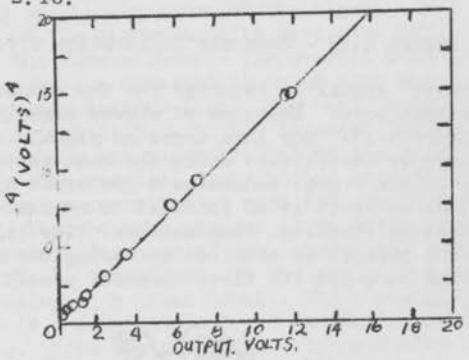

Figure 2.18 - Calibration of a Fourth Power Multiplier

The third power of a signal would be obtained by multiplying the instantaneous mean square with the original.

signal. For this operation the phase shift in the multiplier might be of importance if it occurs at too low a frequency. The calibration of the cube system, or for that matter any odd moment, cannot be done with a pure sine wave. The odd moments are zero for a great number of wave shapes such as sine, triangular, and even a random noise signal. Thus the calibration is usually done with a signal composed of a sine wave and its first harmonic. Firgure 2.19 is a typical circuit designed to calibrate the odd moment multiplier system.

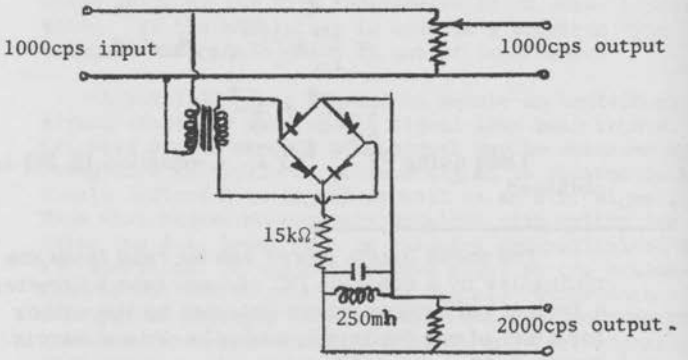

Figure 2.19 - Skewness Calibration Circuit.

A "skewed" signal is required for the odd moments to be other than zero. Examples of skewed signals are shown in figure 2.15. For this types of signal the amplitude is unevenly distributed about the mean value Physically such a signal indicates a preferred direction of fluctuation so it is of interest to evaluate the skewness of turbulent fluctuations. The calibration of the cube circuit is obtained by varing the r.m.s. of the sine wave and its first harmonic according to the relation *

$$\overline{e_1^2 e_2} = \frac{\left(\sqrt{\overline{e_1^2}}\right)^2 \sqrt{\overline{e_2^2}}}{\sqrt{2}} \qquad (2.27)$$

The voltages e_1 and e_2 are fed into one multiplier and

then the output $e_1 e_2$ is multiplied by either e_1 or e_2 to give

$$\overline{e_1^2 e_2} \quad \text{or} \quad \overline{e_1 e_2^2}$$

* For convenience the cosine rather than the sine function is employed in the derivation

Let $e_1 = E_1 \cos\omega t$

$e_2 = E_2 \cos 2\omega t$.

Then

$$\overline{e_1^2 e_2} = \frac{1}{T}\int_0^T e_1^2 e_2 \, d\tau$$

$$= \frac{\omega}{2\pi}\int_0^{\frac{2\pi}{\omega}} [E_1^2 \cos^2\omega t][E_2 \cos 2\omega t]\, dt$$

$$= \frac{\omega E_1^2 E_2}{2}\int_0^{\frac{2\pi}{\omega}} \cos^2\omega t \cos 2\omega t \, dt$$

$$= \frac{E_1^2 E_2}{4}$$

Other types of measurements - The r.m.s. is representative of the magnitude of the random signal, but it tells nothing of the structure of the signal. The measurements of the higher moments give some hint of the structure of the fluctuations. The overall structure of the signal requires a detailed study of both the amplitude and frequency distribution. Two basic measurements are of major interest; that of the spectral distribution of the fluctuations and secondly that of the probability distribution. The spectral distribution is a detailed look at the energy contained at each frequency in the fluctuation. The spectrum appears to be one of the major focal points for much of the theoretical work on turbulence. Thus, techniques for evaluating the spectra have been developed in great detail. The probability distribution is a detailed study of the amplitude of the random signal. From the probability distribution the r.m.s. and all higher moments of the signal can be computed. The probability distribution shows for example such properties as skewness or preferred direction of the

fluctuations.

Spectrum Analysis -

Two methods of studying the frequency distribution of a random signal have been employed. The first obvious approach is to construct a set of filters which pass only a narrow band of frequencies. This narrow band of frequencies can then be examined either by measuring its r.m.s. or any other desired operation. Typical audio frequency spectrometers contain a set of fixed 1/3 octave filters. This means that the filters have mid-frequencies at 1/3 octave distance. In acoustical work there is a set of preferred filter settings which have been standardized, although this is not necessarily of interest in fluid measurements. Electronic filters are also available which allow a selection of any frequency desired.

The second technique of measuring spectra is an analog method. The voltage to be measured modulates a local oscillator output in a balanced modulator circuit. The oscillator operates at a frequency much higher than the frequency to be measured. The balanced modulation causes the local oscillator frequency to be suppressed and only sum and difference frequencies are left in the modulator output circuit. The amplifiers which follow the modulator accept the lower sideband frequency which is in turn read out on a meter. The system is able to select a very narrow band of frequencies to examine. Secondly, a continuous spectra may be measured with no need to select specific frequencies. Both techniques of measuring frequencies have been made automatic so that direct plots of local r.m.s. versus frequency can be obtained.

The specific analysis of a spectrum from measurements with either filters or the analog technique is basically the same. Thus, the present discussion may apply to either type of spectrum analysis. The spectrum is normally defined in terms of the energy density rather than in terms of the r.m.s. This means that the mean square of the velocity is employed. A spectra function is defined from the relation

$$\overline{e^2} = \int_0^\infty \overline{e_f^2}\, F(f)\, df \qquad (2.28)$$

The spectrum energy density function F(f), or F(n) as is sometimes employed, is just the requirement that the sum of the individual frequencies add up to the total $\overline{e^2}$. The term $\overline{e_f^2}$ is the mean square of the voltage fluctuations in the unit band width at frequency f . Thus, $\overline{e_f^2}\, F(f)$ is the contribution from the frequency band f to $f+df$. The physical evaluation of F(f) requires the measurement of $\overline{e^2}_{,e}$ and $\overline{e^2}$ The measurement of $\overline{e_f^2}$ requires two bits of information; one, the mean square of the output of either a filter or the analog spectrum analizer, and two, the effective band width of the filter or analizer. The effective band width is necessary to reduce the measurement to a unit band width. The definition of the effective band width is the width of a rectangle of the same area as that of the actual filter. Figure 2.20 shows typical filter characteristics for both a 1/3 octave filter and an analog equivalent filter. Since the mean square or power spectrum is of importance, the filter characteristics must be plotted as gain squared. The

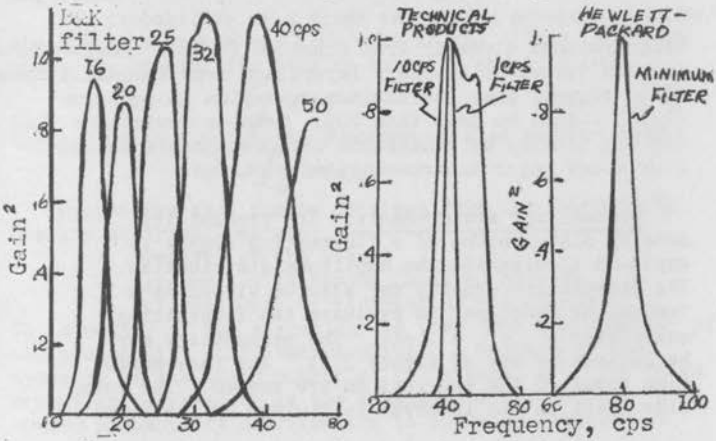

Figure 2.20 - Filter characteristics of spectrum analizers.

area contained within the filter is graphically integrated and a rectangle of the same area and a maximum gain ratio of one is determined. The width of the rectangle becomes the effective band width of the filter. For the 1/3 octave filters a different effective band width must be determined for each frequency. Once determined the effective band width of the analog spectrum analizer will be constant independent of frequency. For a filter of effective band width, b and a measured output, e_b^2 the spectrum energy density function is

$$F(f) = \frac{\overline{e_1^2}}{b\overline{e^2}_{tot}} \qquad (2.29)$$

Several other definitions of effective band width, such as 3db reduction in gain, are to be found in the literature. Depending on the shape of the filter, it is true that the same effective band width can be determined from a simple measurement, however, it must be kept in mind that there is only one correct width for the definition given in equation (2.28). The obvious check of the spectrum measurements is to check the result

$$\int_0^\infty F(f)\, df = 1 \qquad (2.30)$$

which follows directly from equation (2.28). Measurements in both turbulent boundary layers and free turbulent shear flows suggest that the maximum deviation in equation (2.30) should be less than 20%. Greater deviations than 20% are usually an indication of questionable values for b or other major instrumentation problems.

Probability measurements.- The probability density distribution of a fluctuating signal is employed to discribe the amplitude distribution. The probability density may also be viewed as a "weighting function" to evaluate the fluctuating quantities $\overline{e^2}$, $\overline{e^3}$, $\overline{e^4}$, etc. The probability may be defined by use of figure 2.21. The incremental time spent in the interval du are summed. The total time spent in the interval is divided by the total

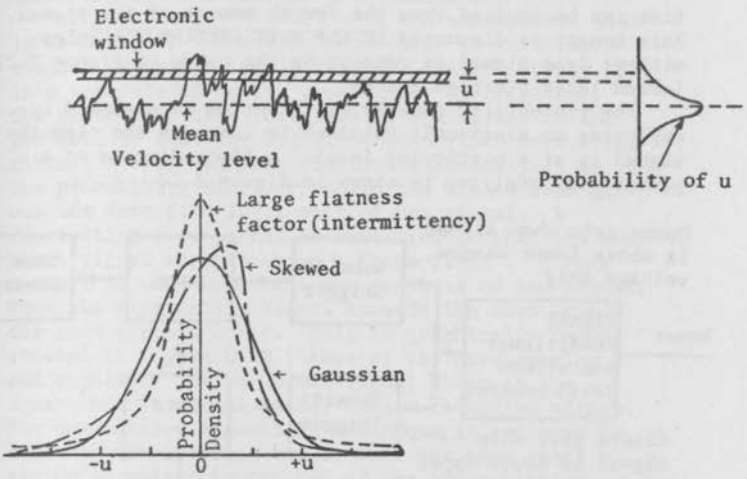

Figure 2.21 - Probability density function

sample time to obtain the probability density P(u) at u_1. The value P(u) defines the probability of occurrence of a given signal magnitude through out the entire range of magnitudes

The probability of a given value of u occurring within the limits of $\pm\infty$ at any time will be one. Thus, the area under the probability density curve is equal to one.

$$\int_{-\infty}^{+\infty} P(u)du = 1$$

Since P(u) is a weighting function it also follows that

$$\overline{u^n} = \int_{-\infty}^{+\infty} u^n P(u)du$$

Properties that can be obtained from the probability density distributions are:

1. Symmetry of the signal
2. Agreement with random Gaussian signals
3. Intermittency or clumping of the signal.

The symmetry of the signal can be seen from the symmetry of the probability distribution curve. A measure of the symmetry is the third moment of the signal, $\overline{u^3}$. The third moment is referred to as the skewness of the signal. A skewed probability distribution is shown on figure 2.21.

The intermittency or clumping aspects of a fluctuation can be implied from the fourth moment of the signal. This aspect is discussed in the next section. A intermittent type signal is denoted by the curve of figure 2.21 labled large flatness factor.

The probability density distribution is measured by employing an electronic "window" to indicate the time the signal is at a particular level. A block diagram of a probability analyzer is shown in figure 2.22.

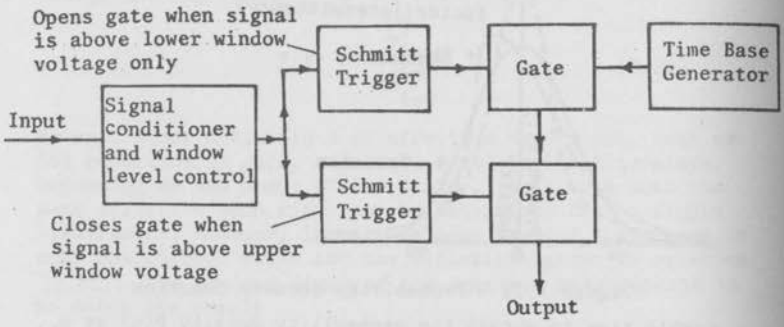

Figure 2.22 - Probability analizer.

The circuit senses when the amplitude reaches the desired voltage level. When the signal enters the "window" the gate is opened and the counting pulse is emitted. The gate is closed when the signal amplitude falls outside the window limits. The frequency response of this type of circuit is determined by how quickly the gates can be opened by the first trigger, but since the second trigger is almost on top of the first, the gate fails to close. It is necessary to restrict the frequency content of the input signal well below the frequency at which the gate does not close.

Intermittency Measurements - A measurement that is becoming of increasing importance in turbulence studies is that of intermittency. Intermittency is in a way related to the probability distribution. The percent of time turbulent is equivalent to the probability that the signal is other than zero. The circuit is basically an electronic window just as in the probability analizer except the window sees all but the zero d.c. level part of the signal. A fluctuating a.c. signal is rectified so that the complete signal appears above a "zero level". A gate circuit is used to detect the presence of the signal. When the fluctuating signal exceeds the zero level the gate circuit opens. This is graphically demonstrated in figure 2.23 (trace of the gate opening and signal). The turbulent signal shown is the square of the signal rather than a rectified signal. For convenience a counting technique is employed to evaluate the intermittency. When the gate opens a series of pulses is fed out of the intermittence circuit. When the gate closes the pulses cease. If a signal is present all the time then the pulses are present all the time. An electronic counter is used to count the number of pulses over a given period of time. A period of time may be chosen so that a multiple of 10 number of counts would occur in the time if the gate remains open the complete time.

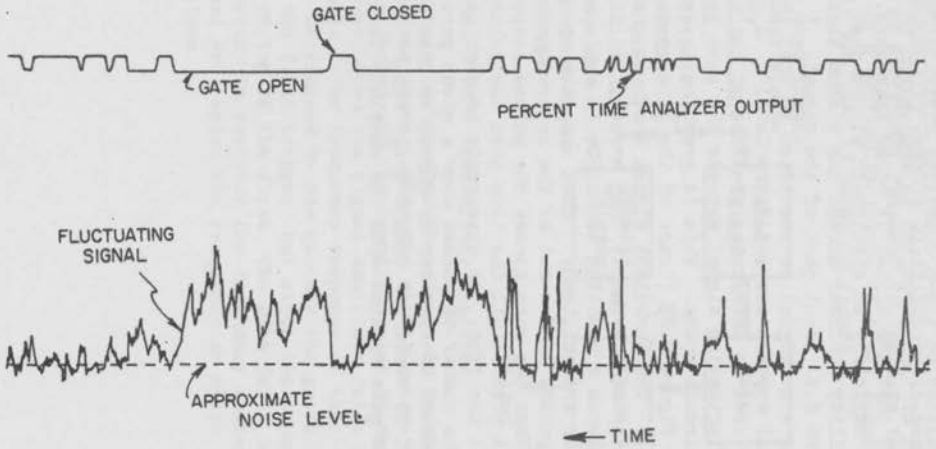

Figure 2.23 - Comparison of percent time analizer output with the fluctuating signal.

The counter output for a given turbulent signal can then be read directly as per cent of time turbulent. For example, the CSU "System" has a pulse rate of 10^5 per second. The pulses are counted on a 5 or greater place counter. The five place counter is set to count for one second, thus for a continuously open gate it counts 10^5 counts. When the turbulent signal is fed into the intermittent circuit the counter only counts, say 70,000 counts, which corresponds directly to 70% of the time turbulent. A six place counter increases the count time by a factor of 10.

The intermittency circuit developed at Colorado State University is shown in figure 2.24.

This instrument is made so that the gate "height" above zero volts can be varied. The circuit is also designed so that the intermittency of either the negative or positive part of the a.c. signal can be measured. This is particularly of value if the intermittency of the squared signal is to be measured.

Circuits, such as shown in figure 2.24, measure very accurately the intermittency of a given signal. Unfortunately it is necessary to determine what part of the signal is due to noise and what part is due to the turbulence. The major problem is the evaluation of the intermittency in the presence of noise. Consider for example the traces shown in figure 2.23.

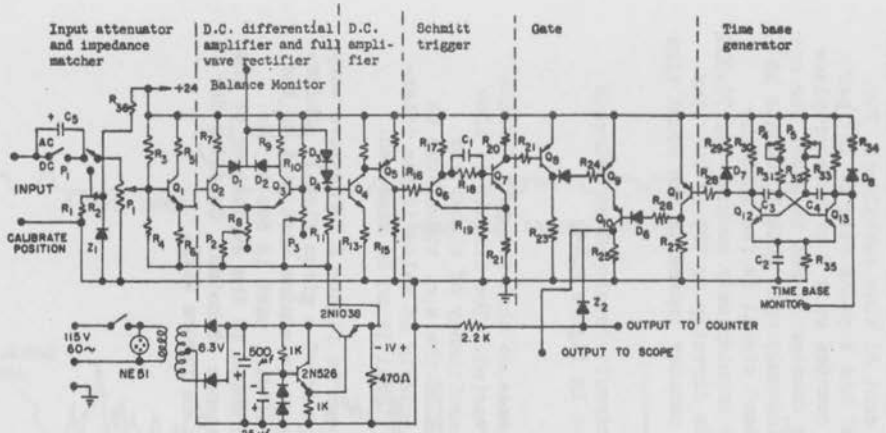

D_1-D_8 - 1N634	Q_{12}-Q_{13} - 2N1304	R_7 - 12K	R_{17} - 3.3K	R_{27} - 3.3K	C_1 - 1000 pf
P_1 - 10K	Q_8-Q_{11} - 2N526	R_8 - 165 Ω	R_{18} - 2.2K	R_{28} - 27K	C_2 - 10 mf
P_2 - 20 Ω	Q_5 - 2N1038	R_9 - 12K	R_{19} - 6.8K	R_{29} - 4.7K	C_3 - 100 pf
P_3 - 5K	R_1 - 10 Ω	R_{10} - 47K	R_{20} - 2.2K	R_{30} - 1K	C_4 - 100 pf
P_4-P_5 - 100K	R_2 - 1K	R_{11} - 100K	R_{21} - 1.8K	R_{31} - 33K	C_5 - 250 mf
Q_1-Q_4 - 2N1304	R_3 - 2.2M	R_{12} - 1K	R_{22} - 27K	R_{32} - 33K	C_6 - 100 pf
Q_6-Q_7 - 2N1304	R_4 - 100K	R_{13} - 1K	R_{23} - 3.3K	R_{33} - 1K	NOTE: ALL RESISTORS
	R_5 - 10K	R_{14} - 100 Ω	R_{24} - 1K	R_{34} - 4.7K	ARE 1/2 WATT
	R_6 - 2.2K	R_{15} - 1K	R_{25} - 1K	R_{35} - 270 Ω	Z_1 - 1N465
		R_{16} - 1K	R_{26} - 1K	R_{36} - 10K	Z_2 - 1N759
				R_{37} - 1K	

Figure 2.24 - Percent time analizer.

Note that the gate does not open until the signal is well above the noise level. This means that the per cent of time turbulent indicated by the gate is less than the actual time. For the example shown in figure 2.23 the gate per cent was 67.1% while a count of the signal directly from the trace indicates 80.8% of the time turbulent. For signals where the signal to noise level is very great the problem would not be as severe as that of figure 2.23.

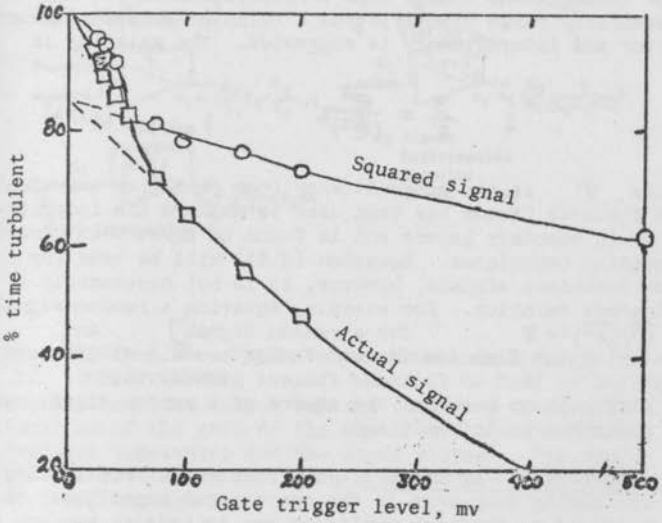

Figure 2.25 - Effect of electronic noise on the percent time turbulent measurement.

Figure 2.25 shows several methods of determining the intermittency of the signal. Several tricks may be employed to obtain the optimum signal. First if the time interval of counting is too short the signal may be tape recorded and played back at a higher speed. Thus, the increase in tape speed increases the actual count time of a given sample. To gain signal in the presence of noise, the signal may be squared. Squaring the signal increases the large amplitude fluctuation much greater than the small amplitude fluctuations. The results of these tricks in evaluating the signal of figure 2.23 are demonstrated in

figure 2.25. The gate height (voltage) is varied in all cases so that an extrapolation to zero voltage level is possible.

A second indirect method is also employed to determine the degree of intermittency. Instead of counting the fluctuations directly the flatness factor, $\overline{e^4}/(\overline{e^2})^2$, of the signal is measured. Physically $\overline{e^4}/(\overline{e^2})^2$ represents a measure of the extent of the "skirts" of the probability density curve, since the fourth power weighs the large values of e heavily. A burst or large amplitude-type intermittent signal will affect the skirts of the probability curve greatly, thus a relation between flatness factor and intermittency is suggested. The relation is

$$\frac{3}{\gamma} = \frac{\overline{e^4}}{(\overline{e^2})^2} \qquad (2.31)$$

where γ is the intermittency (per cent time turbulent). The flatness factor has been used to explore the intermittency in boundary layers and is found to agree with direct measuring techniques. Equation (2.31) will be true for most turbulent signals, however, it is not necessarily a universal relation. For example, squaring a random signal [$\overline{e^4}/(\overline{e^2})^2 = 3$ for a random signal] and measuring the flatness factor of this new signal has been reported to lead to flatness factors greater than 3. It is difficult to see that the square of a random signal can be described as intermittent.

Operational amplifiers - The backbone of modern electronic analog computers is the operational amplifier. This high gain d.c. feedback amplifier can be made to perform a great number of mathematical operations. Typical operations which employ operational amplifiers in hot wire anemometry are; Wide band d.c. amplifiers, sum and difference circuits, absolute value circuit, differentiating circuits, and integrating circuits. Operational amplifiers have also been employed as the d.c. feedback system for the "hot wire anemometer". There are a great number of commercially available operational amplifiers which can be used with hot wire signals. There are, of course, a great range of frequency response systems, so care must be taken to insure that the amplifier can respond at the highest frequency expecte

expected from the hot-wire anemometer output. Figure 2.25 demonstrates the hookup of operational amplifiers for some of the applications.

The operational amplifiers shown in figure 2.25 have a high input impedance so that grid current is

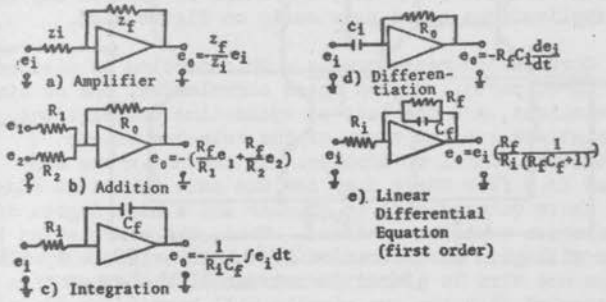

Figure 2.26 - Typical operational amplifier applications.

negligible. The output voltage (e_o) is a complicated function of the gain of the amplifier, the input and feedback impedances and the input voltage. For the general case shown in figure 2.25 the ratio of output to input voltage is

$$\frac{e_o}{e_i} = -\frac{Z_f}{Z_i}\left[\frac{1}{1+\frac{1}{G}\left(\frac{Z_f}{Z_i}+1\right)}\right] \qquad (2.32)$$

For the case where the gain G of the amplifier is very large with respect to unity, equation (2.32) reduces to

$$e_o = -\frac{Z_f}{Z_i}\, e_i \qquad (2.33)$$

where the output voltage is approximately proportional to the input modified by the ratio of feedback to input impedance.

Figure 2.27 is the complete circuit diagram of a sum and difference circuit which employs the operational amplifier system. This circuit was developed at C)S)U. and is an all transistorized unit. The operational amplifier circuits are noted, and could be used in any of the applications noted previously on figure 2.26.

Correlation measurements - This section is divided into three parts. One on space correlation, one on time correlations, and the last on space-time correlations. Correlations are the study of the relation of one fluctuating signal to another. If two hot wires are placed in a flow where they see the same turbulent eddy, then their outputs will be simular and a high degree of correlation would be recorded. Thus, the correlation in space will give an indication of the turbulent eddy size. If the one wire is placed downstream of the other then it is expected that the two signals will have to be adjusted in time for a high correlation. Thus, space-time correlations allow an eddy to be followed in the down stream direction.

Space correlation - Briefly, the mechanics of measuring the space correlation is simply to place two wires in the flow at the two locations where the correlation is desired. The correlation between the two wires can be obtained either by multiplying the outputs together or by using a sum and difference circuit.

The measure of the longitudinal turbulent velocity component is the only one that can be correlated directly. Evaluation of correlations for the two normal velocity components, the cross velocity terms and temperature velocity components becomes difficult. In principal at least enough different operations can be performed so that any of the correlations can be evaluated. However, the accuracy of correlations can never be expected to equal that of the simple normal wire operation.

Time correlation - Time correlations have been used

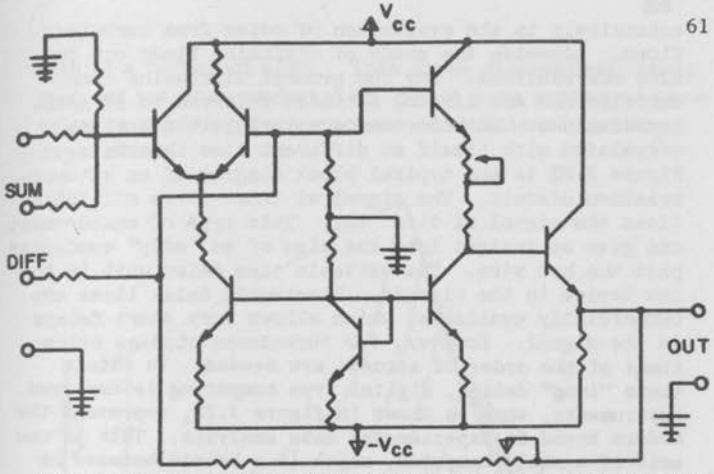

Figure 2.27 - Transistorized operational amplifier, sum and difference circuit.

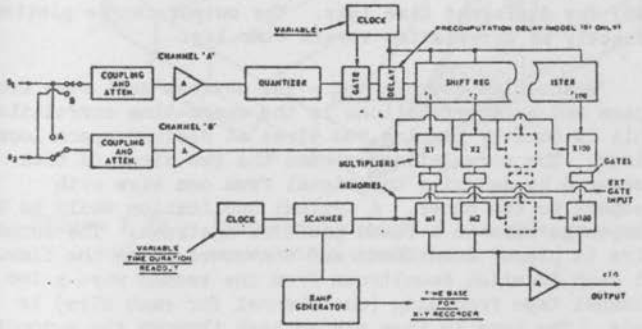

Figure 2.28 - Correlation function computer (from Princeton Applied Research Corp. Tech. Bulletin 149)

extensively in the evaluation of noise from turbulent flows. Likewise the study of diffusion finds use for time correlations. For the present discussion time correlations are limited to those referred to as autocorrelations. In other words a turbulent signal is correlated with itself at different time intervals. Figure 2.28 is the typical block diagram of an autocorrelation circuit. The signal at time t is multiplied times the signal at time $t-\tau$. This type of measurement can give an insight into the size of an "eddy" conducted past the hot wire. The variable time delay unit is the new device in the circuit. Electronic delay lines are commercially available, which allows very short delays in the signal. However, for turbulence studies delay times of the order of seconds are needed. To obtain these "long" delays, digital type computing is employed. Instruments, such as shown in figure 2.28, represent the modern trend in experimental data analysis. This is one unit of a small computer, which is a hybred between an analog and a digital system. The time correlation is composed of a number os memory banks, which compute a predetermined number of correlations (of the order of 100) for different time lags. The output can be plotted directly as correlation versis time lag.

Space-time correlation - The obvious next step from space and autocorrelations is the space-time correlation. This is done by placing two wires at desired space locations. The correlation between the two wires is then measured by delaying the signal from one wire with respect to the other. A typical application would be to place one wire in a fixed position upstream. The second wire is placed downstream and traversed along the flow. At each location downstream from the second wire a two c channel tape recording (one channel for each wire) is made. The tape is then played back through the autocorrelator circuit and the downstream wire signal is delayed with respect to the upstream wire. The results is a set of correlation curves which can be drawn isometrically, as shown in figure 2.29. The time delay to the point of maximum correlation is a measure of the convective velocity downstream of the turbulence. By transversing the second wire not only along the flow but also across the flow at each station, the point of maximum space-time correlation could be determined. This measure would define the average

path of a turbulent eddy. This three dimensional study has not yet been undertaken, but it does appear of great value in studying the structure of turbulent boundary layer flows

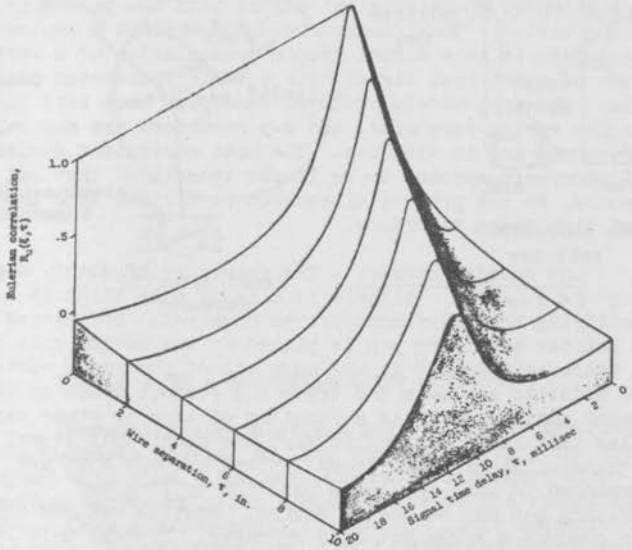

Figure 2.29 - Isometric sketch of example general eulerian correlation coefficient.

B. Recorders - Application of the deflection principal to read the flow of an electrical current in a circuit is the fundamental readout system for a great number of measurements. The basic approach is to vary some parameter, such as time, distance, temperature or other quantity and find the variation of the signal. It quickly becomes convenient to obtain a record of the variation of the electrical signal with the parameter being varied. Thus, modern research employs a number of recorders to make direct grapic presentation of a variation of electrical signal with a varing parameter possible. The most widely employed recorders have used time as the varing parameter, and x-y recorders are now well developed and in wide use. The most convenient division of recorders appears to be in the speed that they can record, so the present discussion is divided into low and high speed recorders.

Low speed recorders - The recording of slowly changing (<1cps) signals is made by only slightly modifying the galvanometer-type movement. If instead of a pointer a writing pen is placed in the moving coil then a trace is produced as the movement of the meter varies. In order to evaluate the trace the readout scale on the meter must be moved as a function of time or other varables that it is desired to plot the electrical signal against. Figure 2.30 shows typical methods that are employed to move the scale past the writing pen. The writing pen may be one of several possible methods used to produce a permanent line on paper. Typical writing systems include: direct writing ink; scratch on a blacken (lamp black? or wax paper, heat burn on wax paper, or light beam exposure of a photographic paper. All of these systems are to be found in use in commercial plotters.

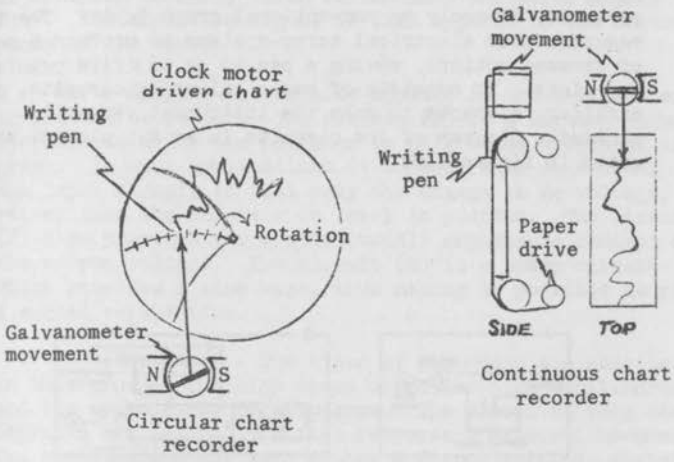

Figure 2.39 - Recording meter movements.

Commercial time plotters are built with accurate servo-driven charts, so that they do not vary the chart speed with time. The more expensive recorders also employ servo-amplifier systems to drive the recording pen. Once a servo-amplifier is used it is convenient to make the recorder into a self-balancing potentiometer circuit rather than a simple meter movement. A servo-motor is used to drive the recording pen as well as the chart paper. Thus, the width of the voltage scale can be expanded out to 10 or more inches and also be maintained linear on the chart. The self-balancing, recording potentiometer is quite commonly employed in the research laboratory.

The most recent step in recorders is the x-y recorder. For most of engineering work a Cartesian coordinate graph is the most often means employed to portray experimental data. Modern x-y recorders speed data interpretation by producing such graphs quickly. An x-y recorder automatically and conveniently plots the

value of an independent variable versus a dependent variable, directly on conventional graph paper. The x-y recorder usas electrical servo-systems to produce a pair of crossed motions, moving a pen so as to write precise x-y plots. It consists of basic balancing circuits, plus auxiliary elements to make the instrument versatile. A schematic diagram of the circuits in an x-y plotter are shown in figure 2.31.

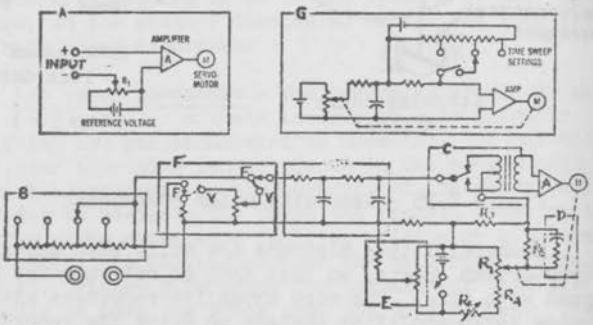

Figure 2.31 - Schematic diagram of the circuits in an x-y recorder (from Hewlett and Packard catalog No. 25)

The self-balancing potentiometer circuit (A) compares an unknown external voltage with a stable internal reference voltage. The difference between these voltages is amplified and applied to a servo-motor to drive a potentiometer in a direction that will null any difference or error voltage. A stepped attenuator or range selector (B) is included for each axis, so voltages as high as 500 volts may be plotted directly. Input resistance of plotters are of the order of 200,000 ohms. A chopper

(C) converts the dc errorssignal into a reversible-phase alternating current, which is fed into the servo amplifier. The amplified signal is then applied to the control phase of the servo.

Servo damping (D) is also applied in the x-y plotter to prevent overshoot. The circuit (F) is a zeroing potentiometer to allow the operator to select the origin of the graph. In many applications it is desirable to off-set the input signal, so that only the change in dc voltage, rather than the complete dc level is plotted. The circuit (F) also provides for a continuously adjustable control on the output voltage. The circuit (G) is a sweep circuit which provides a time base, thus making it possible to plot a signal versus time.

Fast Recorders - Two types of recorders are considered in this group. The high speed direct writing oscillographs and the cathode-ray oscilloscope. The direct writing oscillographs are basically a fast response D'Arsonval movement. The oscillograph may have either a direct writing, stylus movement or a light beam movement. The direct writing oscillographs are usually limited to 100 cps or less, and may employ either ink, pressure-writing or heated styli. The light beam system employs a focused light beam writing on a light-sensitive paper. The frequency response of the light beam galvanometer will be a function of the mass moment of inertia and damping characteristics of the coil and mirror. Present development has produced light beam galvanometers that can follow frequencies greater than 5,000 cps. Commercial recorders can be obtained with as many as ten or twenty galvanometers recording at the same time, so that a great number of events can be recorded at the same time. The speed of the chart can be varied from a matter of inches per hour to upwards of 5 feet per second.

The cathode-ray oscilloscope is an extremely fast x-y plotter which plots an input signal versus another signal or versus time. The "stylus" is a luminous spot which moves over the display area in response to the input voltage. In the usual scope application, the x-axis input is an internally generated linear ramp voltage. This ramp voltage moves the spot uniformly with time from left to right across the display screen. The voltage to be examined is applied to the y-axis input. The spot is moved up or down in accordance

with its instantaneous value. The spot, thus, traces a curve which shows how the input voltage varies as a function of time.

The writing speed of the cathode-ray oscilloscope is nearly unlimited. The electron can be deflected at speeds approaching the speed of light, thus, the limiting features are electronic circuits rather than the "stylus" which is the major factor in the oscillographs. The primary part of the oscilloscope is the cathode-ray-tube (CRT). Figure 2.32 shows the basic oscilloscope circuit.

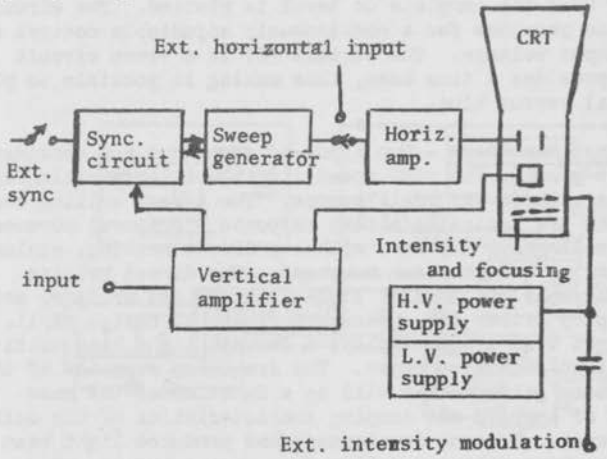

Figure 2.32 - Basic Oscilloscope Circuity.

The CRT is composed of a thermionic cathode which produces electrons. The electron is produced by heating the cathode until electrons are emitted. The electrons are electro-optically focused into a narrow beam. The beam of electrons are accelerated through the optical system. On leaving the electron accelerators, (which is commonly referred to as an electron gun), the electron stream passes between two pair of deflection electrodes. Voltage applied to the deflection electrodes moves the beam up and down or from side to side. These

deflection movements are independent of each other, so that the electron beam can be directed as desired.

The electron beam strikes a phosphor coating at the end of the glass tube. The high energy electrons cause the phosphor to fluoresce. Any number of different chemical salts can be used for the phosphor coating. The selection of a coating will determine color, brightness, decay and speed of response. Oscilloscopes are available with a wide range of phosphor coatings.

The frequency response of oscilloscopes are nearly unlimited. General purpose oscilloscopes have frequency response up to about 500 kilocycles per second. Special oscilloscopes can record signals well above 100 megacycles per second.

Recording of oscilloscope traces are made with special oscilloscope cameras. Oscilloscope cameras are similar to conventional cameras, but have additional refinements for facilitating scope photography. The camera is within a light-tight enclosure, which clamps or bolts over the face of the cathode-ray tube. The optical system is in line with the axis of the CRT, figure 2.38.

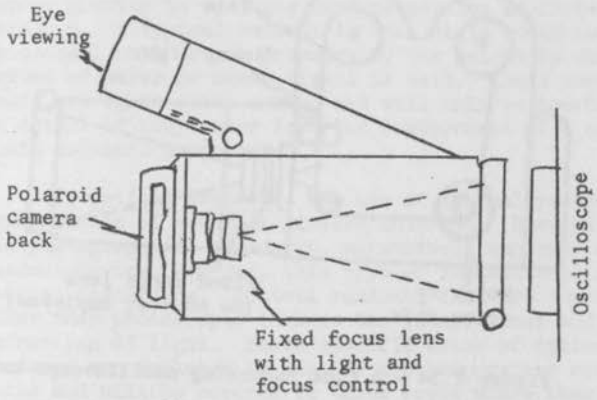

Figure 2.38 - Schematic of an Oscilloscope camera.

A viewing port is provided to permit observation of the oscilloscope face. The camera lens is usually a fixed focus system, with provisions for varable shutter speeds and light stops.

To take a picture of a single trace on an oscilloscope the oscilloscope is triggered to sweep once. In general, the use of shutter speeds on the camera is of no value in photographing a trace. The best procedure is to simply open the camera shutter to the black oscilloscope screen. The oscilloscope is triggered externally, so that the spot makes a single sweep across the screen. The graticule on the oscilloscope can then be illuminated and photographed at a proper shutter speed after the spot trace is recorded.

It is also desirable to obtain long time traces of the fluctuating voltage from an oscilloscope. This long time recording is done with the special type camera shown in figure 2.34. This type a camera supplies the time=

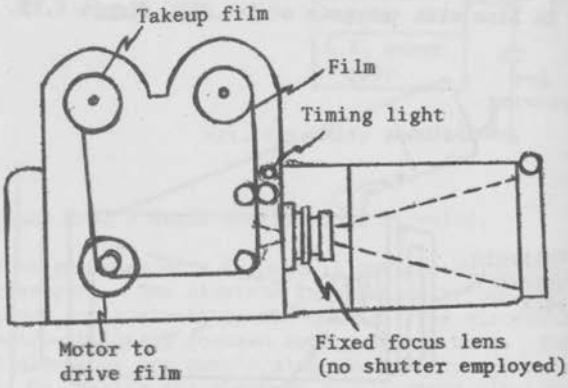

Figure 2.34 - A time recording oscilloscope camera.

axis of the photograph by pulling the film past the vertically varing spot. This camera employs an oscilloscope for which the time or horizontal axis of the scope is not operated. The spot is allowed to move in the vertical direction only. Recording cameras can produce a strip of film traveling at speeds greater than 5 feet per second. The limiting speed of this system is the writing speed, or exposure time of the photographic film.

C. Mechanical Readout - The use of mechanical readouts are, of course, a part of nearly every measuring instrument. The human can only sense movement in a quantitative way. All other human senses are of a qualitative nature. Mechanical readouts are in general familiar to most everyone, so we will not go into detail in their operations. The galvanometer demonstrated the most widely used mechanical device, namely the spring. The elastic property of metals is employed in many ways to convert a physical force into a scale measurement. The elastic property of springs, metal membranes, Bourdon tubes, and many related shapes are employed to evaluate force and torque.

Another class of instruments that would, of course, be included in the mechanical readouts would be those that employ gravity to evaluate such properties as force and pressure. A typical readout in this class would be the manometer, which reads pressure by the height to which a column of water or other liquid is held. These instruments are again quite common and will only be touched upon in detail if they enter into the measurement of a specific fluid mechanic property.

D. Optical Readout - The use of optical readout equipment is of somewhat limited interest. Specifically, the photograph is, of course, extensively employed as a readout device, however, this type of readout need no special discussion. Optical readouts that are employed other than photograpic include the interference and refraction of light. These specific areas of optical readouts are employed in density and temperature measurements and will be covered in those areas where they apply.

Chapter III - Transducer Concepts

In the first chapter a transducer was defined as a device that converts the quantity being sensed into some other form of signal. This is a very general definition and also very vague. Actually, in every measurement we are in a sense comparing the physical quantity to be measured against a known standard. The transducer, thus, becomes the go-between from the standard to the physical quantity. In every case that we will be considering the physical quantity will act upon a sensing element in such a way that a physical device gives a scale deflection that can be read visibly. The transducer may be either the sensing element, transmissions, or readout part of a measuring system. For example, the galavanometer could easily fall into the definition of a transducer since it senses an electrical signal and converts it into a mechanical deflection. For the present discussion the word transducer is simply an energy converter, and we will direct our attention to those converters that are of value in measurements in fluid mechanics.

A. Electrical - In this section we will review briefly some of the basic physical effects that take a fluid flow property and convert it to an electrical signal. The following table is a limited attempt to point out some of the physical changes-electrical change phenomenon that are employed as transducers.

Table III - 1

Phenomenon	Physical Effect	Application
Resistance - Strain	The electrical resistance of a material changes as it is strained	Measure Strain
Resistance - Temperature	The electrical resistance of a material changes with temperature	Measure; temperature, Heat Transfer, Kinetic Energy, Radiant Energy
Photoconductivity	The electrical resistance of a material changes with light	Measure light intensity
Thermoelectric	Dissimular metal junction produces an emf with a change in temperature	Measure; temperature heat transfer, kinetic energy, radient energy
Piezoelectric	Pressure difference produces an electrical charge	Measure pressure
Pyroelectric	Temperature difference produces an electric charge	Measure temperature
Photoelectric	Light liberates electrons and produces a flow of current	Measure light intensity
Capacitance - Displacement	Change in distance produces a change in capacitance	Measure displacement

Table III-I Continued

Capacitance - Pressure	Change in pressure produces a change in capacitance	Measure pressure
Inductance - Displacement	Change in core displacement produces a potential	Measure displacement
Electromagnetic Induction	Change in electrical conductor produces a current	Measure revolutions, electrical conductivity

The effects listed in TableIII-I are a few of the possible phenomenon that can be employed to sense physical quantities. In each case the physical quantity produces an effect which changes the electrical characteristic of the transducer. Thus, an electrical signal can be produced that is proportional to the physical quantity. Only those effects that are of basic importance in fluid measurements are included in the table.

The classification of electrical phenomenon used in instrumentation is extremely poor. Unfortunately, the science of instrumentation is not an accepted study in itself. As a result, the name assigned to a class of instruments may be inadequate. For example there is a large group of transducers that employ the change in resistance with temperature as the electrical phenomenon. This group of transducers might be classified as thermal resistors or contracted to thermistor transducers. Unfortunately, the thermistor is copywritten to apply to only one extremely limited type of material. Thus, each group of names listed in Table II-I is by no means all inclusive as to an electrical phenomenon.

There are several effects that are employed with the above transducers to increase their usefulness. For example, the electrogenerator effects of a coil in a magnetic field. The production of a force in the galvanometer by the interation of a current in a coil in a magnetic field is an important example of the reverse effect of the electrogenerator or electromagnetic induction. Another phenomenon of basic interest is Joulean heating. The flow of an electrical current through a material produces an increase in the temperature of the material. The heating is proportional to i^2R of a material. The cause of the heating may be seen by considering the resistance of a material.

A third electronic phenomenon of basic importance throughout the field of measurements is electron emission. It is this type of electron emission that makes possible the electron vacuum tube, cathode-ray-tube, and many other applications. Electron emission finds use as a transducer in in photoelectric devices, however, it is a work horse in many circuits and readouts employed in measurements. There

are four types of electron emission: 1. Thermonic, or primary, emission 2. Secondary emission 3. Photoelectric emission 4. Field emission. Thermonic emission occurs when a material is heated to incandescence in a vacuum. Secondary emission occurs when a high velocity electron or ion strikes a material in a vacuum and knocks out one or more electrons. Photoelectric emission occurs when energy in the form of light falls upon a surface. Field emission occurs at cold surfaces under the influence of extremely strong fields. In each case the electrons in the material are given an increase in energy to the point where they can escape the "hold" that the material has on them. We will refer to the hold that the material has on the electron as an energy barrier which the electron must overcome before it leaves the material.

RESISTANCE OF MATERIALS

No doubt every one is familiar with the phenomenon of the resistance of materials changing as their temperature changes. The theoretical explanation for the resistance change requires little short of a complete course in solid-state physics, and thus it is not attempted herein. The reader interested in the subject is referred to an article by Bardeen[1] and to the many text books on solid-state physics. Figure 3.1 is a plot of the $\log_{10}$ of electrical resistivity as it varies with temperature for three types of materials. Resistivity, σ, is a physical quantity used to describe the resistance of a material and at the same time make it independent of the material geometry.

$$\sigma = \frac{RA}{l} \qquad (3.1)$$

---

[1] Bardeen, J.: Jour. Appl. Phys., vol. II, 1940, p. 88.

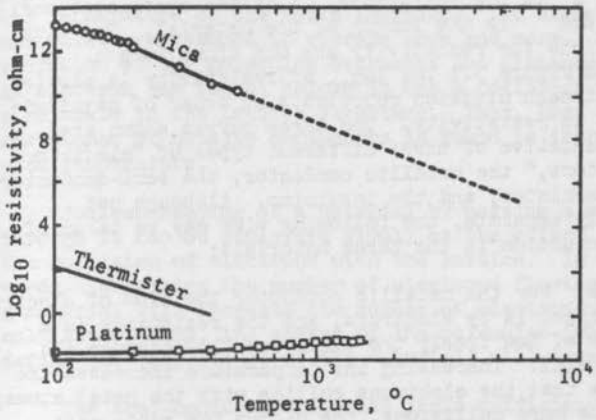

Figure 3.1 - Variation of Electrical Resistivity, With Temperature, of The Basic Types of Conductors.

where R is the resistance, A is the cross-sectional area, and is the length of the material. The usual dimensions for resistivity are ohm times length. Note that in Figure 3.1 the $\log_{10}$ of resistivity is plotted so that each division represents an order of magnitude change in resistivity. The three curves shown are representative of three different types of "electrical conductors," the metallic conductor, the semi-conductor and thermistor, and the insulator. Although not strictly accurate, the following view may be taken of the conduction in the three materials:

(a) For the metallic conductor the flow of electrical current is by electrons, and the resistance is a measure of how freely the electrons flow through the solid metal. Increasing the temperature increases the chances that the electrons collide with the metal atoms; thus the more collisions, the higher the resistance.

(b) For semi-conductors the system may be viewed as electron starved, where not enough electrons are available to conduct the current. As the temperature is increased, more electrons are free to conduct; thus the resistance drops with increasing temperature.

(c) Insulators simply do not have electrons available for conduction. Conduction in insulators is by ions, which become more mobile as the temperature increases; thus the resistivity of the insulator drops with increasing temperature.

There is no sharp division between the different types of conductors. It is possible to find materials that will have nearly any value of resistivity, at a particular temperature, in the range shown in Figure 3.1. In the region of metallic conductors alloys are available with greater resistivity than platinum.

The resistance of a metallic conductor is explained by viewing the metal as if it were a gas. Free electrons are assumed to exist in quantity throughout this "gas". Thus, if a potential difference exists along the conductor, electrons flow from negative to the positive points of the potential difference. Resistance is simply the resistance that the molecular lattice of the metal

offers to the electron flow. In a solid all atoms and molecules are assumed to be fixed in the lattice. As the temperature of the solid increases, the atoms and molecules are assumed to vibrate more and more. The vibration of the molecules decreases the distance that an electron can travel before it has a collision with a molecule in the lattice structure. Thus, the resistance of metalic conductors is found to increase with temperature.

Joulean heating of a material by passing a current through it can be explained simply as the effect of the collision of electrons with the lattice. In other words, increasing the number of electrons flowing through a material will increase the number of electron-molecule collisions, thus, the energy of the molecules (which define the temperature of the material) will increase.

The semi-conductor material lacks sufficient number of electrons to conduct the current. Thus, the major effect of change of resistance of a semi-conductor material has nothing to do with electron-molecule collisions. The most important effect is that increasing the temperature of a semi-conductor material releases more electrons for conduction, so that resistance of semi-conductors decreases with temperature.

For the semi-conductor materials anything that will release electrons in the system will decrease the resistance of the material. A typical example of this is the photoconductive effect, where light striking the material causes a decrease in the resistance. The photo-conductive effect can be detected as a pure photon effect and not related to a radiation heating effect. Radiation energy will, of course, also produce a change in resistance if it heats the material.

The strain of a conductor will in effect compress the lattice of the material and, thus, increase the chance of an electron-molecule collision. Thus, the change of resistance with strain canbbe related to young's modulus and Poisson's ratio for the conductor. The effect of high pressure that compresses the conductor can also be detected as a change in resistance.

For the most part the resistivity of a pure metal conductor is a well explained phenomenon. However, in the remote realm of temperature approaching absolute zero a strange phenomenon occurs. In 1911 the Dutch physicist Heike Kamerlingh Onnes discovered that at 4.2°K all resistance to the flow of an electrical current through mercury disappeared. Onnes also found the same phenomenon occurred in several other metals, such as tin, lead, tantalum, and niobium. Figure 3.2 shows the drop in resistance for several metals near absolute zero. The transition temperature for the superconducting state varies with the metal, as shown in figure 3.2.

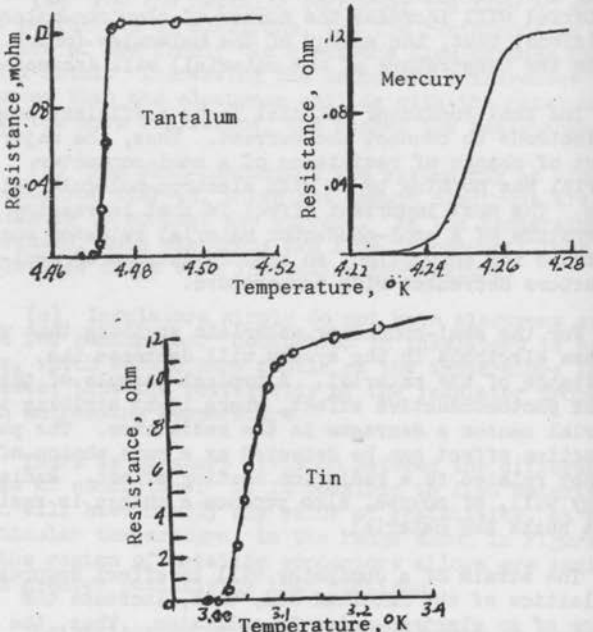

Figure 3.2 - Resistance of Metals in the Superconducting region.

Superconductivity does not occur in all metals. Metals which are comparatively poor conductors at normal temperature are most likely to become superconductors. Strangely, the best conductors at normal temperatures, copper and siliver, do not become superconducting. Explanations of superconducting states are not yet entirely satisfactory. Current theories suggest the vibrating atoms may help to conduct the flow of electrons through the metal in the superconducting state. At low temperatures the atoms in the lattices no longer obstruct the flow of electrons, but rather, they abruptly begin to conduct electrons along in a wavelike manner.

Thermoelectric Effect- If two disimular materials are joined at two junctions, which are at different temperatures, and e.m.f. (called the Seebeck e.m.f., or total e.m.f., or just thermoelectric e.m.f.) is found to flow in the circuit. This phenomenon was discovered by T. J. Seebeck in 1821. Depending on the temperature difference between the junctions the e.m.f. may vary from a few microvolts to the order of volts. Values of the e.m.f. for a given thermocouple pair of conductors are reproducible to a high degree of percision. However, the relationship is empirical and can only be roughly predicted from theory. Atypical thermocouple arrangement is shown in figure 3.3.

The theoretical explanation of the thermocouple effect was for many years a question. The problem was a failure in the ability to measure charge build up in a conductor which is in a thermal gradient. The electrothermal effect is produced simply because electrons from one end are "carried toward the other end of a conductor by a difference in temperature."[1] It is convenient to imagine that the more numerous high-energy electrons from the hotter end migrate to the colder end. The charge generated between the ends depends only on the two particular temperatures at the ends of the conductor. The use of two dissimular metals simply increases the electrothermal effect to a measurable amount.

---

[1] Beam, W. R.; Electronics of Solids, McGraw-Hill, N.Y. (1965)

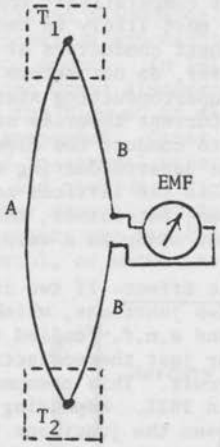

Figure 3.3 - Thermocouple Circuit.

The thermocouple effect is termed the Seebeck effect. There are two other effects identified with the overall thermoelectric phenomenon. The term thermoelectric means the direct conversion of heat into electrical energy (or the reverse). The Seebeck effect is the conversion of thermal energy into electricity, while the Peltier effect is essentially the reverse of the Seebeck effect. For the Peltier effect a cooling or heating of the junction of two dissimilar metals occurs when an electrical current passes through them. The rate of heat output or intake is proportional to the current. The Peltier effect is not in general use as an instrument transducer, however, it is currently being extensively studied in heat pump applications.

The third thermoelectric effect is the Thomson effect. The Thomson effect is a consequence of what was expected from the Seebeck and Peltier effects. While the Peltier heating explains the junction effect in the overall Seebeck effect, the Thomson heating, serves to account for the remaining distribution along the conductor. The Thomson effect accounts for the temperature gradient along the conductors. The Peltier and Thomson

effects taken together are essential to the proofs relating thermoelectricity to thermodynamics.

When a current of density I flows in a homogeneous material in the presence of a temperature gradient, the rate H which heat is developed per unit volume contains a term linear in I and the temperature gradient $\partial T/\partial x$

$$H = I^2R - \tau I \frac{\partial T}{\partial x} \qquad (3.2)$$

where τ is called the Thomson coefficient (a function of the particular conductor.) The third thermoelectric effect was discovered by William Thomson (Lord Kelvin) in 1854.

Piezoelectric Effect - Piezoelectric is the conversion of pressure into an electrical output. The term piezoelectric has come to be applied to a special class of devices. Piezoelectric transducers are that special group of crystals where anplectrical polarization is produced by mechanical strain. In general, it appears that piezoactivity occurs in crystals that do not have a center of symmetry in the lattice structure. Thus, the crystal developespolarization due to shifting of the "center of gravity" of positive and negative charges under the influence of elastic strain. Figure 3.4[1] is the approximate structure of a quartz crystal, which is used in a great number of piezoelectric applications. Quartz is composed of three silicon atoms and six oxygen atoms. The silicon atoms have four positive charges and the oxygen atoms have two negative charges. The charges in the unstrained case are all balanced. A force applied to the x-axis shifts the cells so that the cell becomes polarized.

---

1 Meissner, A.; Uber piezoelectrische Kristalle bei Hochfrequeny; Z. Tech. Phys. vol. 8 (1927).

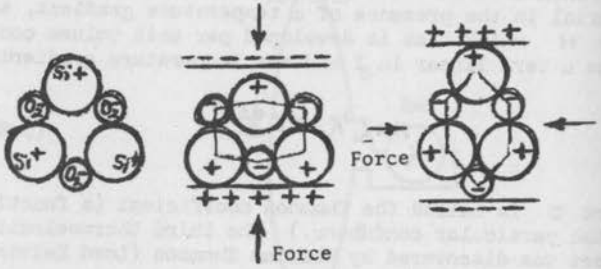

Figure 3.4 - Crystal structure of quartz.

The shift within the crystal produces the charge on the crystal surface. This shift produces electrical forces within the crystal which are not in equilibrium. Thus, the crystal will not remain in this uneven force condition. Actually, in order to produce a polarization of the crystal the force must be applied quickly. A steady state application of pressure will not produce a polarization, so that the piezoelectric, phenomenon is of value only for transient pressure measurements. After a transient pressure is applied to the crystal the charge built up by the polarization will leak off as shown in figure 3.5. The charge leaks away with a time constant RC, where R is the resistance across the gage (resistance of circuit used to readout the charge), and C is the capacitance across the crystal. The readout circuit is necessarily constructed so that the resistance is as great as possible.

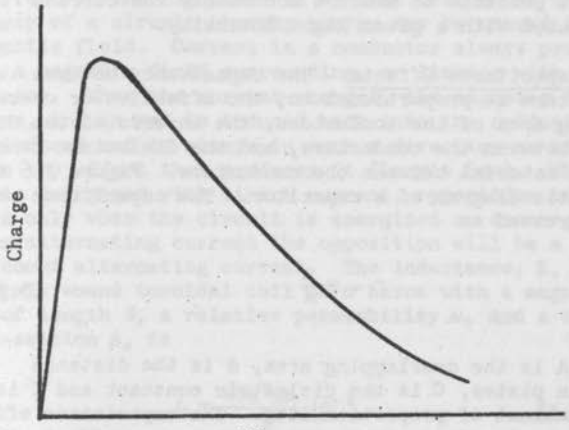

Figure 3.5 - Charge leakage in a Piezoelectric circuit.

Pyroelectric Effect - The pyroelectric effect is nearly identical to the piezoelectric effect, except that the crystal is strained by thermal stresses. In general, the pyroelectric effect is an error in the pressure measurements. The pyroelectric transducer is limited in application, since limited information of transient temperatures have been required. As will be demonstrated in the application of temperature measuring instruments, the device measures heat transfer in the crystal rather than temperature.

Photoelectric Effect - The photoelectric transducers employ the observed phenomenon that photons can give rise to electron emission. In operation a material, such as alloys of antimony and cesium, or silver and cesium, is set in an electrostatic field at conditions slightly below where electron field emission occurs. Thus, when a proton strikes the material electron emission can occur. The yield per photon is at most 0.15

electrons, but this is adequate to produce measurable currents. Special construction of photomultiplier tubes make it possible to measure accurately the current associated with a given light intensity.

Capacitance Effects - The capacitance between two conductors is proportional to; the effective or overlapping area of the conductors, the inverse of the distance between the conductors, and the dielectric constant of the material between the conductors. Figure 3.6 is a schematic diagram of a capacitor. The capacitance can be expressed as

$$C = K\varepsilon\frac{A}{d} \qquad (3.3)$$

where A is the overlapping area, d is the distance between plates, C is the dielectric constant and K is the constant of proportionality. The capacitance effect can be employed to sense area, distance or effects that vary the dielectric constant. The main application of the capacitance effect in measurements in connection with distance or displacement measurements.

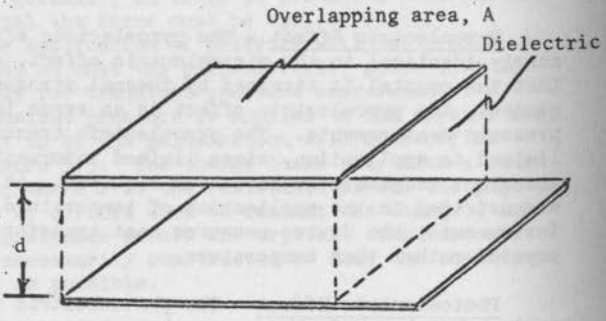

Figure 3.6 - Diagram of a plate capacitor.

Inductance Effect - Inductance is the inherent property of an electric circuit that opposes any change of current in the circuit. It is also defined as the property of a circuit whereby energy may be stored in a magnetic field. Current in a conductor always produces a magnetic field surrounding, or linking with the conductor. When the current changes, the magnetic field changes, and an emf is induced back into the conductor. This induced emf is always in such a direction as to oppose the effect that produces it (Lenz's Law). When a coil is energized with direct current, opposition to flow occurs only when the circuit is energized or deenergized. For an alternating current the opposition will be a continuous alternating current. The inductance, L, for a uniformly wound toroidal coil of n turns with a magnetic core of length ℓ, a relative permeability μ, and a core cross-section A, is

$$L = \frac{4\pi n^2 \mu A}{\ell} 10^{-9} \qquad (3.4)$$

L is measured in Henries if A and ℓ are expressed in cm. If the core of the coil is made vary by sliding a solid rod core in or out, the inductance will vary with the core displacement. The inductance can also be varied by variation in the permeability of the core, so the inductance may be used to evaluate properties that affect permeability.

B. Mechanical.- The mechanical phenomenon used in transducers are listed in Table III.2

These physical phenomenon are the basic part of many transducers. In most cases it is , of course, impossible to take advantage of the mechanical phenomenon without electrical systems being involved. Likewise, the electrical transducers are interrelated with the mechanical phenomenon..

TABLE III. 2

Phenomenon	Physical Effect	Application
Gravity	All bodies at the surface of the earth are accelerated toward the center at a constant rate.	Measure; mass, force pressure
Seismic Mass	A mass in motion tends to stay in motion. A mass at rest tends to stay at rest	Measure : acceleration
Elastic Deflection	A material may be strained and its deflection is proportioned to the straining force. When the force is removed the material returns to its unstrained condition.	Measure: force, pressure weight, electrical current.
Expansion	A material changes its dimensions with temperature.	Measure: temperature

Gravity.- The con stant of the acceleration of gravity is employed as a means of measuring pressure and weight. The gravitational constant is, according to Newton, a factor only of the radius of the bodies involved. The radius of the earth is so great that we need not consider the shape or size of a body used in the transducer. Thus, the height of the column of water is an accurate measure of pressure with no corrections being made for gravity. For very accurate measurements, such as those of a mercury barometer, the scale is adjusted to match the gravity constant at the location of the measurement.

Seismic Mass.- The seismic mass employs the phenomenon of Newton's law of force

$$F = m\,a \qquad (3.5)$$

to measure acceleration. In other words, a force F is the result of acceleration, a, on a mass, m. The same relation in angular systems is

$$I\ddot{\alpha} = T \qquad (3.6)$$

where I is the moment of inertia of the mass, $\ddot{\alpha}$ is the angular acceleration, and T is the torque. Thus, the seismic mass is used to convert an acceleration into a force. We can not record the output force unless we employ another mechanical phenomenon, thus the seismic mass is not a complete self-contained unit.

Elastic Deflection.- Most materials are elastic in that they can be strained to a given length without altering the properties of the material. When the strain is released the material returns to its original shape. This is Hooks law of elasticity. The properties of importance in materials are the moduli of elasticity, E, and rigidity, G. These properties remain reasonably constant over long periods of time, so that stable transducers can be built using the phenomenon. The resistance to strain is a force, so that force is a direct measure from the deflection of the elastic member. The shapes used in transducers vary over a wide range. The most common elastic member is the spring, which may be in any one of several shapes: Cantilever, Beam, Helical, Torsion Bar, or Spiral. Diaphragms are also used as elastic deflection members. The bellows and bourdon tubes are widely used as pressure sensing elastic deflection transducers.

Expansion.- The dimensions of a material, either gas, liquid, or solid is found to change with temperature. The phenomenon is associated directly with the random motion of the molecules of the material. The random velocity of the molecule increases as the temperature increases, thus each molecule with in a lattice structure of a solid requires more space. The same effect is present to a greater extent in liquids and gases.

The expansion of a material is found to be uniform with temperature, so that it can be used to measure the temperature of the material. The liquid-in-glass thermometer is solely dependent on the difference in expansion between a liquid and its glass container. Bi-metalic thermometers employ both the expansion of metals and their elastic properties to indicate temperature. The gas thermometer employs the equation of state, $T = \frac{pv}{\rho R}$, expression to measure low temperatures. The gas thermometer expresses temperature in terms of pressure, volume, and density, and is used as the standard for low temperatures.

C. Optical - The optical phenomenon employed in physical measurements are listed in Table III.3

TABLE III.3

Phenomenon	Physical Effect	Application
Photochemical	Different wave lengths produce different degrees of chemical reaction	Photographs measure light intensity
Interference	Waves of light out of phase interfere with one another	Measure distance and fluid density variation
Schlieren	Refractive indices of light varies through an inhomogeneity	Measure fluid density variation
Absorption	Fluid molecules may absorb radiation	Measure density of specific species of molecules
Scattering	Fluid molecules may reflect light at right angle to beam	Measure molecule density
Radiation	High temperature fluids will emit light	

Table III.3 mainly considers the phenomenon in the visible light range. In recent years major instrument development has taken place over the complete range of electromagnetic wave lengths. Thus, the phenomenon of interference, absorption, scattering and radiation should not be limited to the wave lengths of visable light. Microwave, X-ray, electron beam, acoustic, and infra-red frequencies are currently employed in fluid mechanics measurements. The development of the high intensity, high monochromatic, and coherent laser laser light source has made measurements in the visable range of frequencies more feasible. In the years after World War II, schlieren and interferometers were used mainly as means of making supersonic flows visible. Most attempts to evaluate quantatitive values of density from the systems were usually of limited value. The laser source coupled with the holograph techniques are now opening up a new area of gas density measurements.

Many of the "electromagnetic wave" instruments make use of Doppler's principle, where the frequency emitted (by scattering) from a moving body will be shifted proportional to the velocity of the body.

The optical transducers are somewhat limited, mainly because of the physical properties they measure. The dimension measuring interferometer finds use only for the very accurate measurements not normally employed in most research laboratories. The density measuring interferometers and Schlieren systems are limited mainly to compressible flows, which are encountered at speeds near the sonic velocity in gases and rarely ever found in liquids. The range of application is somewhat increased for thermal flows.

Photochemical - The photograph is mainly employed as a readout process, however, it may also be viewed as a transducer. The phenomenon is based on the fact that chemical change may occur as a function of the light intensity. The effect is even more selective in that the chemical reaction may vary with the particular wave length of light. Thus, we are able to sense only the infrared or ultra-violet wave lengths of light in a given

photochemical change. The phenomenon is associated with the change in energy of the molecules of a material due to the absorption of energy from the light.

Interference - By considering light as composed of waves it is possible to demonstrate that the waves may interfere with one another. Consider the two sets of equal wave length light beams shown in figure 3.7.

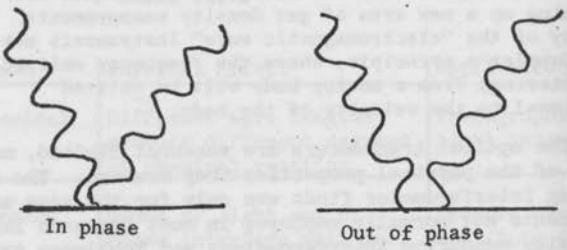

Figure 3.7 The Interference Principle

When the two beams are in phase, the light beams add to produce a bright image. When the beams are out of phase by half a wavelength, the light canceles. Thus, for out of phase light the waves are said to interfere with one another. In application the two light beams are produced by a single monochromatic light source, so the initial beams are of exactly the same wave length. The light beam is "split" into two parts by a half silvered mirror - splitter plate. Interference may be caused by unequal distances of travel of the two split beams, when they are brought back together. Since the optical path length of light is the product of the refractive index, n, and the geometrical path legnth, l, then the interference phenomenon can be used to indicate changes in the refractive index.

Schlieren - The velocity of light in a substance is less than its velocity in free space. In general it is found that the greater the density of a substance the greater is the decrease in the velocity of light. Figure 3.8 shows the variation of the speed of light in air, as a function of the density.

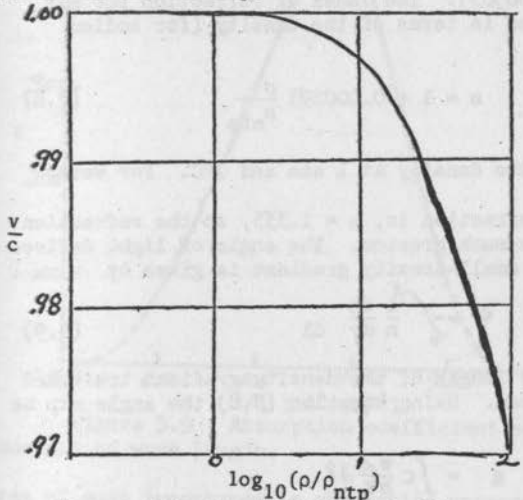

Figure 3.8 Speed of Light in Air.

The Huygen's principle (which states that: every point of a wave front may be considered as the source of small "secondary" wavelets, which spread out in all directions from their centers with a velocity equal to the velocity of propagation of the wave) will lead to the result that a shift in the direction of a wave front occurs as the velocity of light changes. Thus, when a light beam encounters a change in density it will be bent away from its original direction.

The velocity of light in a substance is usually expressed in terms of a ratio

$$n = \frac{c}{v} \tag{3.7}$$

where c is the velocity of light in free space, v is the velocity of light in the substance and n is called the index of refraction.

the index of refraction may vary with the density of the substance and also with the wave length of light. The index of refraction of gases is very close to one. For air n = 1.0002957 for violet light (wave length = 0.00004359 cm) and n = 1.0002914 for red light (wave length = 0.00006563). The index of refraction for air can be expressed in terms of the density (for sodium light)

$$n = 1 + 0.000293 \frac{\rho}{\rho_{ntp}} \tag{3.8}$$

where ρ_{ntp} is the density at 1 atm and 0°C. For water the index of refraction is, n = 1.333, so the refraction effects will be much greater. The angle of light deflection through a small-density gradient is given by

$$\epsilon = -\int_0^l \frac{1}{n} \frac{dn}{dy} \, dl \tag{3.9}$$

where, l is the length of the density gradient traversed by the light beam. Using equation (3.8) the angle may be expressed as

$$\epsilon = \int c \frac{\partial \rho}{\partial s} dl \tag{3.10}$$

Thus, the deflection of light may be employed as a means of evaluating density or density gradients in a fluid flow.

Absorption - If monochromatic radiation (light) passes through an absorption cell of length l, then the intensity of radiation emerging, after absorption in the molecules, is given by

$$I = I_o e^{-\alpha l} \tag{3.11}$$

where I_o is the intensity measured with the cell evacuated, and α is the absroption coefficient in cm^{-1} at NTP. The absroption coefficient is a function of the wavelength of the incident light and depends on the nature of the molecules, their number concentration, their motion and their interaction either with one another or with foreign molecules. Figure 3.9 shows the absorption coefficient for oxygen as a function of the wave length. Since, the

absorption varies from species to species it is possible to indicate the number density of select molecules. The

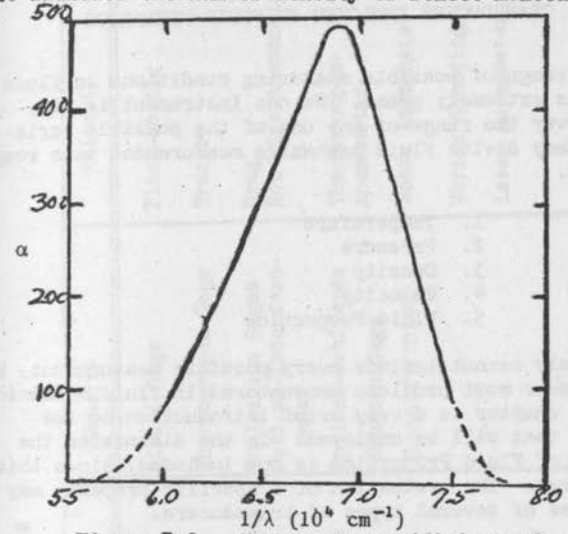

Figure 3.9 - Absorption coefficient of oxygen as a function of wave length.

area of most importance in absorption appears to be in the ultra-violet region.

Scattering - A beam of light may be reflected as it strikes a molecule. The angle of reflection will be a function of the particular molecules. Thus, a measure of the intensity of light at right angles to the initial light beam will be a function of the molecule density. This technique requires large, dense molecules.

Radiation - High temperature gases emit light. This is due to the extremely high vibrational energy of the molecules. In metals the wave length and intensity of light emitted is related to the temperature. For gases the radiation is a complex function of temperature, density and molecular species. The light emitted can be analized spectroscoply to identify specific wave length. Related wave lengths and intensities can be employed to identify radiation from particular molecular species, however, it is extremely difficult to relate the results to temperature and density.

Chapter IV

TRANSDUCERS EMPLOYED IN FLUID MECHANICS

The range of possible measuring conditions in fluid mechanics is extremely great. No one instrument is adequate to cover the range of any one of the possible variables. One may divide fluid mechanics measurement into roughly five groups.

1. Temperature
2. Pressure
3. Density
4. Velocity
5. Fluid Properties

This certainly cannot include every possible measurement, but it should cover most problems encountered in fluid mechanics. The present chapter is a very brief introduction to the transducers that will be employed. In the discussion the fifth group of Fluid Properties is not included, since this is a special area. The evaluation of a specific property may require the use of several types of transducers.

A possible range of flow conditions that can be expected in fluid mechanics laboratories are listed in Table IV.1.

Table IV.1

Measurement	Range
Temperature	$0^{\circ}R$ to 20,000 - 30,000$^{\circ}R$
Pressure	0 to 10,000 psi
Density	0 to ?
Velocity	0 to 100,000 ft. / sec.

The range of conditions stated in Table IV.1 are by no means the maximums that have been obtained. These conditions are roughly the extremes that can be obtained in a fluid mechanics laboratory such as that at Colorado State University.

Table IV.2 is a list of the possible transducers that are employed to make the required measurements.

Table IV.2

Quantity	Temperature	Pressure	Density	Velocity
	Gas Thermometer	Manometer	Pirani Gage	Pitot-Static
	Liquid-in-Glass	McLeod Gage	Thermocouple Gage	Tracer
	Resistance - Thermometer	Diaphragm Gages Bourdon Tube	Ionization Gages Optical-Interferometer	Drag Hot Wire Anemometer
	Thermocouple	Bellows Gages	Optical-Schlieren Knudsen Gage	Thermocouple-Anemometer
	Bi-metalic - Thermometer	Resistance-Pressure Capacitance-Pressure	Spectrometer	Sonic Anemometer Vortex Shedding Laser Anemometer
	Optical Pyrometer	Piezoelectric		
	Sonic-Thermometer	Dead-Weight Tester		
	Kinetic Energy Analizer			

The transducers and sensing elements that are noted in Table IV.2 will be discussed in detail in the following Chapters. These systems represent electrical, mechanical and optical devices.

Chapter V

MEASUREMENT OF FLUID VELOCITY

The measurement of velocity is perhaps the most important measurement in a great deal of problems. The velocity can be measured in any of several ways. Perhaps the most used device is the pitot-static pressure probe, although drag type flow devices are also in wide use. The present discussion is concerned with the steady state and transient velocity measurements. Thus, the chapter includes detailed evaluation of the steady state pressure measurements and also the transient velocity measurements with the hot wire anemometer.

A. Total Pressure Measurement - The Pitot or impact tube is instrument employed to measure the total pressure of a moving fluid stream. The tube is simply an open-end circular or other shape tube facing directly into the fluid flow. The total pressure can be related directly to the total energy of the flowing fluid.

The ideal total pressure $P_{i,\ TOT}$ of a flow is related to the freestream static pressure, P_s by the freestream Mach number M

$$\frac{P_{i,\ TOT}}{P_s} = \left(1 + \frac{\gamma-1}{2} M_\infty^2\right)^{\frac{\gamma}{\gamma-1}} \qquad (5.1)$$

where $M_\infty = \frac{U}{a}$ and $a = \sqrt{\frac{p_s}{\rho_s}\gamma}$ The velocity U is the freestream velocity and ρ_s is the freestream density. For very low freestream Mach number, equation (5.1) can be expanded in a series and only the linear term retained [1] (i.e. $M_\infty^2 (\frac{\gamma-1}{2}) < 1$)

$$\frac{P_{i,\ TOT}}{P_s} - 1 + \frac{\gamma}{2} M_\infty^2 = 1 + \frac{1}{2}\left(\frac{\rho_s U^2}{p_s \frac{P_s}{}}\right) \qquad (5.2)$$

---

[1] $$\frac{P_{i,\ TOT}}{P_s} = \left[1 + \frac{\gamma M_\infty^2}{2} + \frac{\gamma}{2}\left(\frac{2-\gamma}{24}\right) M_\infty^4 + \cdots\cdots\right]$$

The total pressure, P_{TOT} measured by the impact tube may be written as

$$\frac{P_{TOT}}{P_s} = 1 + C\left(\frac{1}{2}\frac{\rho_s U^2}{P_s}\right) \qquad (5.3)$$

C is a numerical factor which is approximately unity for all but very low Reynolds number operation.

For the flow of a gas at supersonic speeds a shock wave will form in front of the impact tube. After the shock the fluid is assumed to decelerate isentropically to the stagnation point of the probe. The total pressure is given by the Rayleigh equation

$$\frac{P_2}{P_1} = \frac{\left(\frac{\gamma+1}{2} M_\infty^2\right)^{\frac{\gamma}{\gamma-1}}}{\left(\frac{2\gamma}{\gamma+1} M_\infty^2 - \frac{\gamma-1}{\gamma+1}\right)^{\frac{1}{\gamma-1}}} \qquad (5.4)$$

where now P_2 is the ideal stagnation pressure after the normal shock wave. Figure 5.1 is a plot of equations (5.1) and (5.4).

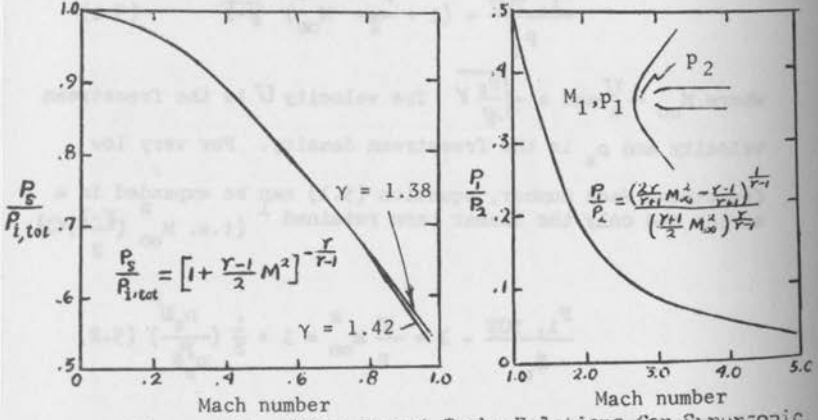

Figure 5.1 - Ideal Impact Probe Relations for Supersonic and Subsonic Flows.

The impact probe does not measure velocity directly. We must, in all cases, know the speed sound at the measured point in order to evaluate the velocity from pressure measurement. For low speeds this may require a measure of density. The measurement in each case can be shown to require an evaluation of total and static pressure, and temperature at the point in question.

Figure 5.2 is a summary plot of experimental values of C obtained for impact tubes. In general the ratio of the impact pressure to the static pressure for the impact tube can be written as

$$\frac{P_{TOT}}{P_s} = \frac{P_{i,TOT}}{P_s}\left[F\left[R_e, M_\infty, P_r, \gamma, \frac{\overline{q'^2}}{U^2}, \frac{\lambda}{r}, \frac{t}{r/U_\infty}, \frac{r_1}{r}, \frac{du}{dr}, \ldots\right]\right] \qquad (5.5)$$

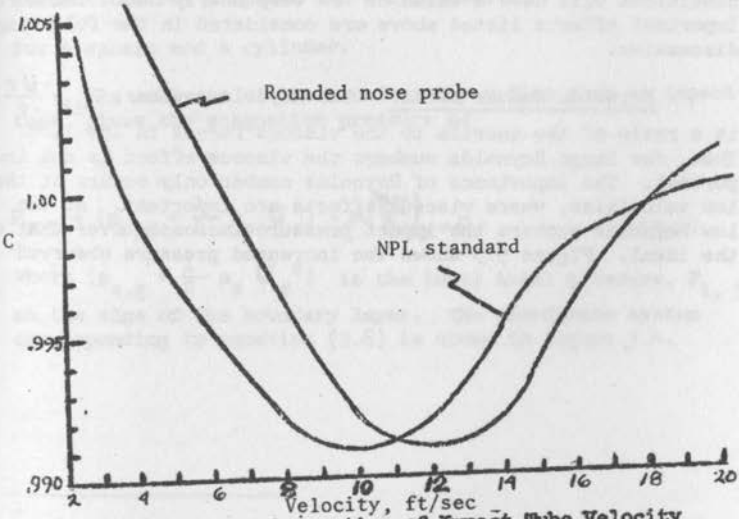

Figure 5.2 - Correction of Impact Tube Velocity Measurements.

where F[1] is a function of the dimensionless quantities:

a) Reynolds number based on probe radius, R_e
b) Local Mach number, M
c) Prandtl number, Pr
d) Specific Heat, γ
e) Turbulent intensity, $\frac{\overline{q^2}}{U^2} = \frac{u^2+v^2+w^2}{U^2}$
f) Knudsen number, λ/r
g) Ratio of relaxation time of a gas to characteristic microscopic times, $t/(r/U)$
h) Angle of attack, θ
i) Ratio of stagnation orifice to external tube, r_1/r.

It will be possible to find regions where the listed effects are quite small. In general the pitot-static tube used in moderate speed (greater than 10 feet/sec.) flows at atmospheric conditions will have a value of F very nearly one. The more important effects listed above are considered in the following discussion.

Reynolds Number Effect - The Reynolds number, $R_e = \frac{Ur}{-\nu}$ is a ratio of the inertia to the viscous forces in the flow. Thus, for large Reynolds numbers the viscous effect is not important. The importance of Reynolds number only occurs at the low velocities, where viscous effects are important. At the low Reynolds numbers the impact pressure increases over that of the ideal. Figure 5.3 shows the increased pressure observed

---

1 Chambre, P. L., and Schaaf, S.A.; The Impact Tube. Physical Measurements in Gas Dynamics and Combustion. Vol. IX Princeton

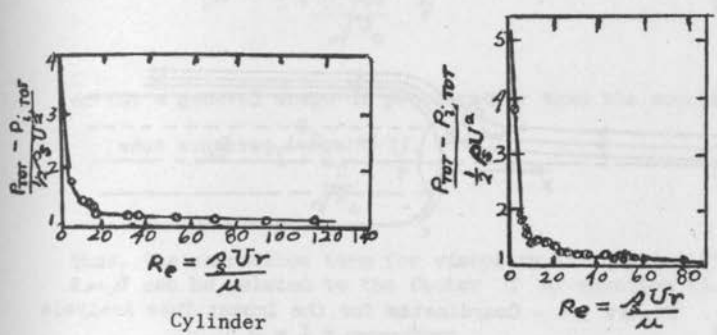

Figure 5.3 - Theoretical and Experimental Viscous Corrections For a Sphere and a Cylinder.

for a sphere and a cylinder.

An analysis of the boundary layer flow over an impact tube[1] gives the stagnation pressure as

$$P_{TOT} = (p_{s,g} + \frac{1}{2} \rho_s U_s^2) - \mu \left(\frac{\partial v}{\partial y}\right)_{y=\delta} \qquad (5.6)$$

where $(p_{s,g} + \frac{1}{2} \rho_s U_s^2)$ is the ideal total pressure, $P_{i,\,TOT}$ at the edge of the boundary layer. The coordinate system corresponding to equation (5.6) is shown in figure 5.4.

---

[1] Chambre, P. L., and Schaaf, S.A.; ibid.

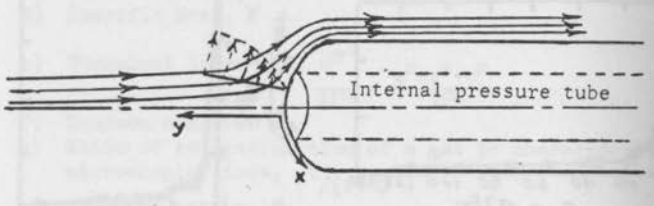

Figure 5.4 - Coordinates for the Impact Tube Analysis

The velocity derivative can be written as

$$\frac{\partial v}{\partial y} = -2\beta \tag{5.7}$$

which is a statement of the assumption that the impact probe can be represented by a potential flow shape, such as that of a source. The velocity potential for a source is

$$\phi = Uy + \frac{r_o^2 U}{\left[x^2+(y+r_o)^2\right]^{1/2}} \tag{5.8}$$

and β becomes

$$\beta = \frac{U}{r_o} \tag{5.9}$$

where r_o is the radius of curvature of the edge of the boundary layer. The boundary layer displacement thickness at the stagnation point is

$$\delta^* = 0.5576 \sqrt{\frac{\nu}{\beta}} \tag{5.10}$$

so that β can be evaluated as

$$\beta = \frac{2}{1 + \frac{0.394}{\sqrt{R_e}}} \frac{U}{r} \tag{5.11}$$

or for a general shape of probe rather than the source

$$\beta = \frac{C_1}{1 + \frac{C_2}{\sqrt{R_e}}} \frac{U}{r} \tag{5.12}$$

Thus, the correction term for viscosity in equation (5.6), $2\mu\beta$ can be related to the factor C of equation (5.3) as

$$C = 1 + \frac{4C_1}{R_e + C_2\sqrt{R_e}} \tag{5.13}$$

For subsonic compressible flow the correction β is given as[1]

$$\beta_{COMPR.} \simeq \beta_{INCOMPR.} (1 - C_3 M^2) \tag{5.14}$$

The constant C_3 for a spherical-shaped probe is

$$C_3 = \frac{83}{330}$$

For supersonic flow the analysis is not applicable and the only information is of an experimental nature. Figure 5.5 shows viscous corrections evaluated in supersonic flows.

---

1 Chambre, P. L., and Schaaf, S.A.; ibid

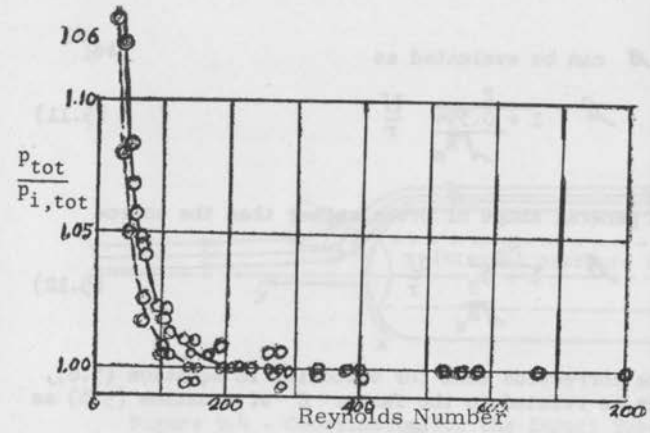

Figure 5.5 - Viscous Corrections to Impact Pressure in Supersonic Flow.

Orifice Diameter Effect - The above analysis does not consider the effect of the size of the orifice. This aspect of the problem is by no means well evaluated, however, it appears that the orifice size will in general lower the actual total pressure reading. Chambre and Schaaf give the following correction for orifice effect

$$P_{TOT,AVE} = P_{TOT,ACT.} - \frac{\beta^2 \rho_s r_1^2}{4} \qquad (5.15)$$

where $P_{TOT,AVE}$ is the average pressure reading by the probe, and r_1 is the orifice radius. An Orifice small compared to probe frontal area is found desirable for supersonic measurements.

Angle of Attack - The above analysis assumed that the flow as directly into the impact tube. If the tube is misalined to the flow, we may expect that the measured total pressure will be too small. Figure 5.6 is a summary of the variation in pressure coefficient observed for impact probes[1]

---

[1] Krause, R.N., and Gettelman: Considerations Entering into the Selection of Probes for Pressure Measurements in Jet Engines, 15A Proc., Vol. 7, p. 134, 1952.

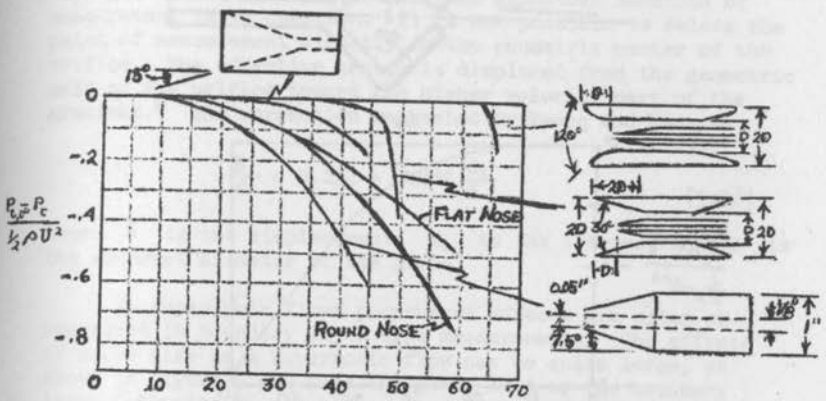

Figure 5.6 - Error Due to Impact Probe Angle of Attack.

The effect of flow angle can be thought of as a simple matter of where the stagnation point is located. As long as the stagnation point is located within the orifice area the angle effect is small. This stagnation point effect is demonstrated by the "wide mouth" type tube showing the least effect to flow angle. The wide mouth probe limits somewhat the point type measurement of the smaller tip geometry, but would be employed when large flow direction changes are expected.

The angle sensitivity of a probe may be employed to determine the flow direction. In this case the probe would be operated at an angle where maximum change with angle occurs. Figure 5.7 shows the sensitivity of a particular probe over a wide range of angles. A typical flow direction probe may employ two or more probes set at 45° to the expected flow direction, as shown in the insert of figure 5.7. The yaw pro is rotated so that a null reading is obtained between the two tubes. The null location would represent the flow direction. The difference in pressure between the two tubes can also be employed as an indication of flow direction, without the need of yawing the tubes. A combination of four tubes rather than two can be employed to find the flow direction in three-dimensions.

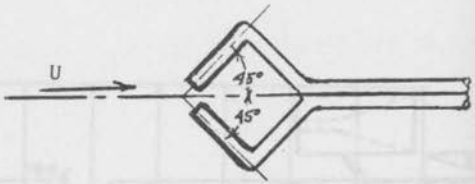

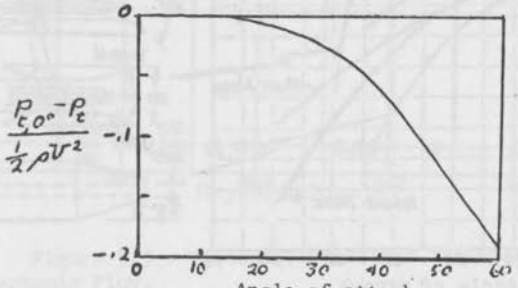

Figure 5.7 - Angle Sensitivity of an Impact Tube

The sensitivity of impact tubes to angle of attack in supersonic flow is shown in figure 5.8. At supersonic speeds the blunter-nosed tubes appear less sensitivity to angle than the slender probes.

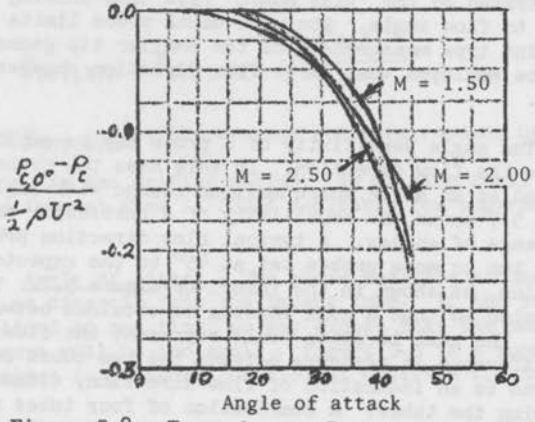

Figure 5.8[1] - Error Due to Impact Tube Angle of Attack in Supersonic Flow.

[1] Wilson: J. Aero. Sci., Vol. 17 585-594 (1950)

Velocity Gradient Measurements - If the impact tube is employed in a velocity gradient, the geometric location of measurement is in question. It is not possible to relate the point of measurement directly to the geometric center of the orifice. The effective center is displaced from the geometric axis of the orifice toward the higher velocity part of the gradient.[2] The correction suggested by Young and Maas is

$$\frac{\delta}{d} = 0.131 + 0.082 \frac{d_1}{d} \qquad (5.16)$$

where δ is the displacement, d_1 is the internal and d is the external diameter of the probe.

In supersonic flows pronounced effects are often encountered in boundary layer type measurements. The effects of probe size in a supersonic flow can be quite large, as shown in figure 5.9. Near the outer edge of the boundary layer (velocity gradient) an overshoot in velocity is noted. This overshoot in velocity is apparently to the probe affecting the upstream flow in the boundary layer.[1] In supersonic boundary layer measurements the shock wave formed in front of the probe may cause a local separation of the boundary layer. The separation of the boundary layer feed information upstream through the subsonic portion of the layer, thus causing a distortion of the complete layer.

---

2 Young, A.D., and Maas, J.N. The Behavior of a Pitot Tube in a Transverse Total-Pressure Gradient. Aeronaut Research Comm., Repts Memo. 1770, 1937

1 Morkovin, M.V., and Bradfield, W.S.; Probe Interference in Measurements in Supersonic Laminar Boundary Layers, Jour. Aero. Sci., vol. 21, p. 785, 1954.

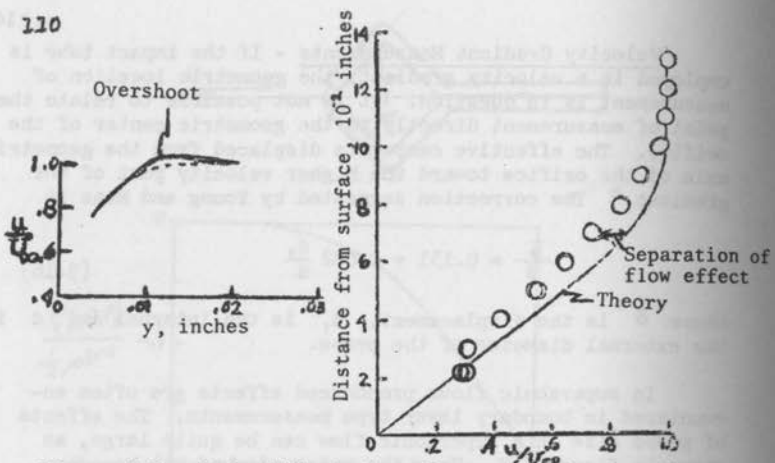

Figure 5.9 - Probe Effects in a Supersonic Boundary Layer.

Turbulent Effects on Velocity Measurements - Goldstein[2] has suggested that the impact pressure P_{TOT} will be equal to

$$P_{TOT} = P_s + \frac{1}{2}\rho U^2 + \frac{1}{2}\rho_s \overline{q'^2} \qquad (5.17)$$

where, $\overline{q'^2} = \overline{u'^2} + \overline{v'^2} + \overline{w'^2}$, is the sum of the turbulent velocity components. Such a relation is found to work reasonably for high turbulent flows. Figure 5.10 shows an example of a pitot-static probe velocity profile compared with a profile measured by a hot wire anemometer.[3] The pitot-static profile corrected for turbulence effects is found to agree reasonably well with the hot-wire profile. For the flow of figure 5.10 the turbulence level is extremely high compared to most fluid flows.

---

2 Goldstein, S.; A Note on the Measurement of Total Head and Static Pressure in a Turbulent Stream. Proc. Roy. Soc. London A155, p 570 (1936)

3 Cho, J. L., and Sandborn, V.A.; - A Resistance Thermometer for Transient Temperature Measurements. Fluid Mech. Paper No. 2. Colo. State Univ., 1964.

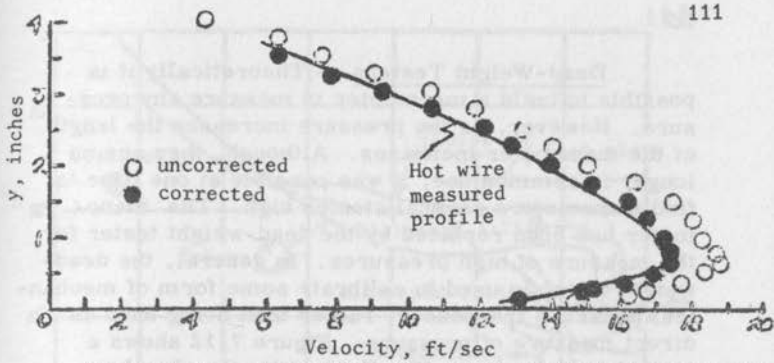

Figure 5.10 - Correction of a pitot static probe Velocity Profile For Turbulence Effects

Rarefied Gas Effects - Rarefied gas flows are defined as those in which the dimensions of the body in question are of the same order as the molecular mean free path. The velocity at the surface of a body is non zero in a rarefied gas flow. The gas "slips" along the surface of a body. Results indicate that the mean pressure at the stagnation point will decrease due to the effect of slip.[1] The effect of slip is to increase the viscous correction to the impact pressure. Figure 5.11 shows the effect of slip on the viscous correction.

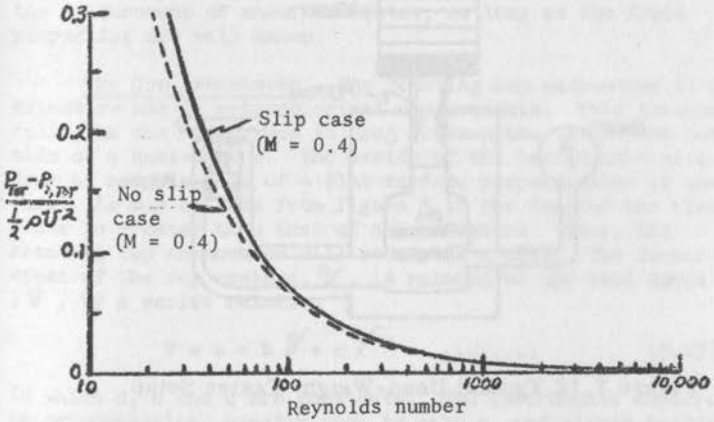

Figure 5.11 - Effect of Slip on the Viscous Correction to Impact Pressure

---

1 Chambre, P.L., and Schaaf, S.A.; ibid.

Dead-Weight Testers. - Theoretically it is possible to build a manometer to measure any pressure. However, as the pressure increases the length of the manometer increases. Although, they are no longer in common use, it was possible at one time to find manometers several stories high. The manometer has been replaced by the dead-weight tester for the measure of high pressures. In general, the dead-weight tester is used to calibrate some form of mechanical pressure transducer, rather than being used as a direct measure of pressure. Figure 7.12 shows a typical tester setup. The fluid within the chamber (an oil) transmits the weights to the gauge and produces a pressure. As long as the friction between the cylinder and piston and flows of oil around the piston are negligible the pressure can be computed. The pressure produced by the weights depends on the effective area of the piston, which depends in turn on the clearance between the piston and the cylinder. The plunger is employed to correct for compression of the oil.

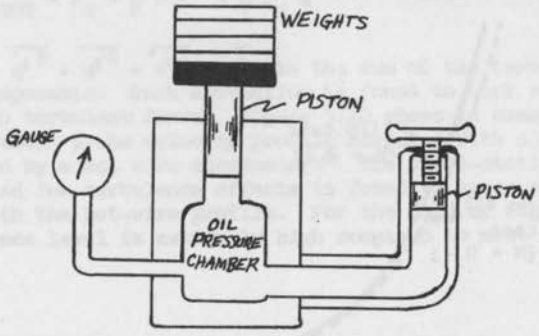

Figure 7.12 Typical Dead-Weight Tester Setup.

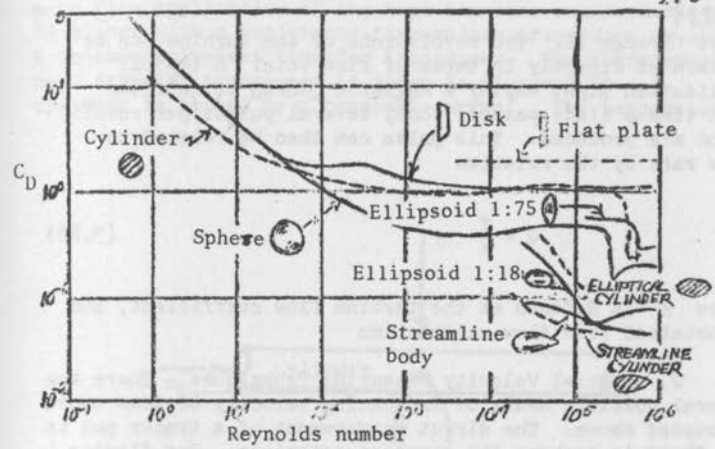

Figure 5.12 - Drag of Different Shapes

The Rotameter - The rotameter relies on the drag of a body in a restricted flow tube. A "floating bob" is raised upward in a tapered tube by the drag and buoyancy force of the flowing fluid. The upward forces are balanced by the weight of the bob. The rotameter measures the mass rate of flow through the tube. These devices are suited to the measurement of mass flow rates, as long as the fluid properties are well known.

The Cup Anemometer - The rotating cup anemometer is in extensive use in meteorological measurements. This instrument relies on the difference in drag between the inside and outside of a hemi-sphere. The inside of the hemi-sphere gives a drag of roughly that of a flat surface perpendicular to the flow. As may be seen from figure 5.12 the drag of the flat plate is greater than that of a hemi-sphere. Thus, the rotating cup anemometer will rotate in a wind. The linear speed of the cup centers, $\mathcal{V}$, is related to the wind speed, V, by a series relation

$$V = a + b\mathcal{V} + c\mathcal{V}^2 + \ldots\ldots \qquad (5.19)$$

in which a, b and c are constants. The instruments employed in meteorological usually seek to make c and higher coefficients zero or very small.

Turbine Flow Meters - The movement of a fluid through a small turbine wheel can be used to measure the mass flow. The drag of the turbine blades produces a rotation as the fluid

flows through it. The revolutions of the turbine can be calibrated directly in terms of flow rate. A typical application might employ a magnetic pickup to indicate each time a blade passes, thus, several pulses per revolution are produced. This pulse can then be related to flow rate by the relation

$$Q = \frac{f}{k} \tag{5.20}$$

where k is defined as the turbine flow coefficient, and is obtained from flow calibration

C. Special Velocity Measuring Techniques - There are several possible means of indicating velocity besides those discussed above. The direct measurement of a tracer put in the fluid is perhaps the simplest technique. For flowing liquids the use of a floating particle is a good indication of the velocity. The tracer must, of course, move along with the flow velocity in order to be of value. The tracer must be carried along by the shear force of the fluid, so that there is a question whether the tracer moves at the velocity of the liquid. Techniques that employ bubbles of the same weight as a flowing gas are also used to measure gas flow. Tracer techniques are at best, first estimates of flow velocity, and not likely to give accurate measurements. Ionized and radioactive tracers are also employed in special cases. These molecular sized particles are quite accurate since they are of the same dimensions as the fluid particles.

Heat transfer techniques are employed to measure velocities in special cases. The heat transfer from a cylinder is found to be related to the mean velocity by the following relation

$$i^2R = A + B\,(U)^n \tag{5.21}$$

where n is of the order of 0.5. The heat transfer is related to the square root of velocity, so it is not as sensitive as the pitot-static relation. On the other hand, the heat transfer is measured in terms of electrical readouts, which can be measured to a much greater degree of accuracy than pressure. As a result, a heat transfer anemometer can be used for accurate measurement of velocities down to less than one foot per second. The major application of the heat transfer anemometer is the Hot Wire Anemometer. The hot wire anemometer is discussed in detail in the section on transient measurements. The

mean flow application of the heat transfer anemometer can be either with a resistance-temperature transducer or with a thermocouple-heat transfer transducer. The thermocouple-heat transfer transducer is shown in figure 5.13. A cylinder is heated by a constant current. The temperature

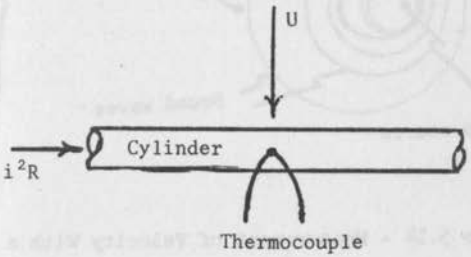

Figure 5.13 - Thermocouple-Heat Transfer Transducer.

of the cylinder is measured by a thermocouple, the output of the thermocouple is a direct measure of the cooling of the cylinder by the air flow. The system is usually calibrated against a standard velocity. These instruments are found to be quite accurate in the measure of velocity. The detailed theory of the device is almost identical with the hot wire which is given in the following section.

The velocity of a fast moving fluid may be measured by the proportion of a sound wave. A source of sound is produced at a point in a flow, figure 5.14. A sound pickup downstream measures the time between the pulse and the arrival of the wave. The velocity of propagation is

$$V = a + U = \frac{\ell}{t} \qquad (5.22)$$

where V is the measured propagation, which is given as ℓ/t,

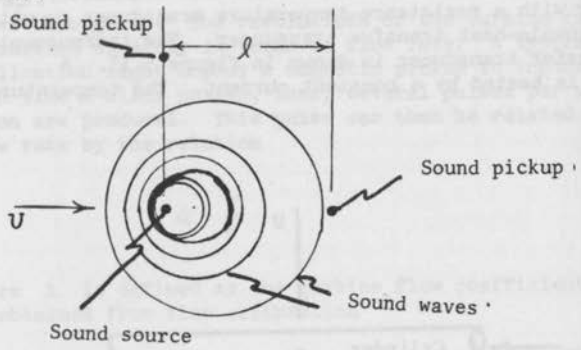

Figure 5.14 - Measurement of Velocity With a Sound Wave.

a is the speed of sound which is a function of the absolute temperature, and U is the velocity of the fluid. For reasonable measurements U must be of the order of a, which is around 1100 ft./sec. Thus, the sonic anemometer is not considered for extreme low velocity measurements. By using two equally spaced sound pickups, one at right angles to the flow, then we can measure directly the speed of sound; and the difference in time between the two pickup readings is equal to the flow velocity. Sonic anemometers are used in meteorolical measurements, because of their ability to indicate transient fluctuations. The measurements are sensitive to changes in temperature and humidity, which limits somewhat the accuracy of calculations. The source of sound may be an expanding crystal or a spark gap. If a spark gap is employed the velocity may also be checked by measuring the propagation of the temperature pulse.

Another system of measuring velocity is the vortex shedding cylinder. This device might best be classed under the heading of a drag instrument. At moderate and low velocities it is found that flow separating from a cylinder produces a regular vortex pattern downstream of the cylinder. The vortex shedding frequency is a direct function of the flow velocity, thus a measure of the frequency will be a measure of the flow velocity. Figure 5.15 is a plot of the Strouhal number, S

$$S = \frac{fd}{U} \qquad (5.23)$$

(where f is the shedding frequency, d is the cylinder diameter and U is the free stream velocity) as a function of Reynolds number.

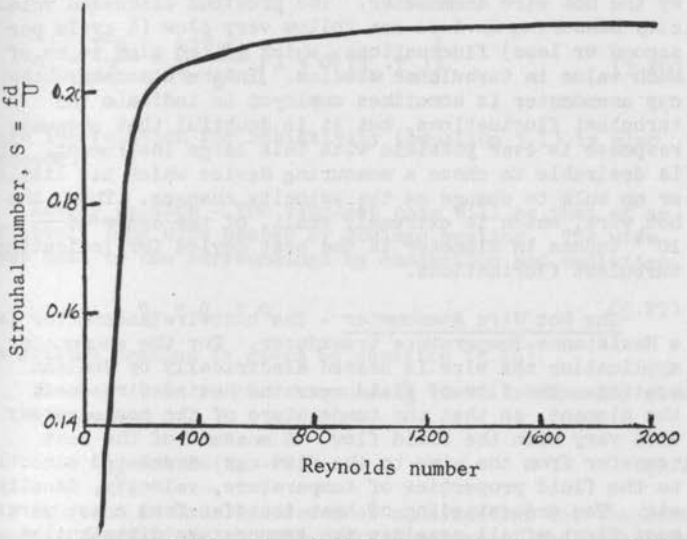

Figure 5.15 - Strouhal Number as a Function of Reynolds Number.

D. Transient Velocity Measurements - The measurement of transient velocities is almost exclusively done by the hot wire anemometer. The previous discussed velocity measuring devices can follow very slow (1 cycle per second or less) fluctuations, which is too slow to be of much value in turbulence studies. In the atmosphere the cup anemometer is sometimes employed to indicate the turbulent fluctuations, but it is doubtful that adequate response is ever possible with this large instrument. It is desirable to chose a measuring device which has little or no bulk to change as the velocity changes. Thus, the hot wire, which is extremely small, of the order of 10^{-4} inches in diameter is the best device for indicating turbulent fluctuations.

The Hot Wire Anemometer - The hot wire anemometer is a Resistance-Temperature transducer. For the anemometer application the wire is heated electrically by Joulean heating. The flow of fluid over the heated wire cools the element, so that the temperature of the heated wire will vary with the fluid flow. A measure of the heat transfer from the wire to the flow can be related directly to the fluid properties of temperature, velocity, density, etc. The understanding of heat transfer from a hot wire must first of all consider the temperature distribution within and along the wire. The temperature distributions can be predicted from energy balances.

Resistance-Temperature Relation - The resistance of a metalic conductor, such as platinum shown in figure 3.1, can be represented by a relation of the form

$$R = R_o \left[1 + \alpha(T-T_o) + \beta(T-T_o)^2 + \ldots\ldots\right] \qquad (5.24)$$

In specific cases the temperature range of the conductor can be restricted to limits where the higher order temperature dependence can be neglected. Thus, for the present discussion we will assume that equation (5.24) is

$$R = R_o \left[1 + \alpha (T-T_o)\right] \qquad (5.25)$$

This relation is adequate for metals such as platinum, tungsten, copper, etc., however it is not valid for materials such as nickel or iron.

The Joulean heating per unit length of a hot wire can be written as

$$q_j = \frac{I^2 R}{\ell} = \frac{4I^2 \sigma_o}{\pi D^2}\left[1 + \alpha (T_w - T_o)\right] \qquad (5.26)$$

where the relation for resistivity (equation 3.1) is also employed.

Energy Balance - The simplest case will be that of an infinitely long wire heated by Joulean heating. The wire loses heat to the surroundings by conduction and radiation.

$$q_j = q_c + q_r \qquad (5.27)$$

The Joulean heating is given by equation (5.26).

The heat loss to the surrounding fluid is normally given by the relation

$$q_c = h\pi D\ (T_w - T) \qquad (5.28)$$

This equation is usually viewed as a definition for the heat transfer coefficient, h. The actual nature of the heat transfer coefficient will depend on the specific application of the anemometer. For normal continuum flow h, varies as the velocity of the fluid flow. The heat transfer coefficient varies from fluid to fluid, and also it varies if the fluid properties change due to temperature or pressure. For the present analysis it is assumed that h is independent of temperature.

The radiation term can be linearized by defining a "heat transfer coefficient of radiation." Consideration of higher order approximations for the wire temperature distribution can include a temperature dependence for the heat transfer coefficient of the form

$$h = h_o + h_1 \Delta T + h_2 \Delta T^2 + \ldots . \qquad (5.29)$$

a relation of this type can be employed to account for the temperature effect on fluid properties. For most heat transfer applications it is desirable to employ some form of a film temperature to produce average fluid properties. However,

the temperature distribution along the wire will vary by several hundred degrees, so that it would be difficult to define a simple film temperature.

The second type of heat loss listed in Equation (5.27) is radiation. For the infinite length hot wire operating in a vacuum radiation may be the only heat loss. For the radiation case the heat loss will depend on the difference of the fourth power of the temperatures. The radiation heat loss is defined in terms of a surface emissivity, ϵ , by the relation

$$q_r = \epsilon \sigma_{sb} \pi D (T_w^4 - T^4) \tag{5.30}$$

where σ_{sb} is the Stefan-Boltzmann radiation constant. The value of ϵ depends on the surface properties of the hot wire.

Equation (5.27) becomes

$$\frac{4I^2\sigma_o}{\pi D^2}\left[1 + \alpha (T_w - T_o)\right] = h\pi D (T_w - T) + \epsilon \sigma_{sb} \pi D (T_w^4 - T^4) \tag{5.31}$$

For a given wire, current input, heat transfer coefficient emissivity, and fluid temperature the infinite long wire temperature can be calculated from Equation (5.31).

For most molar conduction applications the radiation heat transfer can be neglected particularly if the wire temperature is not too great. Neglecting radiation the infinite long wire temperature is

$$T_{w,\infty} = \frac{\frac{4I^2\sigma_o}{\pi D^2}(\alpha T_o - 1) - h\pi DT}{\frac{4I^2\sigma_o \alpha}{\pi D^2} - h\pi D} \tag{5.32}$$

The case of an infinite length wire is of limited use since many of the resistance temperature transducer applications will employ short length wires. Thus, the general energy balance must

include a term for the conduction to the wire supports. Figure 5.16 is a diagram of a typical hot wire geometry. The heat input is still Joulean heating. The heat loss is by; a) conduction to the fluid, b) radiation to the fluid, and c) conduction to the wire supports. For the analysis it is assumed that the wire support temperature is known. Since the supports are usually very large compared to the hot wire, it is found that Joulean heating of the supports can be neglected. Equation 5.27 for the wire of figure 5.16 becomes

$$q_j = q_c + q_r + q_k \tag{5.33}$$

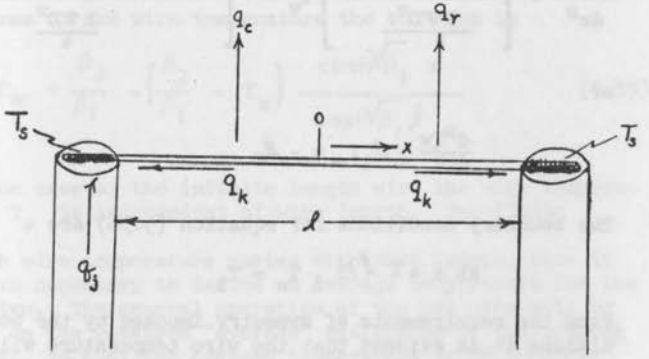

Figure 5.16 - Heat Balance of a Hot Wire Sensing Element.

where q_k is the heat loss by conduction to the wire supports. Thermal conduction within a metal is expressed in terms of the thermal conductivity of the material, k by the relation

$$q_k = - k \frac{\pi D^2}{4} \frac{d^2 Tw}{dx^2} \tag{5.34}$$

Equation (5.33) becomes

$$\frac{4I^2\sigma_o}{\pi D^2}\left[1+\alpha(T_w-T_o)\right] = h\pi D(T_w-T_a)+\epsilon\sigma_{SB}\pi D(T_w^4-T_a^4) - k\frac{\pi D^2}{4}\frac{d^2Tw}{dx^2} \qquad (5.35)$$

A general solution of equation (5.35) is not available. Some computer evaluations for special cases have been worked out.

The case where radiation can be neglected is of specific importance in the anemometer application and for part of the hot wire anemometer range of application. Neglecting radiation equation (5.35) can be written as

$$\frac{d^2Tw}{dx^2} - \left[\frac{h D\pi - \frac{4I^2\sigma_o\alpha}{\pi D^2}}{\frac{k\pi D^2}{4}}\right]T_w = -\left[\frac{h D\pi T_a - \frac{4I^2\sigma}{\pi D^2}(\alpha T_o - 1)}{\frac{k\pi D^2}{4}}\right]$$

or

$$\frac{d^2Tw}{dx^2} - \beta_1 T_w = -\beta_2 \qquad (5.36)$$

The boundary conditions for equation (5.36) are

$$\text{at } x = \pm l/2\ ,\ T_w = T_s$$

From the requirements of symmetry imposed by the boundary conditions it is evident that the wire temperature will be a maximum at x=0. Thus, the boundary conditions can also be expressed as

$$\text{at } x = 0,\ \frac{d\,T_w}{dx} = 0\ .$$

Equation (5.36) is quite common in heat transfer analysis and is solved by change of variable; this gives

$$\theta = -\left(\frac{\beta_2}{\beta_1}\right) + T_w,$$

the following homogeneous differential equation

$$\frac{d^2\theta}{dx^2} - \beta_1\theta = 0 \qquad (5.37)$$

with the boundary conditions

$$\left.\frac{dTx}{dx}\right|_{x=0} = \left.\frac{d\Theta w}{dx}\right|_{x=0} = 0$$

$$\theta_s = (T_s - T_{w,\infty}) \qquad \text{at } x = \pm \left(\frac{\ell}{2}\right)$$

where $T_{w,\infty}$ is the infinite long wire temperature. The solution for equation (5.37) is outlined by Wylie[1], with the results in terms of θ given as

$$\theta = \theta_s \frac{\cosh \beta_1^{\frac{1}{2}} x}{\cosh \beta_1^{\frac{1}{2}} \frac{\ell}{2}} \tag{5.38}$$

In terms of the wire temperature the solution is

$$T_w = \frac{\beta_2}{\beta_1} - \left(\frac{\beta_2}{\beta_1} - T_s\right) \frac{\cosh \sqrt{\beta_1}\, x}{\cosh \sqrt{\beta_1} \frac{\ell}{2}} \tag{5.39}$$

For the case of the infinite length wire the wire temperature T_w is independent of wire length. The finite length wire temperature varies with wire length, thus it appears necessary to define an average temperature for the hot wire. The general operation of the hot wire will be based on the measured "average" resistance of the sensing element, so that the average temperature is of specific importance. The average temperature is obtained by integrating equation (5.39) over the hot wire length.

$$\bar{T}_w = \frac{1}{\ell} \int_{-\frac{\ell}{2}}^{+\frac{\ell}{2}} T_w dx = \frac{\beta_2}{\beta_1} - \left(\frac{\beta_2}{\beta_1} - T_s\right) \frac{\text{TANH} \frac{\sqrt{\beta_1}\,\ell}{2}}{\frac{\sqrt{\beta_1}\,\ell}{2}} \tag{5.40}$$

Figure (5.17) is a plot of equation (5.39) for a typical set of hot wire anemometer conditions. Values of the

[1] Wylie, C.R.; *Advanced Engineering Mathematics*. McGraw-Hill Book Co., 1951.

infinite length, and finite length average wire temperatures are also noted on the figure.

The above analysis applies for the case where heat is transferred from the wire to the fluid stream.

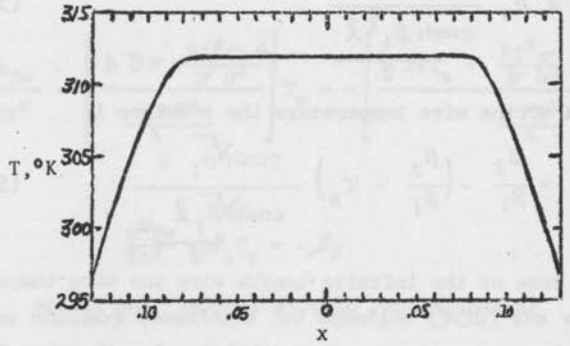

Figure 5.17 - Temperature distribution along a convection controled hot wire.

Length Average Temperature Related to Resistance

The resistance of a hot wire measured by an instrument will correspond to the length average temperature. The length average temperature was computed in the preceeding section for each of the three cases considered. For the convection controled case equation (5.40) is the length average temperature. Thus, the resistance of the convection controled hot wire is obtained by using equation (5.40) for $\bar{T}_w$ in equation (5.25) or perhaps equation (5.24) if a more exact relation is required. For equation (5.25)

$$R_w = R_o \left[1 + \alpha \left\{ \frac{\beta_2}{\beta_1} - \left(\frac{\beta_2}{\beta_1} - T_s \right) \frac{\text{TANH} \frac{\sqrt{\beta_1}\,\ell}{2}}{\frac{\sqrt{\beta_1}\,\ell}{2}} - T_o \right\} \right] \tag{5.41}$$

Thus, the measure resistance of a hot wire can be related directly to the physical properties and the wire support temperature. In application the interest will always be to determine the length average temperature from a measure of the wire resistance.

Circumferential and Radial Temperature Gradients

In the previous section the radial and circumferential temperature gradients that might exist in the wire were neglected. The heat transfer that will be considered in the next section, will be found to vary around the circumference of the hot wire. Such an uneven heat transfer may well require the temperature to vary around the circumference of the wire. These effects will be more important the larger the diameter of the wire. It is usually assumed that the very small anemometer wires (4×10^{-4} cm in diameter), no axial gradient can be supported.

Heat Conduction From the Wire to its Supports - The main use of the resistance-temperature wire will be to measure heat transfer. Accurate measure of the heat transfer must take into account the heat lost to the supports. Thus, if a wire is placed in a flowing medium, it will lose heat to the fluid and to its supports. The energy balance on the entire wire may be obtained by considering 5.18.

$$Q_J = Q_c + 2\,Q_k \tag{5.42}$$

which may be written as

$$I^2 R_w = h \pi d_w \ell \,(\bar{T}_w - T_a) + 2Q_k \tag{5.43}$$

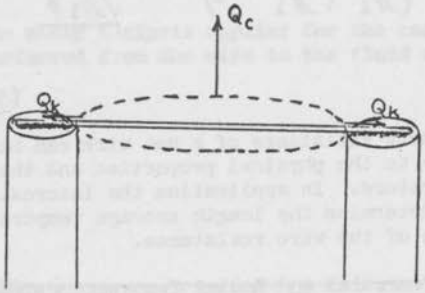

Figure 5.18 - Convection Controlled Energy Balance on a Hot Wire.

The conduction to the supports can be found by applying the Fourier-Biot conduction equation at the point of attachment.

$$Q_k = - K_w \frac{\pi D^2}{4} \left. \frac{dTw}{dx} \right|_{x = \frac{l}{2}} \frac{l}{2} \qquad (5.44)$$

The gradient is obtained by differentiating equation (5.39)

$$\frac{dTw}{dx} = - \left(\frac{\beta_2}{\beta_1} - T_s \right) \frac{\text{SINH} \beta_1^{\frac{1}{2}} x}{\text{COSH} \beta_1^{\frac{1}{2}} \frac{l}{2}} \beta_1^{\frac{1}{2}} \qquad (5.45)$$

or

$$\left.\frac{dTw}{dx}\right|_{x=\frac{\ell}{2}} = -\left(\frac{\beta_2}{\beta_1} - T_s\right)\beta_1^{\frac{1}{2}} \text{ TANH } \frac{\beta_1^{\frac{1}{2}}\ell}{2} \qquad (5.46)$$

equation (5.43) may now be written as

$$I^2 r_o \left[1 + \alpha(\bar{T}_w - T_o)\right] = \pi h D_w (T_w - T_a) + \frac{K_w \pi D^2 \beta_1^{\frac{1}{2}}}{2\ell}\left(\frac{\beta_2}{\beta_1} - T_s\right) \text{ TANH } \frac{\beta_1^{\frac{1}{2}}\ell}{2} \qquad (5.47)$$

Thus, the ratio of the heat loss by conduction to the wire supports to that lost directly to the air stream by convection is

$$\zeta = \frac{K_w \pi D^2}{\ell^2} \frac{\left(\frac{\beta_2}{\beta_1} - T_s\right)\left(\frac{\beta_1^{\frac{1}{2}}\ell}{2}\right) \text{ TANH } \frac{\beta_1^{\frac{1}{2}}\ell}{2}}{\pi K_f Nu_f (T_w - T_e)} \qquad (5.48)$$

where $Nu_f = \frac{hD}{K_f}$. The energy balance, equation (5.47) becomes

$$I^2 ro \left[1 + \alpha(\bar{T}_w - T_o)\right] = \pi K_f Nu_f (\bar{T}_w - T_a)(1 + \zeta) \qquad (5.49)$$

The subscript f denotes conditions evaluated at the average temperature between the fluid and the wire. The major difficulty in evaluating the heat loss due to convection is determining the value of the wire support temperature. The solution of equations (5.48) and (5.49) is difficult,[1] but it can be solved in an adequate form. A simpler technique was developed by Kovasznay[2] by assuming the wire support temperature is that of the free stream. The ratio of the actual heat transfer Nusselt number, N_u, to the measured Nusselt number, N_u'' can be written as

[1] Baldwin, L.V.: Slip Flow Heat Transfer From Cylinders in Subsonic Airstreams. NACA TN 4269, 1958.

[2] Kovasznay: L.S.G.: Turbulent Measurements. Vol. IX Physical Measurements in Gas Dynamics and Combustion. Princeton Univ. Press, 1954.

$$\frac{N_u}{N_u''} = \frac{\frac{\bar{a}}{a^*} + \bar{a}}{1 + \bar{a}} \qquad (5.50)$$

where

$$\bar{a} = \frac{R_w - R_e}{R_e}$$

$$\frac{\bar{a}}{a^*} = 1 - S\left(\frac{a^*}{\bar{a}}\right) \text{ TANH } \frac{1}{S} \left(\frac{\bar{a}}{a^*}\right)$$

$$S = \frac{D_w}{\lambda}\left(\frac{K_w}{K_f}\right)^{\frac{1}{2}} (N_u'')^{-\frac{1}{2}} \left(1 + \bar{a}\right)^{\frac{1}{2}}$$

The reference temperature of the wire, (temperature-resistance calibration), is taken at T_e rather than 32^oF to simplify the calculations. The solution of $\frac{\bar{a}}{a^*}$ as a function of S is shown in figure (5.19). Use of figure (5.19) together with equation (5.50) is a quick means of correcting for the heat loss to the supports.

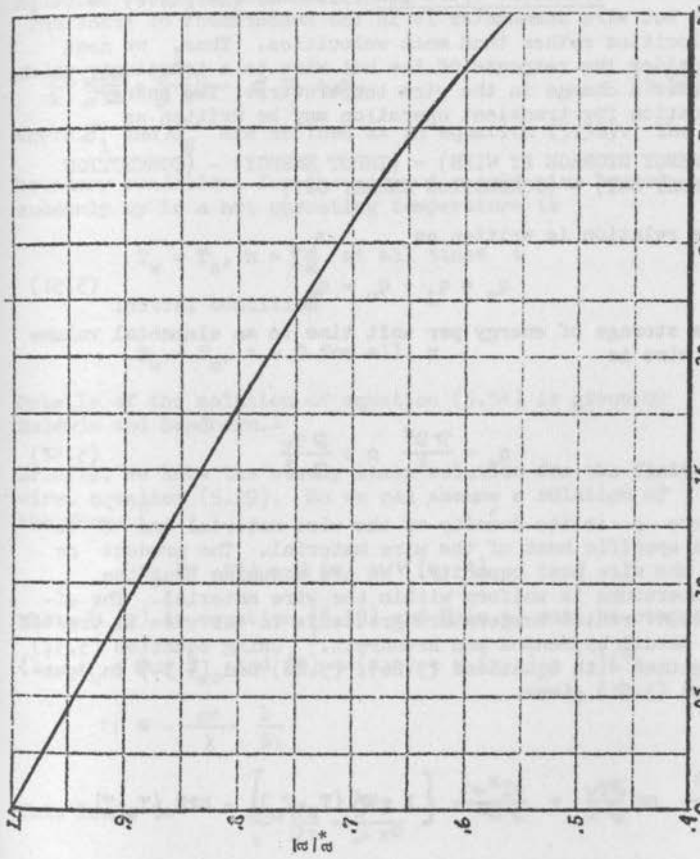

Figure 5.19 - Solution of $\bar{a}/a^*$ as a function of S

Transient Operation - The major application of the hot wire anemometer is in the measurement of transient velocities rather than mean velocities. Thus, we need consider the response of the hot wire to a transient, which causes a change in the wire temperature. The energy equation for transient operation may be written as

(ENERGY STORAGE BY WIRE) = (INPUT ENERGY) - (CONVECTION ENERGY OUT) - (CONDUCTION ENERGY OUT)

The relation is written as

$$q_s = q_j - q_c - q_k \tag{5.51}$$

The storage of energy per unit time in an elemental volume of wire is

$$q_s = \frac{\pi D^2}{4} \rho c \frac{\partial T_w}{\partial t} \tag{5.52}$$

where ρ is the density of the wire material and c is the specific heat of the wire material. The product ρc is the wire heat capacity. We are assuming that the temperature is uniform within the wire material. The effect of radial temperature gradients in the wire is treated in detail by Benson and Brundrett.[1] Using equation (5.52) together with equations (5.26), (5.28) and (5.34) in equation (5.51) gives

$$\frac{\pi D^2}{4} \rho c \frac{\partial T_w}{\partial t} = \frac{4I^2 \sigma_o}{\pi D^2} \left[1 + \alpha (T_w - T_o) \right] - h \pi D (T_w - T) + K \frac{\pi D^2}{4} \frac{d^2 T_w}{dx^2} \tag{5.53}$$

---

1 Benson, R.S., and Brundrett, G.W.; Development of a Resistance Wire Thermometer for Measuring Transient Temperature in Exhaust Systems of Internal Combustion Engines. Temperature, its Measurement and Control in Science and Industry. Vol. 3 (Reinhold Pub. Corp. New York((196)

Equation (5.53) may be written as

$$\frac{\rho c}{k}\frac{\partial T_w}{\partial t} = \frac{\partial^2 T_w}{\partial x^2} - \beta_1 T_w + \beta_2 \qquad (5.54)$$

where β_1 and β_2 are defined as in equation (5.36). The boundary conditions for the case of a cold wire heated suddenly up to a hot operating temperature is

$$T_w = T_s,\ x = \pm\frac{\ell}{2} \text{ at all times } t$$

Initial condition

$$T_w = T_s,\ t = 0 \text{ for all } x$$

Details of the solution of equation (5.54) is given by Baldwin and Sandborn.[1]

Briefly, we know the steady state solution for the finite wire, equation (5.39). So we can assume a solution of the form:

$$t_w(x, t^*) = U(x) + \nu(x, t)$$

where $U(x)$ is equation (5.39) and $U(x,t)$ must be computed

(1) $t_w = \theta + T_{oo}$ and (2) $\nu(x,t) = w(x,t)\, e^{-t/\tau}$,

$$\tau_1 \equiv -\frac{\rho c}{k}\frac{1}{\beta_1}$$

This leads to $$\frac{\rho c}{k}\frac{\partial w}{\partial t} = \frac{\partial^2 w}{\partial x^2}$$

Assume a product solution (e.g. ref., Wylie, C.R. Advanced Engineering Mathematics, McGraw-Hill Book Co. New York, (1951)

---

[1] Baldwin, L. V., and Sandborn, V.A.; Hot-Wire Calorimeter: Theory and Application to Ion Rocket Research NASA TR R-98, (1961).

$$w(x,t) = T(t)\,X(x)$$

the equation becomes

$$(\text{eq}\beta)\ \frac{1}{T}\frac{\partial T}{\partial t} = \frac{\partial^2 X}{\partial x^2}\frac{1}{X} = -\lambda^2$$

or

$$w(x,t) = C\ e^{-\left(\frac{\lambda^2 kt}{\rho c}\right)} \cos \lambda x$$

Only way to fit the boundary conditions is to require:

$$\cos \frac{\lambda \ell}{2} = 0$$

So

$$\lambda_n = \frac{2}{\ell}\left(n\pi + \frac{\pi}{2}\right)$$ eigenvalues, n = 0, 1, 2, 3, etc.

The solution can be written as

$$t_w - \frac{\beta 2}{\beta 1} = \left(T_s - \frac{\beta 2}{\beta 1}\right)\frac{\cosh\sqrt{\beta_1}\,x}{\cosh\sqrt{\beta_1}\frac{\ell}{2}} + \sum_{n=0}^{\infty} C_n e^{-\left(\frac{\lambda^2 k}{\rho c} + \frac{k\beta_1}{\rho c}\right)t} \cos \lambda_n x$$

(5.55)

Where the constants C_n are the Fourier coefficients in the half-range cosine expansion (e.g. Wylie)

The length average solution is

$$T_w = \frac{\beta 2}{\beta 1} - \left(\frac{\beta 2}{\beta 1} - T_s\right)\frac{\tanh\sqrt{\beta_1}\frac{\ell}{2}}{\sqrt{\beta_1}\frac{\ell}{2}} + \sum_{n=0}^{\infty} C_n e^{-\left(\frac{\lambda^2 k}{\rho c} + \frac{k\beta_1}{\rho c}\right)t}$$

STEADY STATE SOLUTION — TRANSIENT SOLUTION

(5.56)

The usual technique employed in transient response analysis leads to solutions of the form $ce^{-t/\tau}$ for a first order system, where τ is termed the time constant of the system. For example, if a simple system, such as a hot wire, were subjected to a change in temperature from T_o to T_1, we might require that the time rate of change $\frac{dT}{dt}$ be proportional to the temperature difference. This would be expressed as

$$\tau \frac{dT}{dt} = (T_o - T_1) \tag{5.57}$$

where the time constant τ is just the constant of proportionality for the relation. Equation (5.57) is a first order system with a solution of the form $ce^{-t/\tau}$. Figure (5.20) shows the solution of equation (5.57) plotted as a function of τ for a ratio $\Delta T_1/\Delta T_o$ so the solution is $1 - e^{-\frac{t}{\tau}}$. As may be seen τ occurs at .63 of the final ratio of 1.0.

Examination of equation (5.56) shows that the transient solution is of the form of

$$\sum_{n=o}^{\infty} C_n^* e^{-\frac{t}{\tau_n}} \tag{5.58}$$

where

$$\frac{1}{\tau_n} = \frac{\lambda^2 n \rho c}{k} + \frac{k \beta_1}{\rho c} \tag{5.59}$$

For this equation the solution is a series of first order solutions, so it is evident that the finite hot wire does not respond exactly as a first order system. However, for general applications it is found that the "higher order" (n = 1, 2, 3 .....) terms in the transient solution can be neglected compared with the n = 0 terms. Thus, the transient solution is approximately

$$\sum_{n=o}^{\infty} C_n^* e^{-\frac{t}{\tau_n}} \simeq C_o^* e^{-\frac{t}{\tau_o}} \tag{5.60}$$

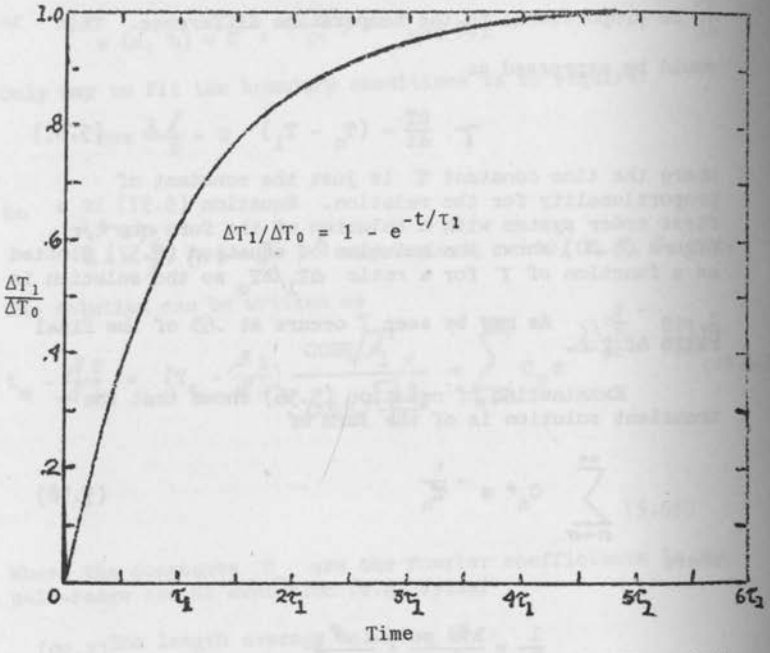

Figure 5.20 - Transient Response of a First Order System to a Step Function.

The relation for the zero order time constant becomes

$$\frac{1}{\tau_o} = \left[\frac{\lambda_o^2 \rho c}{k} + \frac{k\beta_1}{\rho c}\right] = \left[\frac{k}{\rho c}\frac{\pi^2}{\ell^2} + \frac{hD}{\rho c}\frac{4}{D^2} - \left(\frac{4}{\pi D^2}\right)^2 \frac{I^2 \sigma \alpha}{\rho c}\right] \tag{5.61}$$

It can be shown that the exact first order time constant for an infinitely long wire is

$$\frac{1}{\tau_\infty} = \frac{hD}{\rho c}\frac{4}{D^2} - \left(\frac{4}{\pi D^2}\right)^2 \frac{I^2 \sigma \alpha}{\rho c} \tag{5.62}$$

Likewise, the results of Baldwin and Sandborn[1] for a conduction controled wire leads to the result (for roughly the same approximation as made in equation (5.60))

$$\frac{1}{\tau_c} \simeq \frac{k}{\rho c}\frac{\pi^2}{\ell^2} \qquad (\text{for } I \to 0) \tag{5.63}$$

Thus, as might be expected equation (5.61) is a linear combination of the two cases of convection controled and conduction controled heat loss.

A detailed evaluation of the time constant for a resistance thermometer is given in Chapter VI. The actual application of equation (5.61) may be limited, since the conduction term is very small in room air conditions. The conduction term is important only for vacuum conditions where h is very small. For operation of hot wires in the slip region we might expect to find an area where all terms in equation (5.61) are important. The solution, equation (5.55) was obtained by Baldwin in 1961 and we have not had time to check more that the end points of pure conduction and pure convection. Some rough checks[2] were attempted and the trend for the time constant in the slip flow region appeared reasonable, however, the accuracy of the results were extremely limited.

---

[1] Baldwin, L. V., and Sandborn, V. A.; ibid.

[2] Sandborn, V. A.; A Hot-Wire Vacuum Gauge for Transient Measurements. Avco Corp. Wilmington, Mass. RAD-TM-63-41, (1963).

Convective Heat Transfer - The convective heat transfer from hot wires has received much experimental attention. Baldwin, Sandborn, and Lawrence[1] give an extensive review of reported heat transfer measurements from cylinders made up until 1960. The correlations are the basic results upon which the many different applications of the resistance temperature transducers can be related. The general approach in the consideration of convective heat transfer will be mainly to employ experimental data rather than theoretical predictions. The flow around a circular cylinder is complex and as a result theoretical evaluation of the flow is difficult. For potential flow around a cylinder the problem can be handled theoretically, however, for the actual case of a viscous flow the analysis becomes very complex. Numerical solutions have, of course, been obtained over wide ranges of flow conditions, but general relations are not available. For free molecule flow general solutions can, of course, be obtained.

One important fact must be kept in mind in considering the convective heat transfer from cylinders as applied to the applications of the resistance-temperature transducer. This is that it may not be adequate for a particular application to have only an engineering type representation of the heat loss from the wire. If transient applications are considered, the heat loss must be accurately known so that the first derivative of the curve can be obtained. Thus, in the following discussion the very general overall type correlations are not attempted, as they may be very misleading in the transient measurements with the transducer.

In the following sections the convective heat transfer has been considered in several different flow regions. The present division is made basically as to how the density effects the heat transfer. The parameters that determine the heat transfer characteristics are:

---

1 Baldwin, L.V., Sandborn, V.A., and Lawrence, J.C.; Heat Transfer from Transverse and Yawed Cylinders in Continuum, Slip and Free-Molecule Flow.

(1) Nusselt number = $\frac{hD}{k} = N_u$, (2) Reynolds number = $\frac{\rho UD}{\mu} = R$, (3) Mach number = $\frac{U}{a} = M$ and (4) Knudsen number = $\frac{\lambda}{D} = K_u$ where

h - heat transfer coefficient
D - cylinder diameter
k - thermal conductivity
U - flow velocity
μ - coefficient of viscosity
a - speed of sound
λ - molecular near free path
ρ - fluid density

The convective heat-loss rate, equation (5.28) or (5.29), may be taken as a definition of the heat transfer coefficient h. The Nusselt number is a dimensionless heat transfer parameter, which is the ratio of conduction to convection. The Reynolds number is a dimensionless flow parameter, which is the ratio of inertia to viscous forces. The Mach number is a dimensionless compressibility parameter, which is the ratio of flow velocity to the local speed of sound. The Knudsen number is a dimensionless flow regime parameter, which is the ratio of molecular mean free path to wire diameter. The three fluid parameters, Reynolds, Mach and Knudsen number, are interrelated, and any one can be expressed in terms of the other two.

From free molecule flow the mean free path between molecules can be related directly to the density of the gas,

$$\lambda(cm) = \frac{7.746 \times 10^{-9}}{\rho\ (gm/cm^3)} \qquad (5.64)$$

This result is obtained by assuming the gas is composed of hard elastic spheres. This assumption is valid for gases as long as large molecular temperatures are not considered. Using equation (5.64), it is apparent that the Knudsen number represents the effect of density in the problem. Likewise, Mach number represents the effect of velocity in the problem.

Reynolds number contains information about both density and velocity. Again from free molecular flow theory, the viscosity of a rarefied gas composed of hard elastic spheres having a Maxwellian velocity distribution is

$$U = 0.499\,\bar{v}\rho \nearrow \qquad (5.65)$$

where the mean molecular speed can be related to the acoustic speed by

$$a = \bar{v}\sqrt{\frac{\pi\gamma}{8}} \qquad (5.66)$$

where γ is the isentropic exponent. Using these molecular flow relations the relation between Reynolds, Mach and Knudsen number becomes

$$K_u = 1.26\sqrt{\gamma}\ \frac{M}{R_e} \qquad (5.67)$$

Equation (5.67) indicates that only two of the parameters are necessary to express the flow conditions. The most revealing correlation has proven to be a plot of Nusselt number versus Reynolds number, with lines of constant Mach and Knudsen number denoted on the figure. In this type of plot the effect of velocity and density on heat transfer are easily separated. In the sections which follow the discussion is divided into continuum, slip and free molecule flow regimes. These divisions are basically defined in terms of mean free path, and as such can be divided according to Knudsen number.

The subsonic convection of heat from small cylinders in continuum flow has come under theoretical study for many years. The work of Boussineq[1], in 1905 appears to be the first formal attack on the problem. King[2], in 1914 extended the work of Boussineq to the first theoretical application of the hot wire anemometer. The results of King's solution is still taken as the starting point for many modern thesis on hot wire anemometry. As applied to the mean heat loss from hot wires in a subsonic continuum flow the engineering

---

1 Boussineq, 'Comptes Rendus,' vol. 133, p. 257, 1905

2 King, L.V., On the Convection of Heat from Small Cylinders in a Stream of Fluid: Determination of the Convection Constants of Small Platinuum Wires with Application to Hot-Wire Anemometry. Phil. Trans. Roy. Soc. London A 214, 373-432 (1914).

predictions of King are surprisingly good. Unfortunately, the most used applications of the hot wire anemometer is for transient measurement, where the equation for the heat loss must be accurate to the first derivative. King's "potential flow" relation for heat loss may be expressed as

$$\frac{i^2 R}{(R - R_a)} = A + B \sqrt{U} \qquad (5.68)$$

This relation is still employed extensively in many hot wire anemometer studies. Unfortunately, the results of King are limited to at best continuum, high Reynolds number flows. At the limits the power of U can vary from near zero to one. For continuum flow at low Reynolds numbers the sensitivity to velocity becomes

$$\text{Heat loss} = \frac{C\Delta T}{\text{LOG } (d/U)} \qquad (5.69)$$

which is the zero end of the scale. For free molecule flow the heat loss varies as the first power of the velocity. Thus, no one heat loss curve can represent all of the possible relations for heat transfer that can be encountered for the hot wire.

Figure (5.21) shows the possible variation in heat loss, as a function of Mach, Knudsen and Reynolds number for a cylinder in air.[1] The lines of constant Mach number correspond roughly to lines of constant velocity, while constant Knudsen number corresponds to constant density. This curve shows, as might be expected, that the hot wire is sensitive to both velocity and density as well as temperature. The curves of figure (5.21) are an engineering correlation of a great quantity of experimental measurements. Thus, each curve is roughly accurate to $\pm$ 15%, and could never be used as the exact calculation curve for hot wire measurements. Each use of a hot wire will require an individual calibration curve of mean velocity versus heat loss.

---

1 Baldwin, L.V., Sandborn, V. A. and Lawrence, J.C., Jour. of Heat Transfer. ASME Trans., Ser. C., Vol. 82. No. 2. 1960.

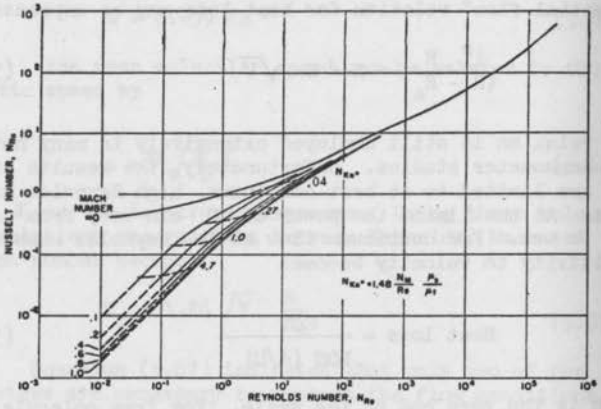

Figure 5.21 - Correlation of convective heat transfer from transverse cylinders.

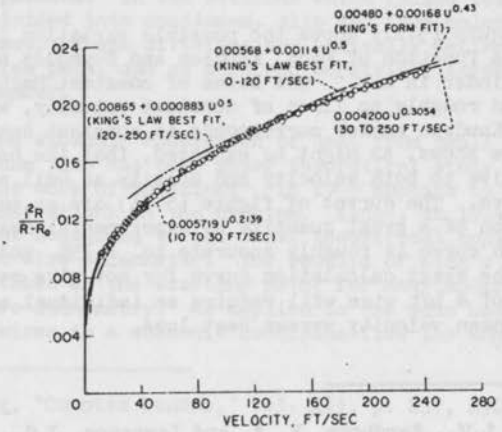

Figure 5.22 - Experimental measurement of the heat transfer from a hot wire.

Figure 5.22 is a plot of measured heat loss from a 0.0002-inch diameter tungsten wire operating near room air flow. Here the dimensional term, $(i^2R)/(R - R_a)$, for heat loss is plotted against measured velocity. The variation of the density was at most 4 percent, and hence for simplicity the data are treated as incompressible ($N_M = 0$). The hot-wire-anemometer output can be analyzed by relating the root-mean-square voltage fluctuation to the corresponding velocity fluctuation graphically by using the best faired curve through the data of Fig. 5.22.

For the evaluation of turbulent fluctuation from anemometer measurements it is preferred to use an empirical equation between heat loss and velocity. The slope of the empirical equation at the measuring velocity will be used to relate the heat loss and the turbulence. Thus, the equation not only must represent the data, but also must give a good first derivative. Several empirical equations are fitted to the data of Fig. 5.22. It was found that, to obtain one equation to fit all the data, the power of the velocity must be less than one-half. An equation of King's form, but with a power of 0.43 gives a good representation over the range of velocities covered. (Note that, for U - 240 ft/sec, N_{Re} of the wire is 22.) The data could be approximated by King's law if two different slopes and intercepts were used. Likewise, simple power laws without an intercept represent the data well over limited regions. The data of Fig. 5.22 were all taken with a constant-temperature hot-wire anemometer at the center of a 4-inch-diameter fully developed turbulent pipe flow.

The relation between the mean heat loss and the mean velocity appears to be best fit by the relation

$$\frac{i^2R}{R-R_a} = A + BU^n \tag{5.70}$$

The value of n is near 0.5, but not exactly 0.5. One may consider the sensitivity of heat loss to velocity $\frac{d(I^2R)}{dU}$, and see that it may make a great deal of difference in the results even for small changes in n.

Flow Direction Sensitivity - The mean heat loss from a hot wire will also be a function of the flow direction. The mean heat loss appears to vary roughly as the component of mean velocity normal to the hot wire axis. Figure 5.23 shows a typical variation of heat loss as a function of wire angle with respect to the flow. This heat transfer curve is compared to a cosine curve, which corresponds to

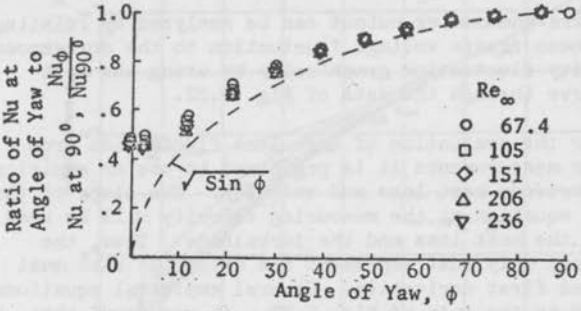

Figure 5.23 - Heat Transfer from a Cylinder as a Function of the Angle Between the Cylinder and Flow.

the case where only the normal velocity component is responsible for the heat transfer. While there is rough agreement between the cosine curve and the measurement it can be seen that a marked deviation would be found if the first derivative of the cosine and measured curves were compared. A general calibration of a hot wire that is to be used at angles to the flow requires a three-dimensional curve such as that shown in figure 5.24. Here the variation to mean velocity as a function of angle is plotted. Actual use of the hot wire requires a series of two dimensional calibration curves at fixed angles and fixed velocities, as shown in figure 5.25, to obtain the velocity and angle sensitivities.

The effect of slip and free molecule flow on the yawed hot wire has been considered by Baldwin, Sandborn and Lawrence.[1] For engineering correlations it is necessary to consider both the Reynolds of the flow normal to the cylinder and the Mach number normal to the cylinder.

[1] Baldwin, L. V., Sandborn, V. A., and Lawrence, J. C.: Ibid.

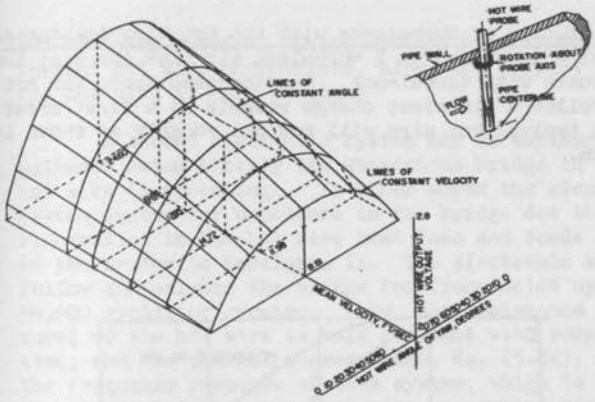

Figure 5.24 - Three-dimensional calibration of a hot wire as a function of flow angle and velocity.

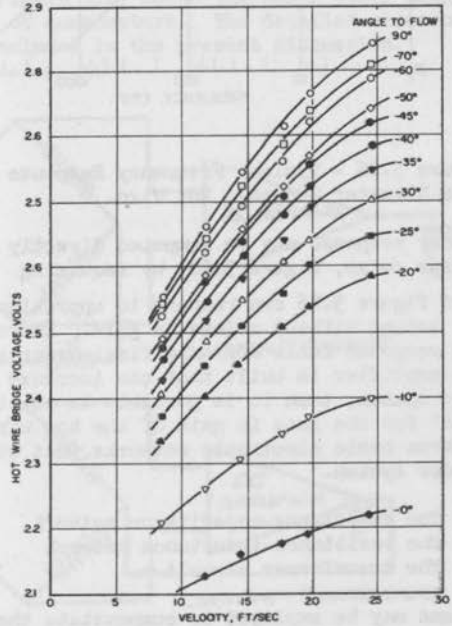

Figure 5.25 - Two-dimensional parametric curves of the calibration of a hot wire to flow angle and velocity.

Evaluation of Turbulence with the Hot Wire Anemometer - If a hot wire is placed in a turbulent air flow the heat loss will fluctuate with turbulence. As discussed above the hot wire can follow a transient change roughly as a first order system. A typical hot wire will respond roughly as shown in figure 5.26.

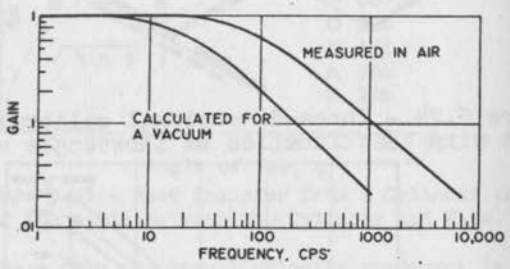

Figure 5.26 - Typical Frequency Response Curve for a 0.0002-inch Diameter Tungsten Hot Wire.

The frequency response may be computed directly from the step response curve, figure 5.20, by requiring $f = \frac{1}{2\pi t}$. The hot wire of figure 5.26 can respond to approximately 70 cycles per second without a loss in gain. Above 70 cycles per second the response falls off as a first order system. If an electronic amplifier is built that can increase gain as a first order system, then it is possible to electronically "compensate" for the loss in gain of the hot wire. There are at least three basic electronic networks that will behave as a first order system.

a) The resistance-capacitance network
b) The resistance-inductance network
c) The transformer circuit

These systems may be employed to compenstate the loss in gain of the hot wire, and thus, increase its frequency response by

two or three decades. These systems are termed constant current hot wire anemometers, since the current through the hot wire is held constant.

A second electronic system may be employed, which balances automatically the wheatstone bridge in which a hot wire is operating. In other words the electronic system senses any unbalance in the bridge due to the fluctuation in the hot wire heat loss and feeds current to the bridge to rebalance it. The electronic system can follow and balance the bridge for frequencies up to 50,000 cycles or greater. Thus, the resistance (temperature(of the hot wire is held constant with respect to time, and the thermal storage term, Eq. (5.52), is zero. The frequency response of this system, which is called the constant temperature hot-wire anemometer, is strickly a function of the frequency limits of the electronic system. Figure 5.27 shows the basic block diagram for the two types of anemometers. The detailed electronic circuits are not included in the present discussion.

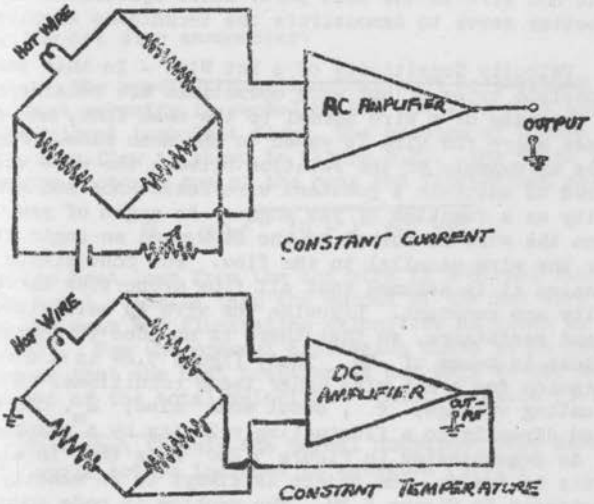

Figure 5.27 - Hot-Wire Anemometer Circuits.

The measurements of turbulence with the hot wire anemometer is based on the fact that the output can follow the instantaneous changes in the fluctuations. The ability to follow the instantaneous variations is accomplished electronically. The present discussion will assume that the anemometer output is following the instantaneous fluctuations. The second assumption required in the measurement of turbulent with the hot wire anemometer is that a mean calibration between the wire heat loss and the quantity to be measured can be used to evaluate the fluctuations. In all cases to be covered it should be kept in mind that the main object is to evaluate the fluctuating quantity once the mean calibration is known.

The first part of the discussion is concerned with the actual relation between the fluctuating voltage and fluctuating velocities. As such, it is intended as a guide to the approximations involved in the evaluation of hot wire anemometer signals. Unfortunately, only a token amount of experimental investigation of the errors involved in hot wire anemometry have been made. Once the approximations are outlined then example sensitivity relations between fluctuating voltages and turbulent quantities can be derived. It was chosen to present the general sensitivity relation for the hot wire in the last part, since specific examples will better serve to demonstrate the techniques involved.

Velocity Sensitivity of a Hot Wire - In this section two possible types of hot wire operations are considered. First the case of a wire normal to the mean flow, and second the case where the wire is yawed to the mean flow. Figure 5.24 is an example of the relation between the wire voltage required to maintain a constant wire resistance and mean velocity as a function of yaw angle. An angle of yaw of 90^{o} is when the wire is normal to the flow, and an angle of zero is for the wire parallel to the flow. For convenience of discussion it is assumed that all flow properties except velocity are constant. Likewise the wire is maintained at a constant resistance, so that there is no need to express the heat loss in terms of ΔR. Thus, figure 5.24 is a complete calibration for a hot wire under these conditions. A fluctuating voltage, e , about some value, E_m, can be related directly to a fluctuating velocity by a graphic solution, as demonstrated in figure 5.28. Note that in all the analysis to follow, the object is always to do exactly that demonstrated in figure 5.28. The problem is made complex only because there is more than one turbulent quantity being sensed

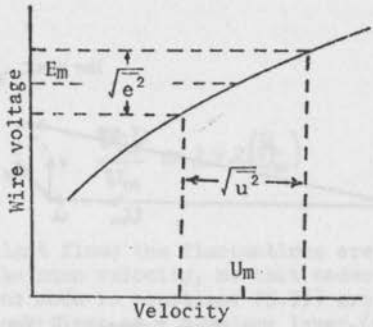

Figure 5.28 - Graphic Solution of Turbulent Fluctuations.

by the hot wire anemometer.

The specific question that must be answered first is what velocity is sensed by the hot wire in a three-dimensional turbulent flow? The problem of a wire normal to the mean flow is shown in figure 5.29. The total velocity is the vectoral sum of the mean and fluctuating velocities.

$$U_{TOT} = \sqrt{(U_m+u)^2 + v^2 + w^2} \qquad (5.71)$$

If the heat loss from the hot wire is a direct function of the total velocity then the output of the hot wire is related to the mean and fluctuating velocities as given by equation (5.71). For the present discussion there is no need to assume that the heat transfer is due only to the normal component of the total velocity.* Thus, equation (5.71) is more

* Note that if only the normal component were assumed, then v^2 would not be included in equation (5.71).

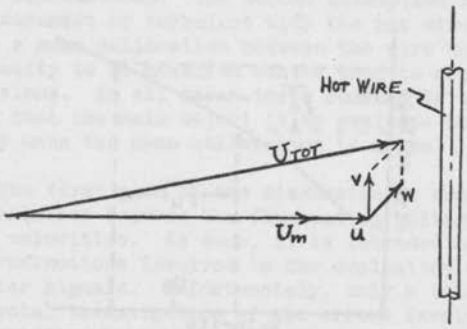

Figure 5.29 - Hot Wire Normal to the Mean Flow.

general than is normally assumed. The fact that in figure 5.24 there is still a velocity sensitivity for a wire parallel to the flow (zero degrees), suggests that some sensitivity to v may be present. The value of v^2, no doubt, should be weighted by a factor somewhere between 0 and 1, therefore equation (5.71) over estimates the wire sensitivity.

Equation (5.71) may be rewritten as

$$\left(\frac{U}{U_m}\right)^2 = 1 + 2\left(\frac{u}{U_m}\right) + \left(\frac{u}{U_m}\right)^2 + \left(\frac{v}{U_m}\right)^2 + \left(\frac{w}{U_m}\right)^2 \qquad (5.72)$$

In order to simplify equation (5.72) it is assumed that $|u| \simeq |v| \simeq |w|$ and $|u| \ll U_m$, thus

$$2\frac{u}{U_m} \gg \left(\frac{v}{U_m}\right)^2 \text{ or } \left(\frac{v}{U_m}\right)^2 \text{ or } \left(\frac{w}{U_m}\right)^2 \qquad (5.73)$$

and

$$\frac{U_{tot}}{U_m} \simeq 1 + 2\left(\frac{u}{U_m}\right) \qquad (5.74)$$

For many turbulent flows the fluctuations are only about one tenth of the mean velocity, so that order of magnitude assumptions made in equations (5.73) are valid. However, for such flows as a boundary layer (near the wall) values of $\frac{u}{U_m}$ as great as 0.4 are obtained. Unfortunately, no information has ever been published to demonstrate just when equation (5.74) is no longer valid. This validity must be determined for each turbulent flow. Throughout the following discussion on the evaluation of hot wire signals it will be assumed that the velocity can be expressed as a mean quantity plus a turbulent component, $(U_m + u')$. The turbulent component u' will be a function of a u, v and w, such as given by equation (5.71), however, for most flows it may be possible to use the relation given by equation (5.74) (i.e. U'=u). Note that in nearly every discussion of hot wire anemometry to be found in the literature, it is assumed that u' = u without a thought being given to secondary effects.

The second problem to be answered is what velocity is sensed by a wire yawed to the mean flow. For this flow it is necessary to assume some further relation between velocity and heat transfer. For the normal wire it was not necessary to assume a specific relation between the total velocity and the wire heat transfer. For the yawed wire case the usual assumption is that only the component of total velocity normal to the wire contributes to the heat transfer. If the heat transfer is due only to the

stagnation line along the leading edge of the hot wire, then the normal component of the velocity is theoretically correct. Unfortunately, for the heat transfer from a hot wire more than the stagnation region must be considered. Thus, the normal component of velocity represents at best a first approximation to the heat loss. For the present discussion it will be assumed that the normal component of velocity is the most important, however, in the final analysis of the hot wire signal the graphic calibration curve is suggested as the only accurate method of evaluating yawed wire data.

Figure 5.30 shows the coordinate system for the yawed wire. The component of total velocity normal to the wire in the x-y plane is

$$U_{n\,TOT\,(x\text{-}y)} = \sqrt{(U_m+u)^2+v^2}\,\left[\sin(\varphi+\delta\varphi)\right] \qquad (5.75)$$

where now $\delta\varphi$ can be either positive or negative depending

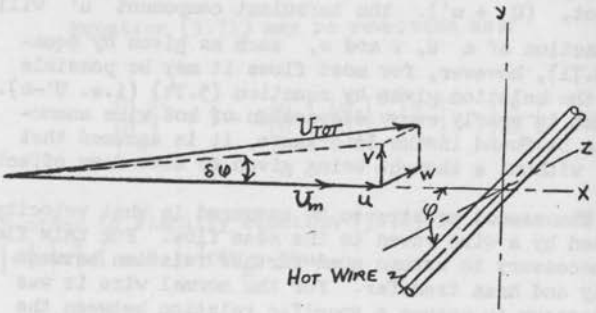

Figure 5.30 - Hot Wire Yawed to the Mean Flow

on the sign of v. The component of total velocity normal to the wire in the xz plane is

$$U_{N_{xz}} = w \tag{5.76}$$

Thus, the total normal component is

$$U_{N_{tot}} = \sqrt{\{(U_m + u)^2 + v^2\}\{\sin^2(\psi + \delta\psi)\} + w^2} \tag{5.77}$$

This relation can be expanded by using the relations

$$\sin(\psi + \delta\psi) = \sin\psi\cos\delta\psi + \cos\psi\sin\delta\psi \tag{5.78}$$

where

$$\sin\delta\psi = \frac{v}{\sqrt{(U_m + u)^2 + v^2}}$$
$$\cos\delta\psi = \frac{U_m + u}{\sqrt{(U_m + u)^2 + v^2}} \tag{5.79}$$

Equation (5.77) may be rewritten as

$$U_{N_{tot}} = \sqrt{(U_m + u)^2\sin^2\psi + 2(U_m + u)v\sin\psi\cos\psi + v^2\cos^2\psi + w^2} \tag{5.80}$$

or

$$\frac{U_{N_{tot}}}{U_m} = \sin\psi\{1 + \frac{3u}{U_m} + (\frac{u}{U_m})^2 + \frac{2v}{U_m}\cot\psi + \frac{2uv}{U_m^2}\cot\psi$$
$$+ (\frac{v}{U_m})^2\cot^2\psi + (\frac{w}{U_m})^2\frac{1}{\sin^2\psi}\}^{\frac{1}{2}}$$

for moderate angles of ψ it is reasonable to assume that

linear approximations can be made

$$\frac{2u}{U_m} \text{ or } \frac{2v}{U_m} \gg \frac{u^2}{U_m^2} \text{ or } \frac{2uv}{U_m^2}\cot\varphi \text{ or } \frac{v^2}{U_m^2}\cot^2\varphi$$

$$\text{or } \frac{w^2}{U_m^2}\frac{1}{\sin^2\varphi}$$

however, for small angles of φ the second order terms cannot be neglected. Again, just where the second order terms start to become important is not known. Most experimenters limit their measurements to angles greater than 30°, however, it is tempting to operate the wire at very small angles in order to obtain greater sensitivity to the v component.

To first order it is assumed that the yaw wire is sensitive to u and v only

$$\frac{U_{n\text{TOT}}}{U_m} = \sin\varphi\sqrt{1+\frac{2u}{U_m}+\frac{2v}{U_m}\cot\varphi} \qquad (5.81)$$

Linearized Evaluation of Small Amplitude Fluctuations - Constant Current Hot Wire Anemometer - The practical evaluation of the hot wire anemometer output requires a minimum of two electrical measurements: The mean, d.c. voltage and the r.m.s. of the a.c. voltage. For a single wire normal to the mean flow these two measurements are sufficient to compute the longitudinal turbulent velocity. Once the mean and fluctuating voltages are measured, it is evident from the discussion in the previous section, that these two measurements can be used with the voltage- velocity calibration curve to compute the turbulent velocity fluctuation. These two measurements are not sufficient to determine much of the detail of the fluctuation, such as symmetry or flow reversal. Thus, the analysis of the present section must assume from the start that the fluctuations are symmetrical about E_m, and no flow reversal occurs. The

general approach to evaluating the anemometer output is to consider the flow composed of a mean velocity, U_m, and a fluctuating component, u. Likewise, the voltage is divided into a mean and a fluctuating component

$$\left.\begin{aligned} U &= U_m + u \\ E &= E_m + e \end{aligned}\right\} \qquad (5.82)$$

the fluctuating component has both positive and negative values. For the present constant current case it is necessary to specify that the fluctuations in wire resistance are small compared to the total circuit resistance, so that no fluctuations in wire heating current occurs.

To demonstrate the procedure in evaluating the anemometer signal, it will be assumed that the voltage-velocity calibration curve can be represented by an empirical relation of the form given in equation (5.70).

$$\frac{i^2 E}{E - i R_a} = A + B U^{n} \qquad (5.70a)$$

where E is substituted for iR. This procedure requires that the mean and instantaneous relations between voltage and velocity are the same. This requirement is present in all the transient evaluations of the resistance-temperature transducers. The error due to the use of the mean calibration curve would enter through the effect of turbulence on the wire heat transfer. This effect is unimportant for most hot-wire anemometer measurements.

Using the definitions, Eq. (5.82), for E and U equation (5.70a) can be written as

$$\frac{i^2(E_m+e)}{(E_m+e)-iR_2} = A + B(U_m+u)^n \qquad (5.83)$$

Equation (5.83) is the general type of relation, between the velocity fluctuation, u, and the voltage fluctuation, e, obtained for the hot wire anemometer. The exact form of equation (5.83) will, of course, depend on the empirical relation used to represent the voltage-velocity calibration curve. The assumptions necessary to obtain equation (5.83) are: 1) no fluctuation in the current i, 2) the mean voltage, E_m, corresponds to the mean velocity, U_m, and 3) the mean and instantaneous relation between voltage and velocity are the same. Actually the second and third assumptions are not independent. To employ equation (5.83) it must be written in terms of the measured quantity, $\overline{e^2}$ or $\sqrt{\overline{e^2}}$. This requires that equation (5.83) be squared and mean values taken.

The mean square expression is

$$\overline{\left\{\frac{i^4(E_m-e)^2}{[(E_m-e)-iR_2]^2}\right\}} = A^2 + 2AB\overline{(U_m+u)^n} + B^2\overline{(U_m+u)^{2n}} \qquad (5.84)$$

where the bar denotes the mean value of the fluctuating quantities. Equation (5.84) is complex and does not yield a unique relation between the measured voltage $\overline{e^2}$ and the fluctuating velocity $\overline{u^2}$. In fact, equation (5.81) shows that no one to one correspondence between $\overline{e^2}$ and $\overline{u^2}$ exists.

Equation (5.84) is of mathematical interest, since it represents the concise relation between the statistical voltage fluctuation and the velocity fluctuations. However, for practical evaluation of the hot wire anemometer output, such a relation as equation

(5.81) has never been employed. The practical approach is to find a relation between $\sqrt{\overline{e^2}}$ and $\sqrt{\overline{u^2}}$ by restricting the analysis to small fluctuations. Starting with equation (5.80), the velocity term, $(U+u)^n$ is expanded in an infinite series

$$(U_m+u)^n = U_m^n + nU_m^{(n-1)}u + \frac{n(n-1)}{2!}U_m^{(n-2)}u^2 + \frac{n(n-1)(n-2)}{3!}U_m^{(n-3)}u^3 + \cdots \frac{n(n-1)\cdots(n-N+1)}{N!}U_m^{(n-N)}u^N \qquad (5.85)$$

The power series places the restriction $|u|<U_m$ on equation (5.85). The mean voltage-velocity relation may be taken out of equation (5.85) to give

$$\frac{-i^3 eR_a}{(E_m-iR_a)(E_m+e-iR_a)}\left[\frac{1}{BnU_m^n}\right] = \left(\frac{u}{U_m}\right) + \frac{(n-1)}{2!}\left(\frac{u}{U_m}\right)^2 + \frac{(n-1)(n-2)}{3!}\left(\frac{u}{U_m}\right)^3 + \cdots \qquad (5.86)$$

coupled with the restriction $|u|<U_m$ is the fact that $(u/U_m) > (u/U_m)^2 > (u/U_m)^3 \ldots$. Thus, to first order it is required that $U_m >> u$, so that higher powers of (u/U_m) can be neglected. Coupled with this first order restriction is the fact that $E_m >> e$, so that equation (5.86) to first order becomes

$$\frac{i^3 R_a e}{(E_m-iR_a)^2}\left[\frac{1}{BnU_m^n}\right] = \frac{u}{U_m} \qquad (5.87)$$

The negative sign in equation (5.87) denotes that an increase in u cools the wire so that e decreases. The relation between r.m.s. voltage and velocity becomes

$$-\frac{i^3 R_a \sqrt{\overline{e^2}}}{(E_m - iR_a)^2 B n U_m^n} = \frac{\sqrt{\overline{u^2}}}{U_m} \qquad (5.88)$$

Equation (5.88) is the linearized relation between the hot wire anemometer measured r.m.s. signal and the velocity r.m.s. An insight into the linearization can be obtained by considering the differential of equation (5.70),

$$-\frac{i^4 R_a}{(E - iR_a)^2} \frac{dR}{n B U_m^n} = \frac{dU}{U} \qquad (5.89)$$

where E replaces iR. If now idR = de is replaced by $\sqrt{\overline{e^2}}$, dU is replaced by $\sqrt{\overline{u^2}}$, and E and U are replaced by the mean values, then equations (5.88) and (5.89) are identical. This demonstrates that the linearization process is equivalent to replacing the calibration curve by its tangent at the point E_m, and requiring that e and u can be neglected compared to E_m and U_m.

The practical evaluation of the constant current hot wire anemometer output usually employs a form quite simular to equation (5.88). The special case, where n=1/2, is of course the classic example

$$\frac{2 i R_a \sqrt{\overline{e^2}}}{(R - R_a)^2 B \sqrt{U_m}} = \frac{\sqrt{\overline{u^2}}}{U_m} \qquad (5.90)$$

(where now $E_m = iR$ has also been used.) The value of B and U_m are obtained from the mean calibration equation. The accuracy of the linearized evaluation will

will depend first on how well the empirical relation (5.70) fits the mean calibration data. As could be demonstrated by equation (5.89), the empirical fit of the mean data must be accurate to the first derivative. This requires that a good deal of care in fitting the empirical relation to the calibration curve. This curve fitting requirement is equally true for either constant current or constant temperature operation of the hot wire.

b) Constant Temperature Hot Wire Anemometer - For constant temperature hot wire anemometer operation the wire resistance is held constant and only the current or voltage varies. Equation (5.70) is assumed for the starting empirical relation for the calibration curve. The equation is modified by employing the voltage instead of the current

$$\frac{E^2}{R(R-R_a)} = A + BU^n \tag{5.70b}$$

The perturbation relation equivalent to equation (5.85) becomes

$$\frac{(E_m+e)^2}{R(R-R_a)} = A + B(U_m+u)^n \tag{5.91}$$

and the relation between the mean square of the voltage fluctuation and the velocity fluctuation is

$$\frac{E_m^2 + \overline{e^2}}{R(R-R_a)} = A + B\overline{(U_m+u)^n} \tag{5.92}$$

Equation (5.92) is perhaps simpler than the constant current relation, Eq. (5.87), but it also indicates that a unique relation between $\overline{e^2}$ and $\overline{u^2}$ only does not exist.

To obtain a useable relation the infinite series expansion of the term $(U_m+u)^n$, which requires $|u|<U_m$, is made.

$$\frac{2E_m e + e^2}{R(R-R_a)} \frac{1}{B n U_m^n} = \left(\frac{u}{U_m}\right) + \frac{(n-1)}{2!}\left(\frac{u}{U_m}\right)^2 + \frac{(n-1)(n-2)}{3!}\left(\frac{u}{U_m}\right)^3 + \cdots \qquad (5.93)$$

To first order, the higher powers of $\left(\frac{u}{U_m}\right)$ and $\left(\frac{e}{E_m}\right)$ are neglected, so that the relation between the r.m.s. voltage and the r.m.s. velocity for the constant temperature hot wire anemometer becomes

$$\frac{2E_m\sqrt{\overline{e^2}}}{R(R-R_a)} \frac{1}{B n U_m^n} = \frac{\sqrt{\overline{u^2}}}{U_m} \qquad (5.94)$$

A simple substitution will show that equation (5.94) is equivalent to the derivative of equation (5.70) if $Rdi = \sqrt{\overline{e^2}}$ and $dV = \sqrt{\overline{u^2}}$. The special case, n=1/2, gives the following relation

$$\frac{4E_m\sqrt{\overline{e^2}}}{R(R-R_a)B\sqrt{U_m}} = \frac{\sqrt{\overline{u^2}}}{U_m} \qquad (5.95)$$

The accuracy of the turbulent velocity evaluation will depend on the accuracy with which the empirical relation, Eq. (5.70), fits the calibration data. In figure 5.22 a calibration curve for a 0.0002 inch diameter tungsten hot wire was shown. This data was taken with a constant temperature hot wire anemometer. The root-mean-square voltage fluctuation was also recorded for each measured point. The hot wire was operating at the center of a 4-inch-diameter fully developed turbulent pipe flow,[1]

[1] Sandborn, V.A.: Experimental Evaluation of Momentum Terms in Turbulent Pipe Flow, NACA TN 3266, 1955.

A direct comparison between the turbulent fluctuations, evaluated by each of the suggested empirically fitted curves shown on figure 5.22, is shown on figure 5.31. As a standard for comparing the different equations, the crosshatched curve represents values obtained graphically from the measured E_{in} and $\sqrt{e^2}$ and the calibration curve. The spread in the graphic evaluated data is in part due to the curve reading. The accuracy of the equations is best at the high Reynolds numbers. None of the relations are adequate at the low Reynolds numbers. Figure 5.31 demonstrates the King's law with n=1/2 is no better than the other empirical relations. This also points up the fact that measurements of the turbulent fluctuations with the so called "linearized" anemometers are not necessarily a great improvement.

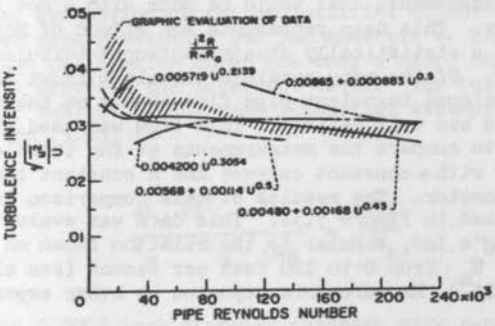

Figure 5.31 - Comparison of turbulent intensity evaluated from several empirical equations for the heat loss

Most of the early measurements with the hot wire anemometer have used the square root relation of King. In many instances it was realized the relation of King did not correlate the calibration data. Much of the misfit was blamed on dirt or other external effects. The

author,[2] encountered the deviations from King's law in boundary layer measurements before it was realized that such effects existed. Under the assumption that dirt was affecting the wire calibration, a new King's law curve was fitted to approximately every four or five points measured in the region near the wall. This technique can be employed to improve the accuracy of the evaluation shown in figure 5.31, however, it soon becomes just as easy to graphically evaluate the fluctuations. Considering the results shown in figure 5.31, it would appear that no one empirical relation of those considered will be adequate over the complete Reynolds number range. Above and below a pipe Reynolds number (based on pipe radius) of between 6 and 8 x 10^4 (hot wire Reynolds number of 6 to 8) the turbulent intensity changes more marked than the empirical relations can indicate. The accuracy with which a set of turbulence measurements are evaluated will, of course, depend on the specific research program. In the past the interest was mainly in trends of the turbulent intensity rather than absolute value, so that only approximate values were necessary.

The turbulence data shown in figure 5.31 is typical of measurements that would be made with a hot wire anemometer. This data represents the effect of Reynolds number on a statistically steady isotropic turbulent intensity. Of the many possible turbulent flows the fully developed turbulent pipe flow should be the most repeatable and well defined. This flow was used by the author[1], to compare the measurements of the turbulent intensity with a constant current and a constant temperature anemometer. The results of this comparison is demonstrated in figure 5.32. This data was evaluated using King's law, simular to the relation shown on figure 5.22 for U_m from 0 to 120 feet per second (see also figure 5.21.) Measurements reported by other experimenters

---

1 Sandborn, V.A,: Experimental Evaluation of Momentum Terms in Turbulent Pipe Flow. NACA TN 3266, 1955.

2 Sandborn, V.A., and Slogan, R.J.: NACA TN 3265, 1955.

are also included on figure 5.32. From an accuracy standpoint there is little to chose between the two methods of measuring the turbulent intensity.

The fully developed turbulent pipe flow is the ideal facility to check out a net hot wire anemometer system. It is recommended that researchers just starting to develop techniques for measuring turbulence with the hot wire consider first attempting to make measurements at the center of the pipe. A check of the turbulent intensity and the trend with Reynolds number will insure that the anemometer is functioning properly.

Several alternate methods of evaluating the hot wire anemometer signal can be found in the literature. Of interest to the engineer needing a quick answer without an elaborate calibration curve is the method which uses the intercept rather than the slope of the calibration curve. A derivation of the intercept method of evaluating constant temperature hot wire anemometer data is given by Lawrence and Landes.[1] The one new assumption of this technique is that a measure of E_m for no flow is sufficient to define the calibration curve intercept. Such an assumption cannot be justified either theoretically or experimentally, but for moderate or high velocities the calibration curve has only a minor dependence on a small error in the intercept value. The resulting relation, subject to the same linearized assumptions as equation (5.95) is

$$\frac{4E_m\sqrt{\overline{e^2}}}{E_m^2 - E_{m,\,U=0}^2} = \frac{\sqrt{\overline{u^2}}}{U_m} \qquad (5.96)$$

For the 0.0002 inch diameter tungsten wire sensing element, equation (5.96) was found to give turbulent intensity values within from 20 to 30 of the values shown in figure 5.32.

---

[1] Lawrence, J.C., and Landes, L.G.; NACA 2843, 1952.

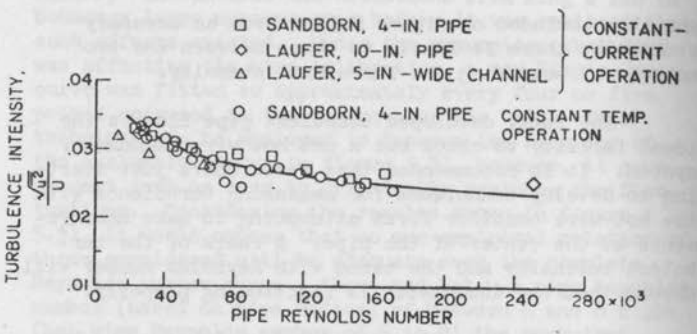

Figure 5.32 Comparison of measured turbulence intensity at the center of pipes from hot wires operated by constant current and constant temperature anemometers.

Measurement of the normal turbulent velocity component - To demonstrate the evaluation of the turbulent fluctuations from the yawed wires, employing an empirical relation, the normal component of the velocity may be assumed to represent the heat loss. The heat loss from the yawed wire, as a function of velocity and angle, is written similar to equation (5.70) as

$$\frac{i^2R}{R-R_a} = A_1 + B_1 U_N^n \qquad (5.97)$$

The relation for U_N, given by Eq. (5.81) is expanded simular to the method employed for Eq. (5.85). The expansion retaining only the first order terms, gives

$$U_N^n = U_m^n \sin^n\varphi + nU_m^n \sin^{(n-1)}\varphi\left[\frac{u}{U_m}\sin\varphi + \frac{v}{U_m}\cos\varphi\right] \quad (5.98)$$

Thus, the output voltage from the hot wire may be related to the velocity fluctuations by

(constant current)

$$-\frac{i^3 eR_a}{(E_m - iR_a)^2}\,\frac{1}{B_1 nU_m^n \sin^{(n-1)}\varphi} = \frac{u}{U_m}\sin\varphi + \frac{v}{U_m}\cos\varphi \quad (5.99)$$

(constant temperature)

$$\frac{2E_m e + e^2}{R(R-R_a)}\,\frac{1}{B_1 nU_m^n \sin^{(n-1)}\varphi} = \frac{u}{U_m}\sin\varphi + \frac{v}{U_m}\cos\varphi \quad (5.100)$$

where B is the slope of the calibration curve of $\frac{i^2R}{(R-Ra)}$ versus $U_m^n \sin^n\varphi$.

An alternate example would be the assumption that the heat loss varies as $(\sin\varphi)^m$, where m is the power determined from the angle calibration data. The anemometer relations become

(constant current)

$$-\frac{i^3 e R_a}{(E_m - iR_a)^2}\,\frac{1}{B_1 nU_m^n \sin^{(m-1)}\varphi} = \frac{u}{U_m}\sin\varphi + \left(\frac{m}{n}\right)\frac{v}{U_m}\cos\varphi \quad (5.101)$$

(constant temperature)

$$\frac{2E_m e + e^2}{R(R-R_a)}\,\frac{1}{BnU_m^n \sin^{(m-1)}\varphi} = \frac{u}{U_m}\sin\varphi + \left(\frac{m}{n}\right)\frac{v}{U_m}\cos\varphi \quad (5.102)$$

The effect of the angle relation shows up directly as a change in the wire sensitivity to the v component only. Thus, equations (5.101) and (5.102) point out the importance of having the correct angle variation.

If equation (5.99) and (5.100) are written in

terms of the mean square voltage and velocity fluctuations, a new velocity term $\overline{uv}$ appears. For the case corresponding to equation (5.97) the relation becomes

$$k^2\overline{e^2} = \frac{\overline{u^2}}{U_m^2}\sin^2\varphi + 2\frac{\overline{uv}}{U_m^2}\sin\varphi\cos\varphi + \frac{\overline{v^2}}{U_m^2}\cos^2\varphi \quad (5.103)$$

where

$$k^2 = \frac{i^6R_a^2}{(E_m - iR_a)^4}\,\frac{1}{B^2n^2U_m^{2n}\sin^{2(n-1)}\varphi} \quad \text{(constant current)}$$

$$k^2 = \frac{4E_m^2}{R^2(R-R_a)^2}\,\frac{1}{B^2n^2U_m^{2n}\sin^{2(n-1)}\varphi} \quad \text{(constant temperature)}$$

The term $\overline{u^2}$ can be determined with the wire normal to the flow, however, the $\overline{v^2}$ and $\overline{w^2}$ components are not evaluated from a wire parallel to the mean flow. As will be seen, the variation of heat loss for the small yaw angles does not follow a simple angle dependency. A systematic set of measurements should be undertaken to decide on the useable range of angles that might be used in the valuation of turbulent velocities. To evaluate $\overline{v^2}$ and $\overline{uv}$ it is necessary to operate the wire at two different angles of yaw. In this way two equations with $\overline{v^2}$ and uv as unknowns can be solved simultaneously. For maximum accuracy two different angles which are equally sensitive to uv and $\overline{v^2}$ would be chosen. Typical angles employed are 45° and 135°. In figure 5.30 it was assumed that a positive value of v was in an upward direction. Consider now the case of a wire yawed at an angle-φ to the mean flow. For an angle-φ the normal component of the total velocity may be written to first order as

$$U_N = (U_m + u)\sin\varphi - v\cos\varphi \qquad (5.104)$$

Thus, for a wire yawed at an angle $-\varphi$ (which would correspond to 135°, since the yaw angle is measured clockwise from the mean velocity direction), the mean square voltage - velocity relation becomes

$$k^2\overline{e^2} = \frac{\overline{u^2}}{U_m^2}\sin^2\varphi - 2\overline{uv}\sin\varphi\cos\varphi + \frac{\overline{v^2}}{U_m^2}\cos^2\varphi \qquad (5.105)$$

As an example, equation (5.103) and (5.105) can be solved for the case $\varphi = 45°$ and $-\varphi = 135°$ to obtain a unique value for $\overline{uv}/U_m^2$

$$\frac{\overline{uv}}{U_m^2} = \frac{(k^2\overline{e^2})_{45°} - (k^2\overline{e^2})_{135°}}{4} \qquad (5.106)$$

The relation for $\overline{v^2}/U_m^2$ is

$$\frac{\overline{v^2}}{U_m^2} = \frac{(k^2\overline{e^2})_{45°} + (k^2\overline{e^2})_{135°} - 2\frac{\overline{u^2}}{U_m^2}}{2} \qquad (5.107)$$

An assumption inherent in evaluating $\overline{uv}$ and $\overline{v^2}$ is that the wire at each angle of yaw sees the same value of $\overline{u^2}$, $\overline{v^2}$ and $\overline{uv}$. If the wire were a point measuring device then the assumption would be exact, however, the wire will have a finite length which sweeps out a finite area as it is yawed. Thus, a question will arise if the turbulent field over the length of the wire is not uniform. A discussion of the effect of nonuniformity of

the turbulence in the evaluation of yawed wires will be covered in more detail in part (c) of this section.

Single Wire Measurements of the Three Turbulent Velocity Components - Two techniques have been used to evaluate the transverse turbulent components from yawed wires. The first is to rotate a single wire to several angles and the second is to employ two hot wires at fixed angles. The two fixed wires will be referred to as ab X-wire and will be discussed in the next section. The single rotating hot wire probe appears to be the best means of measuring the transverse and correlation components. However, there are many times when it is inconvenient to rotate a hot wire probe.

Figure 5.24 is a typical calibration map obtained for a rotating hot wire. The three variables, wire voltage, mean velocity and yaw angle are plotted on the three axis. A two-dimensional calibration plot with yaw angle as a parameter is shown in figure 5.25b. Note that for a wire parallel to the mean flow there is still a dependency of heat loss on the mean velocity. Thus, it is evident that an analysis based on the normal velocity component only is at best only approximate. The most accurate evaluation of the yawed hot wire appears to be a semi-graphic approach, where no specific curve fitting is attempted.

Considering the calibration curves of figure 5.25, it is possible to state that the fluctuating voltage output of a hot wire is a function of the fluctuation in mean flow and flow angle. This may be written as

$$de = \frac{\partial E}{\partial U} u + \frac{\partial E}{\partial \varphi} \delta\varphi \qquad (5.108)$$

The differentials are replaced by pertibations, e, u and $\delta\varphi$. The angle $\delta\varphi$ can by referring to figure 5.30 be expressed as

$$\delta\varphi = Tan^{-1}\frac{v}{U_m+u} \simeq \frac{v}{U_m+u} \propto \frac{v}{U_m} \qquad (5.109)$$

where u and u^2 can be neglected compared to U_m. These assumptions are equivalent to the linerizztion made in connection with equation (5.87). Equation (5.108) may be written as

$$e = \frac{\partial E}{\partial U} u + \frac{\partial E}{\partial \varphi} \frac{v}{U_m} \qquad (5.110)$$

It could have been shown that equation (5.110) is equivalent to equation (5.99) or (5.100). Equation (5.110) can be evaluated directly from the experimental calibration curves by measuring the differentials. Figure 5.33 shows the values of $\partial E/\partial U$ and $\partial E/\partial \varphi$ evaluated from the calibration curves of figure 5.35. A comparison of the terms shows that $\partial E/\partial \varphi$ increases much faster than $\partial E/\partial U$ decreases. As a result, it would be expected that the hot wire output voltage (root mean square) will increase as the wire approaches the parallel condition. Figure 5.34 shows the actual measured output of a hot wire as it is yawed to the flow. The maximum output occurs at an angle of approximately 10 degrees between the hot wire and the mean flow. Evaluation of the hot wire output at these small angles may be of value, since the signal level is much improved. However, it is necessary to reconsider the linearization of the equations. A question is always posed that the hot wire supports may interfere with the flow at the small angles. If interference were of great importance it would be expected that the zero angle output would be much greater than that recorded in figure 5.34. It appears worthwhile to further explore the possibilities of operating the hot wire at angles nearly parallel to the mean flow.

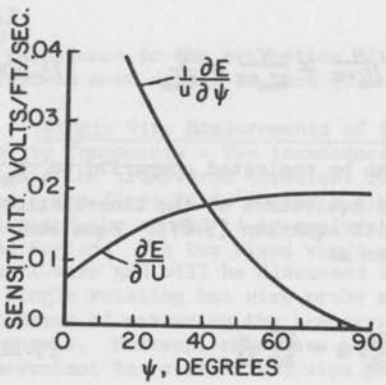

Figure 5.33- Wire sensitivity to velocity and yaw.

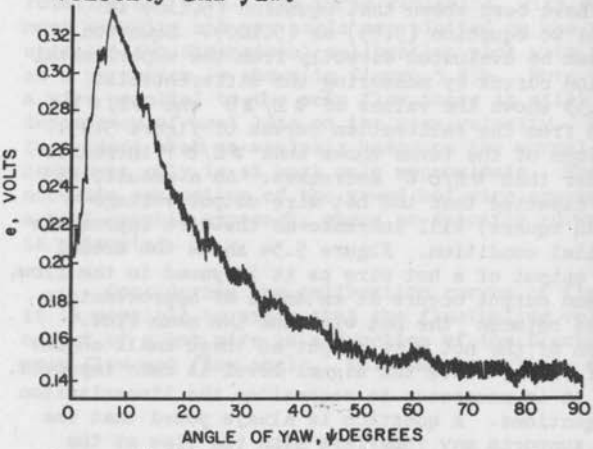

Figure 5.34- RMS output of a hot wire as it is yawed to the flow.

A check of the yawed wire analysis has been made by computing the $\overline{v^2}$ component as a function of angle for the data shown in figure 5.35. This data was taken at the center of a fully developed pipe flow, thus $\overline{uv}$ is equal to zero. The fact that $\overline{v^2}$ is not independent of angle is difficult to understand. A great number of measurements have all indicated that minimum value of $\overline{v^2}$ is always found around an angle of 40 degrees. The variation of $\overline{v^2}$ must be accepted at the present time as the accuracy of the measuring technique. Again further work is indicated to better understand the yawed wire measuring techniques.

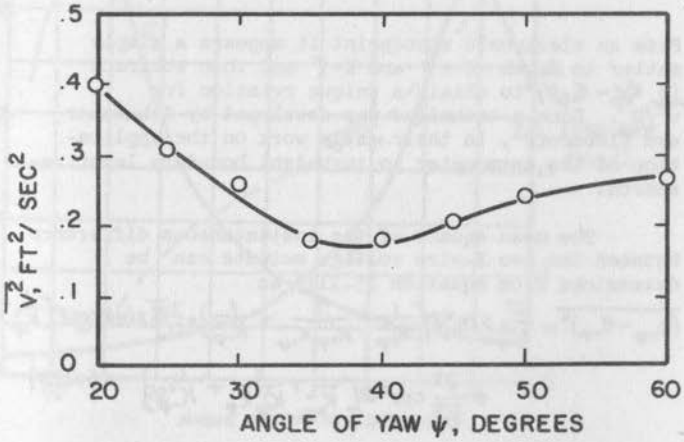

Figure 5.35 - Values of $\overline{v^2}$ as a function of wire yaw angle.

c) X-wire operation - The X-wire probes employ hot wires yawed at angles ψ and $-\psi$ with respect to the mean flow. These wires operate identical to the single yawed wire, so that equations (5.99) and (5.100) can be applied directly. The X-wire probes are used to evaluate both the v and w velocity components, as well as the correlations between the velocity components.

The present discussion treats only the measurement of the v component, but it should be obvious that placing the same probe with its wires yawed in the xz-plane the w component will be measured.

The output voltage from the two wires may be written, following equations (5.99) and (5.100), (the same could also be done for equations (5.101) and (5.102) as

$$(ke)_{+\varphi} = \frac{u}{U_m}\sin\varphi + \frac{v}{U_m}\cos\varphi$$

$$(ke)_{-\varphi} = \frac{u}{U_m}\sin\varphi - \frac{v}{U_m}\cos\varphi \qquad (5.111)$$

From an electronic standpoint it appears a simple matter to match $K+\varphi$ and $K-\varphi$ and then subtract $(e_{+\varphi} - e_{-\varphi})$ to obtain a unique relation for $\sqrt{v^2}/U_m$. Such a technique was developed by Schubauer and Klebanoff[1], in their early work on the application of the anemometer to turbulent boundary layer research.

The mean square of the instantaneous difference between the two X-wire voltage outputs can be determined from equation (5.111) as

$$\overline{(e_{+\varphi} - e_{-\varphi})^2} = \frac{\overline{u^2}}{U_m^2}\sin^2\varphi\left[\frac{1}{K_{+\varphi}^2} - \frac{2}{K_{+\varphi}K_{-\varphi}} + \frac{1}{K_{-\varphi}^2}\right] + \frac{2\overline{uv}}{U_m^2}\sin\varphi\cos\varphi\left[\frac{1}{K_{+\varphi}^2} - \frac{1}{K_{-\varphi}^2}\right]$$

$$+ \frac{\overline{v^2}}{U_m^2}\cos^2\varphi\left[\frac{1}{K_{+\varphi}^2} + \frac{2}{K_{+\varphi}K_{-\varphi}} + \frac{1}{K_{-\varphi}^2}\right] \qquad (5.112)$$

From equation (5.112) it is evident that if $K+\varphi = K-\varphi = K$ then

$$\overline{(e_{+\varphi} - e_{-\varphi})^2} = \frac{4\overline{v^2}}{K^2U_m^2}\cos^2\varphi \qquad (5.113)$$

Equation (5.113) demonstrates the practical

---

[1] Schubauer, G.B., and Klebanoff, P.S.,

problem is one of matching the two wires of the X-wire probe. Schubauer and Klebanoff solved this problem by rotating the X-wires about their axis until the mean voltage from the two wires are equal. Figure 5.36 is a plot, obtained by Schubauer and Klebanoff, of the mean voltage from the two wires of an X-probe, as a function of angle. The difference voltage between the two wires is also plotted on figure 5.36. It may be seen that the curves for the individual wires are far from linear in the region of the angles

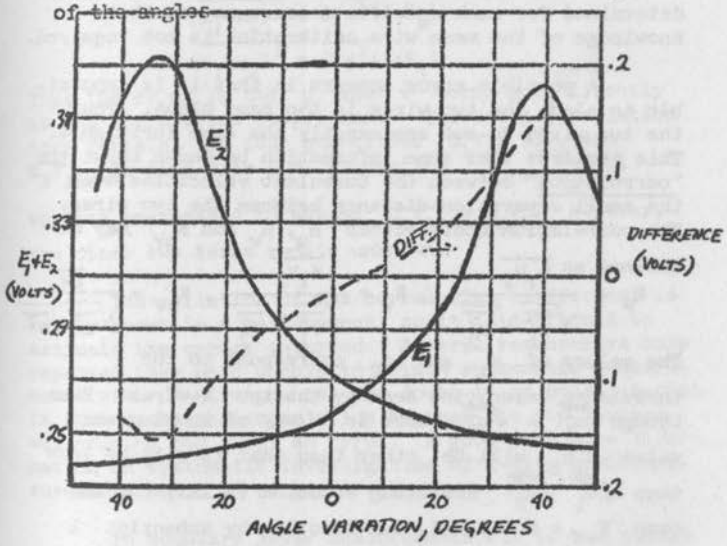

Figure 5.36 - Matching of the X-probe Wires to Measure the v and w Turbulent Velocity Components.

However, the difference voltage is nearly linear over an angle range of 30°. The slope of this voltage different curve is the reciprocal of the sensitivity of the X-wires to v or w. Expressing the slope in volts per radian, there exists the relation

$$\frac{\sqrt{v^2}}{U_m^2} = \frac{\sqrt{(e_{+\varphi} - e_{-\varphi})^2}}{\Delta E/\Delta\varphi} \qquad (5.114)$$

Where $\Delta E/\Delta\varphi$ is the slope, and $(e_{+\varphi} - e_{-\varphi})^2$ is the r.m.s. of the instantaneous difference between the two wires. In operation the value $\Delta E/\Delta\varphi$ can be determined for each specific measurement so that knowledge of the mean wire calibration is not required.

A possible error appears in that it is impossible to place the two wires in the same plane. Thus, the two wires do not see exactly the same turbulence. This requires that some information be known about the "correlation" between the turbulent velocities over the small separation distance between the two wires. The correlation coefficients R_u, R_v and R_{uv} may be defined as

$$R_u = \frac{\overline{u_1 u_2}}{\sqrt{\overline{u_1^2}}\sqrt{\overline{u_2^2}}}, \quad R_v = \frac{\overline{v_1 v_2}}{\sqrt{\overline{v_1^2}}\sqrt{\overline{v_2^2}}}, \quad R_{uv} = \frac{\overline{uv}}{\sqrt{\overline{u^2}}\sqrt{\overline{v^2}}}$$

The values of u_1 and u_2 correspond to the turbulence velocities seen by the two X-wires. Even though $\sqrt{\overline{u_1^2}} = \sqrt{\overline{u_2^2}}$ there is no way of knowing what value $\overline{u_1 u_2}$ will be, other than that it will be less than $\sqrt{\overline{u_1^2}}\sqrt{\overline{u_2^2}}$. Rewriting equation (5.111) for the case $K_{+\varphi} = K_{-\varphi} = K$, but denoting by subscript 1 or 2 the turbulent velocity corresponding to the $+\varphi$ or $-\varphi$ wire, gives

$$\overline{(e_{+\varphi} - e_{-\varphi})^2} = \frac{\sin^2\varphi}{K^2 U_m^2}\overline{(u_1 - u_2)^2} + \frac{2\sin\varphi\cos\varphi}{K^2 U_m^2}\overline{(u_1 - u_2)(v_1 + v_2)} + \frac{\cos^2\varphi}{K^2 U_m^2}\overline{(v_1 + v_2)^2} \qquad (5.115)$$

note that the correlation coefficient can be defined as

$$R_u = \frac{\overline{u_1 u_2}}{\sqrt{\overline{u_1^2}}\sqrt{\overline{u_2^2}}} = \frac{\overline{(u_1+u_2)^2} - \overline{(u_1-u_2)^2}}{4\sqrt{\overline{u_1^2}}\sqrt{\overline{u_2^2}}}$$

or $$\overline{(u_1-u_2)^2} = \overline{(u_1+u_2)^2} - R_u\, 4\sqrt{\overline{u_1^2}}\sqrt{\overline{u_2^2}}$$

$$\overline{(v_1+v_2)^2} = \overline{(v_1-v_2)^2} + R_v\, 4\sqrt{\overline{v_1^2}}\sqrt{\overline{v_2^2}}$$

For the assumption $\overline{u_1^2} = \overline{u_2^2}$ and $\overline{v_1^2} = \overline{v_2^2}$

$$\overline{(u_1-u_2)^2} = 2\,\overline{u^2}(1-R_u)$$

$$\overline{(v_1-v_2)^2} = 2\,\overline{v^2}(1+R_v)$$

Thus the error in the u and v terms goes directly as the correlation coefficient. The cross correlation term contains the four quantities $\overline{u_1 v_1}$, $\overline{u_2 v_2}$ and $\overline{u_2 v_1}$. In line with the assumption $\overline{u_1^2} = \overline{u_2^2}$, it appears reasonable to assume $\overline{u_1 v_1} = \overline{u_2 v_2}$, however, the other two terms remain unknown.

The variation of the correlation coefficient is rarely known in a measurement, so it is difficult to estimate the errors incurred. Several researchers have reported they were unable to obtain reasonable measurements with X-wire probes. No doubt it is possible that in some cases the correlation between the two X-wires was causing too great an error. A good deal more information on systematic investigation of X-wire probe measurements would be of great value.

In boundary layer measurements, it is not always possible to rotate and match the two wires of an X-probe. Thus, a more complex method of evaluating the probe outputs must be employed. Basically, equation (5.106) can be used to evaluate uv and equation (5.107) can be employed to evaluate $\overline{v^2}$ (where $\overline{u^2}$ is obtained from an independent measure with a single wire normal to the flow). Equation (5.106) and (5.107) require only that $\overline{u_1^2} = \overline{u_2^2}$, $\overline{v_1^2} = \overline{v_2^2}$, with no uncertainty entering due to the correlation coefficient. Note that in most cases it is quite reasonable to equate the statistical average velocities, even though the correlation might differ from one. To make X-wire

measurements independent of the normal wire measurements the electronic sum and difference circuit is employed. In this way a third statistical average equation, such as equation (5.115) is obtained. Since there are three unknowns, $\overline{u^2}$, $\overline{v^2}$ and $\overline{uv}$, three relations are needed. It was found convenient to construct the third equation from a measure of both the sum and difference of the X-wire signals. The mean square instantaneous sum, corresponding to the difference equation (5.115) is

$$\overline{(e_{+\varphi} + e_{-\varphi})^2} = \frac{\overline{u^2}}{U_m^2}\sin^2\varphi\left[\frac{1}{K_{+\varphi}^2} + \frac{2}{K_{+\varphi}K_{-\varphi}} + \frac{1}{K_{-\varphi}^2}\right]$$

$$+ \frac{2\overline{uv}}{U_m^2}\sin\varphi\cos\varphi\left[\frac{1}{K_{+\varphi}^2} - \frac{1}{K_{-\varphi}^2}\right] + \frac{\overline{v^2}}{U_m^2}\cos^2\varphi\left[\frac{1}{K_{+\varphi}^2} + \frac{2}{K_{+\varphi}K_{-\varphi}} + \frac{1}{K_{-\varphi}^2}\right] \quad (5.116)$$

Note that substracting equation (5.112) from equation (5.116) gives

$$\frac{K_{+\varphi}K_{-\varphi}}{4}(\epsilon_+^2 - \epsilon_-^2) = \frac{\overline{u^2}}{U_m^2}\sin^2\varphi - \frac{\overline{v^2}}{U_m^2}\cos^2\varphi \quad (5.117)$$

where

$$\overline{\epsilon_+^2} = \overline{(e_{+\varphi} + e_{-\varphi})^2} \quad \text{and} \quad \overline{\epsilon_-^2} = \overline{(e_{+\varphi} - e_{-\varphi})^2}$$

Solving equations (5.103), (5.105) and (5.117) for $\overline{u^2}$ and $\overline{v^2}$ gives

$$\frac{\overline{u^2}}{U_m^2} = \frac{1}{4\sin^2\varphi}\left[K_{+\varphi}^2\overline{e_{+\varphi}^2} + K_{-\varphi}^2\overline{e_{-\varphi}^2} + \frac{K_{+\varphi}K_{-\varphi}}{2}(\overline{\epsilon_+^2} - \overline{\epsilon_-^2})\right] \quad (5.118)$$

and

$$\frac{\overline{v^2}}{U_m^2} = \frac{1}{4\cos^2\varphi}\left[K_{+\varphi}^2\overline{e_{+\varphi}^2} + K_{-\varphi}^2\overline{e_{-\varphi}^2} - \frac{K_{+\varphi}K_{-\varphi}}{2}(\overline{\epsilon_+^2} - \overline{\epsilon_-^2})\right] \quad (5.119)$$

The sum and difference relation, equation (5.117), can be shown to be in error directly as the correlation coefficients, much the same as equation (5.113). However, the uncertainty can be determined by comparing the evaluation of $\sqrt{u^2} / U_m$ from the X-wire measurements with measurements made with a single wire normal to the flow. Figure 5.37 shows such a comparison reported by Sandborn and Slogar.[1] These measurements were made in a turbulent boundary layer. A comparison, such as shown in figure (5.37), gives a good consistency check on the reliability of the other X-wire measurements $-\overline{v^2}$, $\overline{w^2}$ and $\overline{uv}$. For the particular boundary layer flow studied in connection with figure (5.37), it was found that the X-wire measurements checked the single wire data within ± 20%. Obviously, the X-wire data will be subject to a great deal more random error than the single wire data. This means that errors of ± 20% might be expected even in the absence of the correlation error. However, if the error exceeds ± 20% the data of figure 5.37 would suggest that other than random error is being encountered.

Several techniques for evaluating X-wire data have been discussed by other researchers.[2] These methods are simular to those outlined above. Flow Corporation,[2] finds it convenient to work with the instantaneous values, such as $(K_{+\varphi} e_{+\varphi} + K_{-\varphi} e_{-\varphi})$ where the wire sensitivity constant K is handled through the electronic circuits. For a given application this approach can save on computing time. In each and every application it appears necessary to reach an independent conclusion on whether equation (5.99) and (5.100), or the more complex relations (5.100) and (5.102) must be used. As in the wire normal to the flow case, one can not rely on previous reported hot wire evaluation. Only in recent years has it become obvious that the King's Law approach is too restricted. Like the normal wire case, figure 5.22 the mean heat loss relations must be valid to the first derivative in order to accurately evaluate the turbulence.

Correlation Measurements - The importance of correlation terms in turbulence theory make necessary a great number of correlation measurements. The previous discussion on X-wire covered briefly some of the methods of

---

[1] Sandborn, V.A., and Slogar, R.J.; NACA TN 3265, 1955.

[2] See for example: Bulletin No. 68, Flow Corp. 205 Auth Street, Cambridge 42, Mass, 1962.

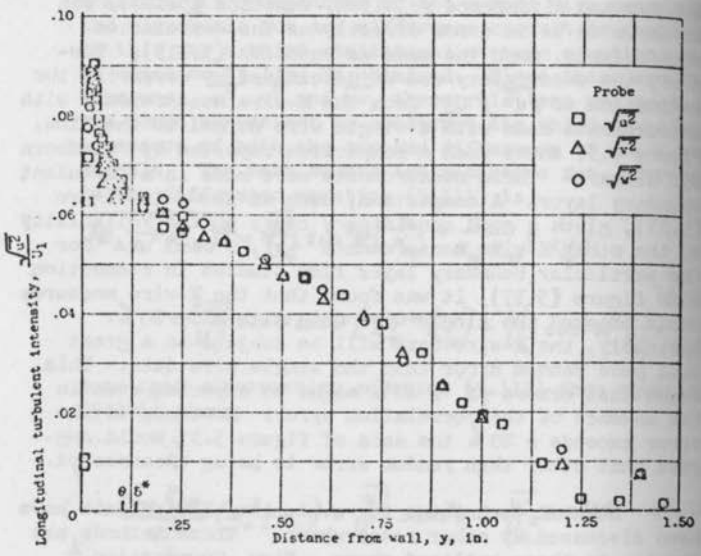

Figure 5.37-Comparison of $\frac{\sqrt{\overline{u^2}}}{U_m}$ measurements made with a single wire and X-wire probes

evaluating correlations. The cross correlation measurements of $\overline{uv}$ and $\overline{uw}$ are obtained directly from the X-wire data, equation (5.106). For turbulent shear flows the uv term corresponds to the turbulent shear and it is important in the equation of motion. (Depending on the particular flow coordinates $\overline{uv}$ or $\overline{uw}$ may be the shear term.) For most turbulent flow fields, symmetry conditions will require that one of the cross correlations terms, usually $\overline{uw}$, be very near zero. Likewise, the term $\overline{vw}$ should be approximately zero in most turbulent flows, so no technique has been developed to measure it.

Terms such as $\overline{u^2v}$ become important in the turbulent energy relations[1]. The triple correlations can be obtained from the X-wire probes by employing an electronic multiplier. Starting with equations (5.111) and obtaining the mean quantities indicated, the following X-wire relations for the triple velocity correlations are obtained.

$$\frac{\overline{u^3}}{U_m^3} = \frac{K_{+\varphi}^3 \overline{e_{+\varphi}^3} + K_{-\varphi}^3 \overline{e_{-\varphi}^3}}{2\sin^3\varphi} - \tfrac{3}{8}(\cot^2\varphi)\left[K_{+\varphi}^3 \overline{e_{+\varphi}^3} + K_{-\varphi}^3 \overline{e_{-\varphi}^3} - K_{+\varphi}^2 K_{-\varphi} \overline{e_{+\varphi}^2 e_{-\varphi}} - K_{+\varphi} K_{-\varphi}^2 \overline{e_{+\varphi} e_{-\varphi}^2}\right] \quad (5.120)$$

$$\frac{\overline{v^3}}{U_m^3} = \frac{K_{+\varphi}^3 \overline{e_{+\varphi}^3} - K_{-\varphi}^3 \overline{e_{-\varphi}^3}}{2\cos^3\varphi} - \tfrac{3}{8}(\tan^2\varphi)\left[K_{+\varphi}^3 \overline{e_{+\varphi}^3} - K_{-\varphi}^3 \overline{e_{-\varphi}^3} + K_{+\varphi}^2 K_{-\varphi} \overline{e_{+\varphi}^2 e_{-\varphi}} - K_{+\varphi} K_{-\varphi}^2 \overline{e_{+\varphi} e_{-\varphi}^2}\right] \quad (5.121)$$

$$\frac{\overline{u^2v}}{U_m^3} = \frac{1}{8}\left[K_{+\varphi}^2 K_{-\varphi} \overline{e_{+\varphi}^2 e_{-\varphi}} - K_{+\varphi} K_{-\varphi}^2 \overline{e_{+\varphi} e_{-\varphi}^2} + K_{+\varphi}^3 \overline{e_{+\varphi}^3} - K_{-\varphi}^3 \overline{e_{-\varphi}^3}\right] \quad (5.122)$$

[1] Townsend, A.A.: The Structure of the Turbulent Boundary Layer, Proc. Cambridge Phil. Soc., Vol. 47, pt. 2, 1951.

$$\frac{\overline{uv^2}}{U_\infty^3} = \frac{1}{8}\left[K_{+\varphi}^3 \overline{e_{+\varphi}^3} + K_{-\varphi}^3 \overline{e_{-\varphi}^3} - K_{+\varphi}^1 K_{-\varphi} \overline{e_{+\varphi}^2 e_{-\varphi}} - K_{+\varphi} K_{-\varphi}^2 \overline{e_{+\varphi} e_{-\varphi}^2}\right] \qquad (5.123)$$

Modern multipliers now exceed any requirements made of them in analyzing hot wire data, so that the four operations required can be done with about the same degree of accuracy as the evaluation of mean square terms from X-wire data.

The usual measured correlation is for two points, however, it can be of any number of points and of any higher moment of the velocity. For the present discussion only two point correlations are considered. It may be kept in mind that the addition of more hot wires and the use of multipliers can produce any degree of correlation required. For the two point correlation either a multiplier or sum and difference circuit may be employed. As introduced previously, the correlation coefficient can be written as

$$R_u = \frac{\overline{u_1 u_2}}{\sqrt{\overline{u_1^2}}\sqrt{\overline{u_2^2}}} = \frac{\overline{(u_1+u_2)^2} - \overline{(u_1-u_2)^2}}{4\sqrt{\overline{u_1^2}}\sqrt{\overline{u_2^2}}} \qquad (5.124)$$

It has only been in the past few years that instantaneous multipliers circuits have become available. Although multiplier circuits were reported in the literature for a good number of years, the operation was marginal. The commercial units presently available give very reliable results. The sum and difference technique was used in the place of multipliers. A simple sum and difference circuit, such as shown in figure 2.20 is quite easy to build and operate.

The correlation coefficients R_v, R_w and R_{uv} can

be determined from two X-wire probes. These correlations measurements are a major undertaking, and as such have not been reported. As an alternate approach, the autocorrelation technique, has been employed. The autocorrelation measures the correlation of the signal from a single wire at two instances in time.

Separation of Velocity, Temperature and Density Fluctuations - The general application of the anemometer to measurements of velocity, temperature and density is by far more complex than the cases treated so far. The approach in the present section will be to introduce the all inclusive hot wire sensitivity relations. Note that the overall sensitivity relations could have been developed at the outset, and all results in the preceding sections derived directly from the general relation. However, it appeared that the concepts of transient anemometry could better be grasped by discussing directly

the simple cases, without bringing in the complexity of the general relations. The general sensitivity equations do in no way eliminate the necessity of individual wire calibration, but rather, they serve as guides to performing the calibrations. The non-dimensional heat-transfer correlation for hot wire can be written as:

$$Nu_t = f(M, Kn, \Delta T, \tau_t, \varphi) \qquad (5.125)$$

The choice of (M,Kn) rather than (M,Re) or (Re,Kn) leads to simpler sensitivity expressions. The use of Reynolds number introduces additional terms in the velocity sensitivity. The "temperature loading" parameter, τ (=Tw-Te/T_t = $\Delta T/T_t$) is employed to account for the second-order, nonlinear dependence of the Nusselt number on air and wire temperature. The effect of τ on Nu in slip flow causes up to 20 percent deviations from the general correlation. The recovery temperature, Te, may be expressed in terms of the recovery temperature ratio, η, and total temperature, Te-ηT_t. The heat loss from a wire may be written as

$$I^2R = \pi \ell k (T_w - \eta T_t) Nu_t \qquad (5.126)$$

Equation (5.126) assumes that Nut is corrected for finite wire length, so that I^2 is the square of the measured wire current times the end-loss correction factor ζI_m^2. Naturally, if a calibration curve for a particular wire is being used, it is possible to set ζ = 1 and correlate data as Nu*.

It will be assumed that the hot-wire resistance (or temperature) is maintained constant by a fluctuating feedback current:

$$2IR\,dI = \frac{\partial}{\partial U}\left[\pi \ell k (T_w - \eta T_t)\right] Nu\, dU + \frac{\partial}{\partial \rho}\left[\pi \ell k (T_w - \eta T_t) Nu\right] d\rho$$

$$+ \frac{\partial}{\partial \varphi}\left[\pi \ell k (T_w - \eta T_t) Nu\right] d\varphi + \frac{\partial}{\partial T_t}\left[\pi \ell k (T_w - \eta T_t) Nu\right] dT \qquad (5.127)$$

If the fluctuating current dI is set equal to i and small finite flow fluctuations are approximated by δ to replace the derivatives, equation (5.127) can be written as

$$i = \left[\frac{\pi \ell}{2IR} k Nu T_t \left(-\frac{\partial \eta}{\partial U}\right) + \frac{\pi \ell}{2IR} k Nu\, \eta \left(-\frac{\partial T_t}{\partial U}\right) + \frac{\pi \ell}{2IR} k (T_w - \eta T_t) \frac{\partial Nu}{\partial U}\right] \delta U$$

$$+ \left[\frac{\pi \ell}{2IR} k (T_w - \eta T_t) \frac{\partial Nu}{\partial \rho} + \frac{\pi \ell}{2IR} k Nu \overline{T_t} \left(-\frac{\partial \eta}{\partial \rho}\right)\right] \delta \rho \qquad (5.128)$$

$$+ \left[\frac{\pi \ell}{2IR} (T_w - \eta T_t) Nu \frac{\partial k}{\partial T_t} - \frac{\pi \ell}{2IR} k Nu\, \eta + \frac{\pi \ell}{2IR} k (T_w - \eta T_t) \frac{\partial Nu}{\partial T_t}\right] \delta T_t$$

$$+ \left[\frac{\pi \ell}{2IR} k Nu T_t \left(-\frac{\partial \eta}{\partial \varphi}\right) + \frac{\pi \ell}{2IR} k (T_w - \eta T_t) \frac{\partial Nu}{\partial \varphi}\right] \delta \varphi$$

The following dimensionless groups are introduced to generalize equation (5.128).

$$\left.\begin{aligned} \frac{\partial}{\partial \rho} &= \frac{\partial K_n}{\partial \rho} \frac{\partial}{\partial K_n} = -\frac{K_n}{\rho} \frac{\partial}{\partial K_n} \\ \frac{\partial}{\partial U} &= \frac{\partial M}{\partial U} \frac{\partial}{\partial M} = \frac{1 + \frac{\gamma - 1}{2} M^2}{a_s} \frac{\partial}{\partial M} \\ \frac{\partial T_t}{\partial U} &= \frac{U}{c_p} \\ \frac{\partial}{\partial T_t} &= \frac{\partial \tau}{\partial T_t} \frac{\partial}{\partial \tau} = -\frac{\tau + \eta}{T_t} \frac{\partial}{\partial \tau} \end{aligned}\right\} \qquad (5.129)$$

Using the above relation in equation (5.128), along with

the relations $M = \frac{U}{a_s}$ and $\frac{I}{2Nu} = \frac{\pi \ell}{2IR} k\,(Tw = \eta T_t)$, results in the following from for the sensitivity relation

$$i = \frac{I}{2}\left[-\left(1+\frac{\gamma-1}{2}M^2\right)\frac{M}{\tau}\frac{\partial \eta}{\partial M} - \frac{U^2\eta}{c_p T_t \tau} + \left(1+\frac{\gamma-1}{2}M^2\right)\frac{M}{Nu}\frac{\partial Nu}{\partial M}\right]\frac{\delta U}{U}$$
$$+ \frac{I}{2}\left[\frac{Kn}{\tau}\frac{\partial \eta}{\partial Kn} - \frac{Kn}{Nu}\frac{\partial Nu}{\partial Kn}\right]\frac{\delta \rho}{\rho}$$
$$+ \frac{I}{2}\left[\frac{T_t}{k}\frac{\partial k}{\partial T_t} - \frac{\eta}{\tau} - \frac{\tau+\eta}{Nu}\frac{\partial Nu}{\partial \tau}\right]\frac{\delta T_t}{T_t} \qquad (5.130)$$
$$+ \frac{I}{2}\left[-\frac{\varphi}{\tau}\frac{\partial \eta}{\partial \varphi} + \frac{\varphi}{Nu}\frac{\partial Nu}{\partial \varphi}\right]\frac{\delta \varphi}{\varphi}$$

Equation (5.130) is the general constant temperature hot wire anemometer sensitivity. It is a linearized relation in that dI was replaced by i and the other derivatives are represented by δ. The relation is also restricted to fluids in which the relations

$\frac{\partial M}{\partial U} = 1 + \frac{\gamma-1}{2}M^2$ and $\frac{\partial T_t}{\partial U} = \frac{U}{Cp}$ apply (for example the relations are not valid for flows of air in which the temperature excees 2000°K).

Equation (5.130) is valid for almost every type of aerodynamic flow obtainable in test facilities. The exceptions are the very high temperature shock tubes and some are heated facilities. The special applications of the transient anemometer to date are for the most part limited to values of $Kn < 0.10$. Restrictions of the hot wire to flows in which $Kn < 0.10$ allows the recovery temperature dependency on Kn and φ to be neglected. Also from figure 5.30 the three dimensional angle $\delta\varphi$ is approximately equal to $\frac{v}{U}$ (i.e. $\tan \delta\varphi \simeq \delta\varphi = \frac{v}{U}$). This assumption is equivalent to assuming that the w velocity fluctuations do not affect the heat transfer from the wire. Inspection of equation (5.130) suggests that simplifications are possible by employing logarithmic derivations (i.e. $\frac{M}{Nu}\frac{\partial Nu}{\partial M} = \frac{\partial Log\, Nu}{\partial Log\, M}$, $\frac{T_t}{k}\frac{\partial k}{\partial T_t} = \frac{\partial Log\, k}{\partial Log\, T_t}$, and $\frac{1}{Nu}\cdot\frac{\partial Nu}{\partial \varphi} = \frac{\partial Log\, Nu}{\partial \varphi}$)

The constant temperature hot wire anemometer sensitivity for continuum and moderate slip flow the sensitivity relation may be written as

$$i = \frac{I}{2}\left[-\left(1+\frac{\gamma-1}{2}M^2\right)\frac{M}{\tau}\frac{\partial\eta}{\partial M} - \frac{\eta}{\tau}(\gamma-1)M^2 + \left(1+\frac{\gamma-1}{2}M^2\right)\frac{\partial \log Nu}{\partial \log M}\right]\frac{u}{U}$$

$$+ \frac{I}{2}\left[\frac{\partial \log Nu}{\partial \varphi}\right]\frac{v}{U} + \frac{I}{2}\left[\frac{\partial \log Nu}{\partial \log Kn}\right]\frac{\delta\rho}{\rho} \qquad (5.131)$$

$$+ \frac{I}{2}\left[\frac{\partial \log k}{\partial \log T_t} - \frac{\eta}{\tau} - \frac{\tau+\eta}{Nu}\frac{\partial Nu}{\partial \tau}\right]\frac{\delta T}{T_t}$$

The derivation of the general sensitivity equation for the constant current hot wire anemometer starts also from equation (5.126). An additional derivative enters such sensitivity term, since the wire temperature is no longer constant. The constant current hot wire anemometer relation, equivalent to equation (5.130), is given below, where IdR =c

$$e = IR\left[\left(1+\frac{\gamma-1}{2}M^2\right)\frac{M}{\tau T_t}\frac{\partial T_w}{\partial M} - \left(1+\frac{\gamma-1}{2}M^2\right)\frac{M}{\tau}\frac{\partial \eta}{\partial M} - \frac{U^2\eta}{c_p T_t \tau} + \left(1+\frac{\gamma-1}{2}M^2\right)\frac{M}{Nu}\frac{\partial Nu}{\partial M}\right]\frac{\delta U}{U}$$

$$+ IR\left[-\frac{Kn}{\tau T_t}\frac{\partial T_w}{\partial Kn} + \frac{Kn}{\tau}\frac{\partial \eta}{\partial Kn} - \frac{Kn}{Nu}\frac{\partial Nu}{\partial Kn}\right]\frac{\delta\rho}{\rho}$$

$$+ IR\left[\frac{1}{\tau}\frac{\partial T_w}{\partial T_t} + \frac{T_t}{k}\frac{\partial k}{\partial T_t} - \frac{\eta}{\tau} - \frac{\tau+\eta}{Nu}\frac{\partial Nu}{\partial \tau}\right]\frac{\delta T}{T_t} \qquad (5.132)$$

$$+ IR\left[\frac{\varphi}{\tau T_t}\frac{\partial T_w}{\partial \varphi} - \frac{\varphi}{\tau}\frac{\partial \eta}{\partial \varphi} + \frac{\varphi}{Nu}\frac{\partial Nu}{\partial \varphi}\right]\frac{\delta\varphi}{\varphi}$$

Morkovin,[1] has defined a different form of equation (5.132), where he considers Nu = f (M,Re,Θ). The quantity $\Theta = T_w/T_t$ is simular to the temperature loading term. He obtains a more general form in that the wire temperature is treated as an independent variable. The derivation does not include the effect of yawed wires. Morkovin's sensitivity relation in the present notation is given below.

$$
\begin{aligned}
e = IR\Bigg[& \frac{d\log k}{d\log T_t} - \frac{d\log u}{d\log T_t}\frac{Re_t}{Nu_t} - \frac{\tau+\eta}{Nu_t}\frac{\partial Nu_t}{\partial\theta} - \frac{\eta}{\tau}\left\{1 - \frac{(1+\frac{\gamma-1}{2}M^2)}{2}\frac{M}{\eta}\frac{\partial\eta}{\partial M}\right. \\
& \left. - \frac{d\log\mu}{d\log T_t}\frac{Re_t}{\eta}\frac{\partial\eta}{\partial Re_t}\right\} - \frac{1}{2}(1+\tfrac{\gamma-1}{2}M^2)\frac{M}{Nu_t}\frac{\partial Nu_t}{\partial M}\Bigg]\frac{\delta T}{T} \\
& + IR\Bigg[\frac{Re_t}{Nu_t}\frac{\partial Nu_t}{\partial Re_t} + (1+\tfrac{\gamma-1}{2}M^2)\frac{M}{Nu_t}\frac{\partial Nu_t}{\partial M} - \frac{\eta}{\tau}\left\{(1+\tfrac{\gamma-1}{2}M^2)\frac{M}{\eta}\frac{\partial\eta}{\partial M}\right. \\
& \left. + \frac{Re_t}{\eta}\frac{\partial\eta}{\partial Re_t}\right\}\Bigg]\frac{\delta U}{U} \qquad (5.133) \\
& + IR\Bigg[\frac{Re_t}{Nu_t}\frac{\partial Nu_t}{\partial Re_t} - \frac{\eta}{\tau}\frac{Re_t}{\eta}\frac{\partial\eta}{\partial Re_t}\Bigg]\frac{\delta\rho}{\rho} \\
& + IR\left[\frac{\theta}{Nu_t}\frac{\partial Nu_t}{\partial\theta} + \frac{\theta}{\theta-\eta}\right]\frac{\delta T_w}{T_w}
\end{aligned}
$$

Morkovin covers in detail the application of this relation to measurements in supersonic flow.

Measurements of Velocity and Temperature Fluctuations - The general sensitivity relation indicates the hot wire responds to fluctuations in total temperature, as well as to velocity and density. In other words the hot wire behaves as an anemometer, resistance thermometer and a manometer all at the same time. The present discussion assumes that it is possible to obtain a turbulent flow in which only velocity and temperature fluctuate. If temperature fluctuations are kept small (of the order of 5° F or less) and velocity is also low, then a turbulent flow field might exist in which fluctuations in density can be neglected. Whether such a case actually exists has

[1] Morkovin, M.V.: Fluctuations and Hot Wire Anemometry in Compressible Flows AGARDograph 24, 1956.

not been completely established, however, measurements have been reported based on the assumption that density fluctuation can be neglected in special flows.

Although there are several papers in the literature which report velocity and temperature fluctuation measurements, there is little information on the general application of the anemometer in this type of flow. Assuming $\delta\rho/\rho=0$, the general equation (5.130) expresses the linearized sensitivity of the constant temperature hot-wire anemometer in an incompressible flow is,

$$e = \frac{E}{2}\left[-(1+\frac{\gamma-1}{2}M^2)\frac{M}{\tau}\frac{\partial\eta}{\partial M} - \frac{\eta}{\tau}(\gamma-1)M^2 + (1+\frac{\gamma-1}{2}M^2)\frac{\partial \log Nu}{\partial \log M}\right]\frac{u}{U} + \frac{E}{2}\left[\frac{\partial \log K}{\partial \log T} - \frac{\eta}{\tau} - \frac{\tau+\eta}{Nu}\frac{\partial Nu}{\partial \tau}\right]\frac{\delta T}{T} \qquad (5.134)$$

Since the flow is limited to the incompressible case the recovery temperature term η is equal to 1, and the Mach number is considered as zero. It is further assumed that the variation of thermal conductivity with temperature may be neglected. Thus equation (5.134) can be reduced to the form

$$e = \left[\frac{\pi \ell}{2I}k(T_w - T)\frac{\partial Nu}{\partial U}\right]u + \left[-\frac{\pi \ell}{2I}kNu + \frac{\pi \ell}{2I}k(T_w - T)\frac{\partial Nu}{\partial T}\right]t \qquad (5.135)$$

where ℓ is the hot wire length, I is the current passing through the hot wire, and t is the fluctuation in temperature. From the definition of Nusselt number

$$Nu = \frac{hD}{k} = \frac{I^2R}{k\pi\ell(T_w - T_a)}$$

the relation, Eq. 5.135, may be expressed in terms of the directly measured quantities.

$$e = \frac{\pi \ell \Delta T}{2I}\left[\frac{\partial(hD)}{\partial U}u + \left(-\frac{hD}{\Delta T} + \frac{\partial(hD)}{\partial T}\right)t\right] = \frac{\partial E}{\partial U}u + \frac{\partial E}{\partial T}t \qquad (5.136)$$

Equation (5.136) may be employed to evaluate the r.m.s. velocity and temperature fluctuation and the velocity-temperature correlation. A typical example of the application of the equation is encountered in the study of thermal boundary layers. It is desired to determine the usual fluctuations and also the correlation of velocity and temperature on a delay basis (auto-correlation). For this application it would be convenient to obtain a hot wire output proportional to only the instantaneous velocity. The instantaneous temperature fluctuation can be obtained by operating the hot wire as a resistance thermometer.

Thus, equation (5.136) indicates that for a hot wire held at constant temperature (electronically), it is necessary to know the variation in wire voltage with flow temperature and velocity. For the case of the resistance thermometer it is possible to operate the "hot wire" at such a low value of current (low temperature) that $\partial E/\partial V = 0$ and equation (5.136) becomes

(RESISTANCE THERMOMETER) $$de = \frac{\partial E}{\partial T} dT \qquad (5.137)$$

where $(I \approx 0)$

The possibility was advanced that $\partial E/\partial T$ does not vary with increase in wire temperature whereas $\frac{\partial E}{\partial \bar{u}}$ increase rapidly with wire temperature. Thus, by operating the hot wire at high temperatures it might be possible to reach a condition where $\frac{\partial E}{\partial \bar{u}} \gg \frac{\partial E}{\partial T}$.

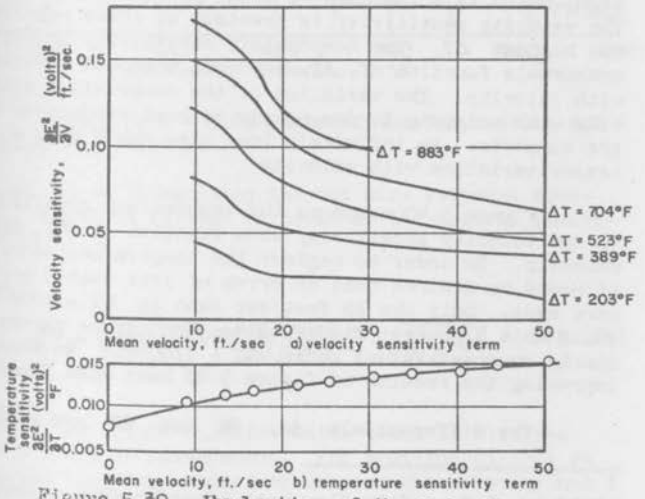

Figure 5.39 - Evaluation of the Velocity and Temperature Sensitivity.

Figure 5.39 is a plot of the velocity and temperature sensitivity terms obtained for a 0.0002 inch diameter 90 percent platinum 10 percent rhodium hot wire. The terms are plotted as $\frac{\partial E^2}{\partial V}$ and $\frac{\partial E^2}{\partial T}$ as a matter of convenience only. For the terms plotted in figure 5.39 equation (5.136) would be written as

$$2E\,de = \frac{\partial E^2}{\partial V}dV + \frac{\partial E^2}{\partial T}dT \qquad (5.136a)$$

These data were obtained by placing the wire normal to the flow in a constant temperature stream. The temperature of the wire, rather than the air temperature was varied. It is known[1] that the heat loss is a function of $(T_w - T)$ rather than the absolute temperature level, so a change in wire temperature is equivalent to a change in fluid temperature (the sign of the sensitivity is reversed). Figure 5.39 shows the velocity sensitivity term, which is a function of both ΔT and flow velocity. The velocity sensitivity is greatest at lower velocities and highest ΔT. The temperature sensitivity is not a measurable function of ΔT, however, there is a variation with velocity. The variation of the temperature sensitivity with velocity is due mainly to heat conduction to the supports. An infinitely long wire would show a lesser variation with velocity

Figure 5.40 compares the temperature sensitivity to the velocity sensitivity as a function of ΔT and velocity. In order to neglect the temperature sensitivity it would be desired that an error of less than 5 percent were made. Only the 10 feet/sec case at $\Delta T = 1000^{\circ}F$ would this 5 percent figure be reached. (The curves are nearly constant values above $\Delta T + 1200^{\circ}F$.) No means of improving the results of figure 5.40 have been found.

The differentials de, dV and dT are replaced

---

1 Baldwin, L.V.: Slip flow heat transfer from cylinders in subsonic airstreams. NACA TN 4369.

by perturbation quantities $\overline{e^2}$ $\overline{u^2}$ and $\overline{t^2}$. This is

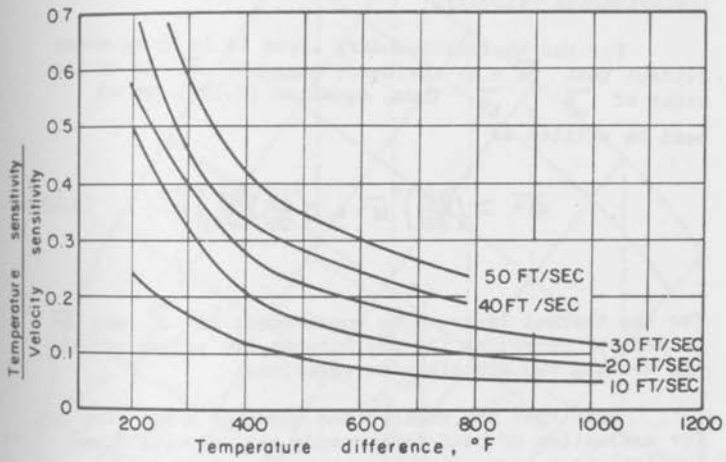

Figure 5.40 - Comparison of the Temperature and Velocity Sensitivity.

equivalent to linearizing the hot wire response equation. Equation (5.136) in terms of the squared quantities is

$$\overline{e^2} = \left(\frac{\partial E}{\partial U}\right)^2 \overline{u^2} + 2\left(\frac{\partial E}{\partial U}\right)\left(\frac{\partial E}{\partial T_f}\right)\overline{ut} + \left(\frac{\partial E}{\partial T}\right)^2 \overline{t^2} \qquad (5.138)$$

This is the actual equation which would be obtained from a hot wire measurement. For equation (5.138) it is noted that the comparison between the velocity and temperature sensitivity terms goes as the square. Thus, for the mean equation it is evident that the temperature term can be neglected compared to the velocity

terms for ΔT greater than about 800°F. Thus, for flows in which $\overline{ut} = 0$ it is possible to measure the r.m.s. longitudinal turbulent velocity in the presence of temperature fluctuations. This is true for the mean quantity only and not applicable for measure of the instantaneous velocity.

For the thermal boundary layer it is by no means evident that $\overline{ut} = o$. Evidence suggests $\overline{ut}$ is of the order of $\overline{u^2} \times \overline{t^2}$. Thus, equation (5.138) can at best be written as

$$\overline{e^2} \simeq \left(\frac{\partial E}{\partial v}\right)^2 \overline{u^2} + 2\left(\frac{\partial E}{\partial v}\right)\left(\frac{\partial E}{\partial t}\right) \overline{ut} \qquad (5.138a)$$

for the thermal layer. The measurement of $\overline{u^2}$ and $\overline{ut}$ is made by operating the hot wire at two values of Δt and solving two simultaneous equations.

Note that the calibration curve of a hot wire for evaluation of both temperature and velocity fluctuations is a three-dimensional curve. Figure 5.41 is a typical calibration curve drawn up a three-dimensional plot. The vertical axis is wire voltage, while the other two axis are flow velocity and temperature difference.

Measurements of Velocity, Temperature and Density Fluctuations - The extension of the hot wire anemometer technique to compressible flow has been underway for about 10 years. The major effort has been in connection with the study of supersonic flows. Historically, Kovasznay[1] introduced the original concepts of turbulence in supersonic flow and applied extended King's law relations to supersonic hot wire measurements. Morkovin,[2] working with Kovasznay has formalized the approach in terms of the general sensitivity equation (5.132) or (5.133). The present discussion follows the general ideas

[1] Kovasznay, L.S.G.: The Hot Wire Anemometer in Supersonic Flow. Jour. Aero. Sci., Vol. 17, No. 9, 1950.

[2] Morkovin, M.V.; ibid.

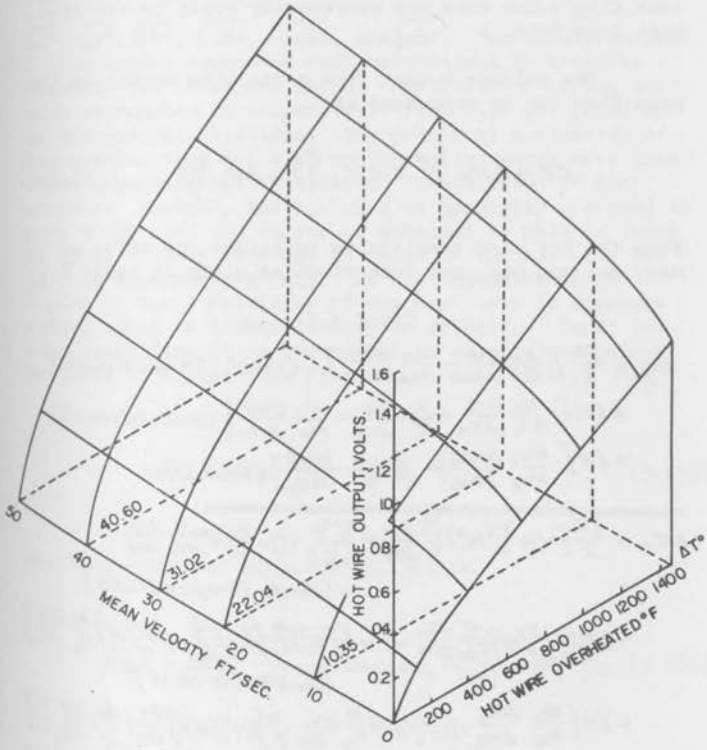

Figure 5.41-Summary of a hot wire velocity-temperature calibration

of Kovasznay and Morkovin, but it will be kept in mind that King's law does not necessarily apply to the mean heat loss data.

The voltage output from a hot wire normal to the mean flow can be expressed as

$$\Delta e = \Delta e_\rho \frac{\delta\rho}{\rho} + \Delta e_u \frac{\delta u}{U} + \Delta e_t \frac{\delta T}{T} \qquad (5.137)$$

From the hot wire sensitivity relations the value of Δe_ρ, Δe_u and Δe_t are determined as given in table V.I.

TABLE V.I.

$$\Delta e_\rho = \frac{IR}{2}\left[\frac{K_0}{\tau}\frac{\partial\eta}{\partial K_n} - \frac{K_n}{Nu}\frac{\partial Nu}{\partial K_n}\right] \quad \text{(Const. temperature)}$$

$$= IR\left[-\frac{K_n}{\tau T_t}\frac{\partial T_w}{\partial K_n} + \frac{K_n}{\tau}\frac{\partial\eta}{\partial K_n} - \frac{K_n}{Nu}\frac{\partial Nu}{\partial K_n}\right] \text{(const. current)}$$

$$= IR\left[\frac{Re_t}{Nu_t}\frac{\partial Nu_t}{\partial Re_t} - \frac{\eta}{\tau}\frac{Re_t}{\eta}\frac{\partial\eta}{\partial Re_t}\right] \text{(Morkovin)}$$

$$\Delta e_u = \frac{IR}{2}\left[-\left(1+\frac{\gamma-1}{2}M^2\right)\frac{M}{\tau}\frac{\partial\eta}{\partial M} - \frac{U^2\eta}{c_p\bar{T}_t\tau} + \left(1+\frac{\gamma-1}{2}M^2\right)\frac{M}{Nu}\frac{\partial Nu}{\partial M}\right.$$

(Const. temperature)

$$= IR\left[\left(1+\frac{\gamma-1}{2}M^2\right)\frac{M}{\tau T_t}\frac{\partial T_w}{\partial M} - \left(1+\frac{\gamma-1}{2}M^2\right)\frac{M}{\tau}\frac{\partial\eta}{\partial M} - \frac{U^2\eta}{c_p\bar{T}_t\tau} + \left(1+\frac{\gamma-1}{2}M^2\right)\frac{M}{Nu}\frac{\partial Nu}{\partial M}\right]$$

(Const. current)

$$= IR\left[\frac{Re_t}{Nu_t}\frac{\partial Nu_t}{\partial Re_t} + \left(1+\frac{\gamma-1}{2}M^2\right)\frac{M}{Nu_t}\frac{\partial Nu_t}{\partial M} - \frac{\eta}{\tau}\left\{\left(1+\frac{\gamma-1}{2}M^2\right)\frac{M}{\eta}\frac{\partial\eta}{\partial M} + \frac{Re_t}{\eta}\frac{\partial\eta}{\partial Re_t}\right\}\right]$$

(Morkovin)

$$\Delta e_t = \frac{IR}{2}\left[\frac{T_t}{k}\frac{\partial k}{\partial T_t} - \frac{\eta}{\tau} - \frac{\tau+\eta}{Nu}\frac{\partial Nu}{\partial\tau}\right] \text{(const. temperature)}$$

$$= IR\left[\frac{1}{\tau}\frac{\partial T_w}{\partial T_t} + \frac{T_t}{k}\frac{\partial k}{\partial T_t} - \frac{\eta}{\tau} - \frac{\tau+\eta}{Nu}\frac{\partial Nu}{\partial\tau}\right] \text{(const. current)}$$

$$= IR\left[\frac{d\log k}{d\log T_t} - \frac{d\log\mu}{d\log T_t}\frac{Re_t}{Nu_t}\frac{\partial Nu_t}{\partial Re_t} - \frac{\tau+\eta}{Nu_t}\frac{\partial Nu_t}{\partial(\tau+\eta)} - \frac{\eta}{\tau}\left\{1 - \frac{\left(1+\frac{\gamma-1}{2}M^2\right)}{2}\frac{M}{\eta}\frac{\partial\eta}{\partial M}\right.\right.$$

$$\left.\left. - \frac{d\log\mu}{d\log T_t}\frac{Re_t}{\eta}\frac{\partial\eta}{\partial Re_t}\right\} - \frac{1}{2}\left(1+\frac{\gamma-1}{2}M^2\right)\frac{M}{Nu_t}\frac{\partial Nu_t}{\partial M}\right] \text{(Morkovin)}$$

The mean square output of the hot wire (equation 5.137 squared) contains 6 fluctuation terms: $\overline{\delta u^2}$, $\overline{\delta \rho^2}$, $\overline{\delta T^2}$, $\overline{\delta u \delta \rho}$, $\overline{\delta u \delta T}$, and $\overline{\delta \rho \delta T}$. This requires that 6 independent equations must be obtained in order to evaluate the turbulent terms. Applications of the hot wire anemometer to compressible flow have not faced up to the general relations. The practical evaluation of information from hot wire measurements, where more than three unknowns were considered, is not known to the authors. Instead, the hot wire is generally operated in such a way that the number of unknowns is held to three or less. Such a case may be found in the use of a hot wire at supersonic speeds. As was demonstrated in Figure 5, the s nsitivity of the heat loss is approximately equal to either density or velocity. Thus, for supersonic flow it is convenient to express the output in terms of a mass flow fluctuation sensitivity, Δe_m,

$$\Delta e = \Delta e_m \frac{\delta \rho u}{\rho U} + \Delta e_t \frac{\delta T}{T} \qquad (5.138)$$

The mean square of equation (5.138) is

$$\overline{\Delta e^2} = \Delta e_m^2 \frac{\overline{\delta(\rho u)^2}}{(\rho U)^2} + 2\Delta e_m \Delta e_t \frac{\overline{\delta(\rho u)\delta T}}{\rho U T} + \Delta e_t^2 \frac{\overline{\delta T^2}}{T^2} \qquad (5.139)$$

Equation (5.139) is the relation used in evaluating the supersonic hot wire anemometer output. The number of unknown fluctuation terms is only three, as in all previous cases considered in detail. To improve the accuracy of measuring the terms the hot wire may be operated at many different temperatures and a statistical approach to the evaluation can be made. Kovasznay,[1] has introduced a

---

[1] Kovasznay, L.S.G.: ibid, and Turbulence in Supersonic Flow. Jour. Aero. Sci., vol. 20, no. 10, 1953.

"fluctuation diagram" graphic technique to improve the evaluation of equation (5.139). Although Kovasznay's technique has been employed mainly for the evaluation of supersonic data, it is apparent that it can be used for any case where three unknowns are present.

Resolution Limits of the Hot Wire Anemometer - The above discussion of the transient hot wire anemometer has attempted to cover the important considerations necessary to make accurate measurements. For the specific areas of application considred the present anemometer systems are adequate. However, as the need for more refined measurements arise and also applications outside the present area of use are made, then it is necessary to consider errors that are normally of second order. The present discussion is concerned with both these second order effects in transient hot wire anemometery measurements, and also the limits attainable with the instrument. The present approach will be to note possible effects and reference literature where more detail is available. It is impossible to ascess the importance of the effects considered.

The ultimate limits of the anemometer will be determined by the electronic and aerodynamic limits on frequency response. The space resolution possible with the hot wire will depend on how small a length can be used. These considerations together with the poise level of the electronic circuits will determine the ultimate measuring ability of the hot wire anemometer.

Problems Associated With Transient Hot Wire Anemometery - Unfortunately, what is a second order problem in one measurement may be a major problem in another application. In the present section two problems of major concern to most researchers are singled out for specific consideration. First the wire breakage problem is discussed. At the start of a program in which hot wires are used for the first time, breakage will cause a great deal of concern. Secondly, the frequency response problem is discussed. This frequency problem can escape the inexperienced researcher and lead to incorrect measurements, which might not be realized.

Wire Breakage - The ultimate objective of the present chapter might be to enable the researcher to obtain a correct turbulence measurements on his first try. Unfortunately, experience indicates that the researcher will be lucky if the first wire lasts until it is mounted in the flow. Unlike other types of measurements, the problem of the hot wire is to get it in the flow intact, rather than just the problem of analyzing the output. To go one step further, once the wire is in the flow the chances are good that it will break or be burnt out upon heating. The only encouragement is that it can be done without breakage, and once perfected wire breakage is a rare occurence. It is doubtful that adequate informati n can be given to prevent some flusteration with the initial attempts at operating the hot wire.

The first attempts at the handling and operating the hot wire in a flow might better be done without the ultimate in perfection. If a 0.0002 inch diameter wire is to be used it is probably best to start with the correct diameter wire. The handling ability between a 0.0005 and a 0.0002 inch diameter wire is quite different. With only a minor amount of caution, the 0.0005 inch diameter wire can be handled and operated by inexperienced people. The 0.0002 inch diameter wire is at least an order of magnitude more difficult to handle. To begin with, a probe with strong wire supports with a minimum amount of "Spring" is recommended. The inertia of the wire alone is not great enough to break the wire even under 50g acceleration loads, but a small movement of the support can stress and break the wire. The jeweler's broaches used in the very fine, minimum disturbence, probes are not recommended for the inexperienced. Instead, a probe with wire supports made from tapered steel "paper clips" are found to work much better if breakage is a problem. Secondly, while it is nice to have a tight strung wire, slack wires last longer. A slight amount of slack in the wire does not greatly affect the output of the wire and at the same time cuts shock breakage to a Kovasznay and Morkovin even go one step further and put a drop of rubber cement at the junction of the support and the jswre. This "shock mounting" technique is found quite useful in obtaining a fairly tight wire, but with slack

available at the ends to prevent wire breakage. Obviously, the shorter the wire supports the less movement occurs.

Once mounted in a flow the wire will not fail due to aerodynamic loads, but rather due to external effects. If a constant current anemometer is being used, the most likely wire failure will be wire burnout. A standard procedure employed by the authors for both constant current and constant temperature anemometers is to employ a probe with a light bulb in place of the hot wire. A standard.... lamp has a tungsten wire filament simular in characteristics to the hot wire. This light bulb probe can be heated up just as a hot wire is heated, and the operation of the circuit checked without fear of burnout. Any sudden surge of current can readily be observed by the light emitted from the bulb. A smooth working current control system is essential to prevent wire burnout. If a wire appears erratic in resistance on heat up, the trouble is most often traced to a poor solder joint between the wire and the support.

The air stream in which the hot wire is operated must be reasonable clean and free of dirt particles. Note that the hot wire has a very small frontal area, so that chance collision of "dirt" particles is great only if there is a large number present. In the large laboratory (NACA-Lewis) air supply it was found that sufficient particles were present to cause trouble. After mahy attempts at filtering the air, it was found that paper filters are by far the best. Such materials as felt were found to increase the "dirt" problem. If at all possible a dry paper air filter should be installed in the upstream air supply before a program with hot wires is undertaken. Paper air filter systems are available for extremely high mass flow rates, so they should not be ruled out in high velocity facilities. For very accurate work with the hot wire anemometer, particles too small to break the wire should also be eliminated from the flow. These particles of "dirt" can possibly change the calibration of the wire. To obtain the very high degree of filtering, paper filters with high electrostatic charges are used to attract and trap the particles.

Frequency Response - Once the wire breakage problem is under control the task of interpreting the data begins. The most common source of error in early anemometer measurements was related to frequency response. Such problems as wire compensation and accurate reproduction of turbulent fluctuations are included in the general problem of frequency response. To properly account for all aspects of the frequency problem the researcher must become familiar with the complex electronics. There is no short cut; some knowledge of the frequency response is necessary. Perhaps the logical approach for the researcher in fluid mechanics is to make measurements of turbulent fluctuations and compare them with known values. Specifically, the turbulence level at the center of fully developed turbulent pipe flow could be used as the known source of turbulence. The measurements of figure 5.16 show the variation of turbulent intensity with Reynolds number. Attempts to measure the turbulent intensity in the center of a fully developed turbulent pipe flow will show if trouble exists. In the development of the constant current anemometer used in the measurements the original bridge design contained wire wound variable resistors. As a result, the bridge had a resonant frequency at about 1000 cycles per second. At low Reynolds numbers the indicated turbulence level was high, but not excessive. However, at higher Reynolds numbers, where the higher frequencies were more important, the turbulent intensity increase with Reynolds number instead of the expected decrease. This result led to a more thorough check of the instrument, including measuring the frequency response, which showed the bridge circuit was not useable.

Instrument Resolution - The resolution of the hot wire anemometer is limited to both space and time. The upper frequency response limit will be the determining factor in the instrument time resolutions while the wire length and size will determine its space resolution. The third factor in resolution is the "noise level" of the complete system, which will determine the minimum signal level that can be measured.

Time Resolution - The time resolution of the hot wire anemometer can be expressed, following Kovasznay[1] in terms of a resolution length in the flow direction. A length $\ell_x \equiv U/2f$ is defined in terms of the mean velocity U and the upper frequency of the anemometer, f. Figure 5.42 shows this resolution length as a function of U and f. The present upper limit for the electronic compensation is between 300,000 cycles per second and 500,000 cycles per second. The limits are imposed by the maximum gain available from the electronic amplifiers now used in anemometers. There is no indication that the actual limit of amplifier design has been reached, so that higher frequencies may be obtainable in the future.

The ultimate limit of time resolution must be determined by the transfer of information from the flow across the viscous layer around the hot wire. In other words the wire boundary layer will determine the upper frequency response of the anemometer. An exact theoretical analysis is not available for the magnitude of this upper limit. An analysis made by Mr. C. E. Shepard of the NACA Lewis Laboratory for the idealized case of a cylinderical boundary layer about the wire. This analysis suggested the ratio of the wire time constant to wire boundary layer time constant is approximately

$$\frac{\tau_w}{\tau_{BL}} \simeq 1100\,Nu \quad (For\ Nu > 20) \qquad (5.140)$$

This relation suggests the upper limit of frequency will be of the order of 2 megacycles. The analysis assumed the "capacitance" and "resistance" of the boundary layer could be lumped together, when in reality they are distributed. However, the simpler relation was employed to obtain an estimate of the ultimate time resolution of the hot wire anemometer. Certainly, the operation in slip and free moleculer flow will not be restricted by this limit.

---

1 Kovasznay, L.S.G.: Physical Measurements in Gas Dynamics and Combustion. Vol. IX (High Speed Aerodynamic and Jet Propulsion) Princeton University Press, 1954.

Space Resolution - The length and diameter of the wire determine the space resolution of the anemometer. The diameter of the wire is negligible compared to the wire length and need not be considered. If the wire length is comparable with the characteristic length in the turbulence, then the space resolution will introduce an error in the measurements. For maximum signal output the hot wire must be quite long, however, the space resolution requires a point source hot wire. Thus, these two requirements are in direct conflict. The space resolution of the hot wire anemometer has received considerable attention. These analyses have been reviewed by Frenkiel,[1] and Corrsin.[2] Corrsin also has examined the problem when conduction along the wire is important. The present discussion follows the development presented by Frenkiel.

The variation of the fluctuating velocity, u, along a wire cannot be neglected. In other words the scale of the turbulence must be larger than the wire length for a true value of u to be measured. To examine the effect of non-negligible the voltage-velocity relation for the hot wire, equations are expressed in the form

$$e(t) = K_1 u(t) \tag{5.141}$$

$$K_1 = \frac{(E_m - iR_a)^2 B n U_m^{n-1}}{i^4 R_a} \quad \text{(Constant Current)}$$

$$K_1 = \frac{R(R-R_a) B n U_m^{n-1}}{2 E_m} \quad \text{(Constant Temperature)}$$

If the turbulent velocity, u, varies along the wire length, then the voltage e(t) may be defined by the integral

$$e(t) = K_1 \int_0^{\ell} u(s,t)\, ds \tag{5.142}$$

---

[1] Frenkiel, F.N.: Aero. Quart. Vol. 5, 1954

[2] Corrsin, S.: Turbulence: Experimental Methods, Handbuch des Physik, vol. 8, 1962.

where s is the coordinate along the length of the wire. The mean square voltage for the case where the length can be neglected is

$$\overline{e^2} = K_1^2 l^2 \overline{u^2} \tag{5.143}$$

and for a wire of non-negligible length

$$\overline{e_l^2} = K_1^2 \overline{\left[\int_0^l u(s,t)ds\right]^2} \tag{5.144}$$

The integral is transformed into a double integral with the condition that the average of the integral is also equal to the integral of the average employed.

$$\overline{e_l^2} = K_1^2 \int_0^l \int_0^l u(s_1,t)\, u(s_2,t)\, ds_1\, ds_2 \tag{5.145}$$

The term in the integral can be expressed in terms of a correlation coefficient (where y is in the direction of s)

$$R_u(y) = \frac{\overline{u(x,0,z,t)\,u(x,y,z,t)}}{\overline{u^2}} \tag{5.146}$$

Also for homogeneous turbulence over the length of the wire it is required that $\overline{u^2} = \overline{[u(x,0,z,t)]^2} = \overline{[u(x,y,z,t)]^2}$

Thus, equation (5.145) can be written as

$$\overline{e_\ell^2} = K_1^2 \overline{u^2} \int_0^\ell \int_0^\ell R_u(s_2 - s_1)\, ds_1 ds_2 \qquad (5.147)$$

The relation can be reduced to a simpler form by setting, $s = (s_2 - s_1)$, and requiring R_u to be an even function, ref.

$$\overline{e_\ell^2} = 2K_1^2 \overline{u^2} \int_0^\ell (\ell - s) R_u(s)\, ds \qquad (5.148)$$

Equation (5.148) gives the value of $\overline{e_\ell^2}$ measured with a wire of non-negligible length. The values $\overline{u^2}$ and R_u are the true values of the turbulent terms. Comparing equation (5.148) to equation (5.143), which is the true value of $\overline{e^2}$ when wire length is negligible, gives the following ratio

$$\frac{\overline{e_\ell^2}}{\overline{e^2}} = \frac{2}{\ell^2} \int_0^\ell (\ell - s) R_u(s)\, ds \qquad (5.149)$$

Since $R_u \leq \ell$, the turbulent voltage measured with a hot wire of non-negligible length is smaller than the true value of voltage.

Signal Resolution - The last major resolution factor for the hot wire anemometer is the minimum turbulence level that can be measured. The noise level of the system will in all cases determine the lower limit of measurement. For measurements of the overall turbulent intensity a ratio of signal to noise of 3 is considered sufficient to obtain reliable data. However, if the spectral distribution of the turbulence is to be measured, then a much greater signal to noise level will be required. The noise spectrum is

generally of constant amplitude which extends over the useable frequencies of the amplifier. On the other hand, the turbulent spectrum decreases rapidly with increasing frequency, so that the two signals may be of equal amplitude at the high frequencies.

Techniques are available in communication work, wherein signals can be extracted from noise. However, in the case of turbulence the signal does not differ greatly in wave form (at a given frequency) from the noise wave form. The practical method of lowering the signal to noise ratio of the hot wire anemometer is to increase the output of the transducer, and at the same time lower the noise level of the amplifier. In the past the constant temperature hot wire anemometer has been viewed with disfavor, since its noise level was somewhat high. The constant current anemometer, being a simpler a.c. amplifier, can be made with lower noise levels. The improvement of the transducer output signal is also a possible line of attack. If, for instance, the semi-conductor elements can be employed as hot wires the output signal can be increased by an order of magnitude. Another approach is to employ a very thin film coated on an insulated cylinder, so that a very high resistance metallic element is formed. Here again, the resolution of the anemometer is more than adequate for most applications, and it has by no means reached the

The Laser Anemometer.- The most recent advances in transient velocity measurements has been in the area of light scattering optical techniques. These advances were made practical by the development of the "Light Amplification by Stimulated Emission of Radiation (LASER)" light source. The laser is in principle equivalent to the electronic sine wave oscillator that employs amplifiers and feedback, except that the laser operates in the range of 10^{14} to 10^{15} hertz.[1] The basic properties of the laser are high intensity, high monochromaticity and directivity of its output beam. Electronagnetic radiation is emitted from a material when atoms of the material drop from one energy level to a lower energy level. The laser action is that of "pumping" or exciting a collection of atoms in the material such that a selected transition will have more atoms in its upper energy level than in its lower energy level. When the excited atoms emitt, they are forced to contribute to the electromagnetic wave that already exists in the neighborhood. Thus, all atoms emitt in phase with the existing wave, and a high degree of time coherence is achieved. The structure of the laser is that of a resonator, so that the frequencies generated are confined to specific modes of the resonator. This confining results in a high degree of space coherence. The wave length of radiation is determined by the energy levels of the active material, which may be either a gas or a crystal. A broad range of frequencies can be obtained by considering all possible materials.

[1] Present discussion taken from; T. H. Gee, An Introduction to the Laser, von Karman Institute for Fluid Dynamics Lecture Series 39: Laser Technology in Aerodynamic Measurements. 1971.

The laser anemometer measures the velocities of microscopic particles suspended in a gas or liquid flow. The principle of the laser anemometer depends on a Doppler shift of the frequency of light scattered from the moving particles. It would be desirable to employ the molecules of the fluid as the light scatters, however, the light intensity required is generally not available in continuous form. Secondly, the magnitude of the light intensity required to measure scattering from molecules would also cause measurable changes in the molecular structure of the fluid. The present laser measurements employ particles which are large compared to the molecules. Major problems of size and dispersion of particles have been encountered. The particles must be able to follow the fluid velocity accurately. One may question whether any particle which is large compared to the molecules can follow accurately the turbulent motion.

Consider monochromatic radiation of wavelength λ_i and speed c, emanating from a non moving source[2]. Figure 5.42 shows the radiation passing in the direction defined by the unit vector k_i and illuminates a particle having a velocity v (where $|v| \ll c$).

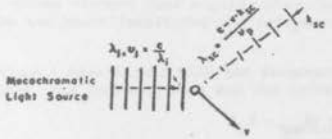

Figure 5.42 Frequency shift for light scattered from a moving particle.

If the particle were motionless, the number of wave fronts passing(or striking) its per unit time would be c/λ_i (or ν_i). From a nonrelativistic viewpoint, the difference between the velocity of the particle and the illumination is

$$c - v \cdot k_i$$

The number of wave fronts incident upon the particle per unit time (or the apparent frequency of the particle) is

$$\nu_p = (c - v \cdot k_i)/\lambda \qquad (5.150)$$

This is also the number of wave fronts scattered per unit time by the moving particles.

Consider now a fixed observer toward which a moving particle is emitting (or scattering) radiation in the direction defined by the unit vector k_{sc}. The apparent frequency to the moving particle is ν_p, and the apparent wavelength is

$$\lambda_p = c/\nu_p = \left\{ c/(c - v \cdot k_i) \right\} \lambda_i \qquad (5.151)$$

After the scattering of one wave front, the particle moves toward that wave front with the speed $v \cdot k_{sc}$. Thus, when the next wave front is scattered after a time interval given by $1/\nu_p$, the first wave front is a distance of

$$(c - v \cdot k_{sc})/\nu_p$$

---

2 The derivation is taken from; Golstein, R. J. and Kreid, D. K., Measurements of Laminar Flow Development in a Square Duct Using a Laser Doppler Flowmeter. ASME Trans. Ser. E. Jour. Applied Mech.Vol.34, p.813, 1962.

away from the particle. Thus, to a fixed observer, the apparent wavelength of the scattered radiation is

$$\lambda_{sc} = \frac{c - v \cdot k_{sc}}{\nu_p} = \lambda_i \left(\frac{c - v \cdot k_{sc}}{c - v \cdot k_i} \right) \tag{5.152}$$

and the frequency of the scattered radiation is

$$\nu_{sc} = \frac{c}{\lambda_i} \left(\frac{c - v \cdot k_i}{c - v \cdot k_{sc}} \right) = \frac{c}{\lambda_i} \left[\frac{1 - \frac{v \cdot k_i}{c}}{1 - \frac{v \cdot k_{sc}}{c}} \right] \tag{5.153}$$

The total Doppler shift ν_D is determined from

$$\nu_D = \nu_{sc} - \nu_i \tag{5.154}$$

For $|v| \ll c$

$$\nu_D = \frac{nv}{\lambda_o} \cdot (k_{sc} - k_i) \tag{5.155}$$

where λ_o is the vacuum wavelength of the incident radiation, and n is the index of refraction in the medium surrounding the particle. If the directions of the incomming and scattered light beams are fixed, the frequency shift gives the component of velocity in a given direction $(k_{sc} - k_i)$.

The Doppler shift for a laser of wave-length 6328 Å (He-Ne) is shown as a function of scattering angle and various angles of incidence is shown in figure 5.43.

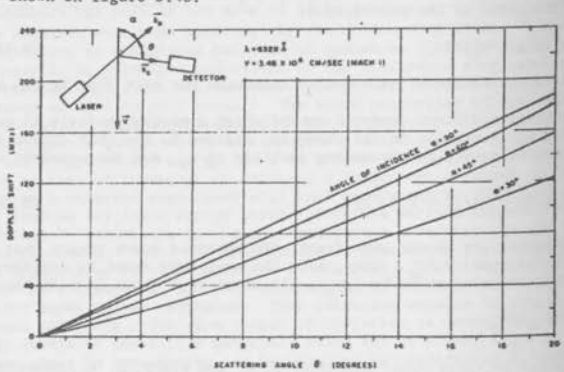

Figure 5.43 Doppler shift versus scattering angle for various angles of incidence. From Rolfe, E., Silk, J. K., Booth, S., Meister, K. and Young, R. M., Laser Doppler Velocity Instrument. NASA CR-1199, 1968.

The frequency shift is determined by optical heterodyning of the scattered laser radiation with an unscattered portion of the beam from the same laser. This is done by combining the two beams on the photocathode of a photomultiplier. The resulting beat signal is analized to determine the frequency difference (Doppler shift) of the two beams. From this value and the geometry of the beams, one can determine the component of the velocity in the direction $(k_{sc} - k_i)$.

The optical system employed by Goldstein and Kreid is shown in figure 5.44. The laser light is incident upon the splitter plate, where there is a division of amplitude of the beam due to partial reflection into a main beam and a reference beam. The main beam is focused by a lens into the flowing fluid. Some of the incident illumination is scattered in the direction of the photomultiplier with a Doppler shift as determined by equation (5.155)

The reference beam is reflected by a mirror and is focused by another lens onto the same region of the fluid as the main lens. The reference beam is directed toward the photomultiplier and the two apertures, which aid in limiting the volume element (and angular direction) that the photomultiplier sees. The two beams (scattered and reference) incident upon

the photocathode produce a heat signal with the frequency of the Doppler shift. For convenience, the incident beam and the reference beam make

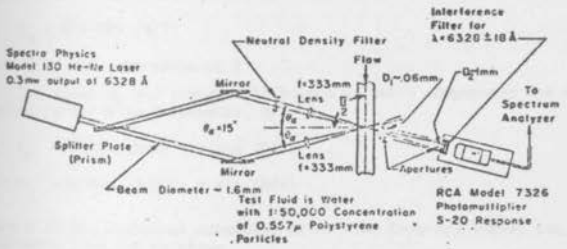

Figure 5.44 Typical Laser Doppler Anemometer.

equal angles with the plane normal to the tube axis. The Doppler shift is therefore proportional to the velocity component parallel to the axis. From equation (5.155) and figure 5.44

$$\nu_D = \frac{2u}{\lambda_o} (\sin \theta_a) \qquad (5.156)$$

The photomultiplier output is scanned with a spectrum analizer. The Doppler shift corresponding to the mean velocity is usually related to the peak output frequency.

Measurements of all three, turbulent, velocity components can be made with the laser anemometer. Recently, the evaluation of the turbulent shear stress, $\overline{uv}$, has also been done with a laser system. Figure 5.45 shows the system employed by Bourke, et. al.[1] to measure the Reynolds stress. The

[1] Bourke, P.J., Brown, C.G., and Drain, L.E., Measurement of Reynolds Shear Stress in Water by Laser Anemometry.DISA Info. No. 12, Nov.1971.

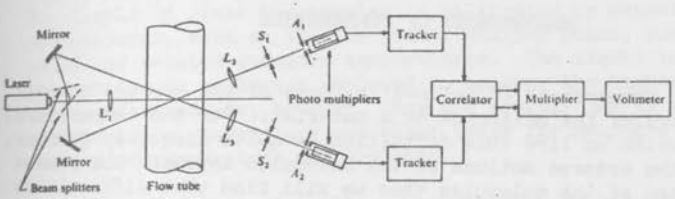

Figure 5.45 Laser Anemometer for measuring the Reynolds Stress.

apparatus measured the velocity components X_1 and X_2 at $\theta/2$ on each side of the axial direction in the tube.

$$X = \frac{\lambda_i}{2n \sin(\theta/2)} v_D \qquad (5.157)$$

The mean velocity was determined from

$$U_m = \overline{X} \,/\, \cos(\theta/2) \qquad (5.158)$$

where $\overline{X}$ is the mean value of X.

The axial u, and radial v turbulent velocity components are obtained, similar to hot wire anemometry, by

$$\begin{aligned} x_1 &= u \cos(\theta/2) + v \sin(\theta/2) \\ x_2 &= u \cos(\theta/2) - v \sin(\theta/2) \end{aligned} \qquad (5.159)$$

where x is the turbulent component of X. The Reynolds stress can be calculated from the relation

$$\overline{uv} = (x_1 + x_2)(x_1 - x_2) / [4 \sin(\theta/2) \cos(\theta/2)] \qquad (5.160)$$

The Doppler technique can be applied to any scattered electromagnetic wave, and is not limited to just the laser light source. Microwave Doppler systems are employed as velocity measuring instruments in the atmosphere. The acoustic Doppler anemometer appears to be of major interest in the measurement of blood flow.

Chapter VI

MEASUREMENT OF TEMPERATURE

Temperature is defined in terms of the average kinetic energy of the molecules of a material. For the temperatures in which we live this definition is quite adequate, however, if the ordered motions of the molecules approach the random motion of the molecules then we will find that difficulties arise in how to; first measure temperature accurately, and second for extreme velocities how to define temperature. Because the motion of molecules are random, temperature has no directional property in the kinetic theory of heat approach. However, if we impart very large uniform motions to the molecules, it is possible to arrive at a condition where, (by defintion). the molecule may have temperatures in the hundreds of thousands of degree in the uniform direction motion and near absolute zero in the direction normal to the uniform motion. Thus, while for most fluid mechanic measurements temperature is well defined, there exists a remote region of free-molecule high energy particle flows where problems in definition can arise.

Through the present discussion we will be mainly interested in the measurement of temperature according to the well defined kinetic energy concept. The measurement of fluid temperatures appears to be well in hand, from temperatures approaching absolute zero to roughly 3,000 or 4,000°F. The upper limit is, of course, vauge because of the calibration ability. No doubt, the "International Temperature Scale" can be defined up to the melting point of materials such as tungsten, but major problems are encountered in the measurement of temperature at these extreme conditions. There is a major interest and effort underway to measure temperatures well above 4,000°F in fluid mechanics and the related special area of plasma physics. Thus, there is still a major area of research type work available in the area of temperature measurements.

A. Mechanical Temperature Measurements - The most common means of measuring temperature is the liquid in glass thermometer. This instrument makes use of the phenomenon that different materials expand at different rates upon being heated. The expansion of glass is extremely small with temperature, while liquids have large variations in expansion with temperature. Liquid in glass thermometers are available with ranges from

-190°C to upwards of +500°C. The upper limit being set by the mechanical properties of glass at the high temperatures. The liquid in glass thermometer is calibrated by established temperatures, such as the ice point, melting point, boiling point and related standard temperatures. The liquid-in-glass thermometer is no longer employed to measure the highest precision of standards, however, they are useful, and in fact indispensable, laboratory and plant tools for making a great variety of temperature measurements.

There are several problems associated with liquid-in-glass thermometers. Thermometer bulbs, whether used or not, are subject to progressive changes in volume. Such changes will not exceed 0.1°C for good grade thermometic glasses, provided the thermometer has not been heated above 150°C. It is for this reason that the National Bureau of Standards will issue certificates showing corrections only to the nearest 0.1°C or 0.2°F for thermometers not graduated above 150°C or 300°F. In addition, to the permanent changes in bulb volume, there are temporary changes resulting from heating, which may require consideration in thermometers graduated in 0.1 or 0.2 degree intervals.

Some liquid-in-glass thermometers are pointed and graduated by the maker to read correct or nearly correct temperatures when the bulb and entire liquid index in the stem are exposed to the temperature to be measured. Other thermometers are so pointed and graduated that they will read correct or nearly correct temperatures when the bulb and a short length of the stem only are in the bath. Thermometers of the former class are known as "total immersion" and those of the latter class are known as "partial immersion" thermometers. Use of these thermometers at other than the calibrated condition requires a correction for stem conduction effects and also for vapor pressure effects within the thermometer.

Tollerances and corrections for liquid-in-glass thermometers are tabulated by Busse.[1]

Metalic expansion thermometers find wide use in direct reading type instruments. These devices are simply not accurate

---

1 Busse, J.; Liquid-in-Glass Thermometers. Temperature Its Measurement and Control in Science and Industry. Am. Inst. Physics. (1941)

enough for research use, and are of interest only for their quick reading.

B. Resistance Thermometer - The possibility of employing the temperature dependency of resistance in metals as a means of measuring temperature is credited to Sir William Siemens (England(in 1871. The idea did not meet with popular approval, and was challenged by a commission of eminent English scientists. Improvement in purety control of metals and in construction techniques has, of course, made resistance thermometers practical. H. L. Callendar was perhaps the best known of the early experiments who developed and demonstrated the essential elements of a resistance thermometer.

The information available on resistance thermometers as steady state temperature measuring instruments is quite extensive. Indeed it would not be difficult to write a complete book on the resistance thermometer alone. The present section is only a brief review of the state of the art as they relate to the resistance- temperature transducer family. The main interest will be the application of the resistance thermometer to transient and fluctuating temperature measurements. The use of the thermometer for transient measurements has received very little attention as compared to steady state applications.

The general concept of resistance temperature transducers was to divide them into three groups: Metalic conductors, Semi-Conductors, and Insulators. The division is maintained for the resistance thermometer. The metalic conductors are of great value in the measurement of temperatures from roughly - 190°C to 1,000°C. The semi-conductors are of specific interest at the very low temperatures, although their large variations in resistance make them desirable at ambient temperatures also. Insulabors are considered for very high temperature measurements.

Metalic Conductors: - Of the many possible conductors, platinum is perhaps the best known and most important as a resistance thermometer. Other metals used for resistance thermometers include copper, nickel, tungsten, silver, iron, tantalum, molybdenum, Iridium, rhodium and their alloys.

a) Platinum - Because of its many desirable characteristics such as high melting point, chemical stability, resistance to oxidation, and availability in a pure form, platinum has been chosen as the international standard of temperature measurement from the liquid oxygen point (-182.97°C) to the animony point

(630.5°C). For this purpose platinum is drawn into wire with utmost care to maintain high purity, and the wire is formed into a coil which is carefully supported so that it will not be subject to mechanical strain caused by differential thermal expansion.

The resistance-temperature relationship for platinum is given by the Callendar-Van Dusen equation.[1]

$$R_t/R_o = 1 + a\left[T - \delta\left(\frac{T}{1000} - 1\right)\left(\frac{T}{100}\right) - \beta\left(\frac{T}{1000} - 1\right)\left(\frac{T}{1000}\right)^3\right] \qquad (6.1)$$

where R_t is the element resistance at $T^\circ C$, R_o is the element resistance at $0^\circ C$, and α, δ, and β are constrants for each individual platinum element. is zero above 0°C, that is, the β term is omitted. Inspection of Equation (5.1) shows that measurement of R_t at any four values for T will permit the constrants R_o, α, δ, and β, to be computed. This is the principle upon which "calibration" of a pure, annealed strain-free platinum sensor is based. R_o is normally measured directly by observation of R_t at 0°C.. Knowing R_o, can be most easily determined by measuring R_t at 100°C. At 100°C Equation (5.1) reduces to:

$$R_{100} = R_o (1 + 100\,\alpha) \qquad (6.2)$$

Where R_{100} is the element resistance at 100°C. δ is determined from a third measurement at the boiling point of sulphur (444.6°C). β is determined from a measurement of the element's resistance at a temperature below 0°C. Usually at the boiling point of oxygen (-182.97°C). Typical values are α = 0.00392, δ = 1.49, β = 0.1 for negative T, and β = zero for positive T.

---

[1] Van Dusen, M.S.: Platinum Resistance Thermometry at Low Temperatures. J. Am. Chem. Soc. Vol. 47, p. 326 (1925).

Figure 6.1 shows the resistance temperature relationship and its rate of change (first derivative, dR/dT) for the pure platinum resistance thermometer.

A good indication of the impurity and built in strain of a platinum element is the value of α (Equation 5.1). For unstrained, annealed, pure platinum wire, a equals 0.003927. NBS certifies platinum temperature sensors with an α of 0.003920 or greater. Typical values of α might lie between 0.00391 and 0.003925.

For most applications the platinum sensing element is protected by some type of housing. An open-wire element would be best for fast response and conduction errors, but it is most subject to strain and dirt. For operation in fluids such as water the element may be ceramic coated to both insulate and protect it.

b) Other Metals - Materials used as resistance thermometers are selected on the basis of their: 1. Temperature coefficient of resistance, 2. Resistivity, 3. Tensile strength and ductibility, 4. Stability, and 5. Linearity.

For a resistance temperature element to be used over long periods of time it must be stable under a wide variety of environmental conditions. The sensing element must be annealed to obtain a stable resistance. In addition resistance thermometry requires the element to be chemically and metallurgically stable over long time periods. Most metallic conductors are quite stable, however, stability is the major objection to semi-conductors.

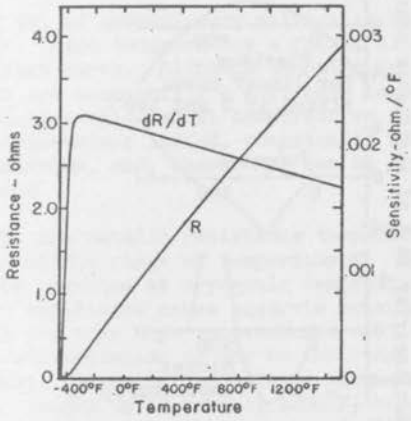

Figure 6.1 - Resistance vs temperature characteristics of a platinum resistance temperature sensor. (Resistance at 32°F is 1.00 ohm.)

Figure 6.2 shows the nonlinearity as a function of temperature for typical resistance thermometer materials. The curves were computed by calculating the deviation of the true curve from a straight line having intercepts at 32 and 932°F. The deviation from the straight line was then plotted as a function of temperature with the ordinate normalized for a 900°F temperature span.

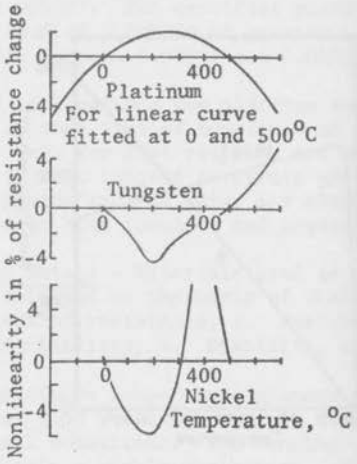

Figure 6.2 - Nonlinear Effect in the Resistance-Temperature Curves of Metals.

Table VI.1 summarzies the properties of various conductors which are used as resistance thermometer elements.

Table VI.1- Resistance Thermometer Materials

Material	Res. 32° F ohm/cmf	ΔR/R/°F x1000	Max. Air Temp. °F	Tensile St. 1000#/in.²
Platinum	59.1	2.18	2200	50-1000
Tungsten	30.3	2.5	400-500	590
Nickel	36	2.4-3.3	1000	120
Copper	9.3	.24	250	30
Rhodium	24.8	2.46	3400	300
Molybdenum	31.1	1.9	400	100-400
Iridium	29.5	2.3	4000	
Silver	8.8	2.1	1200	42
Iron	53.1	3.4	600	
Tantalum	57.3	1.7		
Plat-Ird.(5%)	115	1.1		

Nickel is perhaps the most widely used materials for resistance thermometers. It together with copper are common in applications where temperature control is maintained with the thermometer. Neither nickel or copper are used for great accuracy measurements. The alloy of 70 % Ni - 30 % Fe (Balco) is employed for its large resistance (120) in ohms/cmf. It has a relatively large temperature coefficient of resistance. (2.5×10^{-3} $\Delta R/R/°F$)

Tungsten is, of course, very attractive because of its great strength. Also tungsten has a fairly linear resistance-temperature curve. Although tungsten melts at 6098°F - it is not necessarily a good high temperature material. Tungsten oxidizes at temperatures in excess of 700°F. Of the materials listed, tungsten is least affected by nuclear radiation, and, therefore, can be employed in nuclear reactors.

In general the metalic resistance thermometer is employed for the middle range of temperatures. Metalic elements can be operated at cryogenic temperatures, however, their very low resistance makes accurate measurements difficult. At the very high temperatures most of the elements suffer from oxidation or are so weak that strain problems appear. In general resistance thermometers are available with ranges up to roughly 1800°F, however, most applications are limited to values below 1,000°F.

Operating Techniques for Resistant Thermometers - Several methods can be used to measure the resistance of a resistance thermometer. These may include; potentiometer circuits, as shown in figure 2.6; wheatstone bridges, figure 2.7, or Kelvin bridge, figure 2.10. For moderate accuracy the Wheatstone bridge is employed. For standards type accuracy the Kelvin bridges, such as the special Mueller or Smith bridge, would be used. The Kelvin type bridges are capable of eliminating lead resistance and are available commercially. There are many circuits available commercially to perate resistance thermometers, including servo-balanced systems.

The problems encountered in using resistance thermometers include; Joule heating effects, calibration uncertainty, instability of the sensing element, conduction of heat to the supports, lead resistance, stray thermal e m f and time lag. Also, if the thermometer is in a flowing stream the Mach number effect on recovery temperature must be considered.

The Joule heating will limit the amount of current that can be put through the element before it is heated internally. Any amount of current will produce a heating of the wire. Thus, the problem is strictly one of deciding how accurate the "cold" resistance of the element is to be measured. In other words what is the minimum temperature rise that can be detected by the resistance measuring equipment. The heating of the element can be determined from an experimental measure of the temperature versus current as shown in figure 6.3. The heating will be a function of the physical properties of the sensing element and also of the heat conduction abilities of the surrounding fluid.

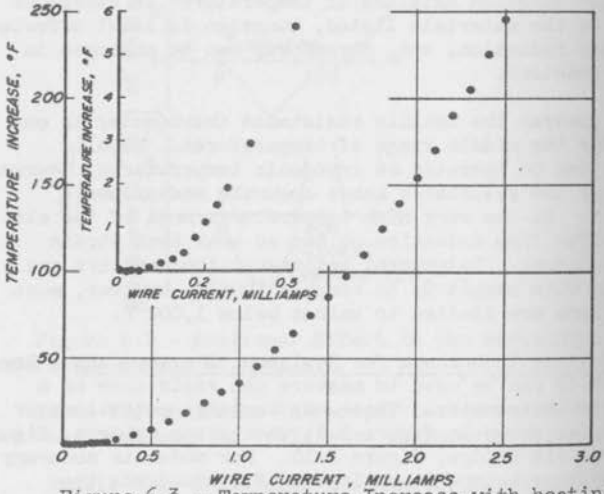

Figure 6.3 - Temperature Increase with heating current for a 90% platinum - 10% rhodium wire at atmospheric conditions.

Figure 6.4 shows a typical temperature rise versus i^2R for an element of 19,000 ohms resistance and the same element material with 100 ohms resistance. The difference in internal heating with the element in air and in water is also demonstrated in figure 5.4.

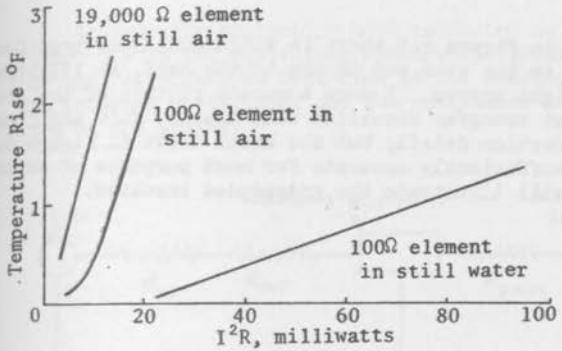

Figure 6.4 - Self-Heating of Typical Commercial Resistance Thermometers.

The calibration of the resistance thermometer is usually done against a known temperature standard. In typical calibration laboratories the standard is a platinum resistance thermometer. The exact calibration technique depends on the known boiling or melting temperatures of certain elements. Once calibrated the accuracy of the resistance thermometer is dependent on the stability of the sensing element.

If the body of the resistance thermometer is not at the same temperature as the sensing element, there will be a loss of heat to the probe body. The present analysis of stem conduction is from the work of Werner, Royle and Anderson.[1]

Figure 6.5 is a generalized sketch of the steady state heat conduction situation for an immersion temperature sensor, illustrating how heat is conducted through the boundary layer of fluid to (or from) the element, and thence along the stem to the head of the sensor (and to the wall or external environment). There is a resistance to heat flow (R_{int}) which cannot always be ignored, and this is also illustrated schematically--an example of R_{int} would be a sensing element mounted inside a thermowell with appreciable air gap between the inside of the well and the external surface of the sensing element. When the stem is exposed to the flow

---

1 Werner, F.D., Royle, R.D., and Anderson, L.E.: Rosemount Engineering Co. Bulletin 9622.

as shown in Figure 6.5 there is additional heat transfer directly to the stem and thence to the head, as illustrated by the light arrows. A more accurate picture of the steady state heat transfer situation will usually show additional heat conduction detail, but the model shown in Figure 6.5 will be sufficiently accurate for most purposes of estimating and will illustrate the principles involved.

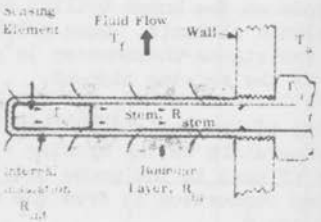

Figure 6.5 - Heat Flow in a Temperature Sensor.

The steady state conduction of heat can be visualized more easily by considering its electrical analog. In this case, a temperature drop corresponds to a voltage drop and the quantity of heat flowing per unit time corresponds to the electrical current. Thus, one recognizes that the equivalent resistence is in the form of degrees per watt, which is the reciprocal of the usual units of heat conductance, watts per degree (or BTU's per degree per second or other units of heat flow rate).

Accordingly neglecting heat conducted to the stem Figure 6.6 is the equivalent electrical circuit showing the resistance to heat flow in the boundary layer, the internal resistance, and the resistance due to the stem of the sensor.

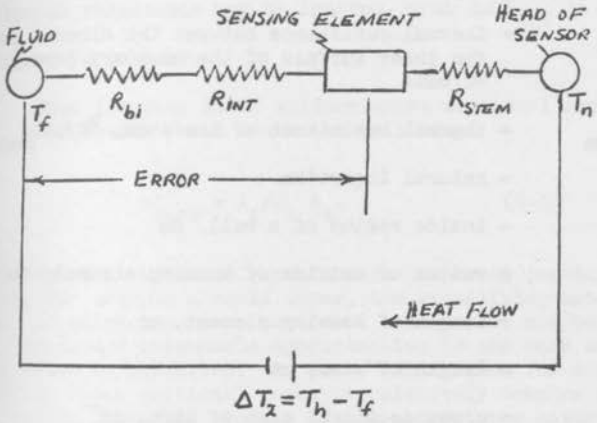

Figure 6.6 - Electrical Equivalent of Simplest Stem Conduction Problem.

From the circuit one can show that the error of temperature measurement is:

$$\delta T_{sc} = \Delta T_2 \, (R_{bl} + R_{int}) \, / \, (R_{bl} + R_{int} + R_{stem}). \quad (6.3)$$

The symbols and suggested units are as follows:

δT_{sc} = error due to stem conduction, ^{o}C.

T_f = fluid temperature, ^{o}C

T_e = sensing element temperature, ^{o}C

T_h = head (or wall) temperature, ^{o}C

T_a = ambient (external) temperature, ^{o}C

ΔT_1 = $T_a - T_f$

ΔT_1 = $T_a - T_f$ °C

ΔT_2 = $T_h - T_f$ °C

R_{bl} = thermal resistance of the boundary layer, °C/watt

R_{int} = thermal resistance between the element and the inner surface of the boundary layer, °C/watt

R_{stem} = thermal resistance of the stem, °C/watt

ln = natural logarithm

r_w = inside radius of a well, cm

r_e = radius of outside of sensing element, cm

l_e = length of sensing element, cm.

l_s = length of stem, cm

A_s = cross sectional area of stem, cm^2

k_s = thermal consuctivity of stem, watt/cm °C

K_g = thermal consuctivity of gap between sensing element and well, watt/cm°C

R_{bl}, the thermal resistance in the boundary layer, is calculated from boundary layer theory, and the methods have been described in detail in various text books. The heat transfer to the sensing element through the boundary layer should be specific among the specifications for an immersion temperature sensor, under definitely stated flow conditions. For other fluids or other flow conditions, the heat transfer theory will allow one to make reasonable estimates, based on this specified condition. It is substantially the same as the "self-heating" effect and will usually be specified under this heading. As cuh, it is usually given in watts per °C (a conductance), and the reciprocal of this number is R_{bl} in °C/watt.

R_{int}, the internal thermal resistance, may be calculated roughly if the details of construction are known, or may be calculated relatively well if this thermal resistance resides mainly in the air gap around a sensing element fitted inside a thermowell, a common industrial practice. In this case,

it is given by

$$R_{int} = \ln (r_w/r_c) / 2\pi l_c k_g. \qquad (6.4)$$

For many kinds of high performance immersion sensors such as often used in missile and rocket testing, the internal resistance may be ignored, that is R_{int} is assumed to be zero.

When the stem is of uniform cross sectional area, R_{stem} is easily shown to be the following:

$$R_{stem} = l_s/k_s A_s. \qquad (6.5)$$

When there is moderate variation in the cross sectional area, for example a small taper, the simplifying assumption of using the cross sectional area at the mid point or some other reasonable approximation to the mean value may often be justified. An exact calculation for non-uniform cross sectional area is relatively complex and is rarely justified because of the approximate nature of the calculations.

Methods of minimizing stem conduction error for installations in tubing are shown in Fig. 6.6.

Dotted lines shown insulation which is always desirable when acceptable. In large pipes or tanks, a long stem on the sensor with deep immersion will ordinarily serve the purpose, and total immersion should be considered where feasible.

In the design of a sensor, stem materials having poor thermal conductivity, such as stainless steel are recommended, and the cross sectional area should be as small as practical, consistent with structural requirements. Heat conduction along the connecting wires inside the stem is usually neglected. For minimum stem conduction errors, attention should be given to providing reasonably good thermal contact between the lead wires and the stem. A hollow stem with numerous holes as large as feasible is highly recommended as a means for suppressing stem conduction. Fins can be helpful, although they usually increase

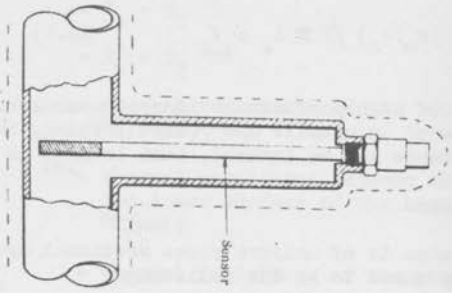

Figure 6.6 - Minimizing Stem Conduction Error.

the diameter of the stem inconveniently.

In the case of nonconducting fluids at moderate or low velocity, perhaps no technique is so effective as the use of a truly "open-wire" element type. By this, reference is made to the resistance sensing element types in which the resistance wire is supported on a cage or on posts so that the fluid can circulate all around the resistance wires. In this case, it is seen that the conduction of heat from the stem must be via the wires of the supporting cage, and thence to the fine wires of the resistance element itself. This gives ample opportunity for exchange of heat with the fluid whose temperature is to be measured, so that stem conduction errors can ordinarily be expected to be quite negligible. Should error estimates be necessary in this cage, the cross sectional areas of the supporting wires of the cage, the lengths of these wires and their thermal conductivities are necessary, so that they can be treated as if they were the stem of the sensor.

The problem of lead resistance can be overcome by employing the Kelvin type bridges. For less accurate measurements the lead resistance is simply measured once and there after accounted for in each reading. The thermal e.m.f. voltage is eliminated by maintaining all

junctions between lead wire and the resistance thermometer at constant temperature. Second, junctions between dissimilar metals are avoided to eliminate the thermocouple effect.

Semi-Conductors - The negative slope of resistance vs. temperature elements such as thermistors, carbon resistors, and technical semi-conductors are considered under the broad heading of semi-conductors. As discussed in Chapter I not all these elements are strictly speaking semiconductors, however, the resistance-temperature characteristics behave in a similar manner.

a) Ambient Temperatures - Figure 3.1 shows a typical comparison of a metallic conductor, semi-conductor (thermistor) and an insulator, temperature-resistance variation. In the range of ambient temperatures it is seen that the thermistor has a much wider variation in resistance than the metallic conductor. Figure 6.7 is a linear comparison of a typical thermistor and common metallic conductors. The sensitivity of thermistors to temperature changes around 0^{o} many times greater than the metallic conductors. The resistivity of the thermistor is many times that of the metallic conductor, so the output voltage of the thermistor will be much greater even at temperature up to $200^{o}C$ or more.

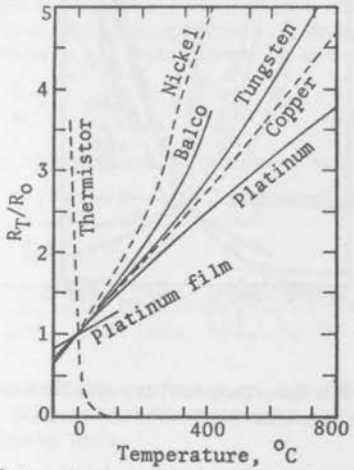

Figure 6.7 - Semi-conductor Resistance-temperature Calibration Compared to a metalic conductor.

The thermistor as a temperature measuring instrument can only recently been developed. Although the semi-conductor resistance-temperature characteristics have been known for 150 years, their potential as a measuring instrument is only now being developed. The problem of producing thermistors with reproducible and stable temperature-resistance characteristics was difficult to over come. Since most of the materials used as thermistors are ceramic in nature, they absorb moisture. Present construction includes a coating of glass or other non-porous material about the thermistor to protect it from absorbing moisture. The repeatability of modern thermistors is extremely good. Thermistor units are presently available commercially in almost any shape or size desired.

b) Cyrogenic temperatures - At temperatures below about 10° K metallic resistance thermometers become relatively useless as a temperature sensor. At the very low temperatures the germanium semi-conductor has been developed as a temperature sensor.

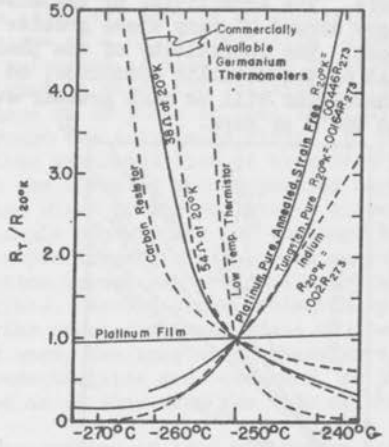

Figure 6.8 - Low Temperature Calibration of Semi-Conductors and Metalic Conductors.

Figure 6.8 shows a set of curves of typical semi-conductor type sensors compared with metallic conductors. Above 15°K the percentage change in resistance for platinum, is actually greater than that for germaium, however, the resistance of platinum is very small as compared to germaium. The carbon resistor is also employed as a resistance thermometer at the low temperatures. The development of the semi-conductor as a cyrogenic thermometer is very recent and no doubt will be of great value as this field of research increases.

Insulators - It is important to note that the insulator is now being considered as resistance thermometers.[1] As temperatures in excess of the melting point of metals are reached and studied, the ceramic insulator is almost the only material that appears possible to withstand the temperature.

Resistance Thermometer Sensitivity - The sensitivity of a given resistance thermometer can be computed directly from the resistance-temperature curve. Figure 6.9 is a typical resistance-temperature curve for a 90 platinum-10° Rhodium wire. This particular wire has been fully evaluated for use as a transient measuring resistance thermometer.[2] Over the range of temperatures shown in figure 6.9 it was assumed that the resistance is a linear function of temperature. Thus, the relation between temperature and resistance is written as

$$R = R_o \left[1 + \alpha (T - T_o) \right] \qquad (6.6)$$

or in terms of the ambient temperature and resistance

$$I \alpha R_o = \frac{I (R_w - R_a)}{(T_w - T_a)} = \frac{\Delta E}{\Delta T} \qquad (6.7)$$

---

[1] Anderson, A.R. and Stickney, T.M.; Temp. its Measur. Control in Sci. and Ind. vol. 3, pt. 2, 1962.

[2] Chao, J.L., and Sandborn, V.A.: A Resistance Thermometer for Transient Temperature Measurements. Fluid Mech. Paper No. 1, Colo. State Univ.

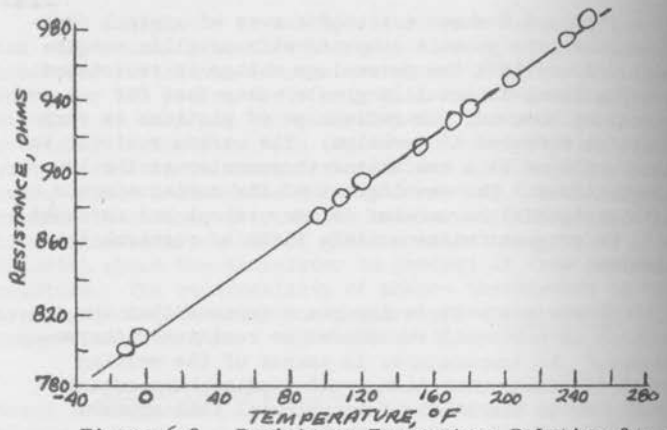

Figure 6.9 - Resistance-Temperature Relation for a 90 % Platinum - 10 % Rhodium Wire.

where I is the current through the wire. Figure 6.10 is a plot of sensitivity. $\Delta E/\Delta T$ computed from equation (6.7) for different length of the wire shown in figure 6.9. The longer the wire the greater the value of R, thus the greater the sensitivity. Note that a steady state resistance thermometer would employ several feet of wire to greatly increase the sensitivity. Equation (6.7) is equally true for either steady state or transient operation. The amount of current through the wire is limited by the self heating problem.

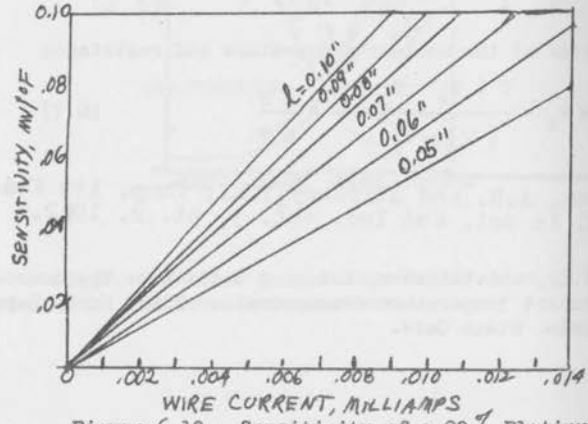

Figure 6.10 - Sensitivity of a 90 % Platinum - 10 % Rhodium Wire To Temperature Changes.

For this particular wire a current of just under 100 microamps causes a measurable heating of the wire. Figure 6.3 demonstrates the actual temperature rise of the wire as a function of current. It is quite possible that the wire will still be a good resistance thermometer eventhough it is heated internally by the detection current. In other words, the actual cross-over temperature at which the anemometer effect of convective heat transfer becomes important determines the limit of use of the heated resistance thermometer. Unfortunately, this limit does not appear to be established. Again the problem is one of how accurately resistance is detected with the electrical readout instruments.

C. Thermoelectric Thermometry[1] - Study in the field of thermoelectricity began in 1821 with the discovery of Seebeck[2] that an electric current flows continuously in a closed circuit of two dissimilar metals when the junctions of the metals are maintained at different temperatures. In the early investigations of thermoelectric effects the results were expressed more qualitatively (in terms of the direction of the current flowing in a closed circuit) than quantitatively, because the relations between the measurable quantities in an electric circuit were not well known at the time.[3]

A pair of electrical conductors so joined as to produce a thermal emf when the junctions are at different temperatures is known as a thermocouple. The resultant emf developed by the thermocouples generally used for measuring temperatures ranges from 1 to 7 millivolts when the temperature difference between the junctions is 100°C.

If a simple thermoelectric circuit (Fig. 6.11) the current flows from metal A to metal B at the colder junction. A is generally referred to as thermoelectrically positive to B. In determining or expressing the emf of a thermocouple as a function of the temperature,

---

1 Present discussion taken from an article by Roeser, W.F.: Thermoelectric Thermometry. Temperature Its Measurement in Science and Industry, Am. Inst. Physics, (1941).

2 Seebeck, T.J. Gilb, Ann, vol. 73 (1823)

3 The relation between the current and potential difference in an electric circuit was first clearly stated by G. S. Ohm in 1826. Schweigger's Journal, 46, 137 (1826).

C, and that of one composed of C and B, both with their junctions at T_1 and T_2.

$$\text{or, } E_{AB} = E_{AC} + E_{CB}$$

From this statement of the law it is seen that if the thermal emf of each of the metals A, B, C, D, etc. against some reference metal is known, then the emf of any combination of these metals can be obtained by taking the algebraic differences of the emfs of each of the metals against the reference metal. Investigators tabulating thermoelectric data have employed various reference metals, such as mercury, lead, copper, and platinum. At present it is customary to use platinum because of its high melting point, stability, reproducibility, and freedom from transformation points.

Law of Successive or Intermediate Temperatures - The thermal emf developed by any thermocouple of homogeneous metals with its junctions at any two temperatures T_1 and T_3 is the algebraic sum of the emf of the thermocouple with one junction at T_1 and the other at any other temperature T_2 and the emf of the same thermocouple with its junctions at T_2 and T_3. Considering the thermocouple as a reversible heat engine and applying the laws of thermodynamics, to the circuit,

$$E = \int_{T_1}^{T_3} \phi \, dT \tag{6.8}$$

from which it follows that

$$E = \int_{T_1}^{T_2} \phi \, dT + \int_{T_2}^{T_3} \phi \, dT \tag{6.9}$$

This law is frequently invoked in the calibration of thermocouples and in the use of thermocouples for measuring temperatures.

Law of Intermediate Metals - The algebraic sum of the thermoelectromotive forces in a circuit composed of any number of dissimilar metals is zero, if all of the circuit is at a uniform temperature. This law follows as a direct consequence of the second law of thermodynamics, because if the sum of the thermoelectromotive forces in such a circuit were not zero, a current would flow in the circuit. If a current should flow in the circuit, some parts of it would be heated and other parts cooled, which would mean that heat was being transferred from a lower to a higher temperature without the application of external work. Such a process is a contradiction of the second law of thermodynamics, and therefore we conclude that the algebraic sum of the thermoelectromotive forces is zero in such a circuit.

Combining this law with that for a homogeneous circuit, it is seen that in any circuit, if the individual metals between junctions are homogeneous, the sum of the thermal electromotive forces will be zero provided only that the junctions of the metals are all at the same temperature.

Another way of stating the law of intermediate metals is: If in any circuit of solid conductors the temperature is uniform from any point P through all the conducting matter to a point Q, the algebraic sum of the thermoelectromotive forces in the entire circuit is totally independent of this intermediate matter, and is the same as if P and Q were put in contact. Thus it is seen that a device for measuring the thermoelectromotive force may be introduced into a circuit at any point without altering the resultant emf, provided that the junctions which are added to the circuit by introducing the device are all at the same temperature. It is also obvious that the emf in a thermoelectric circuit is independent of the method employed in forming the junction as long as all of the junction is a uniform temperature, and the two wires make good electrical contact at the junction, such as is obtained by welding or soldering.

A third way of stating the law of intermediate metals is: The thermal emf generated by any thermocouple AB with its junctions at any two temperatures, T_1 and T_2, is the algebraic sum of the emf of a thermocouple composed of A and any metal

one junction is maintained at some constant reference temperature, such as $0^{o}C$, and the other is at the temperature corresponding to the emf. In Fig. 6.11, T_1 is the reference temperature and the current flows in the direction indicated, the emf of thermocouple AB will be positive, and the emf of thermocouple BA will be negative.

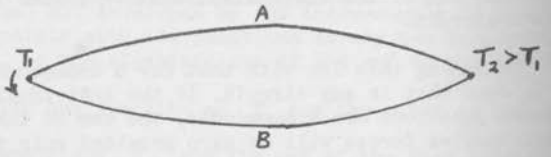

Figure 6.11 - Simple thermoelectric circuit.

The law of the Homogeneous Circuit - An electric current cannot be sustained in a circuit of a single homogeneous metal, however varying in section, by the application of heat alone. As far as we know this principle has not been derived theoretically. It has been claimed from certain types of experiments that a non-symmetrical temperature gradient in a homogeneous wire gives rise to a galvanometrically measurable thermoelectric emf.

In the present paper, we accept as an experimental fact the general statement that the algebraic sum of the electromotive forces in a circuit of a single homogeneous metal, however varying in section and temperature, is zero. As a consequence of this fact, if one junction of two dissimilar homogeneous metals is maintained at a temperature T_1 and the other junction at a

The above are all the fundamental laws required in the measurement of temperatures with thermocouples. They may be, and frequently are, combined and stated as follows: The algebraic sum of the thermoelectromotive forces generated in any given circuit containing any number of dissimilar homogeneous metals is a function only of the temperatures of the junctions. It is seen then that if all but one of the junctions of such a given circuit are maintained at some constant reference temperature, the emf developed in the circuit is a function of the temperature of that junction only. Therefore, by the proper calibration of such a device, it may be used to measure temperatures.

It should be pointed out here that none of the fundamental laws of thermoelectric circuits, which make it possible to utilize thermocouples in the measurement of temperatures, depends upon any assumption whatever regarding the mechanism of interconversion of heat and electrical energy, the location of the emfs in the circuit, or the manner in which the emf varies with temperature.

In a simple thermoelectric circuit of two metals, A and B (Fig. 6.12) there exists four separate and distinct electromotive forces: the Peltier emfs at the two junctions and the Thomson emfs along that part of each wire which lies in the temperature gradient. The only emf that can be measured as such in this circuit is the resultant emf. The identity of the individual emfs can only be established by observations of the reversible heat effects. The Thomson emf will be considered positive if heat is generated when the current flows from the hotter to the colder parts of the conductor, and negative if the reverse occurs.

Thomson took into consideration the reversible heat effects in the temperature gradient of the conductors (Thomson effects) as well as those at the junctions (Peltier effects), and applied the laws of thermodynamics to the thermoelectric circuit. A complete discussion of this application, together with the hypothesis involved, is given in the original paper by Thomson.[1]

Consider a simple thermoelectric circuit of two metals, A and B (Fig. 6.12) and let P and $P + \Delta P$ be the Peltier emfs of the junctions at temperature T and $T + \Delta T$ in degress Kelvin, respectively, and let σ_A and σ_B be the Thomson emfs per degree along conductors A and B respectively. Let the metals and temperatures be such that the emfs are in the directions indicated by the arrows. The resultant emf, ΔE, in the circuit is given by

$$\Delta E = P + \Delta P - P + \sigma_A \Delta T - \sigma_B \Delta T \tag{6.10}$$

$$\Delta E = \Delta P + (\sigma_A - \sigma_B) \Delta T \tag{6.11}$$

or in the limit

$$\frac{dE}{dT} = \frac{dP}{dT} + (\sigma_A - \sigma_B) \tag{6.12}$$

---

1 Thomson, W.; Trans. Roy. Soc. Edinburgh, Vol. 21, p. 123 (1851)/

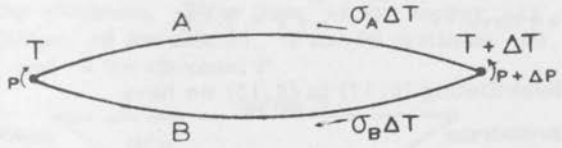

Fig. 6.12. Location of the electromotive forces in a thermolectric circuit

By the second law of thermodynamics $\sum \frac{Q}{T} = 0$, for a reversible process. If then we regard the thermocouple as a reversible heat engine and pass a unit charge of electricity, q, around the circuit, we obtain by considering only the reversible effects.

$$\frac{q(P+\Delta P)}{T+\Delta T} - \frac{qP}{T} + \frac{q\sigma_A \Delta T}{T+\frac{\Delta T}{2}} - \frac{q\sigma_B \Delta T}{T+\frac{\Delta T}{2}} = 0 \quad (6.13)$$

which may be written

$$\Delta\left(\frac{P}{T}\right) + \frac{(\sigma_A - \sigma_B)\Delta T}{T+\frac{\Delta T}{2}} = 0 \quad (6.14)$$

or in the limit

$$\frac{d}{dT}\left(\frac{P}{T}\right) + \frac{1}{T}(\sigma_A - \sigma_B) = 0 \quad (6.15)$$

or

$$(\sigma_A - \sigma_B) = \frac{P}{T} - \frac{dP}{dT} \tag{6.16}$$

Eliminating $(\sigma_A - \sigma_B)$ between (6.12) and (6.16) we have

$$P = T \frac{dE}{dT} \tag{6.17}$$

Substituting (6.17) in (6.15) we have

$$(\sigma_A - \sigma_B) = T \frac{d^2E}{dT^2} \tag{6.18}$$

From (6.17) it is seen that

$$E = \int_t^t \frac{P}{T} dT = \int_t^t \phi \, dT \tag{6.19}$$

which is the expression referred to earlier.

The Peltier emf at the junction of any two dissimilar metals at any temperature can be calculated from Eq. (6.17) and measurements of the variation of the thermal emf with temperature. The magnitude of the emf existing at the junction of two eissimilar metals ranges from 0 to about 0.1 volt for the metals generally used in temperature measurements.

Although the thermoelectric theory as developed above does not enable us to determine directly the magnitude of the Thomson coefficient in any individual metal, the difference between the Thomson coefficients in two metals can be calculated from Eq. (6.18) and measurements of the variation in thermal emf with temperature. Various types of experiments indicate that the Thomson effect in lead is extremely small, if

not zero, at ordinary atmospheric temperatures. Consequently some information regarding the magnitude of the Thomson coefficients in other metals at these temperatures can be determined if it is assumed that this coefficient is zero for lead. On this basis, it is found that the Thomson coefficient at 0° C in microvolts per °C is -9 for platinum, -8 for iron, +2 for copper, -23 for constantan, -8 for alumel, -2 for 90 platinum -10 rhodium, and +9 for chromel P.

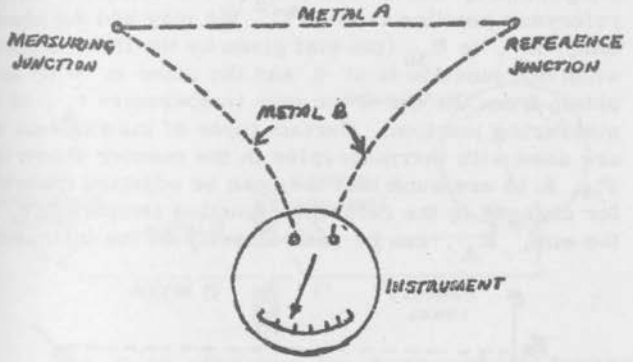

Fig. 6.13. Simple thermolectric thermometer

The simplest form of a thermocouple of two dissimilar metals which develop an emf when the junctions a are at different temperatures, and an instrument for measuring the emf developed by the thermocouple is shown in Fig. 6.13.

As long as the instrument is at essentially a uniform temperature, all the junctions in the instrument, including the terminals, will be at the same temperature and the resultant thermal emf developed in the circuit is not modified by including the instrument. If the reference junction is maintained at some reference temperature, such as 0°C, the emf developed by the thermocouple can be determined as a function of the temperature of the

measuring junction. The device can then be used for measuring temperatures. It is not necessary to maintain the reference junction at the same temperature during use as during calibration. However, the temperature of the reference junction in each case must be known. For example, let the curve in Fig. 6.14 be the relation between the emf, E, and temperature, t, for a particular thermocouple with the reference junction at 0^0C. Suppose the device is used to measure some temperature, and an emf, E_x, is observed when the reference junction is at 30^0C. We may add the observed emf, E_x, to E_{30} (the emf given by the thermocouple when one junction is at 0 and the other at 30^0C) and obtain from the curve the true temperature t_A, of the measuring junction. Certain types of instruments which are used with thermocouples in the manner shown in Fig. 6.13 are such that they can be adjusted manually for changes in the reference junction temperature, and the emf, E_A, can be read directly on the instrument.

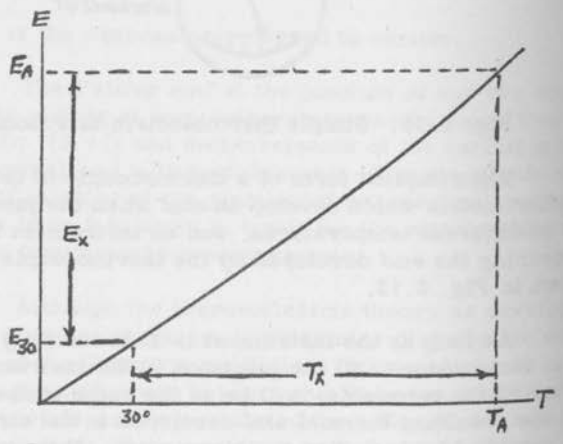

Fig. 6.14. Illustrating how corrections may be applied for variations in the temperature of the reference junction

Inasmuch as the curves giving the relation between emf and temperature are not, in general, straight lines, equal increments of temperature do not correspond to equal increments of emf.

In many cases the thermocouple is connected to the instrument by means of copper leads as shown in Fig. 6.15.

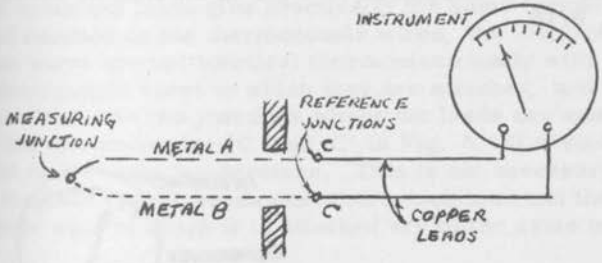

Fig. 6.15. Diagram for thermoelectric thermometer with copper leads for connecting thermocouple to instrument

If the junctions C and C' are maintained at the same temperature, which is usually the case, the circuit shown in Fig. 6.15 is equivalent to that shown in Fig. 6.13. If the junctions C and C' are not maintained at the same temperature, the resultant thermal emf in the circuit will depend not only upon the thermocouple materials and the temperature of the measuring junction but also upon the temperatures of these junctions and the thermoelectric properties of copper against each of the individual wires. Such a condition should be, and usually is, avoided.

Circuits such as those shown in Figs. 6.13 and 6.15 are used extensively in laboratory work where it is usually convenient to maintain the reference junctions, either at $0^{\circ}C$ by placing them in a Thermos bottle filled with cracked or shaved ice and distilled water, or at some other conveniently controlled temperature.

In most commercial installations where it is not convenient to maintain the reference junctions at some constant temperature, each thermocouple wire is connected to the instrument with a lead of essentially the same chemical composition and thermoelectric characteristics as the thermocouple wire, in the manner shown in Fig. 6.16.

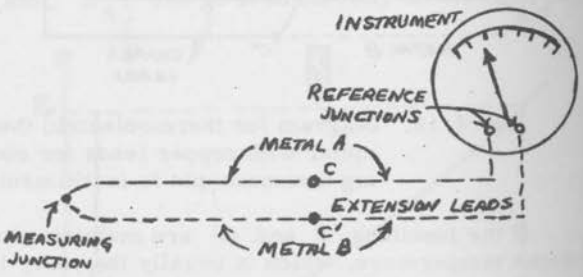

Fig. 6.16. Thermoelectric thermometer with extension leads.

This is equivalent to using a thermocouple with the reference junctions at the instrument terminals. Leads which have the same thermoelectric characteristics as the thermocouple wires are called extension leads. In most installations of this nature the instrument is equipped with an automatic reference junction compensator which automatically changes the indication of the instrument to compensate

for changes in the temperature of the reference junctions, thus eliminating the necessity of measuring or controlling the reference junction temperature. Such automatic devices are usually part of the instrument, and in such cases the reference junctions should be located in or at the instrument or at some point which is at the same temperature as the instrument.

In some cases where expensive thermocouple wires are used, extension lead wires of less expensive materials are available wyich give practically the same temperature emf relation as the thermocouple over a limited temperature range, usually 0 to 100 °C. Although the combined leads give practically the same temperature emf relation as the thermocouple wires, the individual lead wires are not identical thermoelectrically with the thermocouple wires to which they are attached, and therefore, the two junctions where the leads are attached to the thermocouples (C and C' in Fig. 6.16) should be kept at the same temperature. This is not necessary in the case of thermocouples where each lead and thermocouple wire to which it is attached are of the same material.

Although a thermal emf is developed when the junctions of any two dissimilar metals are maintained at different temperatures, only certain combinations of metals have been found suitable for use as thermocouples in the measurement of temperatures. Obviously these thermocouples must be such that:

(1) The thermal emf increases continuously with increasing temperature over the temperature range in which the thermocouple is to be used.

(2) The thermal emf is great enough to be measured with reasonable accuracy.

(3) Their thermoelectric characteristics are not appreciably altered during calibration and use either by internal changes, such as recrystallization, or by contamination from action of surrounding materials.

(4) They are resistant to any action such as oxidation, corrosion, etc. which destroys the wire.

(5) The melting points of the metals used must be above any temperature at which the termocouple is to be used.

(6) The metals are reproducible and readily obtainable in uniform quality.

The combinations of metals and alloys extensively used as thermocouples for the measurement of temperatures in this country are listed in Table VI. 2, together with the temperature ranges in which they are generally used and the maximum temperature at which they can be used for short periods. The period of usefulness of a thermocouple depends upon such factors as the temperature, diameter of wires, accuracy required, conditions under which it is used, etc.

TABLE VI. 2. Types of Thermocouples and Temperature Ranges in Which They Are Used.

Type of Thermocouple	Usual Temperature Range		Maximum Temperature	
	(°C)	(°F)	(°C)	(°F)
Platinum to Platinum-Rhodium	0 to 1450	0 to 2650	1700	3100
Chromel P to Alumel	-200 to 1200	-300 to 2200	1350	2450
Iron to Constantan	-200 to 750	-300 to 1400	1000	1800
Copper to Constantan	-200 to 350	-300 to 650	600	1100

There are two types of platinum to platinum-rhodium thermocouples used in this country, the platinum to 90 platinum-10 rhodium and the platinum to 87 platinum-13 rhodium. These thermocouples develop, at high temperatures, 10 to 14 microvolts per °C as compared to 40 to 55 for the other thermocouples listed in Table VI. 2. The platinum to platinum-rhodium thermocouples at temperatures from about 400 to 1600 °C, being more stable than any other combination of metals, are used (1) for defining the

International Temperature Scale from 660 °C to the freezing point of gold, 1063 °C, (only the platinum to 90 platinum-10 rhodium thermocouple is used for his purpose); (2) for very accurate temperature measurements from 400 to 1500°C; and (3) for temperature measurements where the lower melting point materials cannot be used. They are not suitable for temperature measurements below 0 °C because the thermoelectric power $(\frac{dE}{dT})$ is only about 5 microvolts per °C at 0 °C and decreases to zero at about -138 °C.

The nominal composition of the chromel P alloy is 90% nickel and 10% chromium. Alumel contains approximately 95% nickel, with aluminum, silicon, and manganese making up the other 5%. Chromel P-alumel thermocouples, being more resistant to oxidation than the other base metal thermocouples listed in Table VI. 2, are generally more satisfactory than the other base-metal thermocouples for temperature m measurements from about 650 to 1200 °C (1200 to 2200 °F). The life of a No. 8 gage (0.128") chromel P-alumel thermocouple is about 1000 hours in air at about 1150 °C (2100 °F).

Constantan was originally the name applied to copper-nickle alloys with a very small temperature coefficient of resistance, but it now has become a general name which covers a group of alloys containing 60 to 45% of copper and 40 to 55% of nickel (with or without small percentages of manganese, iron, and carbon) because all the alloys in this range of composition have a more or less negligible temperature coefficient of resistance. Constantan thus includes the alloys made in this country under such trade names as Advance (Ideal), Copel, Copnic, Cupron, etc., most of which contain approximately 55% of copper and 45% of nickel.

Iron-constantan thermocouples give a slightly higher emf than the other base metal thermocouples in Table VI. 2. They are extensively used at temperatures below about 760 °C (1400 °F). The life of a No. 8 gage iron-constantan thermocouple is about 1000 hours in air at about 760 °C (1400 °F).

Copper-constantan thermocouples are generally used for accurate temperature measurements below about 350 °C (660 °F). They are not suitable for much higher temperatures in air because of the oxidation of the copper.

Combinations of metals other than those listed in Table VI. 2 are sometimes used for special purposes. As examples, at temperatures above -200 °C (-300 °F) chromel P-constantan gives a thermal emf per degree somewhat greater than that of any of the thermocouples listed in Table VI. 2 and is sometimes used when the greater emf is required. Graphite to silicon carbide has been recommended[12] for temperatures up to 1800 °C (3300°F) and for certain applicati in steel plants.

Reproducibility of Thermocouples - One of the first requirements of thermoelectric pyrometers for general industrial use is that the scales of the instruments shall be graduated to read temperature directly. Although the indications of the measuring instruments used with thermocouples depend upon the resultant emf developed in the circuit, the scale of the instrument can be graduated in degrees of temperature by incorporating a definite temperature-emf relation into the graduation of the scale. The temperature can then be read directly if the temperature-emf relation of the thermocouple is identical with that incorporated in the scale of the instrument.

All the thermocouples which have the same nominal composition do not give identical relations between emf and temperature. As a matter of fact, in most cases, two samples of metal which are identical as far as can be determined by chemical methods, are not identical thermoelectrically. This is due in part ot the fact that the thermoelectric properties of a metal depend to some extent upon the physical condition of the metal.

It is not practicable to calibrate the scale of an instrument in accordance with the temperature-emf relation of a particular thermocouple and to change the scale each time

the thermocouple is replaced. Consequently the scales of such instruments are calibrated in accordance with a particular temperature-emf relation which is considered representative of the type of thermocouple, and new thermocouples are purchased or selected to approximate the particular temperature-emf relation.

If the temperature-emf relations of various thermocouples of the same type are not very nearly the same, corrections must be applied to the readings of the indicator, and the corrections will be different for each thermocouple. When several thermocouples are operated with one indicator, and when thermocouples are frequently renewed, the application of these corrections becomes very troublesome. For extreme accuracy it is always necessary to apply such corrections, but for most industrial processes, thermocouples can be manufactured or selected with temperature-emf relations which are so nearly the same that the corrections become negligible.

The accuracy with which the various types of thermocouple materials can be selected and matched to give a particular temperature-emf relation depends upon the materials and the degree to which the temperature-emf relation is characteristic of the materials available. The differences in the temperature-emf relations of the new platinum to platinum-rhodium thermocouples available in this country rarely exceed 4 to 5 °C at temperatures up to 1200 °C. Consequently, there is no difficulty in selecting a relation between emf and temperature which is adequately characteristic of these thermocouples. The temperature-emf relations used in this country for platinum to platinum-rhodium thermocouples are such that new thermocouples which yield these relations within 2 or 3 °C up to 1200 °C are readily available.

The differences in the temperature-emf relations of base-metal thermocouples of any one type are so large that the selection of a temperature-emf relation which might be considered characteristic of the type of thermocouple

is difficult and more or less arbitrary. The relations generally used for some of these thermocouples by some manufacturers have been changed from time to time because of differences introduced in the thermoelectric properties of the materials by variations in raw materials and methods of manufacture. However, the relations in use at the present time are such that materials can generally be selected and matched to yield the adopted relations with an accuracy of about $\pm$ 3 °C up to 400 °C and to $\pm$ 3/4 per cent at higher temperatures. In special cases, materials may be selected to yield the adopted relations within 2 or 3 °C for limited temperature ranges.

Temperature-Emf Relations - The temperature-emf relations for all of the common thermocouple metals have been measured in great detail[1]. Figure 6.17 is a plot of the relation for several of the common materials.

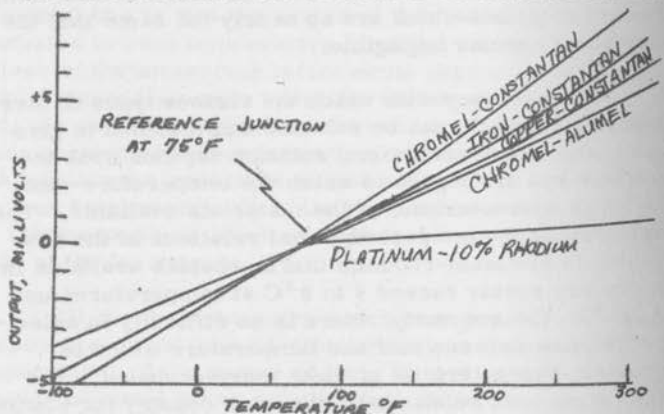

Fig. 6.17. Typical calibration curves for thermocouples

[1] Temperature Its Measurements and Control in Science and Industry. Am. Inst. of Physics, (1941) and (19

Semi-Conductor Thermocouples - The semi-conductor has a high output emf as a thermocouple. As such, the semi-conductor is used mainly for the Peltier cooling effect. The stability problem with semi-conductors has limited its use as a thermocouple.

Comparison of the Resistance and Thermoelectric Thermometers - The thermocouple covers the same range of temperatures as the resistance thermometer. Likewise mechanical thermometers can be used for many applications. The present discussion is limited to only the electrical transducers, although it should be evident that the platinum resistance thermometer has been chosen over all other temperature sensing devices to use as a standard calibration instrument.

Thermocouples have some advantages over the resistance thermometer. The temperature-sensing zone of a thermocouple can be extremely small as compared to steady state resistance thermometer. The thermocouple is better suited for the extreme high temperatures. The tungsten-Rhenium type thermocouples can measure temperatures up to 3000 ^{0}F . The thermocouple is self contained in that an external source of voltage is not required. Neglecting read out equipment, the cost of a thermocouple is a great deal lower than a resistance thermometer.

The advantages of steady state resistance sensors over thermocouples include the following:

1) A much higher output voltage can be obtained.
2) Related recording, controlling, or signal conditioning equipment can be simpler, more accurate, and much less expensive because of the higher possible bridge output signal.
3) The output voltage per degree for resistance sensors can be chosen to be exactly as desired

over wide limits by adjusting the excitation current and/or the bridge design.

4) A reference junction temperature or a compensating device is unnecessary.

5) The shape of the curve of output vs. temperature can be controlled, within limits, for certain resistance sensor bridge designs.

6) Because of the higher output voltage, more electrical noise can be tolerated within resistance sensors; therefore, longer lead wires can be used.

7) Sensitivity to small temperature changes can be much greater.

8) In moderate temperature ranges, absolute accuracy of calibration and stability of calibration for resistance elements can be better by a factor of 10 to 100.

D. Measurement of Temperature in a Flowing Fluid - An unheated cylinder placed in a flowing fluid will reach a steady temperature, which depends on the flow conditions. This is true, whether the cylinder is a resistance thermometer, thermocouple, or a liquid-in-glass thermometer. In a low speed incompressible flow, the cylinder simply measures the static temperature of the fluid. As the velocity increases the cylinder experiences frictional heating. A further increase in velocity produces compression of the fluid in front of the probe with a resulting increase in the temperature of the cylinder. Thus, it is necessary to know the relation between the flow conditions and the temperature of the cylinder.

For gases, both effects may be described by an equation, one convenient form of which is:

$$T_r/T_a = 1 + 0.5\, r\, (\gamma - 1)\, M^2 ,$$

where T_r is the temperature of the surface (or "recovery temperature"), T_a is the temperature of the undisturbed gas (or "static temperature"), r is the recovery factor, γ is the ratio of specific heats c_p/c, and M is the Mach number. In this case, where r is 1.00, equation 6.20 describes the full temperature rise due to compression heating alone, for the case where the gas is decelerated to zero without addition or loss of heat. In this case T_r becomes the total temperature, usually designed as T_o. When there is frictional heating alone, for example when there is a thin flat plate inserted into the flow with flow parallel to the plate, a typical value for r for most gases is 0.85 when the boundary layer is laminar and 0.88 when turbulent. Therefore, it happens in gases that the two sources of temperature rise are of roughly equal magnitude. The fact that the two sources of heating are of comparable magnitude is directly the result of the fact that the Prandtl Number is near to 1.00 (actually it is between 0.7 and 1.00 for gases). The Prandtl Number for liquids is in the vicinity of 0.01 for the liquid metals and above 1.0 for all other liquids, being as high as 10,000 for some liquids. The Prandtly Number Pr is given by:

$$Pr = c_p \mu / k, \qquad (6.21)$$

where c_p is the specific heat at constant pressure, μ is the viscosity, and k is the thermal conductivity. High Prandtl Number is largely the result of high viscosity in the case of oil, and in the case of liquid metals, lower viscosity and high thermal conductivity cause very low Prandtl Number.

For liquids, the theory has been worked out in detail only for a few special cases. For the case of flow parallel to a flat plate at sufficiently low Reynolds Number to give laminar flow, results of established boundary layer theory show a temperature rise as follows:

$$T_f / T_a = 1 + (Pr^{0.5} V^2) / (2 g J c_p T_a), \qquad (6.22)$$

where T_f is the temperature of the plate resulting from frictional heating, T_a is the temperature of the fluid at a distance from the plate where its temperature is undisturbed by the frictional effect, Pr is the Prandtl Number, V is the velocity in fps, g is the acceleration due to gravity, 32.2 fps, J is the Mechanical equivalent of heat, 778.2 ft lb/Btu, and c_p is heat capacity of the liquid in Btu/lb ^{0}F. This equation can be rewritten for CGS units

$$T_f/T_a = 1+(Pr^{0.5}V^2)/(2 \times 10^7 c_p T_a) \qquad (6.23)$$

While these equations apply for laminar flow for a flat plate, and therefore do not apply for reasonably accurate prediction in the case where flow is turbulent or particularly, where the geometry of the part inserted in the flow is not a flat plate, nevertheless calculations of the temperature rise by equation 3 or 4 will give a rough idea of the temperature rise to be expected on a typical temperature sensor. A typical temperature sensor is usually in the form of a cylinder with flow normal to the cylinder, and it is most commonly, though not always, at Reynolds Number sufficiently high to assure turbulent flow. It may or may not have a perforated cylindrical guard outside the temperature sensor. There is reason to expect that for an arbitrary shape, the equation defining the temperature rise may be of the form:

$$T_f/T_a = 1+(f\,Pr^n V^2)/(2gJc_p T_a) \qquad (6.24)$$

where f is arbirarily defined as the "frictional heating factor" and the exponent n may be different from 0.5. By comparison with frictional heating of gases, one may expect that n is determined by whether the flow is laminar or turbulent, and that f is dependent upon the configuration, e.g. a cylinder or other shape. These hypotheses remain to be established.

Table VI. 3 shows calculations for selected liquids according to equations (6.23)or (6.24). It may be noted that the liquids with high Prandtl Number show the effect most prominently. It is evident that temperature measurement of high speed liquids can involve significant errors because of frictional heating.

TABLE VI.3

Friction Heating for Laminar Flow Along a Flat Plate for Various Liquids

The effect is proportional to the square of the velocity. This table will give a rough idea of the error in an ordinary temperature sensor.

Liquid	Prandtl Number	C_p, Btu/lb°F	Temperature °R	Temperature °F
Liquid Hydrogen	2.5	2.5	36.65	-423
Liquid Oxygen	2.1	0.394	162.5	-297
Water	7.5	1.00	528	+68
Engine Oil	10,000	0.44	528	+68
Mercury	0.024	0.033	528	+68
Nitrogen Tetroxide	4.8	0.36	522	+62
JP-4	13.6	0.47	510	+50
MIL-O-5606	392	0.475	510	+50

ERROR

*** V = 1 fps		V = 10 fps		V = 100 fps	
Percent	°F	Percent	°F	Percent	°F
.000034	.000012	.0034	.0012	0.34	0.12
.000045	.000073	.0045	.0073	0.45	0.73
.0000105	.000053	.00105	.0053	0.105	0.53
.00085	.0045	.085	.45	8.5	45
.0000175	.000093	.00175	.0093	0.175	0.93
.0000234	.000122	.00234	.0122	0.234	1.22
.0000161	.000161	.00316	.0161	0.316	1.61
.000104	.000838	.0104	.0838	1.64	8.38

Figure 6.18 is a summary set of figures slowing the measured recovery temperatures over several different shaped bodies.

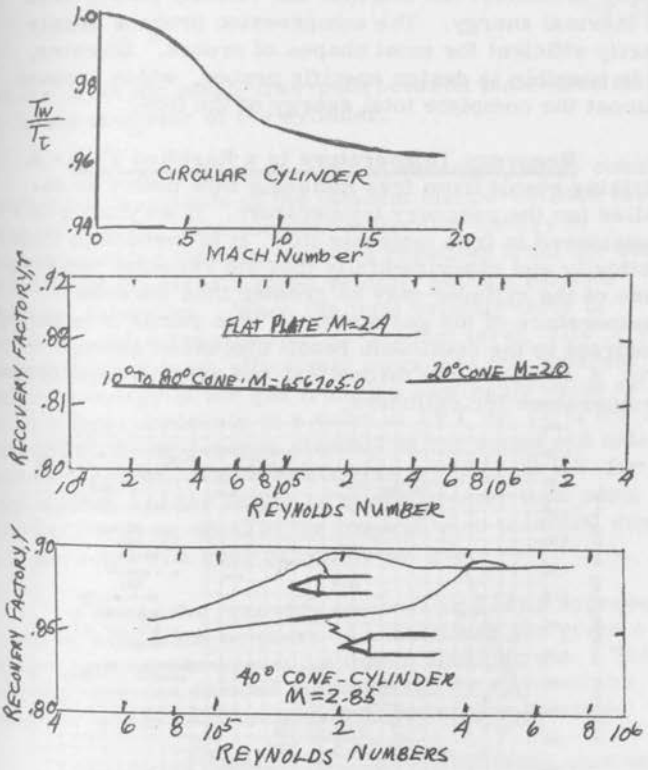

Fig. 6.18. Recovery temperature for different shaped bodies.

As may be seen from Fig. 6.18, the recovery temperature approaches the total temperature of the flowing gas. In other words the body acts as a transducer to convert the thermal and velocity energy back to thermal energy. The compression process is only partly efficient for most shapes of probes. However, if is possible to design specific probes, which recover almost the complete total energy of the flow.

Recovery Temperature in a Rarefied Flow - A striking result from free molecule flow theory is obtailed for the recovery temperature. If a cylinder is considered in free molecule flow, it fs found both theoretically and experimentally that the recovery temperature of the cylinder may be greater than the total temperature of the gas stream. This result is in direct contrast to the continuum result discussed above. Fig. 6.19 shows the theoretical and experimental recovery temperature for cylinders.

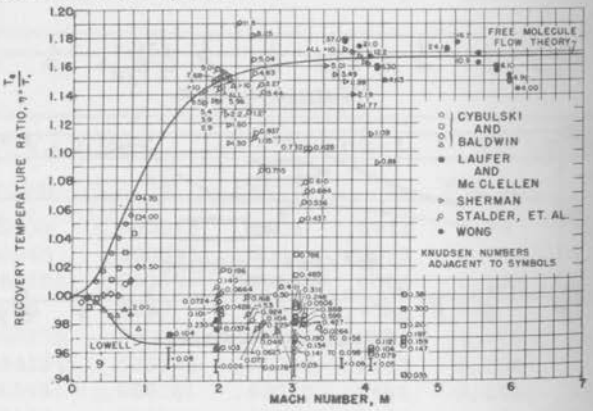

Fig. 6.19. Recovery temperature diameter of the cylinder for a wide range of Knudsen Number

Both Continuum and free molecule results are shown on Fig. 6.19. The parameter that determines if a flow is a continuum or free-molecule is the Knudsen Number, Kn

$$Kn = \frac{\lambda}{d} \tag{6.25}$$

where λ is the mean-free-path between molecules and d is the diameter of the cylinder.

The recovery anomaly can be explained by considering the magnitude of the incident and re-emitted molecular energy.[1] The incident molecular energy is computed using the total velocity resulting from the combination of the stream mass velocity and the random thermal velocities. When the total velocity term is squared, there results a cross-product term, $2Uv$. This cross-product term effectively increases the apparent internal energy of the gas from the continuum value of $(3/2)\,kT$ per molecule to a value of $2kT$ or $(5/2)\,kT$. The actual value depends directly on the speed and orientation of the body. The apparent energy is $(5/2)\,kT$ for the high speeds and for angles of attack greater than zero. The $(5/2)\,kT$ is equal to the internal plus potential energy per molecule of a cube of continuum gas.

For air the recovery temperature ratio approaches 1.168 at high Mach number. A monatomic gas gives a higher recovery temperature than a diatomic gas. The diatomic gas can remove more energy by virtue of the internal energy component due to molecular rotation.

The effect of angle between the cylinder axis and the flow direction effects the recovery temperature. Figure 6.20 shows the recovery temperature as a function of $M \sin \phi$, where ϕ is the angle between the flow and the cylinder axis, for both free-molecule and

---

[1] Stalder, J. R., Goodwin, G., and Creager, M. O., A comparison of theory and experiment for high speed free molecule flow, NACA TN2244, 1950.

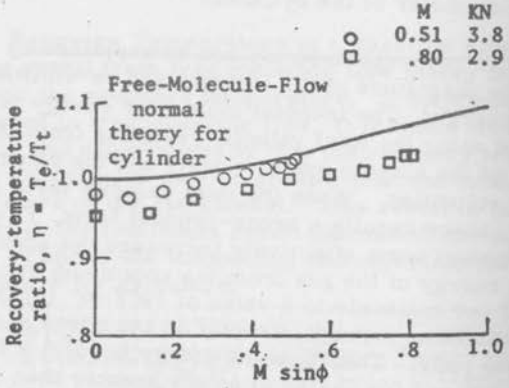

Figure 6.20 - Recovery temperature as a function of flow angle.

continuum flow. It has been assumed that the characteristic length of the wire would change with angle of attack. However, the results of Fig. 6.20 suggest that d is the only length of importance even when the wire is parallel to the flow. More work is needed to fully evaluate the recovery effects of yawed cylinders in supersonic flows.

E. Temperature Evaluation by Sonic Methods - In a still gas the velocity of sound in a gas of molecule weight m m is given by the approximate relation

$$a = \sqrt{\frac{\gamma R T}{m}} \qquad (6.26)$$

Thus, the absolute temperature of a gas may be expressed as

$$T = \frac{m a^2}{\gamma R} \qquad (6.27)$$

The measure of the sonic velocity will in turn be a measure of the temperature for the still gas, since m , γ and R are constant. The measurement of sound velocity is quite simple in a non-flowing fluid, however, it requires the measure of mean velocity in a flowing fluid. Consider Fig. 5.14, which shows a source of sound and a pickup down stream. The source might be pulsed and the transient time to the pickup measured. The velocity of propagation will be $V = a + U = \frac{\ell}{t}$, where t is the time between pulse and arrival. The velocity of sound can be calculated from an independent measure of the flow velocity. A second approach might be to place a second pickup at a position ℓ , away from the source, but not along the direction of flow. The time measured by the two pickups could then be used to solve for both U and a . This procedure requires that we know the mean flow direction. If the mean flow direction is unknown, then a third pickup would be employed to give three equations in terms of t for the unknowns a, U , and flow angle , α .

The sound source may be a small speaker, a spark gap, or a piezoelectric crystal operated in reverse (a voltage suddenly applied to a crystal will produce a change in shape). The sonic pickup is usually a microphone or piezoelectric transducer. These devices have been used in some applications, but they have not found general use. At extreme high temperatues this sonic measurement is not of direct value, since in equation (6.27) neither γ or m will be constant with temperature. This method of measuring temperature is not greatly affected by recovery temperature, if the distance is large compared to the size of the source and the pickup.

F Special Temperature Measuring Techniques - The measurement of temperatures by means of thermal or infrared radiation is widely used. This method is of major importance in the study of solid materials rather than fluids. The use of radiation to measure fluid temperatures is possible, but not as yet well developed. The problem is simply one of how to relate a measured radiation energy from the fluid, such as air to its temperature.

Certain materials, such as "superlinear phosphors" are found to change their luminescence with temperature. This phenomenon is associated with the exciting of the molecular structure of the material. Here also, this technique is of interest in measuring surface temperature, but not a direct indication of the fluid temperature.

The schlieren and interferemometer are techniques which measure density. Thus, these instruments coupled with the measure of pressure can be used to measure temperature. For flow speed flows, where density and temperature vary directly without appreciable effect on the pressure, these optical techniques are used as a direct measure of temperature gradients in fluids.

A possible measure of temperature at the extreme high temperature, low pressure, gas flows is presently being explored at CSU. The concept is to measure directly the kinetic energy of the gas ions in the flow. If the temperature is sufficiently higher than ions of the gas will exist in the flow, and there kinetic energy may be measured. The measurement principal is to employ a "langmuir probe" technique. The Langmuir probe is basically an aerial set in the flow, as shown in Fig. (6.22). The aerial or ion collector is operated at negative voltages, so the ions are attracted to the probe. The number of ions attracted will depend on the voltage of the probe, the number density of ions present in the fluid, and the kinetic energy of the ions.

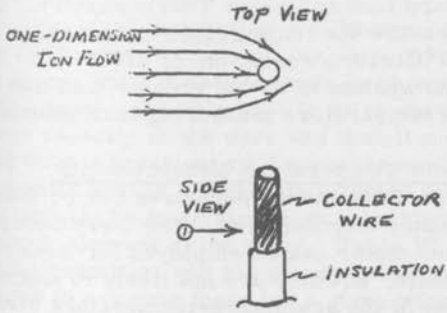

Fig. 6.22. Ion knetic energy measurement

If a ion has a trajectory near the collector, then it can be collected if the attraction of the probe is sufficient to alter its path. A curve of the collected current versus the collector porential will be an indication of the velocity distribution of the ions. If we assume that the ions (and also the molecules) have a Maxwellian velocity distribution, then the relation between the kinetic energy and the

temperature is known. While the collector technique is a possibility theoretically, it still requires a great deal of experimental development.

The resonate frequency of specific crystals is found to vary with the temperature of the crystal. For a quartz crystal plate of generalized orientation

$$f(T) = f(0)(1 + \alpha T + \beta T^2 + \gamma T^3) \qquad (6.28)$$

It is possible to determine a crystal orientation for which the second and third order terms vanish ($\beta = \gamma = 0$)[1]. Thus, a "Linear Coefficient" of frequency with temperature quartz thermometer is commercially available, (Hewlett-Packard Linear Quartz Thermometer). This system can measure the temperature over a range from -40 °C to + 230 °C with a resolution of 0.0001 °C. The accuracy of this system is by far greater than that obtained by most temperature measuring instruments.

G. Transient Temperature Measurements - The measurement of transient temperatures can be done mainly with the resistance thermometer. The thermocouple and sonic thermometer can be employed for moderate transient response, but they are not likely to approach the development of the resistance-temperature element. Thus, the present discussion is limited mainly to the resistance-temperature element. Actually, the response of the thermocouple[2] follows the same laws as the resistance thermometer, with the major limitation being the size to which a wire thermocouple can be made. The response of a thin film type thermocouple can equal that of a thin film resistance-temperature element.

---

[1] Hammond, D. L., Adams, C. A., and Schmit, P., A Linear Quartz Crystal Temperature Sensing Element. ISA preprint No. 11, 2-3-64, 1964.

[2] See for example Shepard, C. E., and Warshawsky, I., NACA TN 2703, 1952.

In Chapter V the general time constant of a wire was given as

$$t = \frac{1}{\frac{k}{\rho c}\left(\frac{\pi}{\ell}\right)^2 + \frac{4}{D^2}\frac{hD}{\rho c} - \frac{\sigma}{\rho c}\left(\frac{4}{\pi D^2}\right)^2 I^2} \qquad (5.61)$$

Thus, the evaluation of the time constant requires a knowledge of the physical properties in Eq. (5.61). For pure materials the physical properties such as; thermal conductivity k, density ρ, specific heat c, and resistivity σ, can be obtained from handbooks. For alloys these properties are not always available. Thus, to fully evaluate a transient resistance thermometer, it is necessary to evaluate the wire physical properties.

Physical Properties - Sufficient information was given in Chapter V to obtain the wire physical properties from steady state measurements (with exception of specific heat). Specific heat is so to speak the heat storage capacity of the wire and thus, it must be determined from a transient type measurement. Fortunately, the specific heat is not greatly affected by alloying, so it can usually be estimated from tabulated properties of the major element of the alloy. Table VI.4 lists the physical quantities and the steady state measurements required to evaluate them for a given wire material.

TABLE VI. 4

Physical Properties Evaluation of a Transient Resistance Thermometer Sensing Element[1]

Parameter	Equation for Evaluating Parameter	Type of Measurement	Remarks
Wire length ℓ		Dimension	Optical type measuring instrument
Wire Diameter D		Dimension	Optical or Electron Microscope instrument
Resistivity σ	$\sigma = \frac{\pi D^2}{4\ell} R_o$ (Eq. 1.5)	Resistance and known dimensions	If σ is known for large wire sample, can use σ to determine wire diameter
Thermal Conductivity k	$k = \frac{\delta R_o \ell}{3\pi D^2} \frac{1}{\frac{\Delta(R/R_o)}{\Delta I^2}}$ (Eq. 2)	Wire resistance versus wire current in a vacuum	Uncertainty due to D^2 which can not be measured with great accuracy
Heat Transfer Coefficient x wire diameter hD	$hD = \frac{I^2 R_w R_o \alpha}{\pi \ell (R_w - R_a)}$	Wire resistance versus wire current in Air	hD is a function of flow Velocity density
Density ρ		Volume-weight measurement	Need determine before drawn into very small wire
Specific Heat c	$c = \frac{k \pi^2}{\rho \ell^2}$	Time constant of wire to a step change in current in a vacuum	Limiting case for $I \longrightarrow 0$ change in current

[1] Chao, J. L., and Sandborn, V. A., A resistance thermometer for transient temperature measurements, Fluid Mech. Paper No. 1, Colorado State University, 1964.

The wire dimensions would be determined from direct measurements if possible. It is sometimes difficult to measure wire diameter. As a result, the resistivity of the alloy might be determined from a large sample, and it in turn used to estimate wire diameter.

The thermal conductivity of the wire material is determined by making resistance-current measurements in a regime where conduction is the major heat transfer mechanism. This regime of conduction controlled heat transfer is the case of a wire in a vacuum. Figure 6.23 shows the measurements made for the platinum-rhodium wire in a vacuum. The value of k calculated from the slope of the curve is noted on the figure. The measurements in a vacuum are affected by radiation heat loss from the wire. The insert on Fig. 6.23 indicates the estimate of radiation heat loss for the wire.

The heat transfer coefficient is obtained from resistance vs. current measurements in a regime where convection is the major heat transfer mechanism. This regime of convection controlled heat transfer is the case of a wire operating in air. The value of hD is a function of flow velocity, density and temperature, so it must be specified for each particular flow in which the wire is to be used.

Figure 6.24 shows the measurements made for the Platinum-Rhodium wire in still ambient air. An estimate of the correction for conduction loss by the wire is shown as an insert on Fig. 6.24.

For the platinum-Rhodium wire evaluated it was assumed that handbook values of ρ and c could be used. A value of ρ for the 90-10 alloy was available in the literature. For c a value was found for a 87-13 alloy, which was only about 10 per cent greater than that of pure platinum. The 87-13 alloy value for c was employed as a first approximation in the evaluation of the wire time

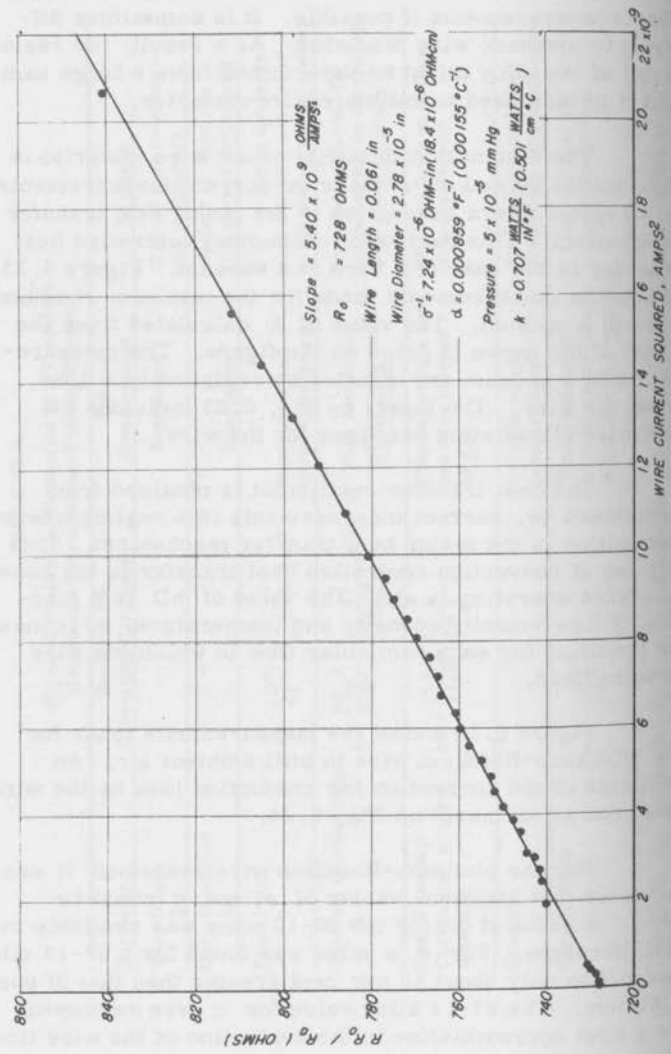

Fig. 6.23 Evaluation of Thermal Conductivity

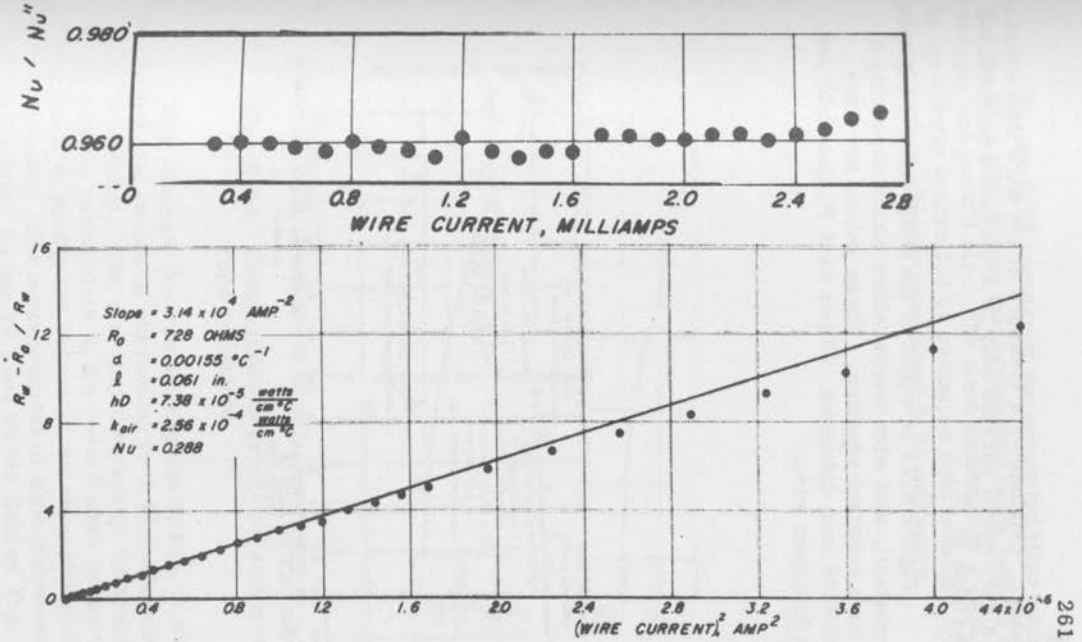

Fig. 6.24 Evaluation of Heat Transfer

constant. Obviously, a measure of the wire time constant for a very small current step in a vacuum was employed as a check of c .

Figure 6.25 is a plot of the convection, conduction (a constant), and wire temperature terms appearing in the time constant equation. These values are for a 0.0000278 inch diameter, 90 per cent Platinum-10 per cent Rhodium wire.

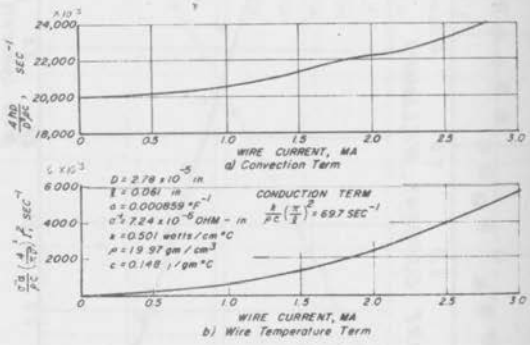

Fig. 6.25. Variation of the thermal time constant terms

Figure 6.26 compares the computed time constant for the wire with actual measurements made both in a vacuum and in still air. The time constant in a vacuum is apparently controlled by radiation heat transfer for wire currents greater than about 0.05 millamps.

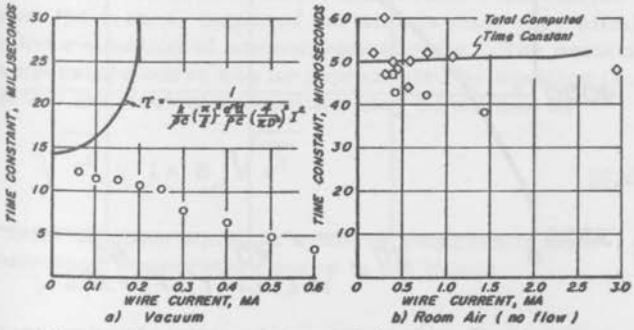

Fig. 6.26. Comparison of predicted and measured time constants.

The estimate for radiation given in Fig. 6.23 had suggested that values of current up to 0.10 millamps would be useable. The fact that the vacuum measurements seen to extrapolate to the $I \longrightarrow 0$ case of the theory would seem to justify the values of the wire physical constants used. The measurement of time constants was somewhat crude, as can be seen by the data of Fig. 6.26.

The computed time constant curve is certainly reasonable, compared to the data, and again justifies the physical constants evaluated.

An idea of the variation of wire time constant with flow conditions is demonstrated in Fig. 6.27.

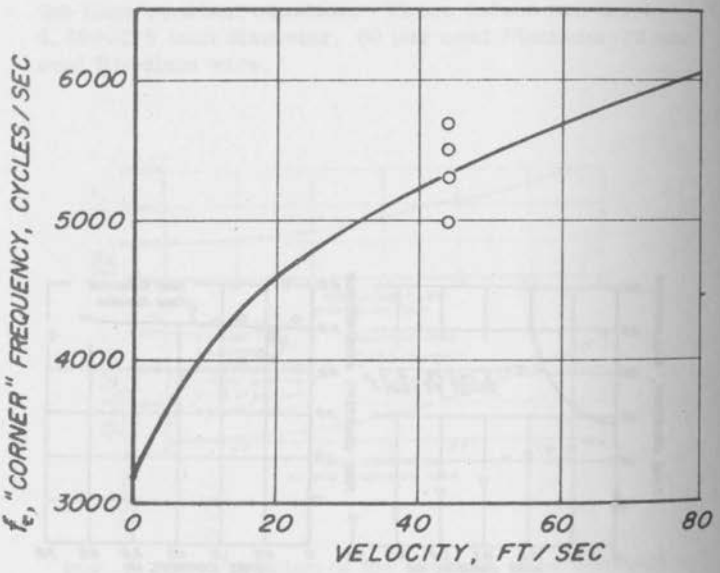

Fig. 6.27. Comparison of predicted and measured time constants in moving air

Using the curves of Fig. 5.21 it is possible to estimate the variation of hD with velocity and/or density. Figure 6.27 shows the value of corner frequency predicted for the platinum-rhodium wire as a function of flow velocity. A set of three measurements taken at a velocity of 45 feet per second is shown for comparison in Fig. 6.27.

Measurements of temperature fluctuations - The platinum-rhodium resistance thermometer is employed in the authors laboratory to measure temperature fluctuations in the boundary layers of a heated flat plate. The frequency response of the bare wire is adequate to measure the fluctuations without need of further electronic compensation. A simple Wheatstone bridge circuit, shown in Fig. 6.28 is employed to operate the wire at a constant current of 0.1 millamp. The output of the bridge was amplified and read with a true r.m.s. voltmeter. The resulting evaluation of both the mean and fluctuating temperatures is shown in Fig. 6.29. The frequency distribution obtained from a spectral analysis of the resistance thermometer output is shown in Fig. 6.30.

The evaluation of the temperature fluctuation from the r.m.s. output of the wire is done very similar to the evaluation of anemometer signals. The resistance temperature curve can be represented by equation (6.6) so that the fluctuation equation may be written as

$$\sqrt{\overline{t^2}} = I \alpha R_o \sqrt{\overline{e^2}} \qquad (6.29)$$

a more complex equation would be required if the resistance temperature curve is not linear.

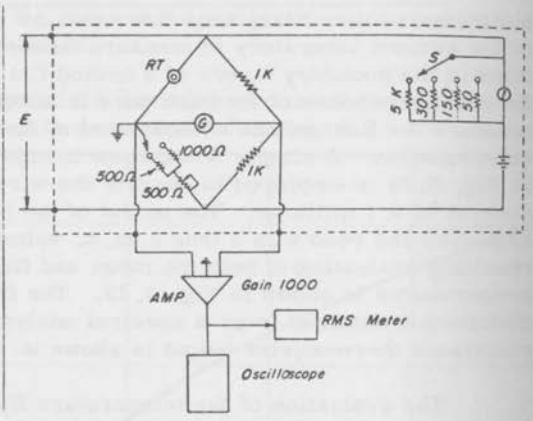

Figure 6.28 - Bridge circuit to operate the resistance thermometer.

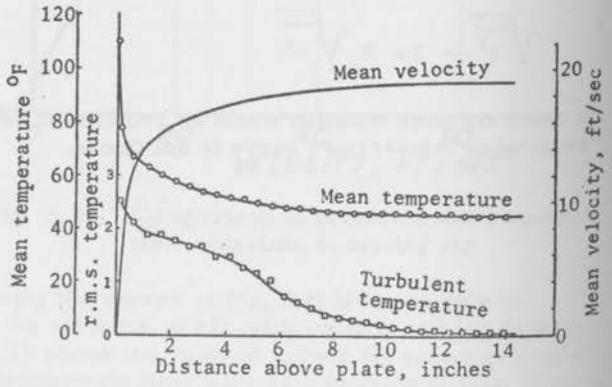

Figure 6.29 - Measured mean and fluctuating temperature distribution.

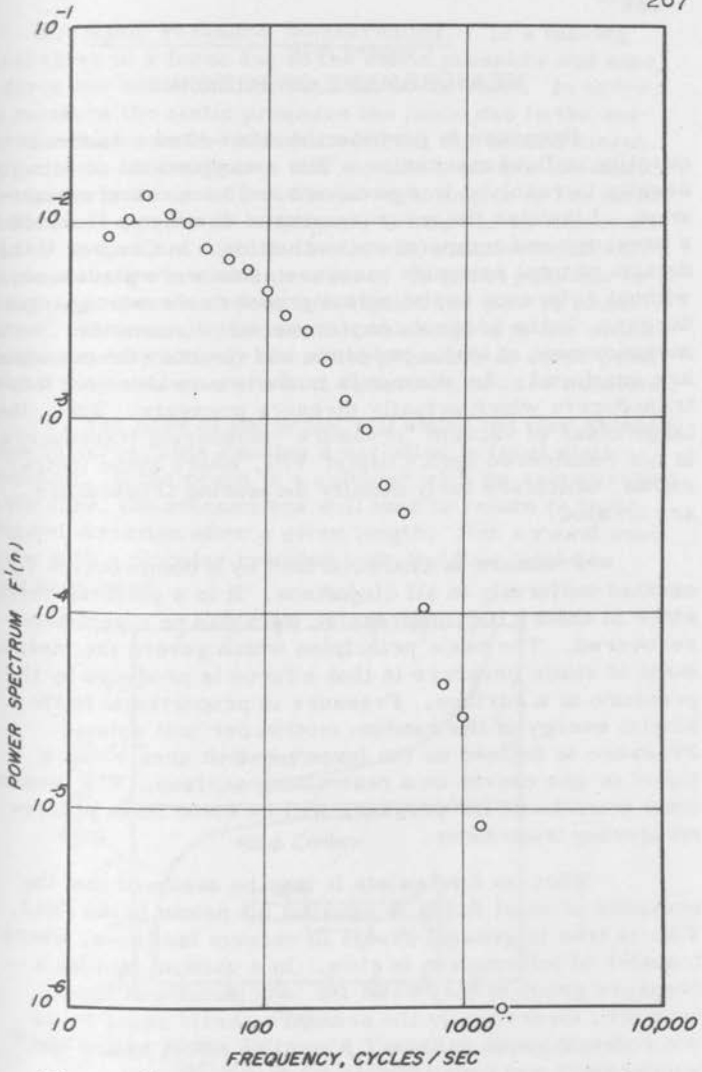

Figure 6.30 - Spectral energy distribution measured by the resistance thermometer.

Chapter VII
MEASUREMENT OF PRESSURE

Pressure is perhaps the most often measured quantity in fluid mechanics. The measurement of velocity usually is resolved to a pressure and temperature evaluation. Likewise the measurement of density is resolved to a pressure and temperature evaluation. In Chapter V the details of total pressure measurements were discussed, without reference to the actual pressure measuring transducers. In the present chapter we will discuss the measurement of static pressure and the transducers which are employed. An attempt is made to consider only those transducers which actually measure pressure. Thus, the large class of vacuum "pressure" measuring transducers is not considered until Chapter VIII, where these instruments, which are turly density measuring transducers, are treated.

Pressure is characterized by a compressive stress exerted uniformly in all directions. It is a potential force, since in theory, its compressive work can be completely recovered. The basic principles which govern the measurement of static pressure is that a force is produced by the pressure at a surface. Pressure is proportional to the kinetic energy of the random motion per unit volume. Pressure is defined as the force per unit area which a liquid or gas exerts on a restraining surface. The measurement transducer for pressure will be some form of force measuring transducer.

When no flow exists it may be assumed that the pressure of most fluids is equal at all points in the fluid. This is true in general except in vacuum facilities, where transfer of information is slow. In a vacuum facility a pressure gradient may exist for long periods of time, however, theoretically the pressure should equal out to one common valve in time. A similar effect exists for temperature and density properties in a vacuum.

A. Static Pressure Measurement.- In a moving fluid there is a force due to the static pressure and also a force due to the uniform motion of the fluid. In order to measure the static pressure the force due to the uniform motion must be eliminated from the measurement. In general, this suggests that we will measure the static pressure-force in a direction at right angles to the mean motion. If a probe is employed, it must be so constructed that it does not disturb the flow in a manner that will cause a change in static pressure. It is not possible to design a probe which does not disturb the flow to some extent. However, it is possible to design a probe which measures very closely the static pressure at some point behind the noise where initial disturbances have subsided.

The nose of the probe will cause the flow streamlines to curve, thus causing a variation in local static pressure. If the probe is a cylinder with its axis paralled to the flow, the streamlines will tend to return to their original direction after a given length. For a round nose probe with a circular cylinder body the flow field has been calculated.

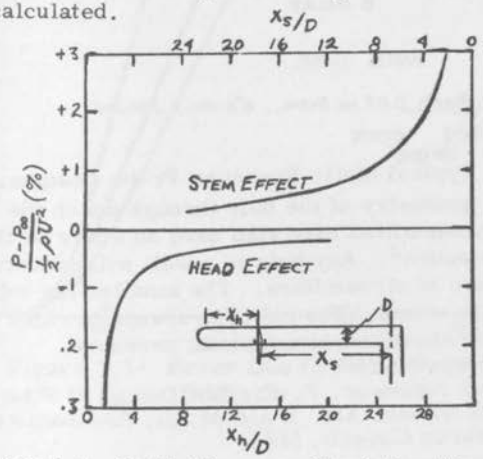

Figure 7.1 - Static Pressure Variation Along the Surface of a Cylinder.

Figure 7.1 shows the variation of local static pressure along such a probe[1]. Also shown on Figure 7.1 is the effect produced by a stem. The general approach to design of a static pressure probe is to optimize the opposing effects of head and stem, so that the two effects tend to cancel each other. Typical static pressure probes are shown in figure 7.2. Holes are equally spaced around the cylinder, so that any non-symmetrical flow effects are reduced.

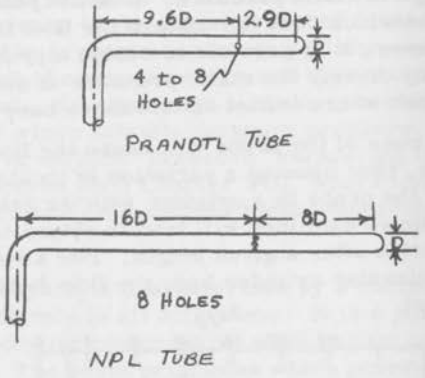

Figure 7.2- Typical Static Pressure Probe Designs.

The geometry of the hole through which the pressure is transmitted may also have an effect on the measured pressure[2]. Any hole in a wall will produce some curvature of streamlines. The smaller the hole the smaller the effect. The effect is always to raise the local pressure above the actual static pressure.

---

[1] Ower, E. and Johanson, F. C.; The Design of Pitot-Static Tubes. ARC R and M 981, Aeronautical Research Council, 1925.

[2] Rayle, R. E.; An Investigation of the Influence of Orifice Geometry on Static Pressure Measurements. M.S. Thesis, Mech. Engr. Mass. Inst. of Tech., 1942.

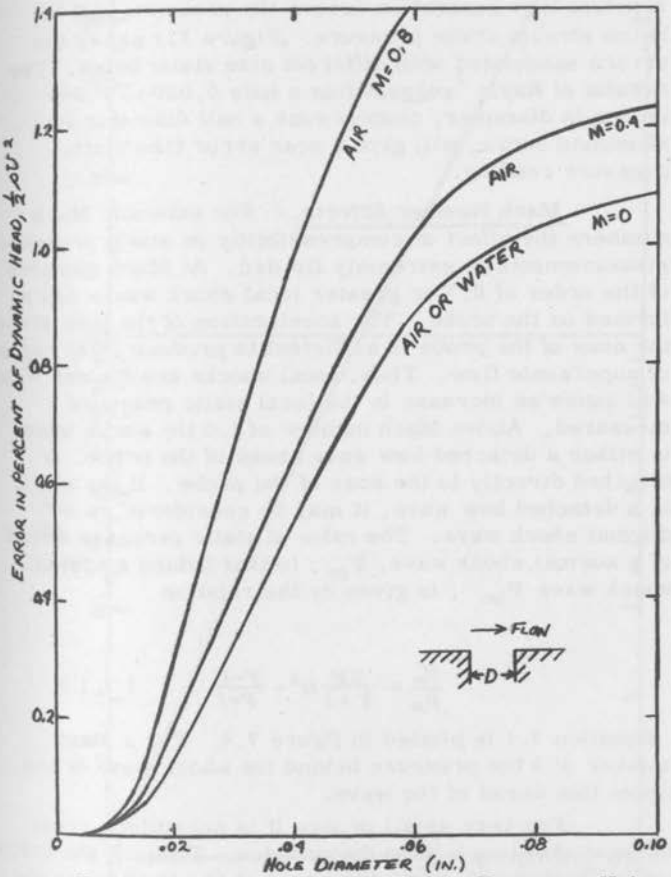

Figure 7.3- Error Due to Static Pressure Hole Diameter.

If actual flow separation occurs the pressure will be below stream static pressure. Figure 7.3 shows the errors associated with different size static holes. The results of Rayle[1] suggest that a hole 0.020 to 0,040 inches in diameter, counter sunk a half diameter to eliminate burrs, will give a near error free static pressure reading.

Mach Number Effects.- For subsonic Mach numbers the effect of compressibility on static pressure measurements is extremely limited. At Mach numbers of the order of 0.7 or greater local shock waves can be formed on the probe. The acceleration of the flow around the nose of the probe is sufficient to produce local regions of supersonic flow. Thus, local shocks are formed which will cause an increase in the local static pressure measured. Above Mach number of 1.0 the shock wave is either a detached bow wave ahead of the probe, or attached directly to the nose of the probe. If the shock is a detached bow wave, it may be considered as a normal shock wave. The ratio of static pressure ahead of a normal shock wave, P_∞, to that behind a normal shock wave P'_∞, is given by the relation

$$\frac{P'_\infty}{P_\infty} = \frac{2\gamma}{\gamma+1} M^2 - \frac{\gamma-1}{\gamma+1} \qquad (7.1)$$

Equation 7.1 is plotted in figure 7.4. For a Mach number of 3 the pressure behind the shock wave is ten times that ahead of the wave.

For very small probes it is possible to treat the bow shock as a local disturbance. Thus, if the static tap is located well behind the nose it is possible for the static pressure to return to the free stream value.

[1] Rayle, R. E.; ibid.

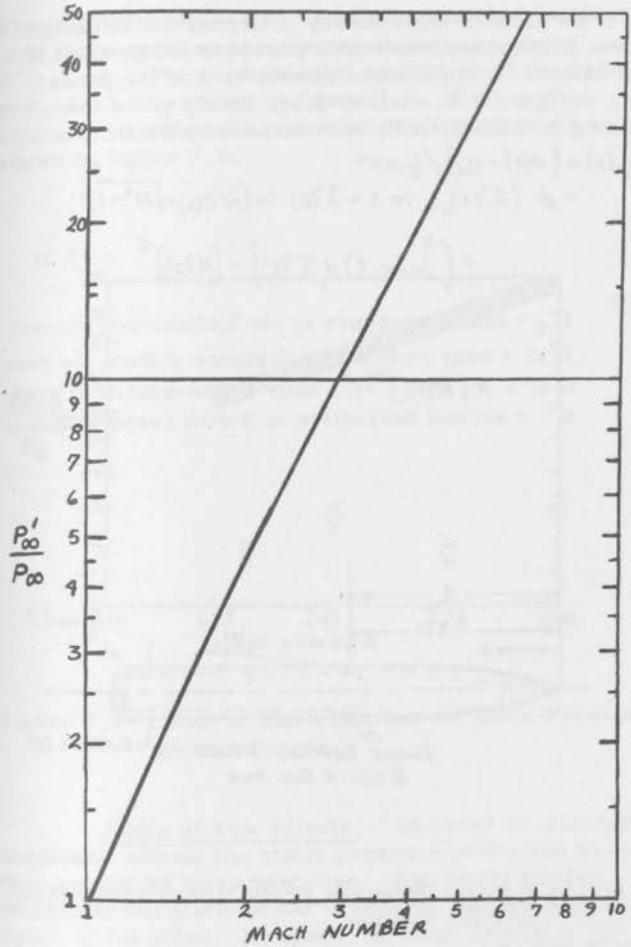

Figure 7.4- Change in Static Pressure Across a Normal Shock Wave.

Also from slender-body theory it is possible to design a probe chich measures static pressure independent of Mach number at supersonic speeds [1]. For the probe shown in figure 7.5, slender-body theory gives the following pressure coefficient variation with x .

$$C_p(x) = \left[p(x) - p_\infty\right] / \tfrac{1}{2}\rho U^2$$
$$= \frac{1}{\pi}\left\{S''(x)_{x=0} \ln x + S''(x) \ln\left[2/R(x)\sqrt{M^2-1}\right] + \int_0^x \ln(x-t)\, d\, S''(t)\right\} - \left[R'(x)\right]^2 \qquad (7.2)$$

where

P_∞ = static pressure in the undisturbed stream
$R(x)$ = body radius at a distance x from the nose
$S(x) = \pi\left[R(x)\right]^2$ the body cross-sectional area
S'' = second derivative of S with respect to x.

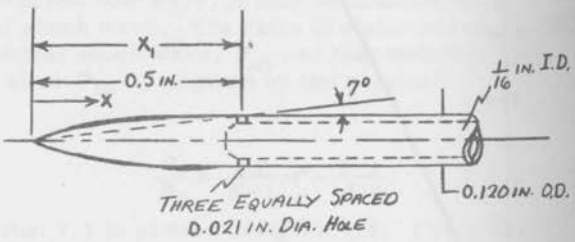

Figure 7.5- A Static Pressure Probe that is Independent of Mach Number.

---

[1] Mollo-Christensen, Landahl, and Martuscelli; A Short Static-Pressure Probe Independent of Mach Number. Jour. Aero. Sci., 1957, p. 625.

The pressure coefficient Cp (x) becomes independent of M if the orifices are placeat at point x, where $S''(x_1) = 0$. The experimental evaluation of the probe in figure 7.5 is shown in figure 7.6. A 5- degree conically tipped probe pressure coefficient is also shown on figure 7.6.

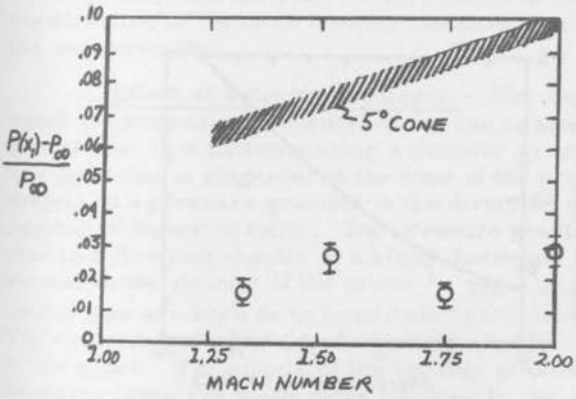

Figure 7.6- Effect of Mach Number on Static Pressure Measurements.

Angle of Yaw Effects.- In order to minimize angularity effects the static pressure probe has several taps around its circumference. For small angular deviations the static probe is usually insensitivity because of the holes. However, at large angles of yaw the flow may actually separate on one side of the probe.

Figure 7.7 demonstrates the effect of flow direction on a typical static pressure probe. In general the probe in insensitivity to small changes in flow direction, but has a marked effect at larger angles. One may employ a static type pressure probe to determine the actual flow direction.

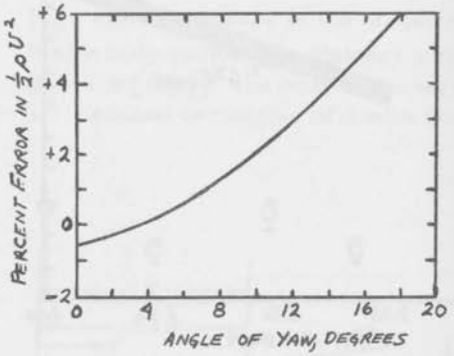

Figure 7.7- Effect of Flow Angle on Static Pressure Measurements.

Effect of Turbulence.- The pressure indicated by a pressure tap is the stagnation pressure of the gas in the hole. For the ideal flow of a gas directly past the hole the pressure should be equal to the stream static pressure. If turbulence exists in the stream it will alter the streamlines of the fluid such that we may find a velocity component directed into the static hole. For this case the pressure measured by the probe will be

$$P_{\infty_i} = P_\infty' + \frac{1}{2}\rho\overline{v^2} \qquad (7.3)$$

An error of 1 % in static pressure measurements would be obtained for a 10% turbulence level.

For a static pressure probe the holes are located symmetrically around the probe, so that the effect of turbulent fluctuations is not as well predicted. If the fluctuations are symmetrical then it appears that no measureable pressure effect could be predicted. Secondly, one may show that if the static pressure probe is insensitivity to yaw angles of the order of ± 10 degrees, then the effect of turbulence in changing the direction of the total velocity can have no effect on the measurement.

Effect of Velocity Gradients.- For flows in which the stagnation pressure varies can cause three dimentional flow patterns along a circular cylinder. The fluid that is stagnated at the nose of the probe is subject to a pressure gradient in the direction of the regions of higher velocity. The pressure gradient gives rise to a flow that results in a slight downwash of the stream in the vicinity of the probe.[1] The viscous forces also are such as to contribute to the downwash. The downwash is equivalent to a slight change in yaw of the probe. The effects of the velocity gradient in a boundary layer are made more complex by the presence of the wall. In general the static pressure probe is not recommended for boundary layer measurements, however, there is a need to evaluate static pressure across the boundary layer. The equation of motion in the vertical direction in a turbulent boundary layer appears to be[2]

$$\rho \overline{v^2} = p - p_w \qquad (7.4)$$

---

[1] Volluz, R. J.: Wind Tunnel Instrumentation and Operation, Handbook of Supersonic Aerodynamics, NAVORD Report 1488 (Vol. 6).

[2] Sandborn, V. A. and Slogar, R. J.: Study of the Momentum Distribution of Turbulent Boundary Layers in Adverse Pressure Gradients. NACA TN 3264, 1955.

Thus, it is possible to evaluate the static pressure from a measure of the vertical turbulent velocity component. Unfortunately equation (7.4) has not been checked experimentally with sufficient accuracy to completely justify its use.

B. PRESSURE TRANSDUCERS.- There are many possible forms of transducers that are employed to measure pressure. We have discussed pressure measurements which are employed to evaluate velocity as well as the more direct static pressure measurement. Obviously, the same transducer can be used to measure either static or total pressure, however, it may be necessary to use different transducers for different magnitudes of pressure. As noted in Table IV.1 it is possible to require pressure measurements from 0 to 10,000 psi in even limited areas of fluid mechanic research.

The major instrument employed to measure pressure is the manometer. This instrument uses the force of gravity to counter balance the force produced by pressure. The manometer is closely related to the dead weight testor, which employs a solid mass rather than a liquid column to indicate force. There are many electro-mechanical devices that have been developed and used as pressure transducers. Figure 7.8 is a schematic diagram of typical systems employed both to change pressure into a measureable movement, and also the electrical read out system.[1] The different types of transducers are covered in detail in the following discussion.

---

[1] Lion, K. S.: Pressure Transducers Survey, ASME Symposium on Measurements in Unsteady Flow. Worchester, Mass., 1962.

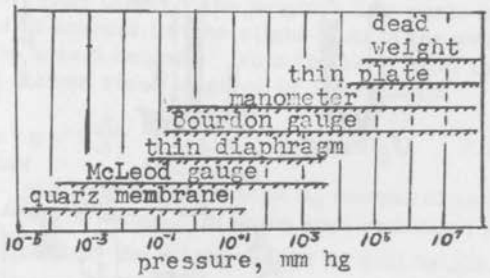

Figure 7.9 - Range of Pressure Transducers

Figure 7.9 is a summary of the range of the different types of pressure transducers. There is of course many ways in which the range of a given type of transducer may be extended, so the end points of each instrument is somewhat uncertain. In the vacuum range of pressures (below 10^{3} mm Hg) the transducers do not measure pressure, but rather the number density of the molecules are measured.

Manometers.- The most widely used pressure transducer is the liquid manometer. The manometer may serve as a laboratory standard for pressure. The manometer takes advantage of the gravitational force on a column of liquid. Figure 7.10 shows the types of manometer employed in pressure measurements. The simple U-tube manometer is the most common employed manometer. The pressure can be computed from the height h of the column of fluid. For a manometer fluid of density ρ_m and a fluid of density ρ_f in which the pressure is measured, the unknown pressure is

$$p = gh(\rho_m - \rho_f) + p_a \qquad (7.5)$$

If the fluid in which the pressure is measured is air and the manometer fluid is water for example, then it is evident that $\rho_m \gg \rho_f$ and so ρ_f can be neglected.

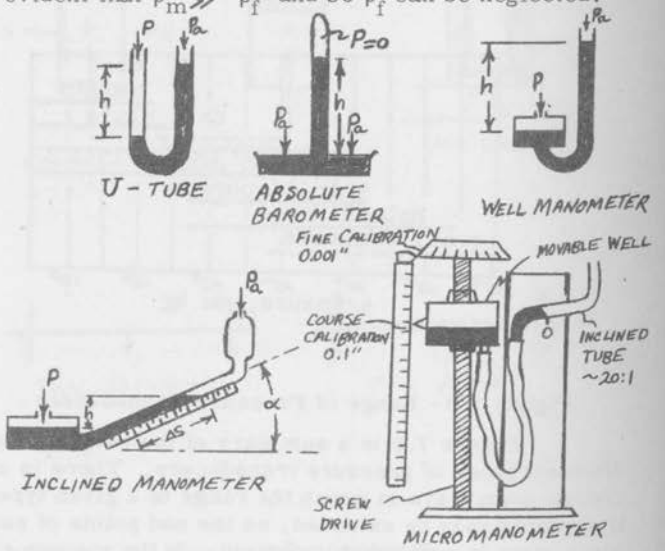

Figure 7.10- Liquid Manometers

The height h is in all cases the vertical height of the column, so that the gravitational mass of the fluid is properly accounted for. The slant tube manometer is designed to produce a large movement of the fluid column for only a small vertical rise in h. The slant tube is a means of expanding the variation in pressure over a greater scale.

The density of manometer fluids are a function of their temperature. Thus, accurate evaluation of the pressure requires that the effect of temperature on manometer fluid be accounted for. Figure 7.11 is a typical plot of the density variation with temperature for various manometer fluids.

The well type manometer is a common type of pressure measuring manometer. This type manometer usually employs a scale along the smaller diameter tube which reads directly the height. The scale is calibrated to account for the slight drop in the well level. The actual height h' from the zero level to which the column rises is given by the relation

$$\rho = g h' \left(\frac{A_2}{A_1} + 1 \right) (\rho_m - \rho_f) + P_a \qquad (7.6)$$

For a well with a very large area A_1 compared to A_2 the factor $\frac{A_2}{A_1}$ is small. In some applications it is possible to neglect the slight change in well height.

For the measure of very small pressure differences the movable well type micromanometer is employed. It is possible to indicate variations as small as 0.0001 inches in the column with a micromanometer.

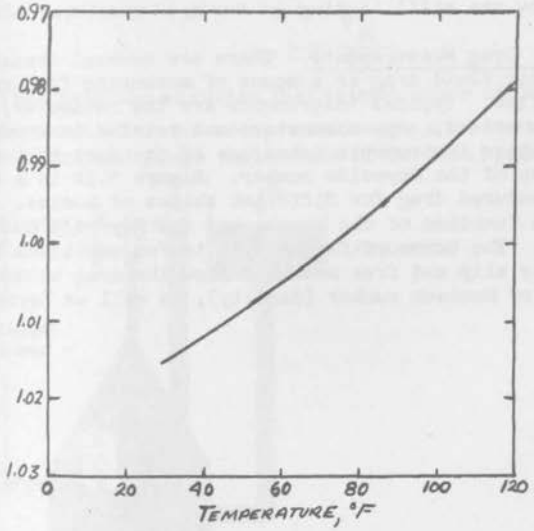

Figure 7.11- Specific gravity characteristics of Merriam Unity Oil.

For pure free molecule flow the molecular mean free path is large compared to the body dimensions. For free molecule flow the following relation is obtained.[1]

$$\frac{p\rho}{p_s\rho_s} = \left\{ e^{-\left(\frac{\gamma}{2} M_\infty^2\right)} + M_\infty \sqrt{\frac{\pi\gamma}{2}} \left[1 + \operatorname{erf}\left(M \sqrt{\frac{\gamma}{2}} \right) \right] \right\}^2 \tag{5.18}$$

Pressure measurements in freemolecule flow is complex in that pressure may not be equal at all places along a tube. Detailed experimental studies of the impact tube in free molecule flow are still lacking.

B. Drag Measurements - There are several transducers that employ fluid drag as a means of measuring flow velocity or mass flow. Typical instruments are the rotameter, turbine flow meters, cup-anemometers and related instruments. Each of these instruments makes use of the fact that drag is a function of the Reynolds number. Figure 5.12 is a summary of the measured drag for different shapes of bodies. The drag is a function of the shape, and the Reynolds number of the flow. The curve of figure 5.12 is for continuum flow only. For slip and free molecule flow the drag becomes a function of Knudsen number (density), as well as Reynolds numbers.

---

[1] Chambre, P. L., and Schaaf, S. A.; ibid.

McLeod Gauge. - A special type of manometer employed in the measure of low pressure was described by McLeod[1]. Figure 7.13 shows a typical McLeod Gauge. The chamber, A, is first exposed to the pressure, p, to be measured as shown in figure 7.13. . The mercury is then raised into the chamber traping the original gas at pressure p in the chamber. As the mercury is raised past the point "s" the gas in chamber A is compressed. The final reading has compressed the original volume of gas in chamber A, denoted by V_A, to the small volume contained in the capillary, denoted by V_c. The pressure of the gas in the capillary is given by

$$p_c = p \frac{V_A}{V_c} \qquad (7.7)$$

This relation assumes that temperature of the gas before and after the compression are still identical. Thus, the McLeod gauge makes use of the ideal gas equation of

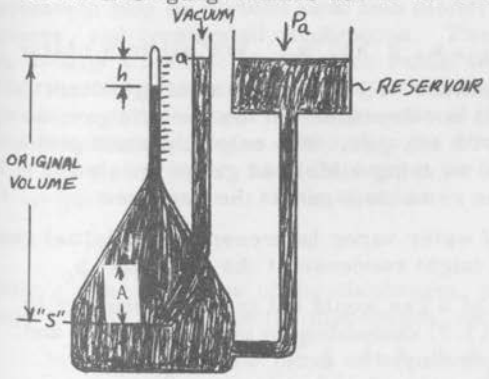

Figure 7.13 The McLeod Gauge

[1] McLeod, H.: Phil. Mag. Vol. 48, p. 110, 1874

state. The actual pressure p_c in the capillary is given by the manometer relation (neglecting ρ_f, and setting $p_a = P$) as

$$p_c = g\, h \rho_{Hg} + p \tag{7.8}$$

The volume of the capillary may be expressed as a constant, v, times the length h, ($V_c = vh$). Thus, the initial pressure, p may be expressed as

$$p = \frac{vg\, h^2\, \rho_{Hg}}{V_A - v\, h} \tag{7.9}$$

Note that V_A is much larger than $V_c = v\, h$, so that the pressure is given approximately as

$$p \sim \frac{v\, g\, \rho_{Hg}\, h^2}{V_A} \tag{7.10}$$

Thus, since V_A, v, g and ρ_{Hg} are all very nearly constant the pressure will be a function of h^2 directly. Equation (7.7) is not dependent on the specific gas, so it can be used with any gas. The only important problem encountered in using a McLeod gauge is to make sure that the gas remains a gas at the pressure p_c.

For example, if water vapor is present in the initial gas sample, then it might condense at the pressure p_c.

The condensing of a gas would act in such a manner to make equation (7.7) unusable. In practice filters and cold traps are employed to avoid the introduction of condensible vapors into the sample gas.

Elastic Deformation Pressure Transducers.- Nearly all modern pressure transducers are based upon the elastic deformation and the resulting mechanical displacement of a member under the influence of pressure Lion [1] lists the following types of elastic deformation elements

1. Membranes
2. Bourdon tubes or spiral
3. Bellows
4. Tubes (which expand under pressure)
5. Pistons (rarely used)

These elements are shown schematically in figure 7.8. The output of the elastic elements is a displacement, which may be either measured directly or converted into an electrical signal. The electrical readout of the displacement is discussed in the following section.

The membrane types of elastic deformation elements may be divided into: thin diaphragms, thin plates, and corrugated diaphragms. The thin diaphragm is usually a metalic sheet under radial tension. The thin diaphragm has no stiffness to bending, thus, if a pressure force is applied to one side of the diaphragm the membrane deflates outward in the shape of a sphere. For a flat, circular, thin diaphragm the displacement d (shown in figure 7.14) is equal to

$$d = \frac{a^2 P}{4 S} \qquad (7.11)$$

where a is the radius of the diaphragm, p is the pressure and S is the tension in the diaphragm. As long as d does

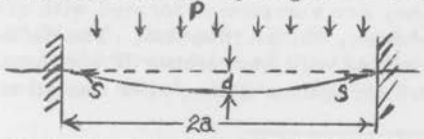

Figure 7.14 - Displacement of a Thin Diaphragm

[1] Lion, K. S., *Ibid*

not exceed approximately 0.005a the deflection is linear with pressure. The thin diaphragm is used in a wide number of pressure transducers. The major application is for very small pressure variations as commonly encountered in air and gas flows. The diaphragm type microphone is employed to measure fluctuating pressures.

The thin plate membrane shown in figure 7.15 is simular to the thin diaphragm except it has stiffness to bending.

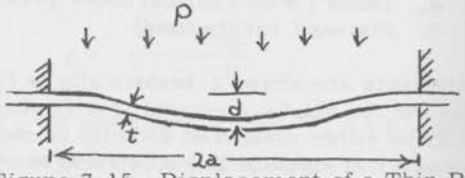

Figure 7.15 - Displacement of a Thin Plate.

The equation for the displacement d, is

$$d = \frac{3(1-\nu^2)a^4 p}{16 E t^3} \qquad (7.12)$$

where ν is Poisson's ratio, E is Young's modules and t is the thickness of the plate. The deflection is linear with pressure so long as d does not exceed 0.5 t. The thin plate as a pressure transducer is of value for moderate and high pressure variations.

A survey of the application of flat diaphragms and circular plates to instruments is given by Wahl [1].

In order to increase the physical deflection of diaphragms they are sometimes formed with corrugations or catenary shapes, rather than flat. The deflection will in general increase with the number of corrugations and decrease with corrugation depth. The design of corrugated

---

[1] Wahl, A. M.; Recent Research on Flat Diaphragms and Circular Plates with Particular Reference to Instrument Applications. Trans. Amer. Soc. Mech. Engrs. vol. 79 p. 83-87, 1957.

diaphragms is covered by Haringx [1] and by Wildhack, Dressler and Lloyd[2]. The corrugated diaphragms find use in pressure gauges which range from vacuum pressures to roughly 350 psi.

The Bourbon type tubes are employed because of their large deflections. These elements are particularly useful when a direct mechanical readout of the deflection is desired. The angular deflection for the simple, elliptical crossectional, C - tube Bourdon gage is given by

$$\frac{\phi}{\phi_o} = \frac{1.16\ pr^2}{t\ E\ b} \qquad (7.13)$$

where ϕ in degrees is the angle of rotation of the tip of the tube, ϕ_o is the sector angle of the original tube, p is the pressure, r is the radius of the tube, t is the wall thickness, E is Young's modulus for the tube material, and b is the minor axis of the elliptical-shaped tube (from middle of the walls). The design of Bourdon tubes is covered by Goitein. [3] The Bourdon tube is used extensively in industrial instruments for pressure up to at least 15,000 psi.

The metallic bellows are capable of giving large deflections for a given pressure. The bellows are less stable structurally than the other types of

---

[1] Haringx, J. A.; Design of Corrugated Diaphragms. Trans. Amer. Soc. Mech. Engrs. vol. 79, p. 55-64, 1957.

[2] Wildhack, W. A., Dressler, R. F., and Lloyd, E. C. Investigation of the Properties of Corrugated Diaphragms. Trans. Amer. Soc. Mech. Engr., vol 79, p. 65-82, 1957.

[3] Goitein, K.; A Dimensional Analysis Approach to Bourdon Tube Design. Instrum. Practice, vol 6, p. 748, 1952.

elastic gauges, thus it is somewhat limited in application. Bellows gauges are employed as absolute pressure gauges, in that a known pressure can be sealed within the gauge. A typical application is the recording barometer.

It should be evident that either the displacement or physical strain of the elastic deformation material can be employed as a measure of pressure. The expanding tube shown in figure 7. 8 is an example where it might be more desirable to measure strain. The expanding tube is the limiting case of a bellows and would be of most value for moderate and high pressures. The expanding tube proves of value in measuring pulsating pressures.

The piston type transducer is not generally employed as a measurement transducer, but rather it finds extensive use as a check valve on excess pressure.

Electrical Readout of Pressure Transducers. - The elastic deformation type pressure transducers all require a displacement, d_1, to be sensed. Figure 7. 16 is a schematic diagram[1] of the electrical phenomenon which are used to sense a displacement. The electrical readout systems can be explained in the following manor.

1. Slide Wire - The displacement, d, causes a change in resistance of the potentionmeter voltage divider. For a constant battery voltage, the output voltage E_o is directly proportional to the change in resistance as d varies.

---

[1] Lion, K. S. ; Ibid.

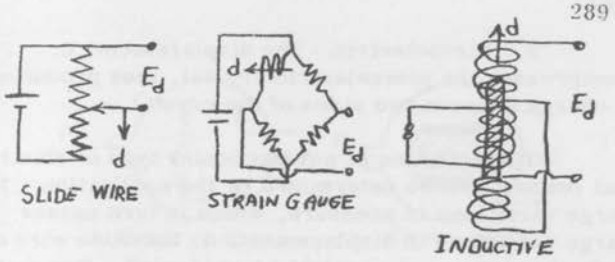

Figure 7. 16 - Electrical Sensing of Displacement.

2. Strain Gauge. - A resistance wire strain gauge (unbonded or bonded) or a foil gauge is attached to the elastic member so it is strained when the member is displaced. The change in resistance of the strain gauge is proportional to the displacement, d, of the elastic member.

3. Inductive. - The change in the core element extension into the coil produces a reluctance variation in an inductive circuit. This change is usually sensed by the eddy currents caused by the inductance of a radio-frequency driven coil.

4. Capacitive. - The displacement, d, between the two plates, produces a change in capacitance, C. The change in capacitance is usually sensed by a radio-frequency circuit.

5. Piezoelectric. - The displacement, d, compresses the piezoelectric crystal, thus producing a charge between two sides of the crystal.

The selection of any particular type of electrical readout will be determined by the application. For large variations in pressure, which in turn causes large variations in displacement, d, the slide wire or inductive type readout might be preferred. For small variations in pressure, the strain gauge or capacitive type readout is usually employed. The piezoelectric readout is mainly for use in transient-type pressure measurements.

Electro-Mechanical Pressure Transducers. - In figure 7. 16, we have noted that several electrical phenomena may be employed to sense the displacement of a mechanical pressure transducer. The direct conversion of pressure (or force) into an electrical signal is also possible. If a material is placed in high pressure, it is possible that it can be compressed to a point where its resistance will change. Likewise, the dielectric constant of a material and the permeability of a material may change with pressure. Figure 7. 17 is a schematic diagram of possible electro-mechanical pressure transducers. [1]

The resistance of materials as a function of pressure has been reviewed in detail by Bridgman. [2] The resistance of several metals are shown in figure 7. 18. The variation of resistance with pressure is

---

[1] Lion, K. S. ; Ibid.

[2] Bridgmen, P. W. ; The Physics of High Pressure. G. Bell and Sons, Ltd. , London, 1949.

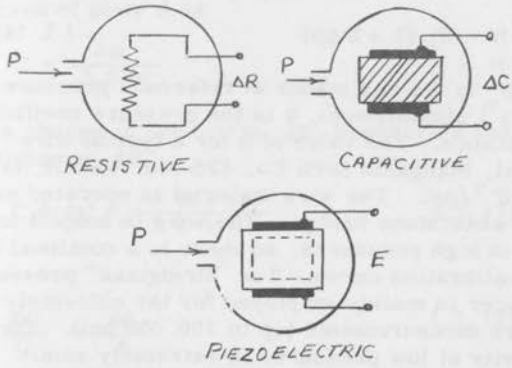

Figure 7. 17 - Electro-Mechanical Pressure Transducers.

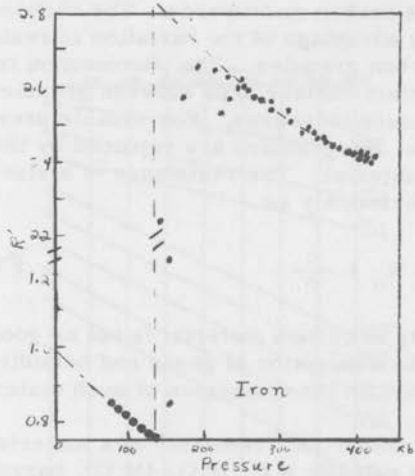

Figure 7. 18 - Variation of Resistance with Pressure

given approximately by the relation

$$R = R_o (1 + b\Delta p) \qquad (7.14)$$

where R_o is the resistance at reference pressure (such as 1 atmosphere), b is the pressure coefficient of resistance. The value of b for a typical wire material, Manganin (84% Cu, 12% Mn, 4% Ni), is 1.7×10^{-7}/psi. The wire material is operated as one arm of wheatstone bridge. The wire is subject to ageing in high pressures, so there is a continual shift in the calibration curve. The "Bridgman" pressure transducer is mainly employed for the extremely high pressure measurements (up to 100,000 psi). The sensitivity at low pressures is extremely small.

A special case of the resistance-pressure transducer is the carbon microphone. The carbon microphone takes advantage of the variation in resistance through carbon granules. The phenomenon is basically that the contact surface area between granules increase as the pressure increases. For useable pressure transducers, the granules are replaced by thin disks of carbon material. The resistance of a stack of disks varys approximately as

$$R = R_o + \frac{c}{p} \qquad (7.15)$$

The stability of carbon material is not as good as metals. The absorption of gases and humidity cause a continual shift in the resistance of such materials.

The dielectric "constant" of a material, such as Rochelle salt ($Na\ K\ C_4\ H_4O_6\ 4H_2O$), barium titanate, MgO, KCl, and KBr, will change with pressure. Neubert [1] has computed the relations for a general

[1] Newbert, H. K. P. ; Instrument Transducers, Oxford University Press, 1963.

dielectric variation capacitor. The capacitance for two plates separated by a dielectric, ϵ, of thickness d and area of plate A is

$$C = \frac{A\epsilon}{3.6\pi d} \qquad (7.16)$$

Thus, a change in dielectric, $\delta\epsilon$, produces a change in capacitance, δC,

$$C + \delta C = \frac{A(\epsilon + \delta\epsilon)}{3.6\pi d} \qquad (7.17)$$

or

$$\frac{\delta C}{C} = \frac{\delta\epsilon}{\epsilon} \qquad (7.18)$$

Figure 7.19 shows a plot of the variation of ϵ with pressure for several typical materials. The variable

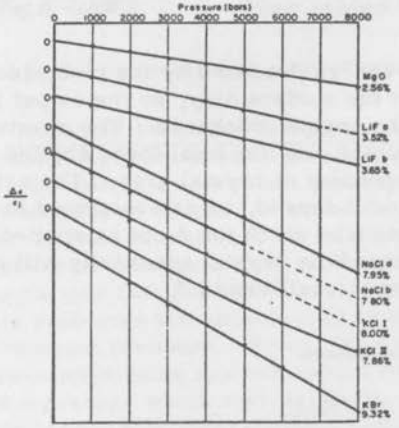

Figure 7.19 - Variation of the Dielectric Constant with Pressure.

dielectric pressure transducer is limited to moderate and high pressures because of the elastic properties of the material.

It has also been suggested that an elastic material be employed as the dielectric. [1] In this case, the dielectric is simply thinned out by the pressure, and the capacitance physically reduced. This type of transducer has not been developed in detail, but it might be of extreme value for low pressures.

In figure 7. 16 the piezoelectric phenomenon was suggested as a means of sensing deflection of a mechanic diaphram type transducer. The piezoelectric transducer may, of course, be employed directly to indicate pressure. The piezoelectric crystal actually requires an almost negligible deformation to produce a measurable charge build-up. The major difficulty has been the requirement of more complex electrical circuits, in order to operate the high impedance crystals.

The charge produced by the piezoelectric crystal is at the surface only, so the output is independent of the crystal thickness. The crystal is in effect measuring only the total force applied to the crystal independent of crystal area. The actual output of a crystal will depend, as demonstrated in figure 3. 4, on the direction in which the force is applied. Thus, an expression of the crystal sensitivity will be in terms of at least three coefficients. [2]

---

1 Lion, K. S. ; Ibid.

2 Neubert, H. K. P. ; Ibid.

Figure 7.20 demonstrates several possible shapes of piezoelectric crystals employed in pressure measurements, together with typical califrations. In some cases, it is possible to place the crystal in a shear or bending moment and greatly increase the force applied to the crystal.

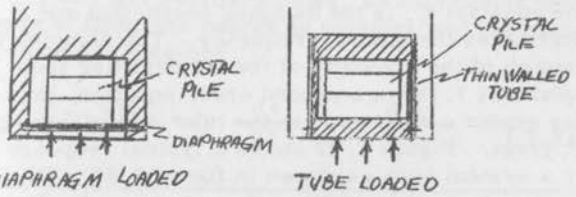

Figure 7.20 - Piezoelectric Pressure Transducers.

C. Transient Pressure Measurements. - There are many applications which require the measurement of fluctuating or transient pressures. The major application is of course the sound-measuring microphone. In fluid mechanics, we will be interested in both pressures related to sound, and also in the pressure variations that produce forces on structures. Two specific problems are encountered in the evaluation of a trancient pressure. First, the response of the pressure-transmitting system, which is composed of a fluid in a passage which may be elastic. Second, the response of the transducer-sensing element must be considered.

Transmitting System Response - When the pressure changes, there must be some motion of the transmitting fluid, since the connecting passage and the transducer itself is elastic. Consider the pressure-transmitting system shown in figure 7. 21. If the flow in the connecting tube is laminar, and the fluid and pressure transducer respond elastically, the governing equation is[1]

$$\frac{d^2 p_t}{d t^2} + C_1 \frac{d p_t}{d t} + C_2 p_t = C_2 p \quad (7.19)$$

The constant C_1 is the damping coefficient and C_2 determines the natural frequency. The damping is a function of the viscosity of the transmitting fluid. Equation (7. 19) is a second order equation, thus we may expect a resonance in the tube if the damping is not great. Figure 7. 22 shows a typical response curve for a system such as shown in figure 7. 21. This system shows a resonance at 40 cycles per second. The resonance frequency of the system is given by the relation

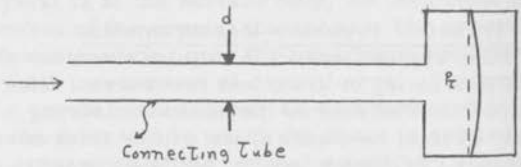

Figure 7. 21 - Model for the Transient Response of a Pressure Transducer System.

---

[1] Hubbard, P. G. ; Interpretation of Data and Response of Probes in Unsteady Flow. ASME Symposium on Measurements in Unsteady Flow, 1962.

$$f = \frac{1}{2\pi}\left[\frac{\left(\frac{\Delta p}{\Delta V}\right)A^2}{\left(m - \frac{4}{3}\rho L\frac{A^2}{a}\right)}\right] \qquad (7.20)$$

where A is the effective area of the sensing element, $\Delta p/\Delta v$ is the ratio of pressure change to volume change for the transducer and tubing, m is the mass of the transducer diaphragm, ρ is the specific mass of the fluid, L is the length of the tubing, and a is the cross-sectional area of the tube.

For rigid capillary tubes, an expression between the rate of flow, the change in volume, and the change in pressure is obtained

$$RT\frac{dm}{dt} = -p\frac{dv}{dt} - v\frac{dp}{dt} \qquad (7.21)$$

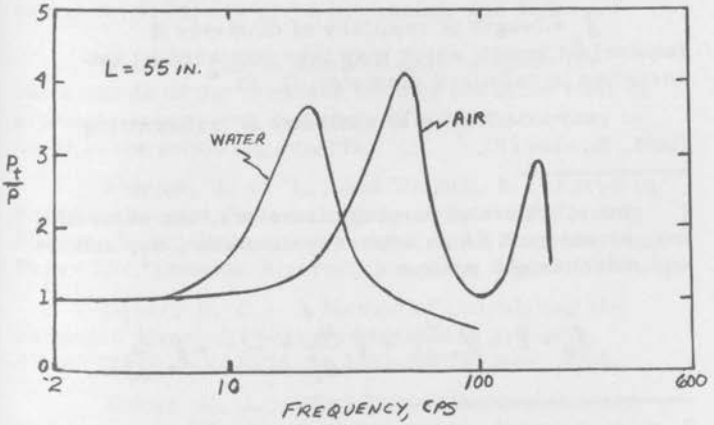

Figure 7.22 - Response of a Transducer System to Sinusoidal Pressure Fluctuations.

Details of this relation and its solution are given by Sinclair and Robins.[1] The solution for the response time is

$$t = \frac{128 \mu \ell_e}{\pi d^4}\left[\frac{V_1}{P_1} \ln \frac{(P_0 - P_1)(P + P_1)}{(P - P_1)(P_0 + P_1)} + \frac{3 V_d}{P_0 - P_1} \ln \frac{P_0 + P_1}{P + P_1} + \frac{V_d}{P_0 - P_1} \ln \frac{P_0 - P_1}{P - P_1}\right] \qquad (7.22)$$

where

v_1 = entire air volume of system from orifice to and including the manometer or transducer, Ft.^{3}

v_d = volume displaced by motion of manometer fluid or by deflection of transducer, Ft.^{8}

d = diameter of the capillaries, Ft. *

ℓ_e = length of capillary of diameter d (equivalent length which may take into account the variation in capillary diameter d), Ft. *

u = coefficient of viscosity of transmitting fluid, lb.-sec/Ft.^{2}

(* for a system of varying diameters, the value of d may be selected as an arbitrary diameter, d_1, and the equivalent length written as

$$\ell_e = \ell_1 + \ell_2 \frac{d_1^4}{d_2^4} + \ell_3 \frac{d_1^4}{d_3^4} + \cdots + \ell_n \frac{d_1^4}{d_n^4} \quad)$$

---

[1] Sinclair, A. R., and Robins, A. W.; A Method for the Determination of the Time Lag in Pressure Measuring Systems Incorporation Capillaries. NACA TN 2793, 1952.

Figure 7.23 shows a comparison of the computed and measured response time for a typical capillary system reported by Sinclair and Robins.[1] The capillary size will limit the response time. Equation (7.22) suggests the time response can be reduced by making the capillaries as large as possible. Expressing the equivalent length ℓ_e as

$$\ell_e = \ell_e' + \ell_x \frac{d^4}{d_x^4} \qquad (7.23)$$

the expression for the optimum diameter d_x is approximately

$$d_x \approx \sqrt[6]{\frac{8 V_1' d^4}{\pi \ell_e}} \qquad (7.24)$$

which results in the optimum diameter being independent of its length. Details of the application of equation (7.24) are given by Sinclair and Robins.[1]

Working charts are available to speed the calculations of the response time of pressure time of pressure-measuring systems. These charts may be found in the following reports:

Aldrich, J. F. L., and Tripoli, S.: Error in Non-Equilibrium Pressure Measurements Following Step and Ramp Pressure Changes. SAE Engineering Paper 587, Douglas Aircraft Company, March 1958.

Bauer, R. C.: A Method of Calculating the Response Time of Pressure Measuring Systems. AEDC TR 56-7 (ASTIA No. AD-98978) Nov. 1956.

Volluz, R. J.: Wind Tunnel Instrumentation and Operation, Handbook of Supersonic Aerodynamics, Sec. 20, NAVORD Report 1488, vol. 6, 1961.

---

[1] Sinclair and Robins, Ibid.

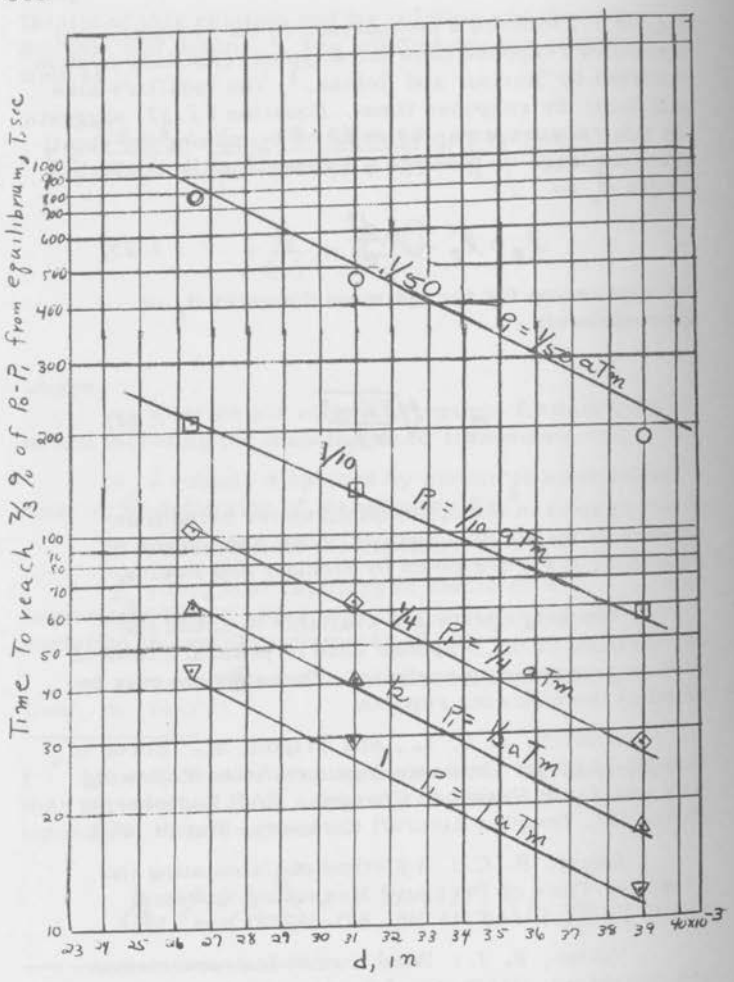

Figure 7.23 - Typical Response Time in a Capillary Tube.

Transducer Response.[1] - In general, the pressure transducer will be a system which has more than one mode of response oscillation. The system will have spring constants and damping factors associated with the modes of oscillation. A mechanical model of the transducer will be an idealized vibrating system. The model must consist of at least one inertial mass, a spring, a viscous resistance, and an external driving or exciting force. For the ideal transducer, the spring force and the viscous resistance are linear. The idealized mechanical models are shown in figure 7. 24. Both a single-degree-of-freedom, and a two-degree-of-freedom model are shown. The movable-plate condenser-capacitive transducer (microphone) and the piezoelectric transducer are examples of an approximate one-degree-of-freedom transducer. The strain gauge transducer is a fair approximation of a two-degrees-of-freedom model.

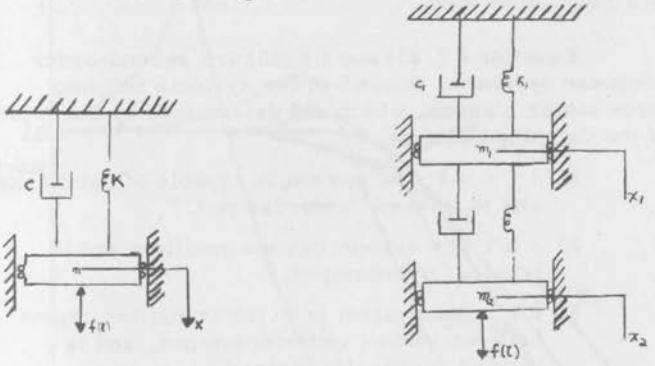

Figure 7. 24 - Mechanical Models of a Vibrating Pressure Transducer.

[1] See, for example; Methods for the Dynamic Calibration of Pressure Transducers. By Schweppe, J. L., Eichberger, L. C., Muster, D. F., Michaels, E. L., and Paskusy, G. F , Nat. Bur. St. Monog. 67, 1963.

The characteristic differential equations which describe the motion of the systems shown in figure 7. 24 are

[one-degree-of-freedom] $$m\ddot{x} + c\dot{x} + kx = f(t) \qquad (7.25)$$

[two-degree-of-freedom]

$$\begin{cases} m_1\ddot{x}_1 + c_1\dot{x}_1 + k_1 x_1 - c_2(\dot{x}_2 - \dot{x}_1) - k_2(x_2 - x_1) = 0 \\ m_2\ddot{x}_2 + c_2(\dot{x}_2 - \dot{x}_1) + k_2(x_2 - x_1) = f(t) \end{cases} \qquad (7.26)$$

where c is the damping constant, k is the spring constant, and f (t) is the external driving force which is a function of time.

Equation (7. 25) and (7. 26) are second-order response systems. Second-order systems fall into three major classes, which are determined by the value of the damping constant, c.

1) $0 \leq c < 1$; the system is capable of oscillation and is termed "underdamped. "
2) $c > 1$; the system can not oscillate and is termed "overdamped. "
3) $c = 1$; the system is in the transition region between under- and overdamped, and is termed "critically damped."

If $c = o$, a disturbance to the system will cause an oscillation which never dies out. A system with $c = o$ is not physically possible, since it would violate the second law of thermodynamics. However, conditions are sometimes encountered where the simplifying assumpition $c = o$ is useful.

Figure 7.25 shows typical solutions of the second-order equation (7.25) for different values of damping constant. For a step change in pressure, the output response of an underdamped system will start with a zero slope, pass through a point of inflection, approach the final pressure, overshoot the final pressure, and oscillate about the final pressure with continually decreasing amplitude. The amplitude of the oscillations will be greatest for small values of c and less for large values of c. The frequency or period of the oscillations is usually expressed in terms of the natural frequency of the sensing element. The natural frequency for typical diaphragms are listed on the following page. [1]

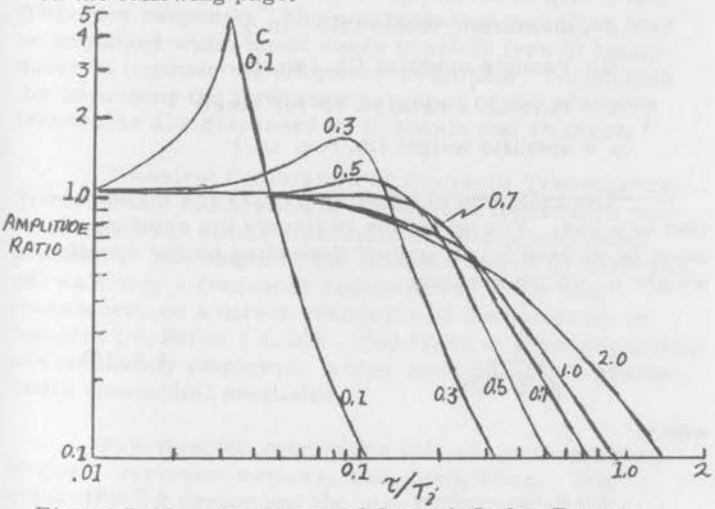

Figure 7.25 - Responses of Second-Order Pressure Transducers.

---

[1] Neubert, H. K. P.; Ibid.

Membrane $$f_o = \frac{1.20}{\pi a}\sqrt{\frac{gS}{\mu t}}$$

Thin Plate $$f_o = \frac{2.56t}{\pi a^2}\sqrt{\frac{gE}{3\mu(1-\nu^2)}} \qquad (7.27)$$

where:

t = plate thickness (in.)

2a = diaphragm diameter (in.)

g = gravitational constant (386 in./sec^2)

s = membrane tension (lb./in.)

E = Young's modulus (lb./sq. in.)

ν = Poisson's ratio (0.30 for steel)

μ = specific weight (lb./cu. in.)

The relations of equation (7.27) are for operation in a gas. For operation in liquids the relation must be altered by an amount depending on the specific weight μ_L of the medium

$$f_1 = \frac{f_o}{\sqrt{(1+\beta)}} \qquad (7.28)$$

where

$$\beta = 0.66\ \frac{\mu_L\, a}{\mu\, t} \qquad (7.29)$$

The useable response of a pressure measuring system can never be as much as the natural frequency. If the system is underdamped, then care must be taken not to exceed frequencies of more than approximately 1/2 f_o.

If frequencies as great as the natural frequency are present, then the output of the transducer may be far too great for the actual pressure present. For membrane pressure transducers, it is possible to obtain usable frequency response of 1000 cycles or more. Since the natural frequency depends on the inverse of the membrane diameter, while the pressure sensitivity goes directly as the diameter, it is found that low pressure transducers have less response than high pressure transducers.

If the output of a pressure transducer is known as a function of frequency, the output can be, in principle, electronically compensated to give a flat frequency response. The compensation technique may be employed with almost every possible type of transducer to improve the frequency response. Techniques for improving the frequency response of the pressure transducer are discussed by Michaels and Paskusz. [1]

Transient Calibration of Pressure Transducers.- The transient calibration of a pressure transducer may be obtained for either a periodic or nonperiodic input pressure. The output of the transducer can be expressed, as either a frequency response curve for the transducer, or a direct evaluation of the constants of equation (7. 25) or (7. 26). Two types of input pressures are commonly employed: a step function, or an approximate sinusoidial oscillator.

Step-function generators include quick-opening devices, explosive devices, and shock tubes. The quick-opening device and the shock tube are similar.

---

[1] Schweppe, J. L., Eichberger, L. C., Muster, D. F., Michaels, E. R , and Paskusz, G. F. : Ibid. , Nat. Bur. St. Monog. 67, 1963.

In each case a pressure pulse in the form of a step function is produced. The shock tube is simply a tube with a high and a low pressure section separated by a diaphragm. The diaphragm is ruptured between the section and a "shock wave" travels down the low pressure section. Figure 7.26 shows a typical output trace from a pressure transducer in a shock tube.[1]

---

[1] The frequency of oscillation of the trace demonstrates the natural frequency of the transducer. The actual constants are given by the relation

$$\text{Oscillation period} = \frac{T}{\sqrt{1 - c^2}}$$

where T is the period of the natural oscillation. The envelope of the peak of the oscillations is a pair of exponential curves having apparent time constants of approximately

$$\tau/2C^2 = \frac{T}{2\pi c}$$

Thus, from the measured period and the oscillation amplitude damping the natural frequency and damping constant can be determined.

Sinusoidal pressure fluctuations in a gas are limited to small amplitudes, since large amplitudes develop into shock fronts. Only sound wave type pressure amplitudes are possible in gases. Microphones are calibrated using diaphragm type speaker pressure generators. Periodic-function generators, such as rotating valves, sirens, piston-in-cylinder devices, and mechanical oscillators are employed. These devices produce periodic pressure waves, however, the mathematical discription of the wave may be complex. In incompressible liquids, it is possible to produce fairly good sinusoidal pressure waves. [1]

Turbulent Pressure Measurements. - The evaluation of fluctuating pressures in a turbulent pipe flow have been reported by Corcos. [2] The problems are very similar to those encountered in the use of hot wires to measure turbulent velocities. The static pressure probe is built with a piezo-electric element replacing the static holes, such as shown in figure 7.26. As shown in figure 7.26, the probe experiences a cross-flow which results in additional pressure fields. The relative order of magnitude of this effect depends on the probe geometry and on the Reynolds number of the cross-flow. If the sensing element is far downstream of the nose, the resultant presure field is nearly a function only of the instantaneous cross-flow. The side-force exerted on the probe is approximately

$$\begin{aligned} &\text{(High Reynolds number)} \quad \sqrt{f^2} \sim \rho \left(\overline{v^2} + \overline{w^2} \right), \ell d \\ &\text{(Low Reynolds number)} \quad \sqrt{f^2} \sim \mu \left(\overline{v^2} + \overline{w^2} \right)^{1/2} \ell \end{aligned} \qquad (7.30)$$

---

[1] Melville, A. W.; Hydraulic Oscillator for the Dynamic Calibration of Pressure Recording Systems. J. Sci. Inst. vol. 36, p. 422, 1959.

[2] Corcos, G. M.; Pressure Measurements in Unsteady Flows. ASME, Symposium on Measurements in Unsteady Flow, Worcester, Mass., 1962.

where v and w are the lateral components of velocity, d is the probe diameter, and ℓ is the probe length. The pressure due to the weighted average of the cross-flow is not necessarily proportional to the cross-flow drag. Minimizing the effect of cross-flow on the probe is an empirical design problem. This is done by testing the probe in turbulent flows where pressure fluctuations are very small. By yawing the probe to the flow, the sensitivity to cross-flow fluctuations is evaluated. The fluctuations due to the lateral turbulent velocity components tends to be of the same order as those of the static pressure fluctuations.

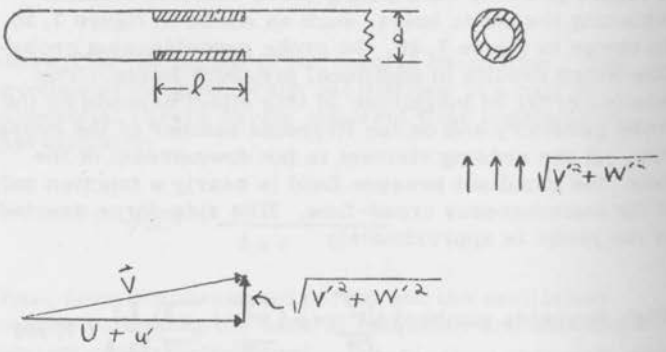

Figure 7.26 - Piezo-Electric Static Pressure Probe.

The measurements of turbulent wall pressure fluctuations have been reported in great detail. Both microphones and piezo-electric pressure transducers are employed. Corcos[1] has employed lead zirconate crystals to measure the fluctuations at the wall of a pipe. These crystals range in diameter from 0.03 to 0.10 unches. Their frequency range is from 35 cps to 100,000 cps. Figure 7.27 shows the measured ratio of root-mean-square pressure to shear at the wall as a function of Reynolds number for a pipe. Note that the results of figure 7.27 are very similar to the turbulent velocity variation shown previously in figure 5.32. The spectra of the pressure is shown in figure 7.28.

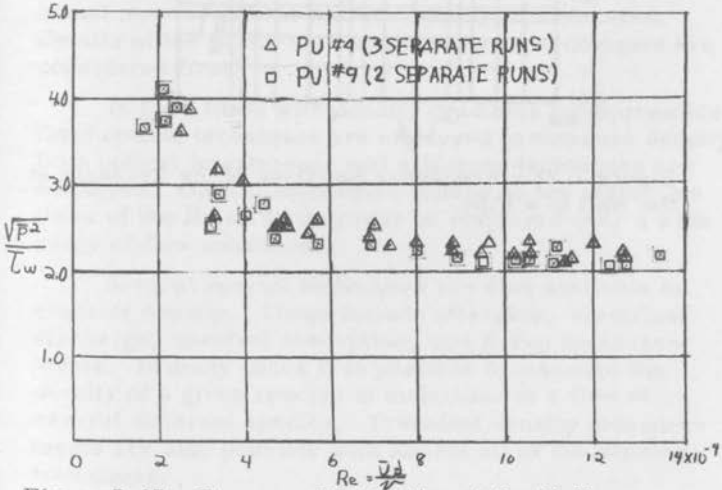

Figure 7.27 - Pressure Fluctuation at the Wall as a Function of Pipe Reynolds Number.

---

[1] Corcos, G. M., Ibid.

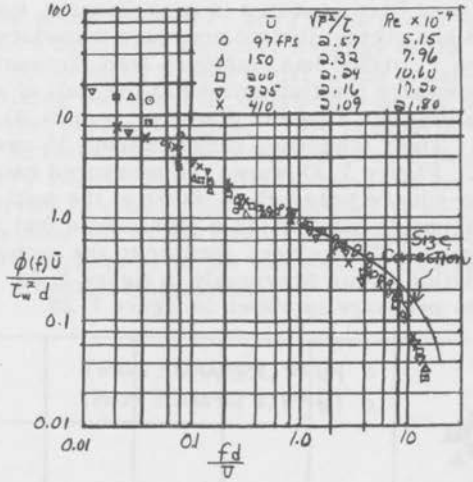

Figure 7.28 - Frequency Spectrum of the Pressure at the Wall of a Pipe.

Chapter VIII

MEASUREMENT OF FLUID DENSITY

The measurement of fluid density depends very much on the fluid. For liquids, the measure of density is simply a measure of volume and weight. For gases, the measure of density is done by measuring pressure and temperature. At low pressures it is easier to measure density of a gas rather than pressure . As a result, most vacuum pressure gages are actually density measuring transducers. The heat transfer, ionization and mass spectrometer instruments all represent an actual measure of the number density of molecules. Details of the number density measuring techniques are considered first.

In fluid flows with density gradients (compressible flow) optical techniques are employed to measure density. Both optical interference and schlieren techniques are employed. Optical techniques depend on the refractive index of the fluid, so they may be employed over a wide range of flow conditions.

Several special techniques are also available to evaluate density. These include afterglow, electrical discharge, spectral absorption, and X-ray measurements. In many cases it is possible to measure the density of a given species of molecules in a flow of several different species. Transient density measurements are also possible with almost all of the sensing techniques.

A. Number Density Measurements - For normal atmospheric conditions density is usually measured indirectly in terms of pressure and temperature. The equation of state

$$P = \rho RT \tag{8.1}$$

relates pressure, P, density, ρ, and temperatures, T, in terms of a constant of proportionality; the gas

constant, R . Equation (8.1) is for an ideal gas, however, most gases follow the relation. The gas constant, R , is the same for all gases, and has a value

$$R = 8.314 \times 10^7 \text{ ERGS/DEG.} = 1.9865 \text{ CAL/DEG.}$$

At extreme conditions of pressure or temperature, where the approximations of an ideal gas are no longer valid equation (8.1) must be modified. At these extreme conditions the equation of state is modified to the form

$$P = Z \rho RT \qquad (8.2)$$

where Z is the departure from perfect gas behavior. The value Z is commonly termed the compressibility factor. This compressibility factor is not to be confused with the use of compressibility to describe a fluid flow. The deviations from ideal gas behavior were first investigated for gases under high pressure, thus, the origin of compressibility factor was related to the high pressure. In recent research the compressibility factor has become increasingly important in the study of high temperature gases, such as encountered in re-entry aerodynamics and plasma physics. Gases which require the use of equation (8.2) have been termed real gases. The compressibility factor, Z , may be viewed as the ratio of the molecular weight of air under normal conditions to the mean molecular weight of the equilibrium gas. Figure 8.1 shows the variation in Z as a function of temperature and pressure for air. The variation of Z depends on the chemical changes in the gas. As noted on Figure 8.1, the dissociation of oxygen and nitrogen contribute greatly to the variation of Z .

The value of Z can be calculated from equilibrium chemistry, so it is well known for gases where it is important. For non-equilibrium changes it would be extremely difficult to predict the variation of Z . We will consider in a later section the problem of evaluating of density in a shock tube where the non-equilibrium processes are not well defined.

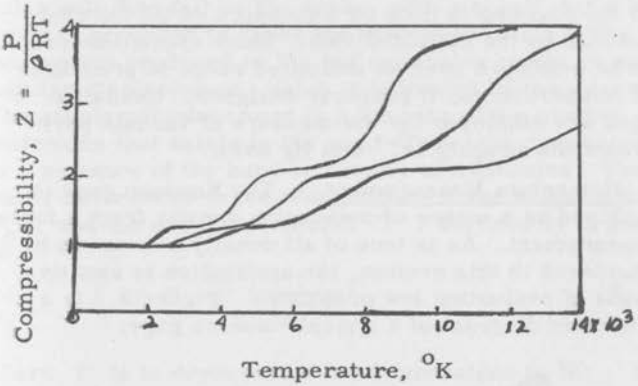

Figure 8.1 - Compressibility Factor for Air in Equilibrium (Hansen and Heims, NACA TN 4359, 1958)

At extreme pressures liquids will also show a compressibility effect, which must be accounted for in evaluation of their density. For normal pressures most liquids are not compressible, so the measurement of density is a matter of measuring a known volume and weight. The density of a liquid will be expected to vary with temperature only, such as demonstrated for the manometer fluid in Figure 7-11.

There are several means of indicating directly the number density of molecules in a flow. Most of these devices are limited to the regions of extreme low densities. The density of molecules may be measured by indirect effects, such as imparting a definite momentum to each molecule and then measuring the resultant force. A second method measures the heat transfer from a heated element, which is a direct function of the gas density. Direct means of

measuring number density employ a method of "tagging" the molecules and then collecting and counting them. The tagging is generally done by ionization of the molecules and the counting is done by a measure of the current produced by the collected ions. Mass spectrometers can be employed over an unlimited range of pressures and temperatures, if properly designed. Ionization gages are employed for the measure of vacuum pressures from roughly 10^{-3} mm Hg down.

Momentum Measurement - The Knudsen gage is employed as a means of measuring density from a force measurement. As is true of all density sensors to be considered in this section, the application is usually a means of evaluating low pressures. Figure 8.2 is a schematic diagram of a typical Knudsen gage.

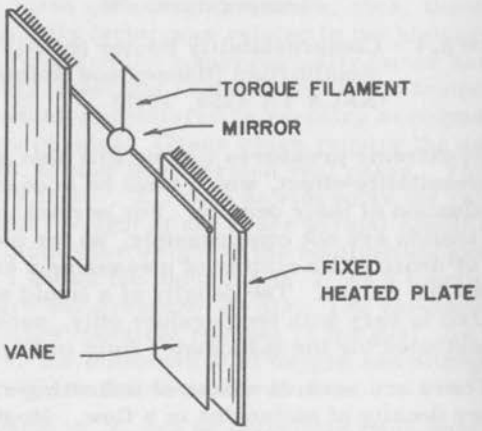

Figure 8.2 - Schematic Diagram of a Knudsen Vacuum Gage.

The gage consists of two vanes on the end of a rod, which is suspended by a filament which resists rotation. Any rotation of the rod is indicated by the light beam-mirror system. Two heated plates at a distance less

than the mean free path between molecules are mounted opposite the vanes. The heated plates increase the energy of molecules which strike them. The hot molecules will then fall on the vanes, with a result that a net force is produced to cause the system to rotate. The net momentum produced by the hot molecules produces an angular displacement, which is indicated by the mirror. The angular displacement is a function of the number of molecules that exists in the gas. Thus, the displacement is a measure of the number density of molecules. For small differences in the temperature of the heated plates, T_p , and the gas temperature, T , the density is given as

$$\rho = \frac{4F}{R}\left(\frac{1}{T_p - T}\right) \qquad (8.3)$$

where F is in dryness and the temperature is ^0K . If the gage is used to measure pressure the pressure is given by

$$P = 4F\,\frac{T}{T_p - T} \qquad (8.4)$$

The Knudsen gage is used over a pressure range from 10^{-8} to 10^{-2} mm Hg. The sensitivity of the Knudsen gage should be independent of the gas composition. The Knudsen gage is sometimes employed as a pressure standard at the low pressures. There is of course many possible uncertainties in the measure of small forces, so the gage is not a National Bureau of Standards accepted measure of pressure.

Thermal Conductivity Gauges - These transducers sense the rate at which heat is lost from a solid surface to a surrounding gas. The rate of loss depends on the number of molecules available to transport the heat. Secondary effects of the interaction of molecules and the exchange of energy at the surface makes the heat transfer depend on the actual gas used. The range of

application of the thermal conductivity gauges will be determined at the upper end by free convection heat transfer over-powering the molecular conduction. The lower end of the usable range will be when heat transfer by thermal radiation is greater than molecular conduction. As in velocity measurements, the thermocouple and the resistance-temperature transducers are employed as vacuum gauges.

Hot Wire Manometer - The hot wire manometer is commonly termed a Pirani gauge. The hot wire may be viewed as the same as described for velocity measurements. The practical Pirani gauge may of course be made of a much longer wire than that used for the anemometer. In general the calculation of the wire temperature will be that given by equation (5.38), where the molecular conduction term given by equation (5.29) is employed. If a sufficient number of molecules exists around a hot wire, then the transfer of heat will set up a free convection type flow. The conduction of heat due to the free convection will be much greater than the molecular conduction, so that the heat conduction is a function of the flow and not of the molecular density. When free convection occurs the Pirani gauge is insensitive to the gas density. Figure 8.3 shows the heat loss expected at different pressures

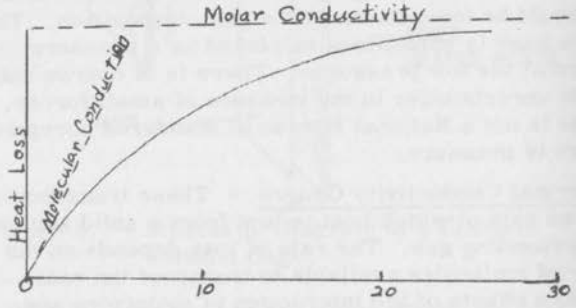

Figure 8.3 - Heat Loss from a Hot Wire as a Function of Pressure.

The Pirani gauge can be used over the range shown in figure 8.3, as long as the sensitivity of the solid curve does not become too small. The determination of the molar conduction limit will depend on the size of the hot-wire compared to the mean-free-path between the molecules.

The wires most often used for the sensing elements of Pirani gauge are platinum, tungsten and nickel. The availability of small diameter wires is the main determining factor in the selection of material. The requirement of each of the heat transfer applications of the resistance-temperature transducers is much the same. A high resistivity and a high value of the thermal coefficient of resistance are desired. Conduction to the hot-wire supports is improved if the wire material has a poor thermal conductivity. For small wire lengths the conduction to the wire support may be a large effect. The ratio of total heat loss by molecular conduction to the total heat loss by conduction can be obtained from equation (5.39) as

$$\frac{Q_{gas}}{Q_c} = \left(\frac{hD}{K}\right)\left(\frac{\ell}{D}\right)^2 \left(\frac{T_w - T_s}{T_{w,\infty} - T_s}\right) \left(\frac{1}{\frac{\eta\ell}{2}\,\mathrm{TANH}\,\frac{\eta\ell}{2}}\right) \quad (8.5)$$

Figure 8.4 is a plot of equation (8.5) for a platinum-iridium wire (0.00025 inch diameter). The actual wire lengths shown in figure 8.5 are smaller than would normally be employed in commercial Pirani gauges. The wires of figure 8.5 were of particular interest in the measure of transient pressure, or density.[1]

The diameter of the hot wire will determine the range of pressures for which it may be used. Theoretically, the classical work of Knudsen shows that the heat transfer from a body to a rarefied gas is a fundamental function of the mean free path between the molecules,

[1] Sandborn, V. A.: A Hot-Wire Vacuum Gauge for Transient Measurements. AVCO Corp. RAD-TM-63-41, 1963.

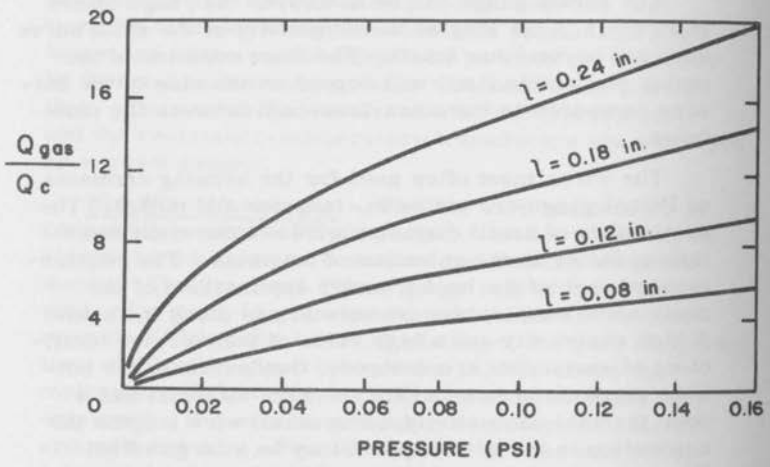

Figure 8.5 - Ratio of Molecular to Support Heat Loss for a Platinum - 20% Iridium Wire.

and of the accommodation coefficient. The accommodation coefficient, a , (where $a \leq 1$) is necessary to express the imperfect exchange of energy between the wire surface and the molecules. The accommodation coefficient is roughly a constant for a given element surface and gas, so it represents a constant of proportionality in the heat transfer relation. The non-dimensional parameter of importance in expressing the heat transfer is the Knudsen number.

From kinetic theory the mean free path between molecules is inversely proportional to the gas density.

$$\lambda = \frac{7.746 \times 10^{-9}}{\rho\ (gm/cm^3)} = \frac{1.502 \times 10^{-8}}{\rho\ (slugs/ft.^3)} \qquad (8.6)$$

Equation (8.6) is for air. The predictions of λ are plotted in figure 8.6.

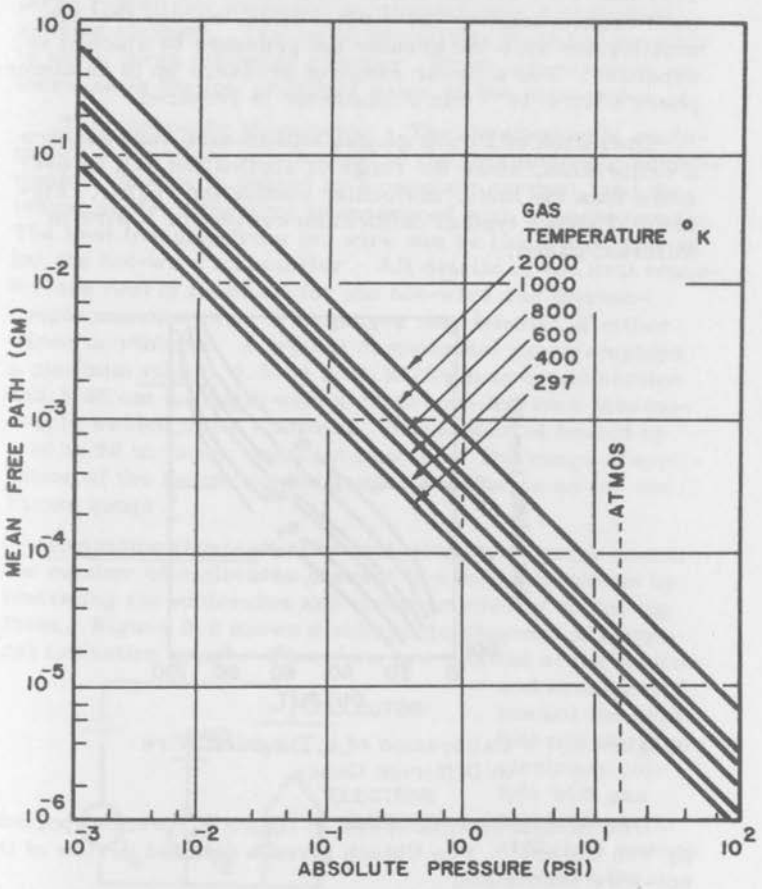

Figure 8.6 - Mean Free Path Between Molecules in Air (Ideal Gas, Z = 1).

Heat transfer measurements suggest that the wire must be at least one fifth of the mean free path in order that free molecular results apply. For example, a 0.01 mm wire the molecular conduction would be dominate out to approximately 10^{-2} psi. Thus, we see that the smaller the wire the greater the pressure to which it is sensitive. For a linear range of pressure up to an atmosphere a wire 10^{-6} mm in diameter is required.

Operation of Pirani gauges will in each case require a calibration, since the range of application will be over more than the linear molecular conduction region. Figure 8.7 shows typical calibration curves for a wire in different gases.

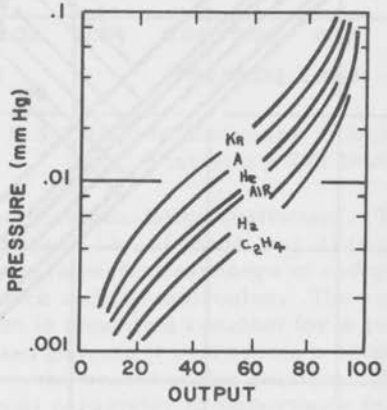

Figure 8.7 - Calibration of a Tungsten Wire in Different Gases.

The measurements shown in figure 8.7 were reported by Von Ubisch[1]. Von Ubisch gives a detailed review of the hot-wire manometer.

[1] Von Ubisch, H.: On the Conduction of Heat in Rarefied Gases and Its Manometer Application. Jour. Appl. Sci. Res., Vol. A2, 1951.

Modern development in Pirani gauges appear to be centered on the use of semi-conductor elements. The large negative thermal coefficient of resistance and the large resistivity make the semi-conductor a desirable sensing element. The large resistivity makes it possible to use a large diameter cylinder, which can result in an increase in the low pressure range of the manometer.

Thermocouple Manometer - The thermocouple manometer is identical in principal to the thermocouple anemometer. A wire is heated by a constant current, and the temperature of the wire is measured with a thermocouple. The heat transfer from the wire can be calibrated just as for the hot-wire manometer. All details of the heat transfer are nearly identical for the hot-wire and thermocouple manometers. The gauges may consist of either wires or ribbons. A typical commercial gauge employs a platinum ribbon 0.0234 by 0.0078 cm in cross section and 3.66 cm in length with a Nichrome-Advance thermocouple welded to its midpoint. The ribbon is heated by a 30 to 50 m. amp. constant current. The range of application of the thermocouple gauge is the same as for the Pirani gauge.

Ionization Gauges - The ionization type gauge counts the number of molecules present in a vacuum system by ionizating the molecules and electrostatically collecting them. Figure 8.8 shows a schematic diagram of a typical ionization gauge. Electrons are emitted at the emitter and accelerated toward the grid. The accelerated electrons collide with gas molecules with sufficient energy to ionize the molecules. For fine wire grids the electrons do

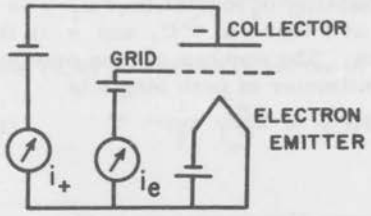

Figure 8.8 - Schematic Diagram of Ionization Gauges.

not strike the grid, but oscillate back and forth through the space between the emitter and collector. As the energy of the electron decreases, it is finally collected by the grid. The ionized molecules are collected by the collector. Design of gauges are such that most of the gas molecules are ionized in a given region. There is of course a calibration problem in that the ionization process may not be 100% efficient. The efficiency of a gauge will depend on the number and collision probability of the electrons. Also, the energy of the electrons must be sufficient to produce ions when a collision occurs. Grid voltages normally run from +120 volts to +200 volts. The plate voltages vary from -6 volts to -100 volts[1].

For an electron to ionize a molecule upon collision the electron kinetic energy must equal or be greater than the ionization potential of the molecule. The ionization potential of molecules varies from 3.89 e V for cesium to 24.6 e V for helium. All gases will fall within the above range of ionization potentials. Thus, the energy of electrons in an ionization gauge needs to be greater than the 24.6 electron volts.

The probability of ionization will depend on the cross section for an ionization collision by the electrons, and the number of molecules present

$$P_i = n_1 \sigma \tag{8.7}$$

where P_i is the probability of ionization, n_1 , is the number of molecules at 1 torr and 0^0C, and σ is the collision cross section. The number of ions produced by an electron per centimeter of path length is

$$n^+ = \frac{273}{T} P n_1 \sigma = \frac{273}{T} P_i P \tag{8.8}$$

---

[1] Leck, J. H.: Pressure Measurements in Vacuum Systems, Inst. Phys., Phys. Soc., Chapman and Hall, Ltd. Lond., 1964.

The term $\frac{273}{T} P$ converts the number of molecules at 1 torr and 0^0 C to the total number at pressure P an temperature T . The probability of an ionization for some common gases is shown in figure 8.9[1] .

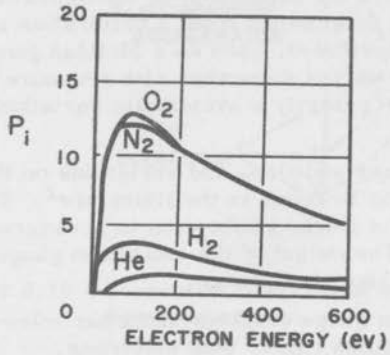

Figure 8.9 - Probability of Ionization of Common Gases[1].

As shown by figure 8.9 the maximum in P_i occurs in the range of voltage between 60 and 200 volts. This maximum indicates the reason for selecting the grid voltage. If all the ions are collected then

$$\psi = \frac{273}{T} P_i P_{i_e} \tag{8.9}$$

Equation (8.9) is written in terms of pressure as

$$P = \frac{1}{S} \frac{i_+}{i_e} \tag{8.10}$$

---

[1] Tate, J. T. and P. T. Smith: Phys. Rev. Vol. 39, p. 270, 1932.

or density as

$$\rho = \frac{1}{S_1} \frac{i_+}{i_e} \qquad (8.11)$$

where S or S_1 is the sensitivity of the ionization gauge. In practice S is determined from a calibration against some other measurement, such as a McHead gauge. The gauge sensitivity varies somewhat with pressure[1], however, it is not necessarily a systematic variation with pressure.

There are many additions and variations on the basic ionization gauge to be found in the liturature[2]. The magnetron gauge has a linear calibration to pressures as low as 10^{-13} torr. The output of the ionization gauges is usually in the micro-amp. range.

The Alphatron gauge employs alpha particles to ionize the gas molecules rather than electrons.

Mass Spectrometers - All of the "vacuum" gauges discussed above measure the total number density of molecules present. Detailed study of a gas requires not only the total number density but also, the number density of each species of molecules present in the gas. The mass spectrometer separates the species according to their molecular weight. Figure 8.10 is a schematic diagram of a simple mass spectrometer. The gas to be analized enters at the left. The gas is ionized just as in a normal ionization gauge. The ionized gas is then accelerated to a known velocity with an electrostatic accelerator. The accelerated ion beam is then subjected to a magnetic field which deflects the ions. The amount of deflection will be a function of the kinetic energy of the ions. If all the ions are travelling at the same velocity,

---

1 Nottingham, W. B., and F. L. Torney: 1960 Vacuum Symposium Transactions, Pergamon Press, Lond. 1961.

2 See for example: Van Atta, C. M.: Vacuum Science and Engineering, McGraw-Hill, 1965.

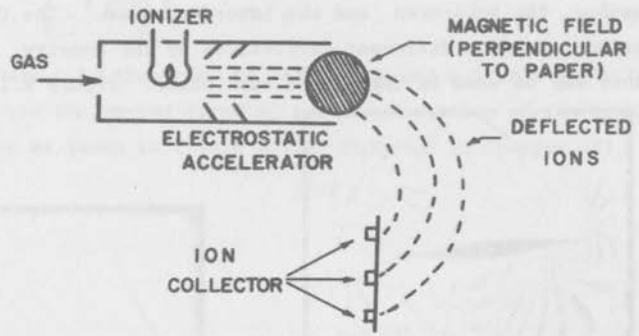

Figure 8.10 - Schematic Diagram of a Mass Spectrometer.

then the light ions will be deflected more than the heavy ions. Thus, we may place a collector at several locations in the deflected beam and measure the number of each ion of a given mass.

B. Electromagnetic Waves- Refraction of light- As shown in figure 3.8 of Chapter III, the refraction index of light is a function of the air density. Optical schlieren techniques, which make use of the change in refractive index, are employed to observe fluid density and density gradients. The word schliere from German could be defined as the locus of inhomogeneities which deflected the light passing through it into a direction other than the original direction. The early development of the schlieren techniques is credited to Toepler in 1866. The interferometer technique was developed by Mach in 1889. Three specific techniques are now generally noted in the literature; the direct-shadow

method, the schlieren and the interferometer.[1] The three methods produce different derivatives of the density, so they may be used to compliment each other. Figure 8.11

(a) Interferometer photograph of the flow past a two-dimensional aerofoil

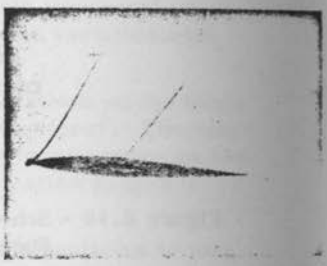

(c) Direct-shadow photograph of the flow past a two-dimensional aerofoil

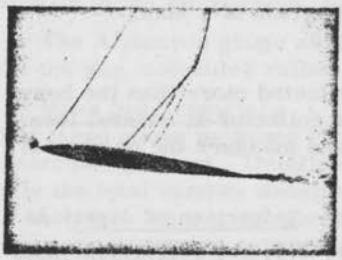

(b) Toepler schlieren photograph of the flow past a two-dimensional aerofoil

PLATE 1

Figure 8.11- Comparison of an interferometer, schlieren and direct shadow photograph.

taken from the paper of Holder and North shows photographs of the flow past a two-dimensional airfoil taken by the three techniques.

The radius of curvature of a light ray in a non-uniform density field is

---

[1] For a general review of the techniques see: Holder, D.W., and North, R. J.; Schlieren Methods. Notes on Applied Science No. 31, National Physics Laboratory, England, 1963.

$$\frac{1}{R} = \frac{\text{grad } n}{n} \sin \psi \qquad (8.11)$$

where n is the index of refraction and ψ is the angle between the vector (grad n) and the direction of the light ray as shown in figure 8.12. As noted in Chapter III,

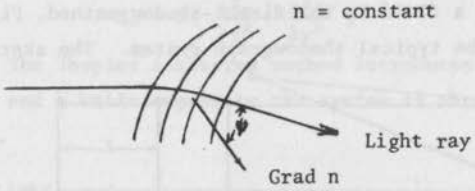

Figure 8.12 - Deflection of a light ray

the index of refraction depends directly on the density

$$n = 1 + k\rho \qquad (8.12)$$

The total angular deflection of a ray as it passes through a density gradient is

$$\varepsilon = \int (1/R) ds \qquad (8.13)$$

where s is the distance along the path of the ray. The deflection of the ray is caused by the projection of grad n upon the plane normal to the light path (grad n sin ψ).

The term grad n sin ψ, will have components $\partial n/\partial x$ and $\partial n/\partial y$ in the x-and y-direction. Thus, the angular deflections in the x- and y-direction are

$$\varepsilon_x = \int k \frac{\partial \rho}{\partial x}\, dz \quad \text{and} \quad \varepsilon_y = \int k \frac{\partial \rho}{\partial y}\, dz \tag{8.14}$$

The deflection is always toward the region of highest density.

The simplest technique to optically view the density variation in a fluid is the direct-shadow method. Figure 8.13 shows the typical shadowgraph system. The sketch

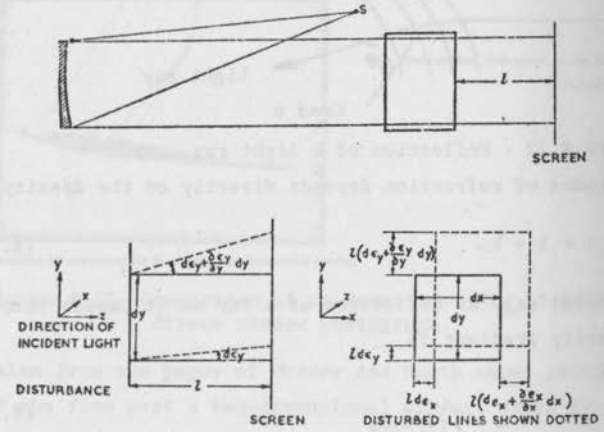

Figure 8.13- Typical shadowgraph system.

taken from Holder and North illustrates the change of illumination seen on the screen. The light that originally illuminated an area on the screen dxdy is deflected to illuminate an area increased by an amount given

approximately by

$$I\,dx\,.\,dy\left(\frac{\partial \varepsilon_x}{\partial x}+\frac{\partial \varepsilon_y}{\partial y}\right),$$

so that the change of illumination on the screen in terms of the initial illumination is

$$\frac{\Delta I}{I}=-I\left(\frac{\partial \varepsilon_x}{\partial x}+\frac{\partial \varepsilon_y}{\partial y}\right). \qquad (8.15)$$

use of equation (8.14) to evaluate $\partial\varepsilon_x/\partial x$ and $\partial\varepsilon_y/\partial y$ lead to the result that the change in illumination is proportional to the second derivative of the density

$$\Delta I = k\left(\frac{\partial^2 \rho}{\partial x^2}+\frac{\partial^2 \rho}{\partial y^2}\right) \qquad (8.16)$$

The Toepler schlieren method introduces a second lens and a knife edge into the system as shown in figure 8.14.

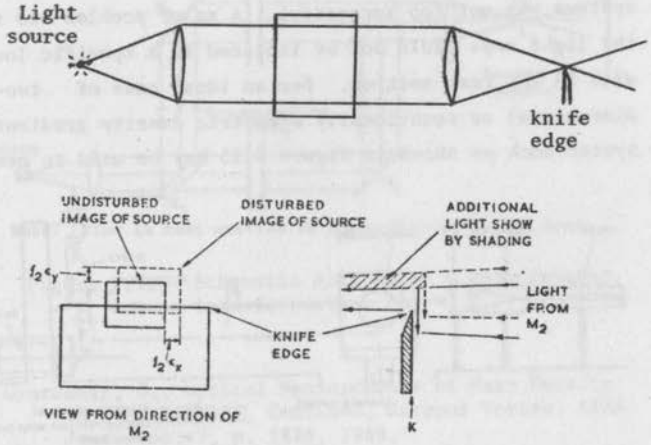

Figure 8.14 - Toepler schlieren system

The second lens produces an image of the source at the lens focal point. The knife edge acts as an optical filter to block out the unwanted light at the focal point. As noted on the sketch of figure 8.14 (from Holder and North) the image is displaced by an amount $f\varepsilon$ in the x and y directions due to density gradients. The constant, f, is related to the focal length of the second lens. The illumination of the image can be increased or decreased according to whether the deflection is toward or away from the knife edge. The knife must be set perpendicular to the direction in which the density is to be observed. The lens knife edge acts as an intergrater of the shadow picture, so that the intensity is proportional to the first derivative of the density.

The early attempts to evaluate density from schlieren systems was not too successful. A major problem was that the light rays could not be isolated to a specific location with in the test section. For an ideal case of two-dimensional or rotationally symmetric density gradients a system such as shown in figure 8.15 may be used to measure

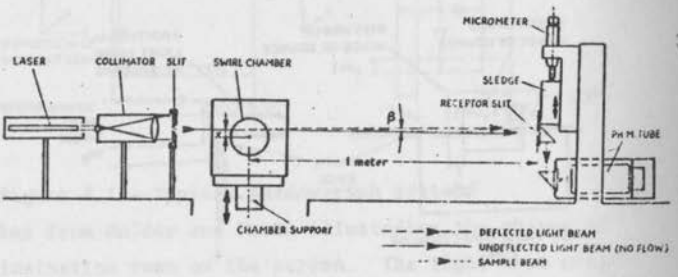

Figure 8.15- Schematic drawing of a quantative schlieren density measuring device.

the deflection of a beam of light.[1] For the rotationally symmetric case of figure 8.15 the deflection can be written in the form of an integral equation of Abel's type, which is solved numerically for the density profile.

The most recent development of holography will remove the problem of two-dimensional assumptions from schlieren techniques and allow three-dimensional density flow fields to be evaluated. The holography techniques is a means of storing the light wave information and regenerating it to construct the complete three-dimensional flow field. Recent work at the Naval Post Graduate School[2] has produced detailed supersonic flow field calculations.

The interferometer technique is able to measure directly the change in refractive index. The basic Mach-Zehnder

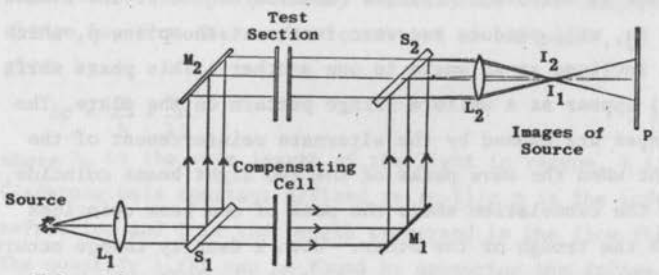

Figure 8.16 - Schematic diagram of a Mach-Zehnder interferometer.

---

1 Gyarmaty, G., Optical Measurements of Mass Density in a High-Speed, Confined, Gaseous Vortex. AIAA Jour. Vol. 7, p. 1838, 1969.

2 Collins, D. J. (Talk given at "Workshop on Flow Visualization and Flow Measurement Techniques", Oct. 1971 NOL, Silver Springs, Maryland.

interferometer is shown in figure 8.16[1]. Light from a monochromatic, coeherent light source passes through a collimating lens, L_1. The collimated light beam is divided by the splitter plate, S_1. Part of the beam is reflected to the mirror, M_2, where it is reflected through the test section to the splitter plate S_2. The beam passes through S_2 to the lens, L_2, which forms an image on the photographic plate, P. The second part of the original beam is transmitted from S_1 through the compensating cell to the mirror M_1. The beam is then reflected from M_1 and S_2 through L_2 to the photographic plate. If S_1,S_2, M_1 and M_2 are all parallel and the lengths of the two light paths are identical, the illumination on the screen is uniform. A slight rotation of one of the elements, say S_2, will produce two wave fronts at the plane p, which are inclined at an angle to one another. This phase shift will appear as a uniform fringe pattern on the plate. The fringes are caused by the alternate reinforcement of the light when the wave peaks of the two light beams coincide, and the cancelation where the peak of one beam coincides with the trough or the other. When a density change occurs in the test section, the speed of light alters the beam such that the fringes will move either up or down. A comparison of the distorted with the undistorted position of the fringes will allow the evaluation of the charge in refractive index, and hence of the density.

---

[1] The discription is taken from: Handbook of Supersonic Aerodynamics, sect. 20 Wind Tunnel Instrumentation and Operation, NAVORD Report 1488 (Vol. 6).

Figure 8.17 is a plot of the light intensity for a typical case of "no flow" and "flow". The light intensity

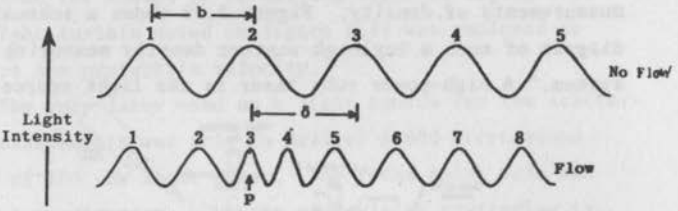

Figure 8.17 - Shift in fringes in a typical flow case.

is measured along a line perpendicular to the fringes. The distance from one bright (or dark) band to another in the no flow case is noted as the fringe width, b. For a point, P, on the flow case the displacement, δ of the fringe from its no-flow position may be measured. The density change, $\Delta\rho$, from the no flow condition at the point, P, is given by

$$\Delta\rho = \frac{\delta}{b} \cdot \frac{\lambda_o}{kL} \tag{8.17}$$

where λ_o is the wave length of the light in vacuum, k is the Gladstone-Dale constant defined as $(\eta-1)/\rho$, η is the index of refraction and L is the length traversed in the flow field. The quantity λ_o/kL can be found by measuring the fringe shifts across known density changes. Accurate evaluation of the density from the interferometer requires a great deal of effort. Detailed studies of the evaluation are reported by Howes and Buchele.[1] The application of laser light sources and holograph techniques have greatly improved the value of the interferometer.

[1] Howes, W. L., and Buchele, D. R.: A theory and method for applying interferometry to the measurement of certain two-dimensional gaseous density fields. NACA TN 2693, 1952. (See also NACA TN 3440 and TN3507).

Scattering. The scattering of electromagnetic waves from the molecules of gases can be employed to make point measurements of density. Figure 8.18 shows a schematic diagram of such a Rayleigh scatter density measuring system.[1] A high-power ruby laser is the light source,

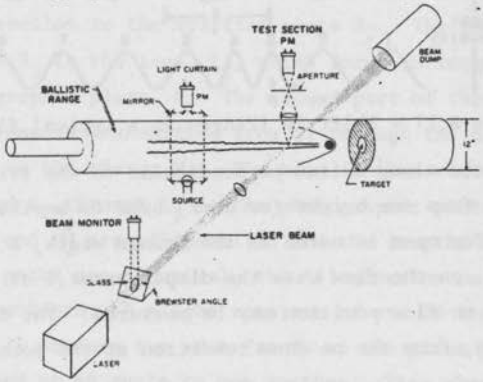

Figure 8.18- Rayleigh scattering density measurements.

which is focused at the point to be measured. The light scattered by the gas at the focal point is measured by the test section photomultiplier. The scattered light is perpendicular to the light beam. The volume of gas sampled is controlled by the size of the laser beam and the aperature size. A second photomultiplier was employed to indicate both the wave form and power of the laser light source. The laser beam, after passing through the test section, is absorbed by a beam "dump". The dump is a blackened cylinder containing a slender circular cone pointed toward the laser.

[1] Locke, E., Point Measurements of the Time Averaged Turbulent Wake Density by Rayleigh Scattering. AIAA Jour. Vol. 5, p. 1888, 1967.

The beam makes many reflections before it leaves the dump, such that the amount of re-emitted light is negligible. The light curtain noted on figure 8.17 was employed to measure the projectile velocity.

The ruby laser used as a light source for the scattering measurements was able to deliver a 600 microsecond pulse of 100 -Kw light power. The focal point size was about 1 mm diameter. The use of Rayleigh scattering is basically a technique of counting molecules. The difficulty with this technique is of course the very large power required for the light pulse. This amount of power can alter the molecular structure of the flow. The gas must also be free of dust particles, as their scattering power will be many times greater than the molecules. It is possible that the technique can be employed to measure the density of the dust particles, or even specific molecules of different Rayleigh scattering cross section. Scattering techniques are not limited to light waves, but also may employ electron beams, x-rays, etc.

Radiation.- Several methods have been suggested to evaluate the density of gases from radiation properties. The technique most often employed in recent years appears to be the electron beam- fluoresence phenomenon. A high energy electron beam is directed across a low density gas flow. The electrons impart energy to the gas moledules causing them to emit visible light. The output is proportional to the density of the gas. The emission at each point along the beam can be used to map the local density

distribution. Figure 8.19 is a schematic diagram of an electronic beam system.[1]

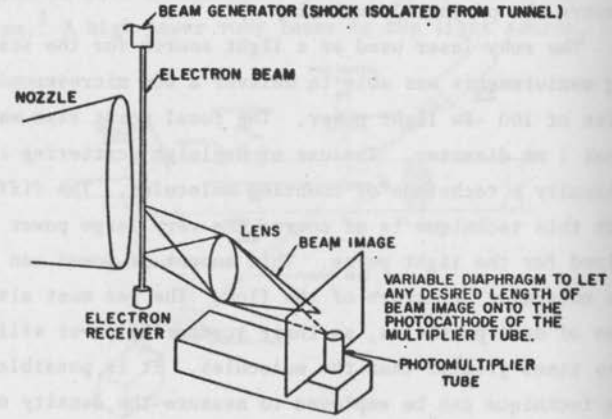

Figure 8.19 - Electronic beam excitation system.

The emission observed due to electron beam excitation in nitrogen, for example, is the prominent emission observed in the auroral spectrum. This process involves direct excitation to an excited state of the ion N_2^+, followed by a spontaneous emission to the ground state of the ion.

---

[1] Muntz, E. P., Harris, C. J. and Kaegi, E. M., Techniques for the experimental investigation of the properties of electrically conducting hypersonic flow fields. Second Nat. Symp. on Hypervelocity Techniques, Denver Res. Inst. Denver, Colo. (See also Muntz, E. P. and Marsden, D.J.; Electron excitation applied to the experimental Investigation of rarefied gas flows. Third Int. Rarefied Gas Dynamics Symp. ed. by J. A. Laurmann, Vol. II. Academic Press, N. Y. 1963.

At gas densities which are low enough to preclude non-radiative de-excitation processes, the fluorescence intensity is a linear function of gas density and electron beam current. The technique is limited mainly to low pressure (below 1 mm Hg.), since it is difficult to maintain a narrow, well-defined beam over large distances at higher pressures. For absolute number density measurements it is important that the beam being observed maintain a constant current density. The measurements are also limited to flows where no significant background or natural radiation exists.

Electron beam of the order of 100-Kv and current of 1 Ma are employed for the measurements. The system can be calibrated under static conditions. Tardil and Dionne[1] suggest the output of the potodetector, S, can be related to the local density by the following relation

$$S = k\,[a\rho/(a+\rho)] \tag{8.18}$$

where k is a normalizing factor and a is a parameter to fit the curve shape. The parameter a is determined from the static calibration data. The normalizing factor is equivalent for known conditions a the time of the test (i.e. free-stream conditions). The calibration will depend on the molecular composition of the gas.

---

1 Tardil, L. and Dionne, J. G. G., Density distribution in turbulent and laminar wakes. AIAA Jour., Vol. 6, p.2027 1968.

Spectral Absorption.- Equation (3.11) notes that the intensity of electromagnetic radiation passing through a gas depends exponentially on the absorption coefficient of the particular gas. The absorption coefficient is a function of the molecules of the gas, the incident electromagnetic wave length, the number concentration of the molecules, and to a lesser extent it depends on the molecular motion and interaction among molecules. Figure 8.20 taken from the

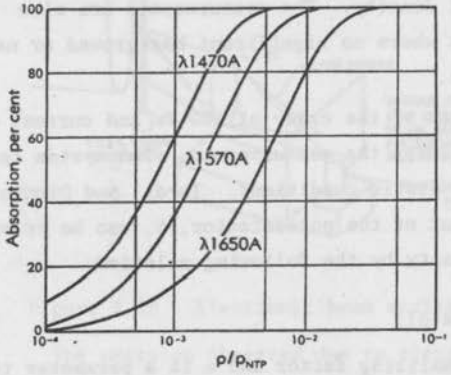

Figure 8.20 Absorption as a function of air density of several wave lengths of light.

paper of Winkler[1] shows the variation of the absorption of several wave lengths of light as a function of density. In air the absorption is actually measuring the number concentration of the oxygen molecules only. With the current ability to control very accurately the wave length of the

---

[1] Winkler, E. M., Spectral absorption method. Physical measurements in gas dynamics and combustion. Vol. IX High Speed Aerodynamics and Jet Propulsion, Princeton University Press. 1954.

radiation it is possible to evaluate the number density of select molecules in a gas mixture. This new ability is of great value in the chemical analysis area. Of specific interest in fluid mechanics is the change in absorption of ultraviolet radiation between atomic, molecular and the ozone states of oxygen.

The absorption of soft x rays has been of value in the measurement of density near solid surfaces. The x ray is not affected by refraction or defraction phenomena which are a problem near surfaces and in steep density gradients. The x ray absorption method can be used over a wide range of density by a suitable selection of the wave length. Figure 8.21 shows the absorption of x rays in air as a

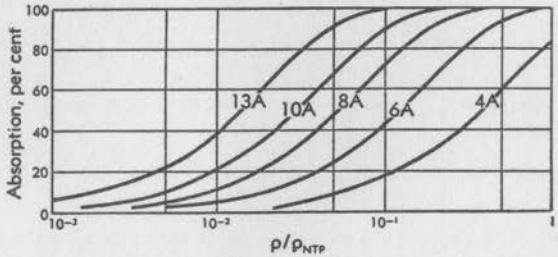

Figure 8.21- Absorption of x rays in air

function of the density for various wave lengths (from Winkler). Electron beams are also employed for measurements of density.